GLOBAL

FINAL REPORT

GEOPHYSICAL SURVEY
SALT POLLUTION STUDY
(DOVE CREEK SITE)
STONEWALL COUNTY, TEXAS

A Geophysical Services Company

SDII GLOBAL

SDII Global Corporation
Main Office
4509 George Road
Suite 200
Tampa, Florida 33634
813.496.9634
Fax 813.496.9664

July 12, 2000

Judge Bobby McGough
County Judge's Office
Stonewall County
P.O. Box 366
Aspermont, Texas 79502-0366

Subject: Final Report - Geophysical Survey
Salt Pollution Study (Dove Creek Site) –
Stonewall County, Texas
SDII Project No. 1011520

Dear Judge McGough:

SDII Global Corporation (SDII) is pleased to submit the final report for the above referenced project. The purpose of the investigation was to utilize geophysical surveys to determine the configuration of the source reservoir and connected conduits/fractures contributing to surface salt-water pollution associated with the Dove Creek area.

SDII appreciates the opportunity to have assisted Stonewall County on this project. If you have any questions or comments about the report, please contact us.

Sincerely,

SDII GLOBAL CORPORATION

Thomas L. Dobecki, Ph.D.
Principal Geophysicist

TABLE OF CONTENTS

LIST OF FIGURES

EXECUTIVE SUMMARY

A geophysical survey was conducted at the Dove Creek Area in Stonewall County, Texas with the objective of locating optimal drilling locations for brine productions wells. The best potential locations for such brine production wells would be in areas where there are several such brine-filled fracture conduits and where the reservoir is known to exist. Traditional methods of locating possible fractures include ground geologic reconnaissance coupled with analysis of photolinear trends. The geophysical survey was designed to determine which linear features correlate with brine-carrying fractures. One task/objective of the geophysical investigation was to perform a combination of Very Low Frequency (VLF) electromagnetic and electromagnetic terrain conductivity (EM34) methods to map the trend and locations of brine-filled fractures. The other task/objective was to use Time Domain Electromagnetic (TDM) surveying to help identify the existence, depth and thickness of the brine reservoir across the project site. The combination of the three techniques was intended to build a three-dimensional model of the brine reservoir-conduit system at a series of specific locations within the site study area. There were six primary survey areas (Area A through Area F as defined on attached Figure 2) within the overall study area where all three surveys were applied. An additional ten sites (also defined on Figure 2) were selected for TDM-only investigation to determine depth to the brine reservoir. The results of the geophysical program can be summarized as follows.

The VLF and EM34 data have demonstrated that we can see discrete vertical conductive bodies that we interpret as brine filled fractures at all sites except Areas D and E. At these two areas, we consider the brine level in the fractures to be so deep below ground surface that these near-surface geophysical devices do not detect it. In the other areas (A, B, C, and F), we were able to detect areas where brine must be locally closer to the surface (in vertical fractures). We can sometimes correlate the positions of these discrete, high conductivity areas from line-to-line in order to determine apparent fracture azimuth across these areas.

There is no consistent, dominant fracture azimuth that is observed over the entire site. Rather it would seem that, like the multiple azimuths seen in Bob Rodgers' of RWR Associates photolinear analysis, there are several fracture orientations and the orientation preference varies around the site.

The dominant anomaly positions at the six main test areas have been staked in the field as potential, recommended drilling locations. The positions of these stakes have been surveyed (GPS) by RWR Associates.

The TDM data analysis has shown that the subsurface resistivity model over majority of the site area may be represented by a three-layered resistivity structure. The uppermost layer is considered to be dry sediments with a typical resistivity of 40-90 (average = 62) Ω-m. This is underlain by a layer (Layer 2) of decreased resistivity (average = 24 Ω-m) that may represent the water table or an increase of clay content at depth. The deepest layer seen (Layer 3) has a very low resistivity (1 Ω-m) and is interpreted as the top of the brine reservoir. We do not see the Childress Formation as a discrete layer because it is probably higher resistivity (more difficult to see with TDM) and may be rather thin as compared with its depth of burial. Except in areas on the river/creek bottoms where saturated brines are seen at ground level, we typically find the top of the brine layer to be at or just below the level of the Top of the Childress formation as taken from structural contours of the Top Childress provided by RWR. The most significant exception to this normal situation is in the SW portion of the study area (Location #13 and Location #14; see Figure 2) where low resistivity brines are interpreted as being in excess of 150 ft above the level of the Childress. This would suggest that in these areas, the Childress is fractured or missing for it is not effectively serving as a barrier to upward movement of brines.

From a standpoint of suggested drilling locations, SDII has already staked the principal anomalies within each of the six main sites. We would also recommend test drilling in Locations #13 and #14 as it would appear the depth to brine is significantly less in these areas than in the other areas surveyed.

1.0 INTRODUCTION

1.1 Background

The project site is a ranch property in far northwestern Stonewall County, Texas approximately 25 miles northwest of the county seat, Aspermont, Texas (Figure 1). The County of Stonewall ("County"), in cooperation with the Texas Brazos River Authority (BRA) and with grant support from Texas Water Development Board (TWDB), is currently evaluating concepts for reducing/eliminating salt pollution of surficial creeks and rivers in the area. This surface water drainage ultimately contributes to the high salinity of the Salt Fork of the Brazos River – a principal drainage system for this part of Texas. The simplified model of the salt pollution system for this area includes a) a brine reservoir situated at depth and b) a system of vertical fractures, which act as permeable conduits bringing the deep brines up into contact with the surface water drainage. One of the remedial concepts being considered involves drilling of high volume production wells into the reservoir and transporting the produced water to a proposed desalination plant.

1.2 Purpose

The best potential locations for such brine production wells would be in areas where there are several such brine-filled fracture conduits and where the reservoir is known to exist. Traditional methods of locating possible fractures include ground geologic reconnaissance coupled with analysis of photolinear trends. The Dove Creek Area (see Figure 2), however, offers numerous photolinear trends at various orientations across the site. The key analytical factor would be determining which linear features correlate with brine-carrying fractures. With this in mind, there is a two-fold purpose for the geophysical surveying in the Study Area. One objective of this investigation is to perform a combination of Very Low Frequency (VLF) electromagnetics and electromagnetic terrain conductivity (EM34) methods to map the trend and locations of brine-filled fractures. The other objective is to use Time Domain Electromagnetic (TDM or EM47) surveying to help identify the existence, depth and thickness of the brine reservoir across the project site. The combination of the three techniques would be to build a three-dimensional model of the brine reservoir-conduit system at a series of specific locations within the site study area. As shown of Figure 2, there were six primary survey areas (Area A through Area F) within the overall study area. These six areas were defined by Bob Rodgers of RWR Associates, Richmond, Texas – the geological consultant to the County. Mr. Rodgers defined these areas based upon his analysis of photolinear trends in the area, the occurrence of springs, and the results of a preliminary drilling program conducted by RWR in 1999.

In addition to these six defined areas, SDII also acquired TDM (only) data at other discrete locations of interest (see Figure 2) defined by RWR.

1.3 Scope of Work

SDII implemented the following scope of work to complete this investigation:

- Mobilize to the project site and perform a combined VLF/EM34 investigation at the six defined site areas specified by RWR personnel (Figure 2);
- Based upon the results of the VLF/EM34 surveys, select locations and acquire TDM (EM47) soundings, as required, at each of the six defined sites
- Acquire TDM survey data at other, secondary sites surrounding the primary study area as also defined by RWR (also Figure 2)
- Demobilize from the site and analyze the total geophysical data set to determine the brine reservoir/conduit system; and
- Prepare a final report that summarizes the geophysical methodologies, field procedures and results of the investigation.

1.4 Site Descriptions

The project site is located along the north side of County Road 350 northwest of Aspermont, Texas in the far NW corner of Stonewall County, Texas (Figure 1) near the common junction of Dickens, King, and Stonewall counties. The study area consists of six, discrete study areas of varying size and shape. Figure 2 shows the locations of the six primary study areas. At the time of the SDII field investigation, the site was covered by grass, brush and mesquite as well as several salt flat areas associated with Dove Creek. The area was prone to flash flooding although only one day of hard rain was encountered during the field program (May 30th through June 8th, 2000). Based on regional geological information, near-surface soils consisted of a sand stratum.

<u>Area A</u>

Area A (Figure 2) is the southernmost of the research sites and is situated on an upland high area above and south of Dove Creek. Because of the narrow area of level ground between steep drop-offs to either side of the access road, the area available for geophysical surveying was quite limited (see Figure 3). The dominant trend in photolinears in this area, as with Areas B and C as follow, is N27°E and N55°W with an EW trend as well. The orientation and location of geophysical survey lines and TDM loops as shown on Figure 3 were dictated by access and topography, primarily, and by the trends of photolinear features as well as could be accommodated.

Area B

Area B is the topographically lowest of the six site areas and is also located towards the southern end of the study area. It is a rectangular area (see Figure 4) that is, approximately, 1000 ft by 800 ft with the long axis oriented along the (magnetic) N45°E direction. Area B includes an extensive crossing of Dove Creek, which had only minimal water but had damp surficial sediments. Outside of the creek bed area, this site had substantial vegetation but was relatively flat except for a few side channel drainages into Dove Creek. Because of the through-going road at a N45°E (magnetic) bearing, the grid of data lines (Figure 4) was laid out with this orientation. In addition to the creek bed, this site is also considered an important site because it is the location of an old well (also on Figure 4) that, when drilled, encountered artesian flow of briny water before being plugged and abandoned (Bob Rodgers, personal communication). Photolinear alignments in this area show several strong orientations including (approximately) N35-40°E, N55°W (Dove Creek), and nearly EW.

Area C

Area C is an irregular, almost triangular shaped area along the upland slope above (north of) Dove Creek. Because of vegetation and steep topography, access was limited to a couple of roadways flanking the area and part of the area between the roadways as shown on Figure 5. Area C was selected because a) there is a spring along Dove Creek almost due east of the Area and b) the spring is along a linear segment (N80°E) of Dove Creek. This linear feature projects back to the west through Area C. We should also note that the spring is actually at the intersection of two linear features: the one just mentioned plus another (N27°E) that actually projects back towards Area A to the South. The geophysical survey lines (Figure 5) were limited to any areas that were accessible within the area as dictated by topography and density of vegetation.

Area D

Area D is the largest (1000 ft by 1000 ft, or 25 acres) area surveyed. It was also an area of high surface elevation and contained what appear to be the beginnings of sinkholes on its western boundary (see Figure 6). There were three apparent photolinear directions crossing this area. These were (approximately) nearly NS, N55°W, and N35°E. Vegetation ranged from dense in the lower portions of the area to fairly open grassy areas in the higher areas. Because of the size of the area, four adjacent TDM soundings were conducted across the area (Figure 6).

Area E

Area E lies on the western trend of a large, straight gully/drainage that trends N97°W from the east into Area E (see Figure 2). A single line and TDM loop (Figure 7) were run along the existing road across this photolinear trend to see if it was coincident with any possible fracturing. This area, like Areas D and F, are at some of the higher elevations in this study.

Area F

Area F is the northern-most and the topographically highest of the six areas of investigation. The surveyed area is, approximately, a 500 ft by 500 ft (Magnetic North by Magnetic East) rectangle that includes a large, water-filled stock tank and a large, collapsed sinkhole structure. The lines for the EM34 and VLF surveys plus the single TDM loop location are shown on Figure 8. These lines were oriented along magnetic north and east directions. The west and southwest portions of the survey area had dense vegetation. The only inaccessible portions of the site were the pond, the sinkhole, and a drainage leading into the sinkhole from the north. The general trends of photolinears in this area were approximately NS and the sinkhole itself exhibits an elongation in the EW direction. Spelunkers report the cave area extends in a somewhat EW orientation as well. The orientation of the geophysical survey lines was selected to be perpendicular to these trends.

2.0 METHODOLOGIES

2.1 VLF Equipment and Principles

VLF stands for the Very Low Frequency electromagnetic surveying method. The *very low* aspect of the VLF method is derived from the method's use of military radio transmission signals in the 15-30 kiloHertz (kHz) band to probe the subsurface. The VLF was first developed for mineral prospecting as it is particularly sensitive to vertical, highly (electrically) conductive bodies such as ore veins. Because water-filled fractures satisfy many of the same descriptive features as an ore vein (electrically conductive fluid contained within a more resistive rock background), the VLF method has found increasing application to fracture characterization programs.

The basis of the VLF method is the precise analysis of the behavior of radio waves as they travel across a site. Global military agencies have set up powerful radio transmitters in the VLF frequency range at locations around the world – primarily for communications with submarines. These radio waves, as they spread out from the transmitter area, form planar electromagnetic waves that interact with the subsurface geology along their pathways. In crossing a site, if the radio waves encounter a body having increased electrical conductivity (e.g. a brine-filled fracture), the wave causes small currents to flow in that body. These induced currents create their own small magnetic fields, which tend to oppose the magnetic fields of the radio wave and, therefore, interact and interfere with the "normal" radio wave characteristics. In essence, this interaction with a buried conductor causes the measured composite (normal plus interaction with body) to show tilt (i.e. a horizontal as well as a vertical field component) whereas the normal radio wave has only a horizontal magnetic component. The effect of a body then is to create a non-zero reading on the instrument. After data manipulation and filtering, the VLF anomaly over a conductive fracture can be made to look quite simple – a peak value over the fracture (see Figure 9, for example). The strength of the anomaly depends on many factors including the contrast in conductivity between the fluid and the rock, the size of the fracture, and the angle between the strike of the fracture and the direction from the site to the transmitter. Regarding the latter point, the anomaly is maximized if this angle is zero (i.e. the fracture is pointing directly at the station). Since we cannot choose the strike of the fracture it would seem that only some fractures, of a specific orientation, could be mapped. This dilemma is resolved by the fact that there are numerous stations around the world so that by picking among the several stations available, a wide spectrum of fracture azimuths may be mapped using VLF.

2.2 VLF Field Procedures

SDII used the ABEM Instruments "Wadi" VLF unit. This is a compact system composed of an antenna system to measure the radio signal characteristics and a console unit. The console allows the user to select the most appropriate VLF transmitter for the site and line orientations, to collect the data, and to display the results in real time on a hand-held computer screen. The data are stored digitally for further display and analysis.

The VLF investigation was performed over the time period May 31 - June 4, 2000. VLF data were acquired over the sets of transect lines shown for each of the six areas (see Figures 3 – 8). For each line, the following procedure was followed.

1 Stand at start of line facing in the direction of the line
2 Use the instrument's automatic scan feature to determine which of the many VLF stations provides the proper signal strength and direction to the station for the particular line orientation
3 Using that particular station, acquire VLF data at 20-ft intervals until the end of the line is reached
4 Move to next line and repeat procedure

2.3 EM34 Equipment and Principles

The EM34 Terrain Conductivity Meter (EM34) is an active geophysical technique for measuring the *in situ* electrical conductivity of the subsurface. By an "active" technique we mean that we use a controlled source to inject electromagnetic waves into the ground and then record how the earth responds to our source. Electrical conductivity is a physical property of soils, rock, and any material that determines how well that material will support the conduction of electrical currents. As such, materials such as dry quartz sands would have very low electrical conductivity, clays would have higher conductivity values, and saline groundwater would have very high conductivity. Generally, electrical conductivity of an earth material will increase with increases of porosity, clay content, saturation, and specific conductance of the saturant. The units of electrical conductivity are milli-Siemens per meter (mS/m) in SI units.

The EM34 accomplishes this measurement of the bulk ground electrical conductivity using a pair of wound wire coils (see Figure 9). One coil, the transmitter coil, is fed an alternating electrical current. This current in a loop of wire creates an alternating magnetic field ("primary field") whose dipole direction is perpendicular to the plane of the coil just like an electromagnet or old-fashioned doorbell. The alternating magnetic field then interacts with the subsurface materials. If those materials have some electrical conductivity, then the alternating magnetic field causes small eddy currents to flow in the ground materials, much like a car's alternator creates electrical current by spinning a magnet near a conductor (copper wire coil). Finally, those small currents flowing in the ground cause their own weak magnetic field ("secondary field"), which is slightly out of phase with the primary field and is detected by a second wound coil ("receiver coil"). The component of the secondary field that is 90° out of phase ("quadrature phase") with the primary field has been shown to be directly proportional to the conductivity of the ground materials. Making this measurement of the quadrature phase is how the EM34 system measures ground conductivity. The depth of penetration for any electromagnetic conductivity system depends upon, among other factors, the distance between the transmitter and receiver coils as well as the orientation of the coils (vertical dipole or horizontal dipole – see Figure 9). Generally, the farther the two coils are separated, the deeper the system "sees". The vertical dipole (i.e. coils laying flat on the ground) mode sees deeper (approximately 1.5 times the coils spacing) than the upright coils, horizontal dipole mode (0.75 times the coil separation).

2.4 EM34 Field Procedures

SDII used the EM34 system manufactured by Geonics Ltd., which offers multiple (10 m, 20 m, or 40 m) coil separations. We utilized, primarily, the 20-m coil separation and measured in both the vertical as well as horizontal dipole modes, yielding an effective depth of investigation from 15 – 30 meters (50 – 100 ft). Data stations were spaced at 20-ft intervals along each of the EM34 transect lines for each of the six primary study areas (see Figures 3-8).

The EM34 investigation was also performed over the time period May 31 – June 4, 2000.

2.5 TDM (EM47) Equipment and Principles

The EM47 Protem Time Domain Electromagnetic (TDM) Sounding system is another active geophysical technique for measuring the *in situ* electrical conductivity of the subsurface. Unlike the EM34 system, which rapidly assesses *lateral* variations in electrical conductivity (profiling), the EM47 enables interpretation of the *vertical* distribution (depth and thickness) of subsurface layering.

The EM47 accomplishes this measurement of the vertical electrical conductivity using a large transmitter loop and a central, small receiver loop (see Figure 10). The large loop or transmitter coil, is fed an alternating square wave of electrical current (see Figure 12). At the moment of current shut-off, a large magnetic field transient is generated and sent downwards into the ground. This field moves downward and outward from the loop interacting with deeper layers as time progresses. The interaction with the subsurface layers causes secondary magnetic fields to be generated. The receiver coil (see Figure 11) detects these secondary fields. By monitoring the receiver coil voltage as a function of time after current shut-off, we are able to determine resistivity (or conductivity) versus depth.

2.6 TDM (EM47) Field Procedures

SDII used the EM47 system manufactured by Geonics Ltd., which controls the current to the transmitter loop (nominally 200-250 ft on a side) and records the output from the receiver coil. The receiver coil output versus time after current shut off is digitally sampled and stored in the EM47 unit. The digital files are then converted to resistivity versus depth soundings by using a specialized computer program (TEMIX ™ by Interpex, Ltd.).

The number of soundings made at a given area was determined by a) the size of the area and b) accessibility/topography of the area. Most of the six primary site areas had only a single loop location. Two areas (Area B and Area D) had two or more soundings (see figures 3-8 for location of TDM transmitter loops). In addition to the six primary areas, SDII also acquired TDM soundings at an additional 10 sites surrounding the area (see Figure 2). Bob Rodgers of RWR determined these locations.

The TDM soundings were conducted over the time period June 5 – 8, 2000.

3.0 RESULTS

3.1 Fracture Characterization

The process of detecting potential brine water filled fractures in each of the six designated areas was accomplished using the complementary interpretation of VLF, EM34, and photolineament data sets. From a geophysical perspective, a brine-filled, nearly vertical fracture of limited width (opening) should present the following anomalous observations on the VLF and EM34 data sets. For a linear fracture which is trending perpendicular to the orientation of the geophysical transect line (or nearly so), we would expect to see the following anomalies:

- On the VLF profile, we would expect to see a localized positive peak directly over the fracture
- On the EM34 profile, we would expect to see a localized increase in ground conductivity if the fracture zone is wide (tens of feet wide)
- However, on the EM34 profile, we could also expect to see a very complex response including a localized increase in conductivity on the horizontal dipole measurement coupled with a decrease or even negative conductivity on the vertical dipole when over the fracture. This complex signature is what is often seen, for example, when an EM34 survey is conducted perpendicular to a steel pipeline – another excellent linear conductor.

The actual nature of the response predicted would be a function of several factors including the angular strike between the line and the fracture, the salinity of contained waters within the fracture, if any, and the width of the fracture/fracture zone. In the following area results descriptions, we will focus on the geophysical response and implications on fracturing. We shall also, whenever possible, try to correlate anomalous responses from one geophysical line to the other in order to interpret fracture azimuths crossing the areas. Note that in the description of results from each of the six designated areas, we shall provide illustrative examples of the VLF and EM34 data that are typical for that area. *All* plots of EM34 (horizontal as well as vertical dipole, when measured) data profiles are attached to this report in Appendix A. *All* plots of filtered VLF data are also attached to this report in Appendix B.

3.1.1 Area A. Figure 12 displays an example of the VLF data acquired along one of the lines in Area A. On the figure, we note a narrow segment of the line where the filtered VLF data show a localized, positive peak. The magnitude of this peak is very small. That is, the VLF indicates a possible fracture, but the size of the anomaly is quite low indicating the depth to the brine-filled part of the fracture is large or the fracture plane itself is only slightly conductive. We compare these data with the EM34 data taken along the same transect (Figure 12). Over essentially the same line distance interval (340 ft – 420 ft marks), the EM34 shows a localized increase in the conductivity seen by the horizontal dipole data with a corresponding decrease in conductivity seen by the vertical dipole. This behavior, is consistent with EM34 data taken perpendicular to (or nearly so) a linear electrically conductive body. We would interpret this anomaly (coincident VLF and EM34 anomalies) as indicating a brine-filled fracture. The VLF data may be used to estimate a depth to the top of the brine-filled portion of the fracture. The VLF analysis for this feature suggests a depth to the conductor of approximately 30-50 ft depth.

Figure 13 is a re-plot of the geophysical lines for Area A (same base map as Figure 3) showing the locations of the VLF positive peak anomalies and the anomalous EM34 segments noted along each line. Because of similar character and shape of the anomalies seen on the series of transect lines acquired, we have linked up those anomalies that we feel represent the same subsurface fracture (correlation between lines). These correlations are also shown on Figure 13. The trend of fracturing in Area A is interpreted to have a N80°E bearing, which is close to some of the large EW photolinear trends in canyons to the South. Some anomalies, however, were not seen on multiple lines, so these are noted as only anomalous areas. Those areas exhibiting both a VLF as well as an EM34 anomaly are those we consider having the higher probability of being a fracture.

Also noted on Figure 13 are the locations of 4 wooden stakes that we annotated and drove into the ground within the major anomalies.

3.1.2 Area B. Figure 14 is a similar plot of the general characteristics of the VLF/EM34 data from Area B as compared with Area A (see Figure 12). Because Area B includes Dove Creek and its flood plain, there are segments within Area B where extremely high conductivity fluids are right at the ground surface while the more upland areas of Area B look more like Area A, but still exhibit conductivities that are much higher. This is shown dramatically by the behavior of the EM34 data crossing Dove Creek (Figure 14). Within the creek bed, the horizontal dipole (very shallow) data show a significant increase in conductivity while the vertical dipole (deeper) goes to extreme negative conductivity values. We have also observed this exact behavior when acquiring EM34 data over seawater bodies. The surficial brines basically cause the vertical dipole data to go negative conductivity values – a physical impossibility! This also points out how significant drops in localized vertical dipole conductivity can be indicative of a brine filled fracture. Figure 14 also shows (circled) a small area in the upland part of this transect where a more normal fracture indication is seen. This small feature is overwhelmed by the magnitude of the anomaly caused by the creek. Note that the VLF over this same line is better behaved and continues to show singular peaks that we interpret as potential fractures. We must caution that, for the orientation of this line, the VLF data were a bit on the unstable side (weak station), so the amplitudes of the anomalies are not accurate. A second transect (Figure 15) is wholly within the upland area (i.e. does not go into the creek bottom). Its shows distinct VLF and EM34 anomalies, which we were able to correlate with a parallel line to the north. The trend of the geophysical anomalies overlies a surface depression that RWR interprets as a potential sinkhole in early stages of development. This also lends confidence to the correlations we are making from one line to the next. Finally, Figure 16 is the aerial map of Area B with the superposed locations of the VLF and EM34 anomalies and our interpretation of fracture trends. The dominant fracture trend we interpret is N29°E – very close to the trend of the photolinears associated with the major offsets of Dove Creek. Because of the major geophysical response of Dove Creek itself, we must also consider the Creek itself (locally, N53°W) as possibly being fracture controlled. Analysis of the VLF data suggests a broad depth range to the brine in the fractures of approximately 30-ft.

Also noted on Figure 15 are the locations of 6 wooden stakes that we annotated and drove into the ground within the major anomalies.

3.1.3 <u>Area C.</u> Figure 17 is a sample plot of the VLF and EM34 data for Area C. We first note from the values of the conductivity profile that this area has typical conductivity values (e.g. similar to Area A but much less than Area B) for normal soils and not soils having brine contamination. We also note the same combination of peaked VLF response and downward trends in the Vertical Dipole conductivity data in two locations that we interpret as potential brine filled fractures. Figure 18 is the aerial map of Area C with the superposed locations of the VLF and EM34 anomalies and our interpretation of fracture trends. The dominant fracture trend we interpret is N10°W. This trend is close to some of the photolinear trends of minor drainage immediately south of Area C and some of the major drainages (e.g. Haystack Canyon) to the East. There is a possible secondary trend of N67°E, but more lines would be needed to verify this trend. Analysis of the VLF data suggests a broad depth to brine within the fractures of approximately 45-ft.

Also noted on Figure 18 are the locations of 7 wooden stakes that we annotated and drove into the ground within the major anomalies.

3.1.4 <u>Area D.</u> Figure 19 is a sample plot of the VLF and EM34 data for Area D. We first note from the values of the conductivity profile that this area has typical conductivity values (e.g. similar to Areas A and C but much less than Area B) for normal soils and not soils having brine contamination. However, throughout Area D, the values of measured conductivity are very uniform. That is the conductivity value is about 20 mS/m ± 5 mS/m (at most a 20% variation). The combination of peaked VLF response and downwards trends in the Vertical Dipole conductivity data is very subdued as shown by the circled, questioned anomaly on the right end of the example profile. If there are fractures in the area, and if they have brine water fill, then the depth to the brine must be very deep to explain the uniform conductivity and the subdued VLF response. Figure 20 is the aerial map of Area D with the superposed locations of the weak VLF and EM34 anomalies and our equally weak interpretation of fracture trends. The dominant fracture trend we interpret is N50-55°E. This is similar in trend to some minor photolinear trends in the area.

3.1.5 <u>Area E.</u> Figure 21 is a presentation of the full VLF and EM34 data set taken on the one transect line of Area E. The line was laid out to be perpendicular to the photolinear trend of the large, EW trending canyon to the East, so fracturing associated with that feature, if existing, would be towards the middle of this transect. We see that the behavior of the geophysical data for Area E is very much like the behavior at Area D (see Figure 19). That is, the data are very uniform with little in the way of anomalous character. As with Area D, we feel that if there is fracturing crossing the area, then the depth to the brine within the fractures is to deep to have any great effect on the recorded geophysical data. We cannot, therefore, detect any fracturing potential within Area E although such fracturing may indeed exist. We did not place any stakes within this area.

3.1.6 <u>Area F.</u> Figure 22 is an example of the VLF/EM34 data typical of Area F. Even though this area is of similar ground surface elevation as Areas D and E, we see significantly more anomalous character to the geophysical data from Area F than in the data from those two areas. Specifically, on Figure 22 we see two anomalous areas where there is a peaked VLF response coupled with an anomalous drop in the vertical dipole conductivity with a rise in the horizontal dipole conductivity. We interpret this combined response as due to fracturing. Given the Area contains a large dissolution feature (sinkhole) that breaches the surface, it is highly probable that this area would be fractured. Figure 23 is the aerial map of Area F with the superposed locations of the VLF and EM34 anomalies and our interpretation of fracture trends. One of two alternative fracture trends we interpret is N65-70°W. This trend was chosen by requiring the major anomalies to correlate with the location of the sinkhole. That is, the sinkhole would be located on a large fracture so the major anomalies should link up through the sink position. Also, spelunkers have indicated a more EW trend to the underground cave. However, there are few strong photolinears in the immediate area having this same trend.

The second alternative trend shown on Figure 23 is N10-20°W. This trend was interpreted by tying together those anomalies that have the most similar looking character. This trend is also close to the same trend as some of the major drainages just to the east as well as south of Area F. Therefore, we have two alternative interpretations of fracture azimuth for Area F. A more important observation, however, is that even though Area F is at an even higher elevation than Areas D and E, it shows indications of shallower depths to brine within the fractures. Perhaps the fractures in Area F are more open (permeable) allowing brine to come higher in elevation along them than in areas D and E. Analysis of the VLF data suggests a broad depth to the brine in the fractures of approximately 50-60 ft.

Also noted on Figure 23 are the locations of 2 wooden stakes that we annotated and drove into the ground within the major anomalies.

3.2 TDM Sounding Results

The time domain (EM47) soundings collected at the 20 locations described, for the most part, have a common interpretation. That is, almost all the TDM sites show a basically three-layered (electrical resistivity) subsurface model. Figure 24 is the illustration of a reduced (apparent resistivity versus time) TDM sounding curve and the inversion, or resistivity-versus-depth model that provides the best fit to the observed data. The typical model results consists of:

- A surficial layer (typically less than 30 ft thick) of reasonably high (50-100 ohm-meters, Ω-m) electrical resistivity.
- An intermediate layer beneath the surface layer (variable thickness) of reduced (approximately 20-30 Ω-m), which could correlate with the water table or a layer with increased clay content
- A deeper, bottom layer where the electrical resistivity drops to extremely low (0.5-1 Ω-m) values. We interpret this as the level of the brine reservoir. The mobile ions of the brine cause the observed, extremely low electrical resistivity.

The variation in thickness and/or the absence of some of these layers are what provide insight into the hydrogeology of the brine reservoir.

Note on the model of Figure 24 that the depth model has also provided several alternative interpretations ("equivalence models") which would yield almost as good a fit as the best model. The amount of scatter of these dashed line models around the best model indicates how good that best model is. Typically, the best (tightest cluster of alternative values) results are for the depth to and resistivity value of the interpreted brine layer. *All* TDM soundings and inversion results are presented in Appendix C attached to this report.

Table 1 presents a basic summary of the results of TDM sounding for all twenty locations taken across the Site area. In it we present, for each location, a) the approximate ground level elevation for the location (from USGS Topographic Map), b) the estimated elevation of the Top of the Childress Formation (confining unit above the brine reservoir) as taken from a map provided by RWR, and c) the estimated depth to saturated brine condition (very low resistivity layer ≈ 1-2 Ω-m) as determined from the TDM analyses.

TDM Location	GL Elev.1 (ft)	Top Childress2 Elev. (ft)	Top Brine3 Elev. (ft)
A	1840	1680	1635
B1	1740	1680	1686
B2	1740	1682	1684
C	1780	1683	1654
D1	1880	1693	1665
D2	1880	1693	1669
D3	1880	1693	1672
D4	1880	1693	1673
E	1870	1685	1644
F	1900	1693	1659
Low Water Crossing	***1660***	***Above Ground***	***1660***
Well 1	1850	1670	1662
#13	***1850***	***1660***	***1747***
#14	***1922***	***1640***	***1828***
#15	***1850***	***1650***	***1678***
#16	1890	1680	1668
#17	1968	1688	1695
#18	1900	1690	1644
#19	1885	1680	1645
#20	1870	1685	1677

1 – from Topo Map   2 - from RWR Map   3 - top of low resistivity layer

In most cases seen on Table 1, the top of the brine layer is situated some 0-46 ft below the Top of the Childress giving an average estimated thickness of the Childress of some 23 ft (assuming the brine is directly below the Childress. The amount of variation seen is attributable to very limited actual data regarding the elevation of the Top of the Childress and normal error in the TDM interpretations. However, specific instances shown in Table 1 show locations where the depth to the brine is less than the depth to the Childress. These locations are highlighted in bold, italicized text. One, the Low Water Crossing location, is in an area where the Childress does not exist or is above ground level at the area of the TDM sounding (past the outcrop position), so this is not surprising. The other three locations highlighted in italics show brine substantially above the Top of the Childress – high enough that the discrepancy may not due to normal error in analysis (e.g.

uncertainty in ground elevation, elevation of Top of Childress, and actual ground position). We feel Location #15 actually does show a reasonably normal situation – that is, there is enough uncertainty in position and known depth to the Childress that the observed height difference of approximately 28 ft (implied brine above the Childress) is still within error bounds. The other two sites – Location #13 and Location #14 – are truly anomalous for two reasons.

- First, the height of the brine (Layer 3) above the estimated Top of Childress is 87 ft and 188 ft, respectively, for these two – too large to be attributed to noise.
- Secondly, the value of the second layer resistivity is much lower (approximately 2 Ω-m) than other sites (average resistivity of Layer 2 = 24 Ω-m).

The only other sites that exhibit such shallow, low resistivities are the Low Water Crossing and Soundings B-1 and B-2, which are essentially in the Creek bottoms (near surface brine saturation). Locations #13 and #14, however, are situated in upland areas, not within the creek beds. Therefore, Locations #13 and #14 are indeed anomalous in that they both show very low resistivity materials (2 Ω-m) within 50-55 ft of the ground surface. This means briny waters, if we consider 2 Ω-m resistivity as being brine saturated sediments, at these two locations are on the order of 150-250 ft higher than the suspected Top of the Childress. That is, we interpret Layer 2 in these two locations as being the top of the brine. If the brine is normally contained by the Childress and is under artesian conditions (as demonstrated by the flowing brine encountered in the abandoned well within Area B), this would mean that the Childress in the areas of Location #13 and Location #14 (southwestern side of the study area) is not serving as a barrier to upward movement of the brines as it does in other areas. The Childress would have to be either missing or highly fractured in this area in order for the brines to be this high in the area.

3.3 Results Summary

The VLF and EM34 data have demonstrated that we can see discrete vertical conductive bodies that we interpret as brine filled fractures at all sites except Areas D and E. At these two areas, we consider the brine level in the fractures to be so deep below ground surface that the geophysical devices do not detect it. In the other areas (A, B, C, and F), we are able to detect areas where brine must be locally closer to the surface (in vertical fractures). We can sometimes correlate the positions of these discrete, high conductivity areas from line-to-line in order to determine apparent fracture azimuth across these areas.

There is no consistent, dominant fracture azimuth that is observed over the entire site. Rather it would seem that, like the multiple azimuths seen in RWR's photolinear analysis, there are several fracture orientations and the orientation preference varies around the site.

The dominant anomaly positions at the six test areas have been staked in the field as potential, recommended drilling locations.

The TDM data analysis has shown that the subsurface resistivity model over majority of the site area may be represented by a three-layered resistivity structure. The uppermost layer is considered to be dry sediments with a typical resistivity of 40-90 (average = 62) Ω-m. This is underlain by a layer (Layer 2) of decreased resistivity (average = 24 Ω-m) that may represent the water table or an increase of clay content at depth. The deepest layer seen (Layer 3) has a very low resistivity (1 Ω-m) and is interpreted as the top of the brine reservoir. We do not see the Childress Formation as a discrete layer because it is probably higher resistivity (more difficult to see with TDM) and may be rather thin as compared with its depth of burial. Except in areas on the river/creek bottoms where saturated brines are seen at ground level, we typically find the top of the brine layer to be at or just below the level of the Top of the Childress formation as taken from structural contours of the Top Childress provided by RWR. The most significant exception to this normal situation is in the SW portion of the study area (Location #13 and Location #14; see Figure 2) where low resistivity brines are interpreted as being in excess of 150 ft above the level of the Childress. This would suggest that in this area, the Childress is fractured or missing for it is not effectively serving as a barrier to upward movement of brines.

From a standpoint of suggested drilling locations, we have already staked the principal anomalies within each of the six sites. We would also recommend drilling in Locations #13 and #14 as it would appear the depth to brine is significantly less in these areas than in the other areas surveyed.

4.0 LIMITATIONS

The geophysical assessment of this site is based on our professional evaluation of the geophysical data gathered and our experience with the properties of ground penetrating radar in the geological setting of the site area. The geophysical evaluation rendered in this report meets the standards of care of our profession. No other warranty or representation, either expressed or implied, is included or intended.

FIGURES

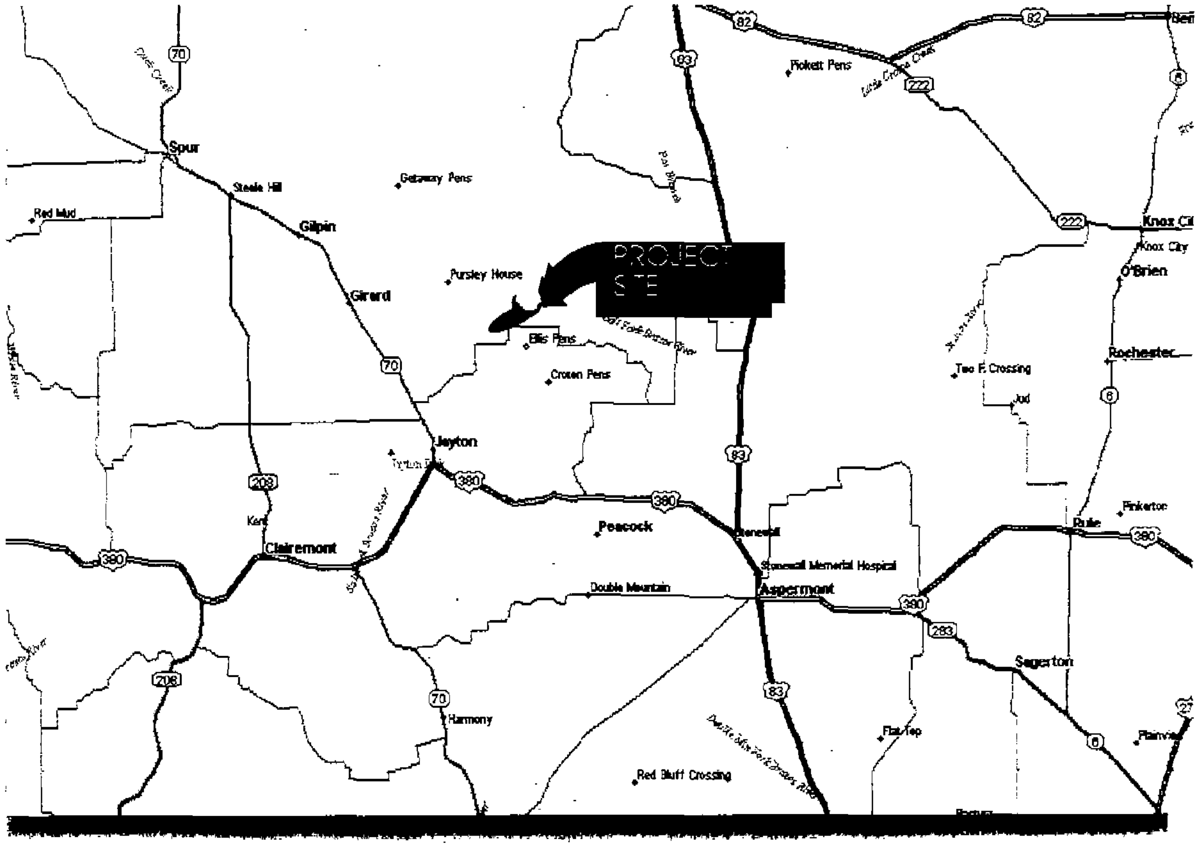

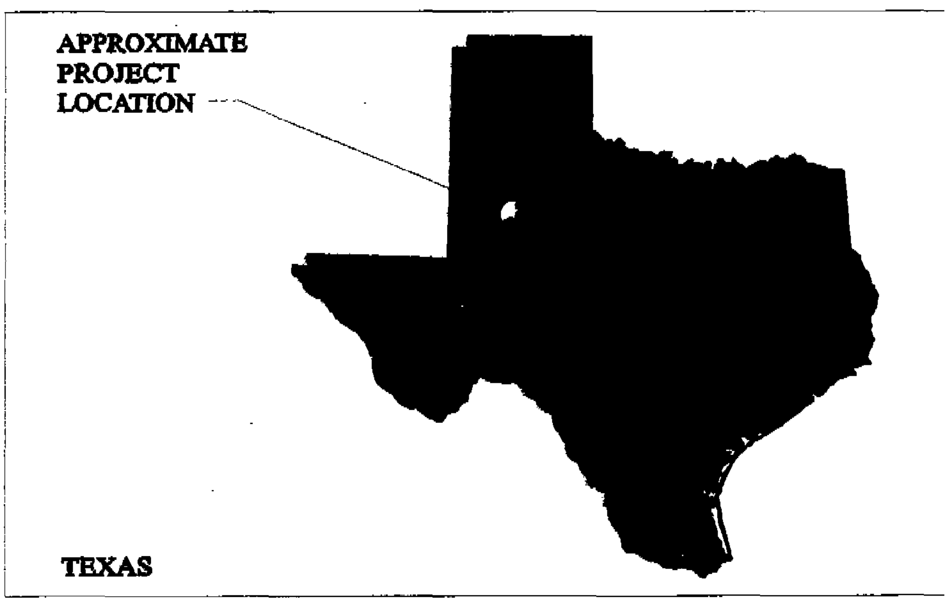

N
NOT TO SCALE

JUDGE'S OFFICE STONEWALL COUNTY, TEXAS	SDII GLOBAL	PROJECT SITE LOCATION MAP SALT POLLUTION STUDY STONEWALL COUNTY, TEXAS	
		DESIGNED BY: TLD CHECKED BY: TLD DRAWN BY: JMW	PROJECT NO.: 1011520 DRAWING NO.: LOC DATE: 07/12/00	FIGURE 1

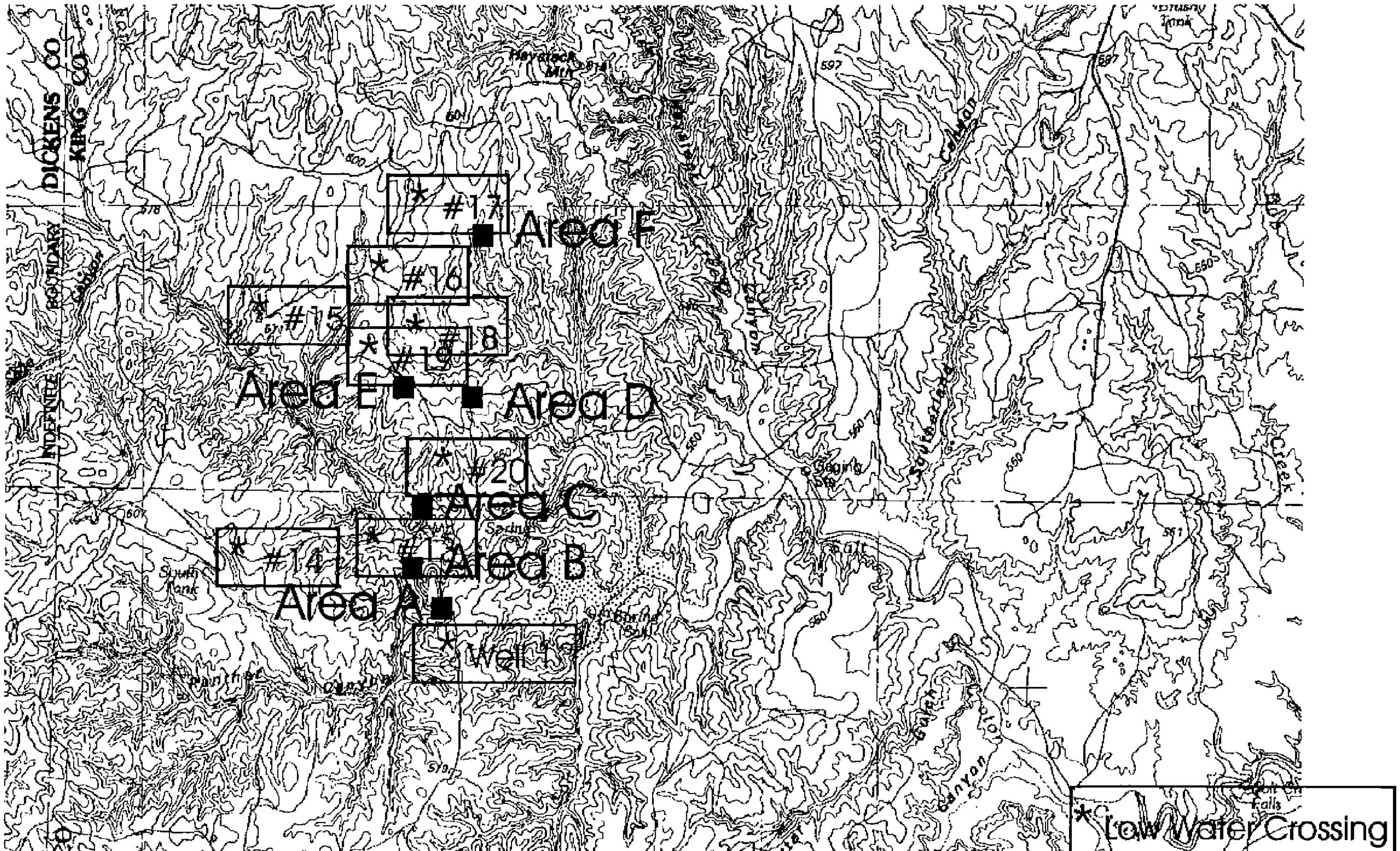

* #16	Location for TDM Sounding
■ Area A	Location for VLF, EM34, and TDM Surveys

JUDGE'S OFFICE STONEWALL COUNTY, TEXAS	SDII GLOBAL	SITE PLAN SHOWING SURVEY AREAS AND DISCRETE TDM SOUNDINGS SALT POLLUTION STUDY STONEWALL COUNTY, TEXAS

DESIGNED BY: TLD	PROJECT NO.: 1011520	FIGURE
CHECKED BY: TLD	DRAWING NO.:	2
DRAWN BY: JMW	DATE: 07/03/00	

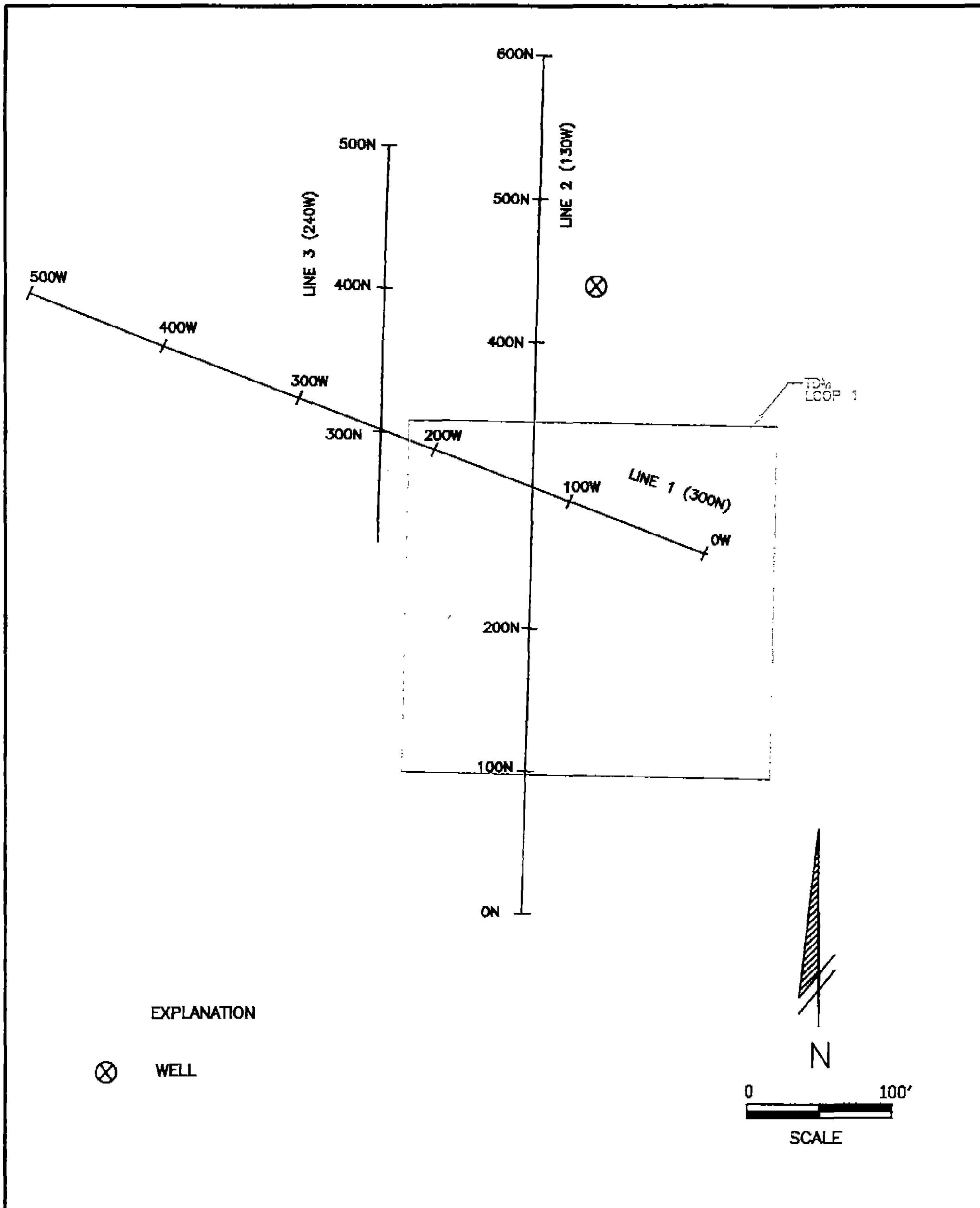

JUDGE'S OFFICE STONEWALL COUNTY, TEXAS	SDII GLOBAL CORPORATION	SITE MAP SHOWING APPROXIMATE LOCATION OF GEOPHYSICAL LINES – AREA A SALT POLLUTION STUDY STONEWALL COUNTY, TEXAS				
		DESIGNED BY:	TLD	PROJECT NO.:	1011520	FIGURE
		CHECKED BY:	TLD	DRAWING NO.:	1520-3	3
		DRAWN BY:	JMW	DATE:	07/12/00	

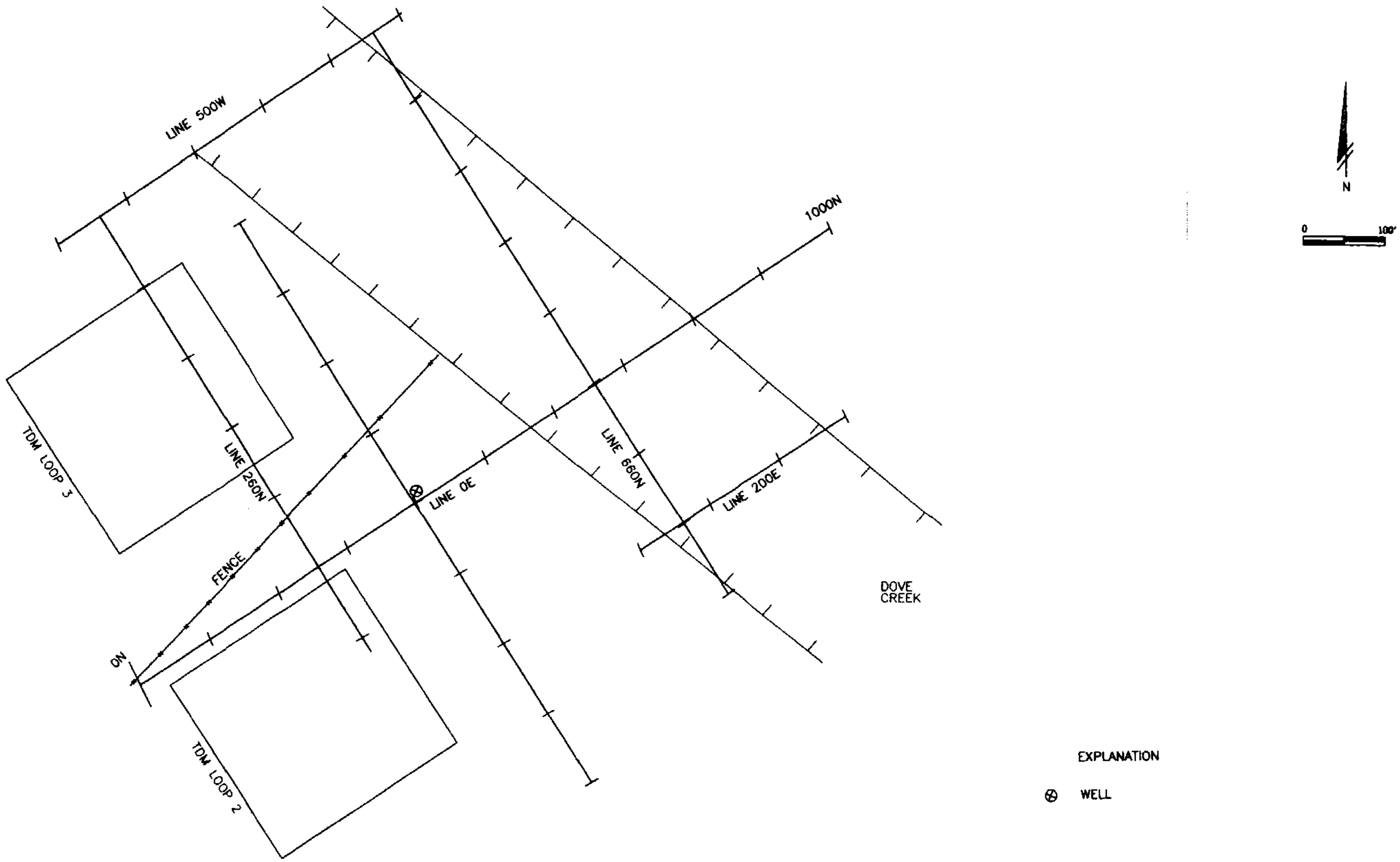

JUDGE'S OFFICE STONEWALL COUNTY, TEXAS	SDII GLOBAL CORPORATION	SITE MAP SHOWING APPROXIMATE LOCATION OF GEOPHYSICAL LINES – AREA B SALT POLLUTION STUDY STONEWALL COUNTY, TEXAS	
		Designed By: TLD Checked By: TLD Drawn By: JMW	Project No: 1011520 Drawing No: 1520–4 Date: 07/12/00
		FIGUR	4

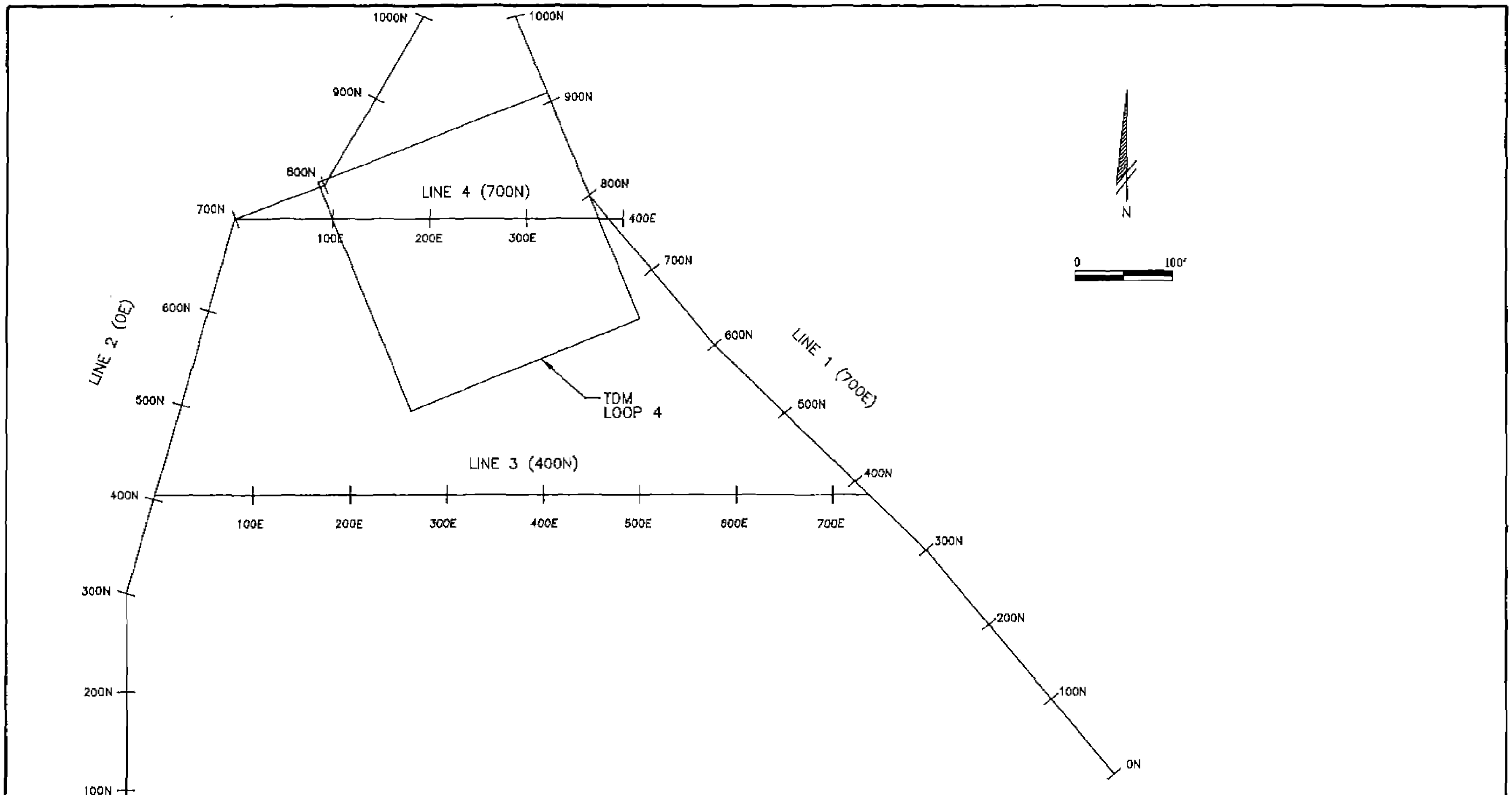

JUDGE'S OFFICE STONEWALL COUNTY, TEXAS	SDII GLOBAL CORPORATION	SITE MAP SHOWING APPROXIMATE LOCATION OF GEOPHYSICAL LINES – AREA C SALT POLLUTION STUDY STONEWALL COUNTY, TEXAS		
		Designed By: TLD Checked By: TLD Drawn By: JMW	Proj. No. 1011520 DWG 1520-5 Date: 07/12/00	FIGURE 5

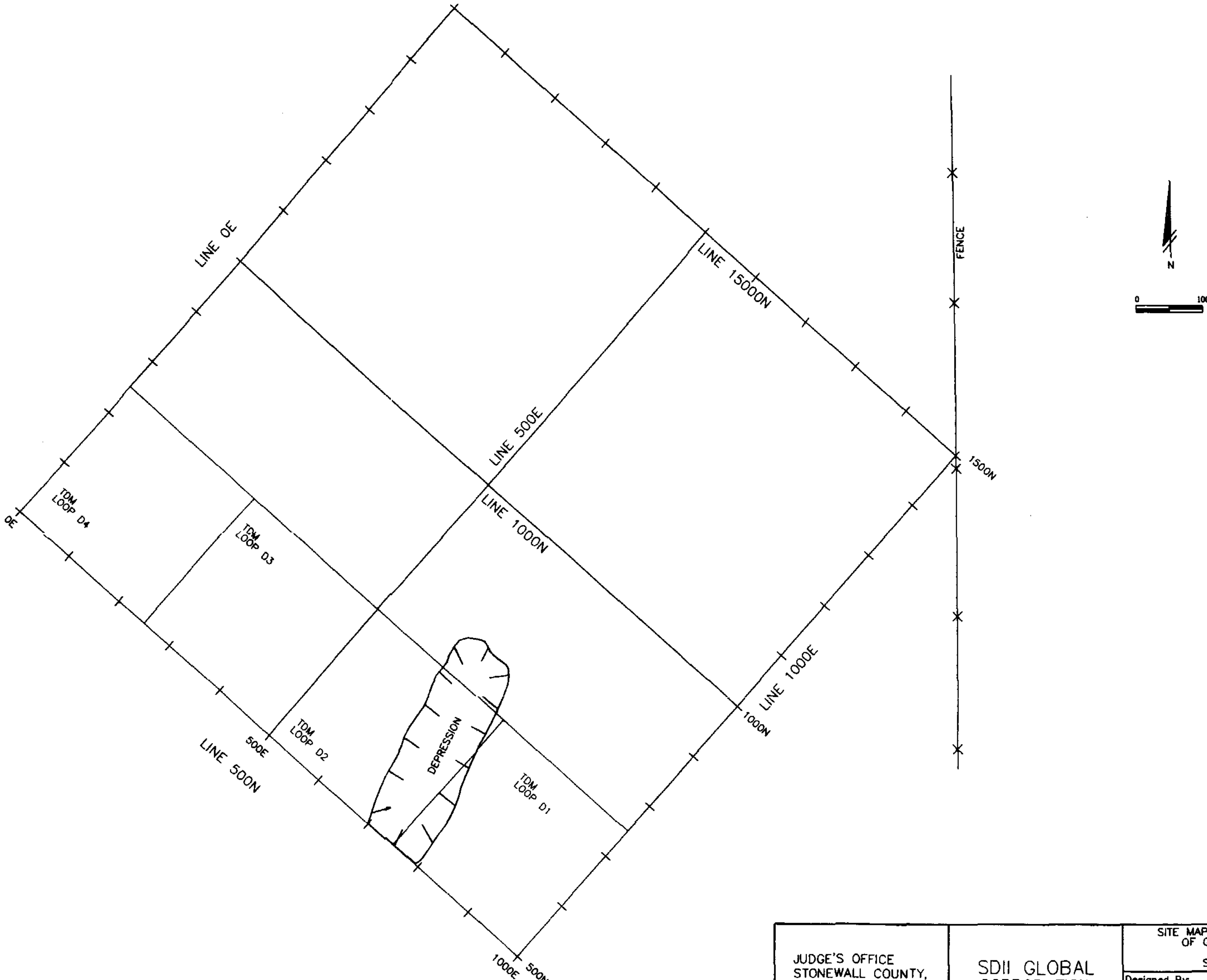

JUDGE'S OFFICE STONEWALL COUNTY, TEXAS	SDII GLOBAL CORPORATION	SITE MAP SHOWING APPROXIMATE LOCATION OF GEOPHYSICAL LINES – AREA D SALT POLLUTION STUDY STONEWALL COUNTY, TEXAS	
		Designed By: TLD Checked By: TLD Drawn By: JMW	Project No: 1011520 Drawing No: 1520-6 Date: 07/12/00

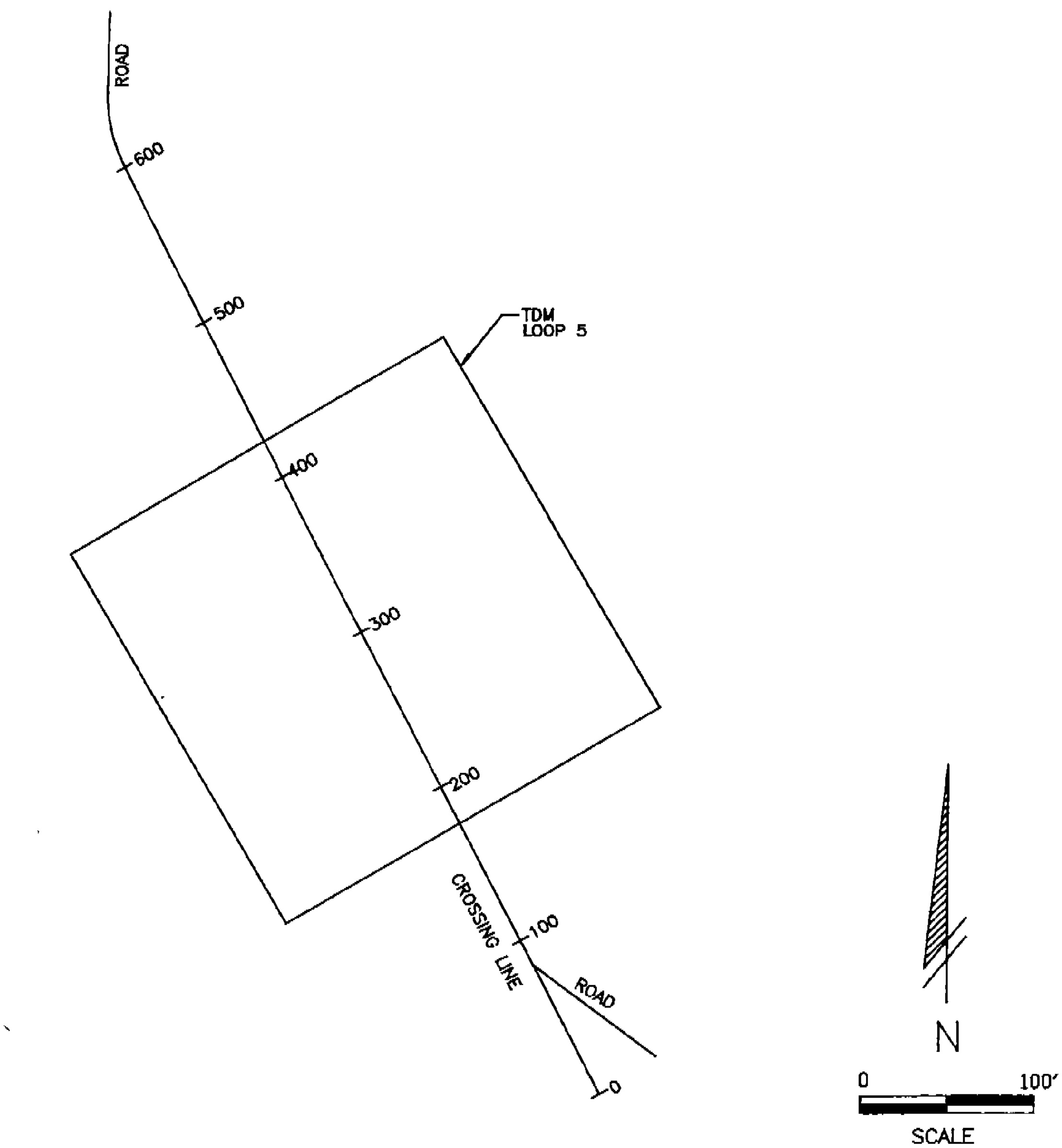

JUDGE'S OFFICE STONEWALL COUNTY, TEXAS	SDII GLOBAL CORPORATION	SITE MAP SHOWING APPROXIMATE LOCATION OF GEOPHYSICAL LINES – AREA E SALT POLLUTION STUDY STONEWALL COUNTY, TEXAS

DESIGNED BY:	TLD	PROJECT NO.:	1011520	FIGURE 7
CHECKED BY:	TLD	DRAWING NO.:	1520–7	
DRAWN BY:	JMW	DATE:	07/12/00	

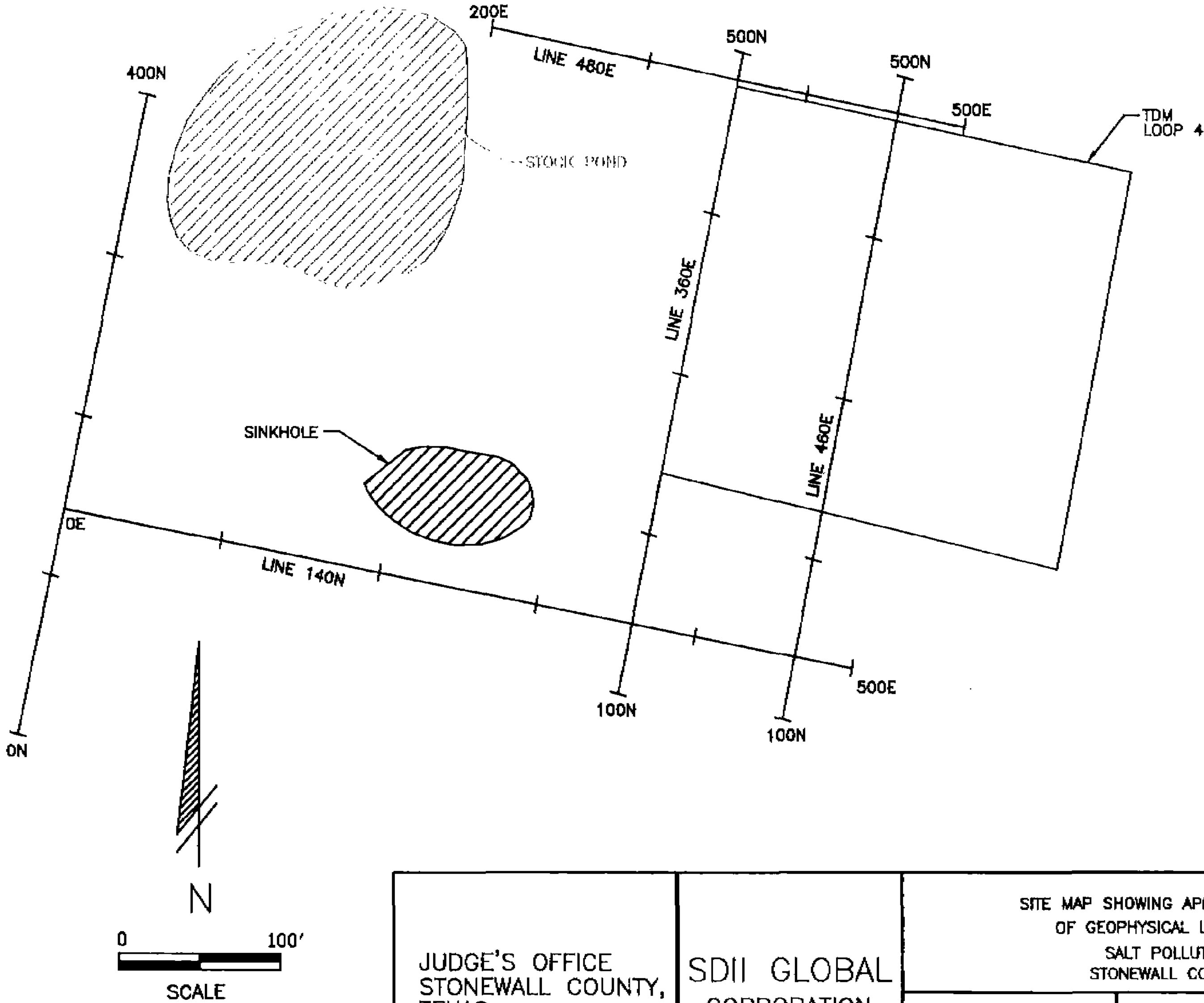

JUDGE'S OFFICE STONEWALL COUNTY, TEXAS	SDII GLOBAL CORPORATION	SITE MAP SHOWING APPROXIMATE LOCATION OF GEOPHYSICAL LINES – AREA F SALT POLLUTION STUDY STONEWALL COUNTY, TEXAS	
		DESIGNED BY: TLD CHECKED BY: TLD DRAWN BY: JMW	PROJECT NO.: 1011520 DRAWING NO.: 1520–8 DATE: 07/12/00
			FIGURE 8

Vertical, Parallel Coils = Horizontal Dipole Mode

Horizontal, Parallel Coils = Vertical Dipole Mode

JUDGE'S OFFICE
STONEWALL COUNTY, TEXAS

FIELD SETUP FOR EM34 CONDUCTIVITY SURVEY
SALT POLLUTION STUDY
STONEWALL COUNTY, TEXAS

DESIGNED BY:	TLD	PROJECT NO.: 1011520		FIGURE
CHECKED BY:	TLD	DRAWING NO.:		9
DRAWN BY:	JMW	DATE:	06/18/00	

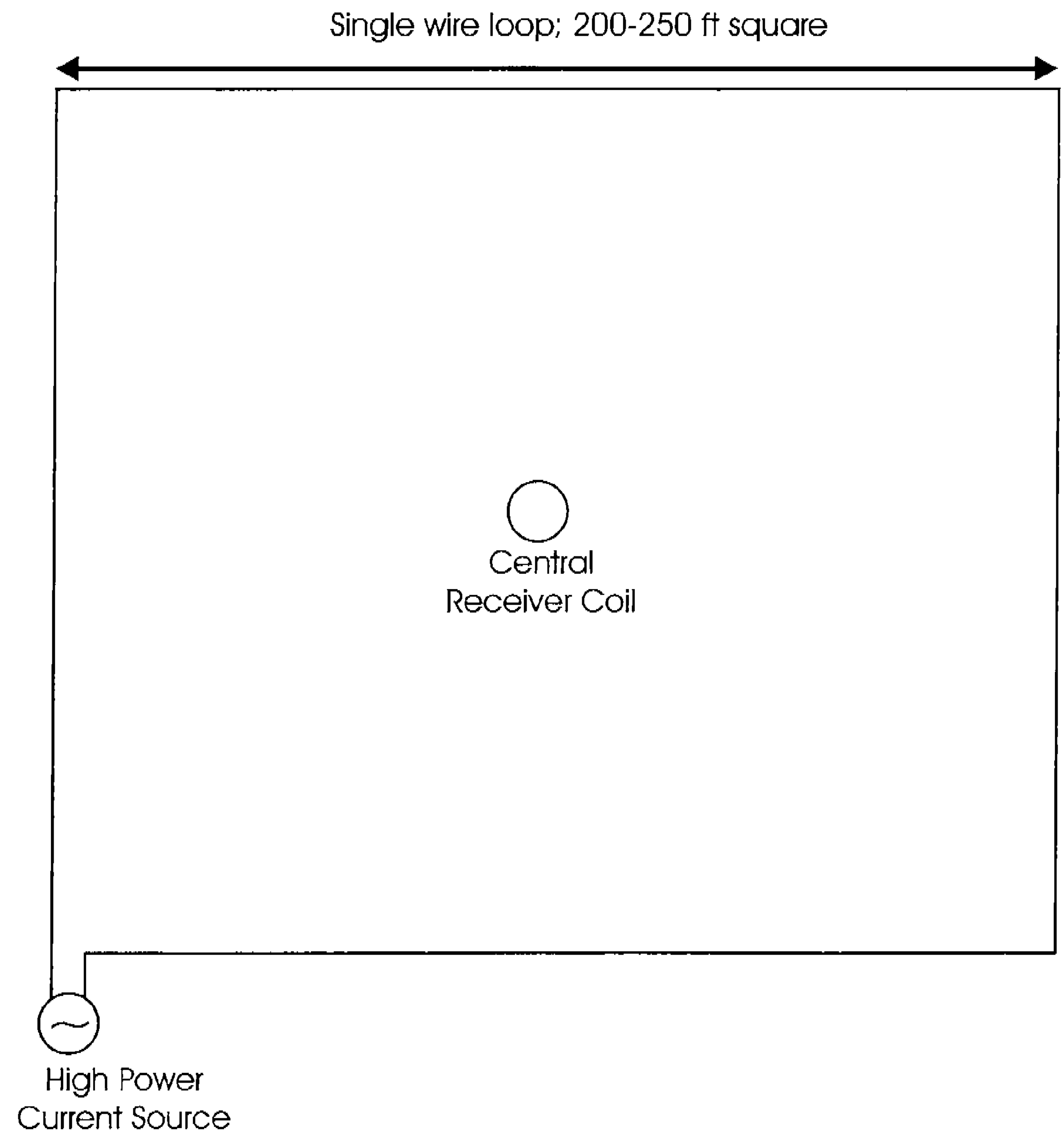

PLAN VIEW

JUDGE'S OFFICE STONEWALL COUNTY, TEXAS	SDII GLOBAL	FIELD SETUP FOR TIME DOMAIN EM SOUNDING SALT POLLUTION STUDY STONEWALL COUNTY, TEXAS		
		DESIGNED BY: TLD CHECKED BY: TLD DRAWN BY: JMW	PROJECT NO.: 1011520 DRAWING NO.: DATE: 06/18/00	FIGURE 10

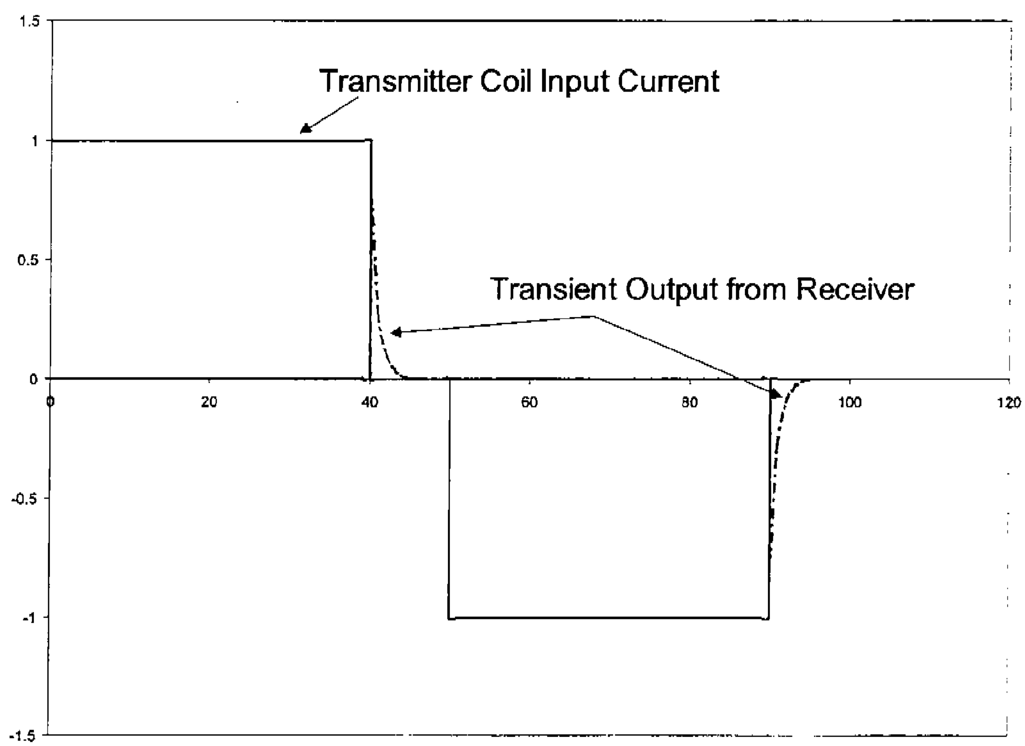

JUDGE'S OFFICE STONEWALL COUNTY, TEXAS	SDII GLOBAL	EXAMPLE CURRENT/VOLTAGE WAVEFORMS FOR TDM SURVEY SALT POLLUTION STUDY STONEWALL COUNTY, TEXAS	
		DESIGNED BY: CT CHECKED BY: TLD DRAWN BY: JMW	PROJECT NO.: 1011520 DRAWING NO.: DATE: 07/03/00
			FIGURE 11

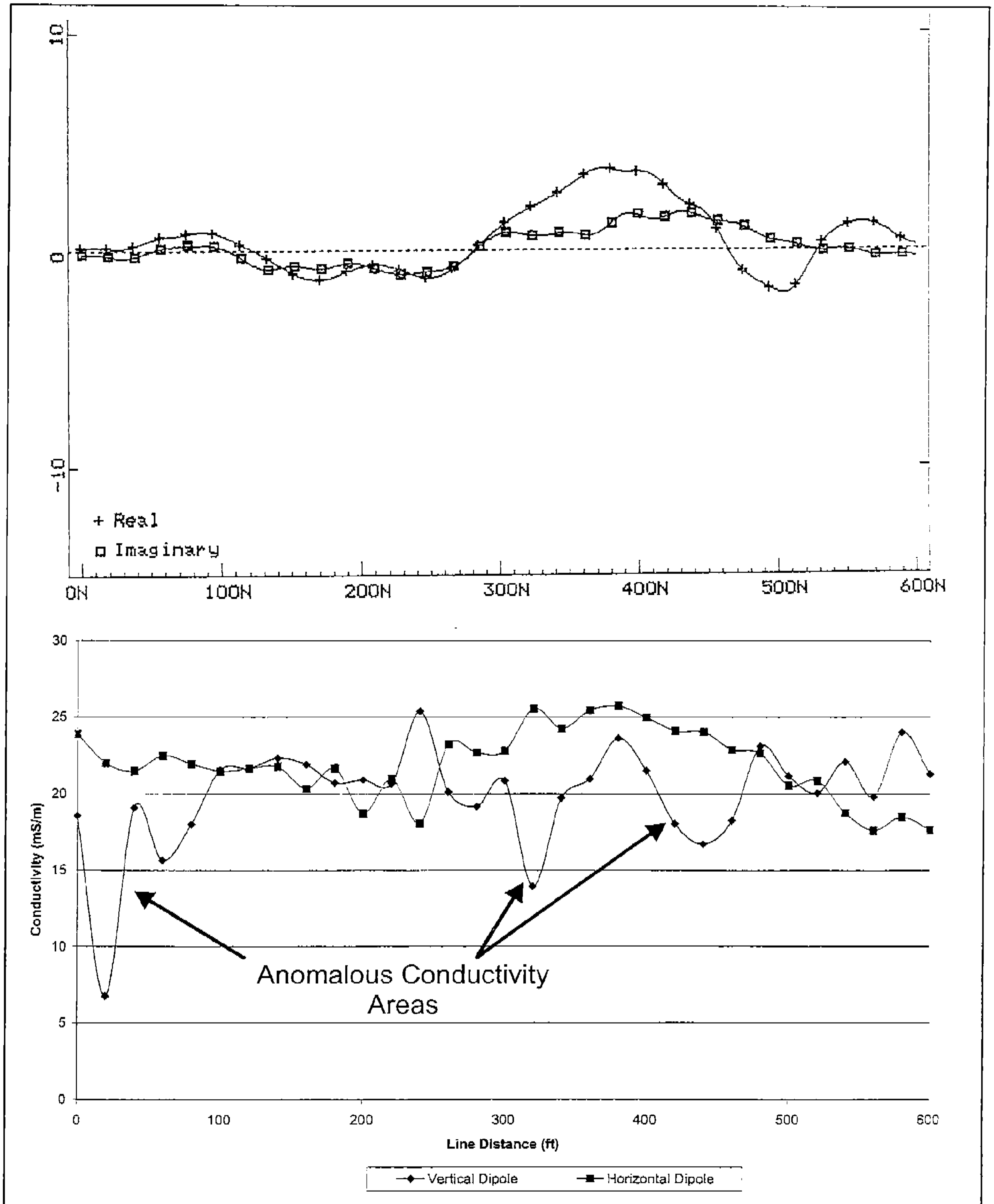

JUDGE'S OFFICE STONEWALL COUNTY, TEXAS	SDII GLOBAL	EXAMPLE OF VLF (UPPER) AND EM34 (LOWER) DATA TRANSECT - AREA A SALT POLUTION STUDY STONEWALL COUNTY, TEXAS		
		DESIGNED BY: CT CHECKED BY: TLD DRAWN BY: JMW	PROJECT NO.: 1011520 DRAWING NO.: DATE: 07/10/00	FIGURE 12

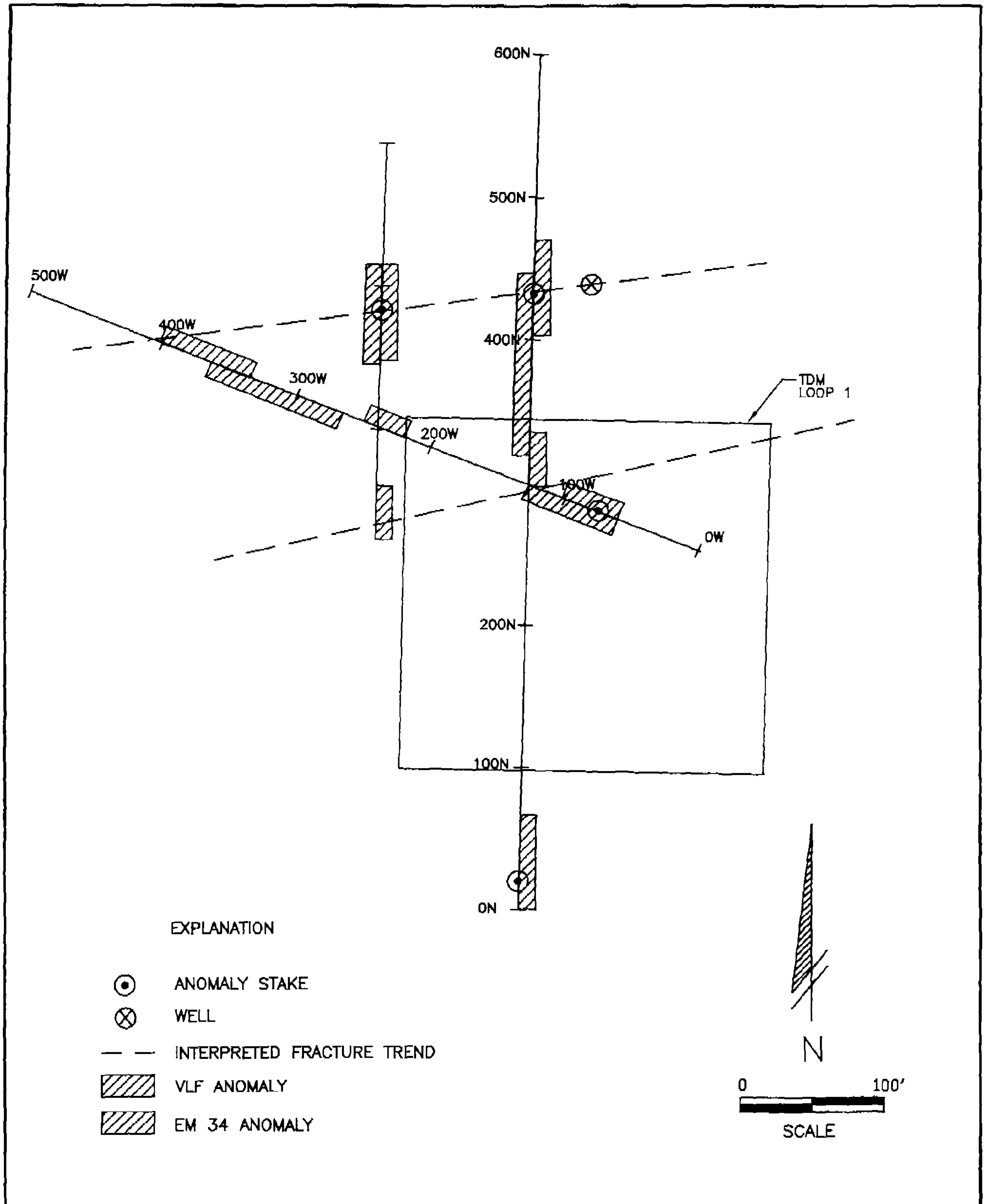

JUDGE'S OFFICE STONEWALL COUNTY, TEXAS	SDII GLOBAL CORPORATION	SURVEY AREA A GEOPHYSICAL LINES AND CONDUCTIVE ANOMALIES SALT POLLUTION STUDY STONEWALL COUNTY, TEXAS		
		DESIGNED BY: TLD	PROJECT NO.: 1011520	FIGURE
		CHECKED BY: TLD	DRAWING NO.: 1520-13	

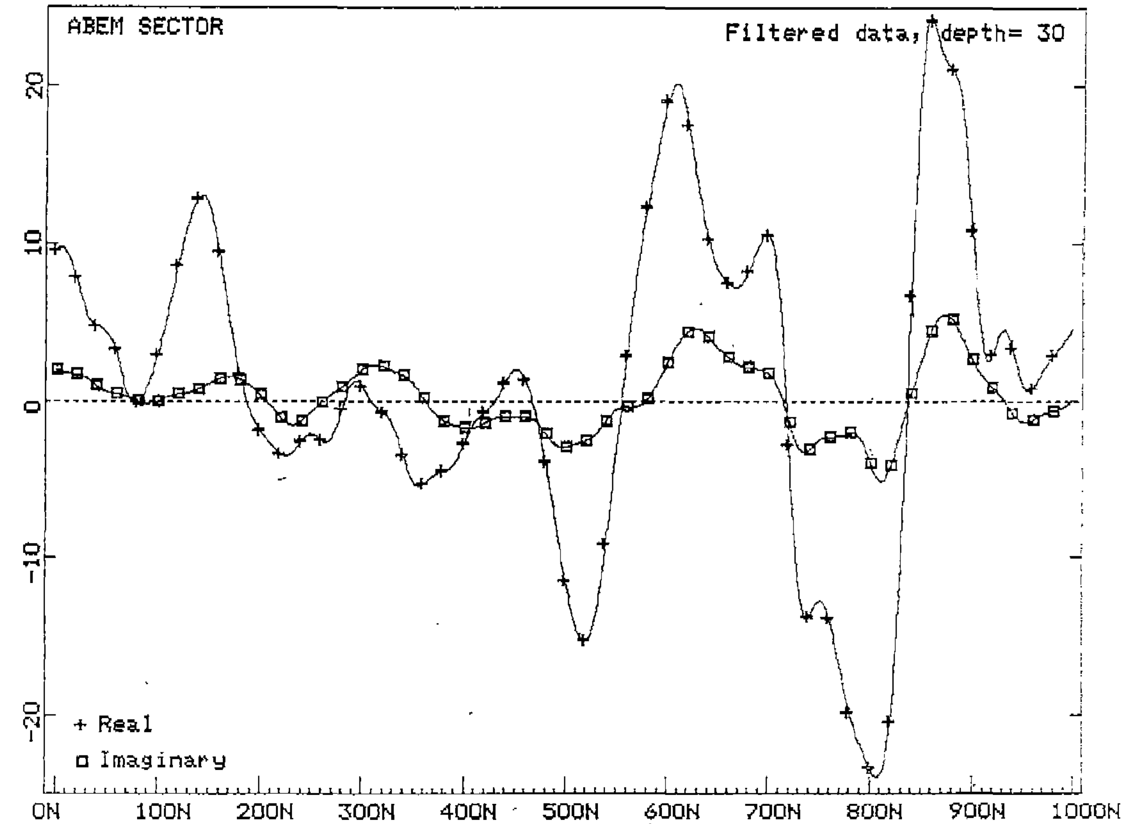

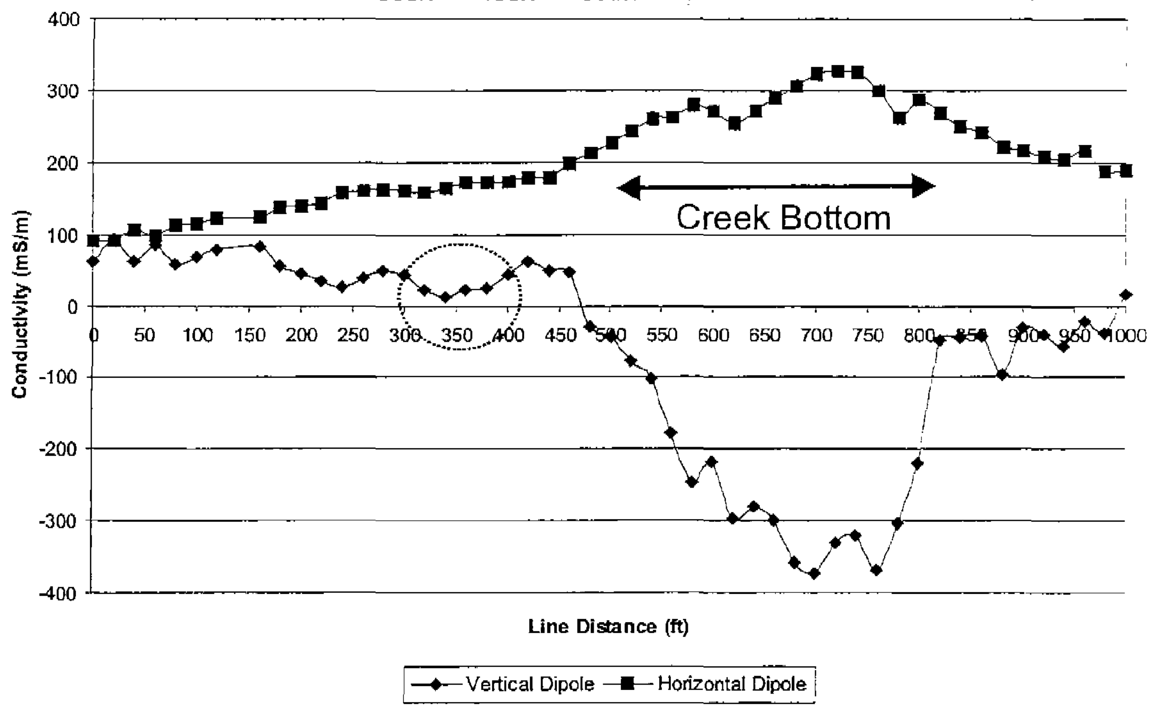

JUDGE'S OFFICE STONEWALL COUNTY, TEXAS	GLOBAL	EXAMPLE OF VLF (UPPER) AND EM34 (LOWER) DATA TRANSECT - AREA B SALT POLUTION STUDY STONEWALL COUNTY, TEXAS

DESIGNED BY:	CT	PROJECT NO.: 1011520	FIGURE
CHECKED BY:	TLD	DRAWING NO.:	14
DRAWN BY:	JMW	DATE: 07/10/00	

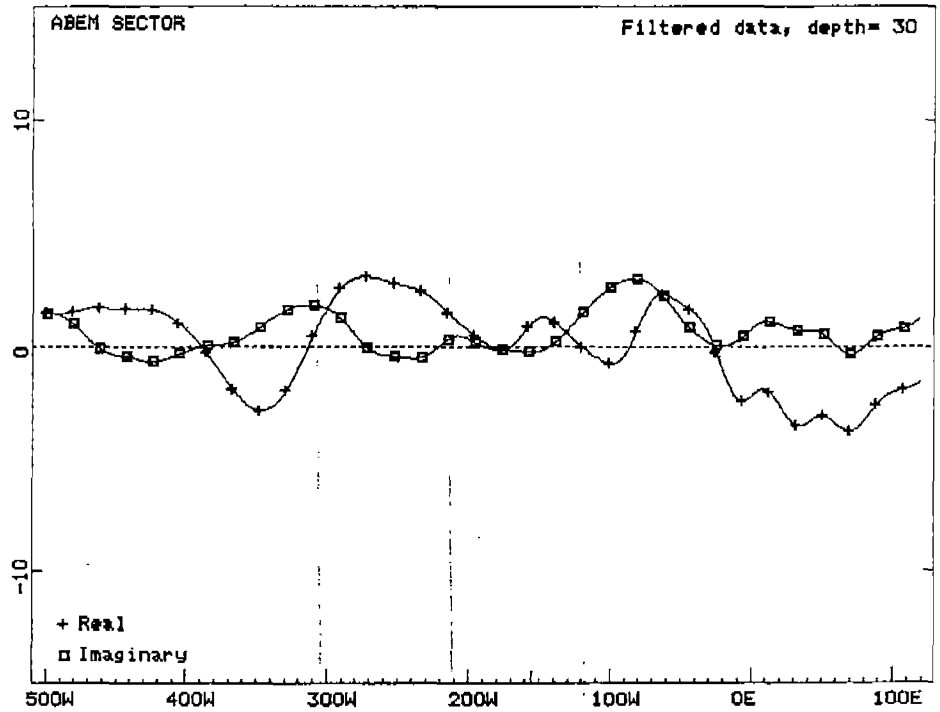

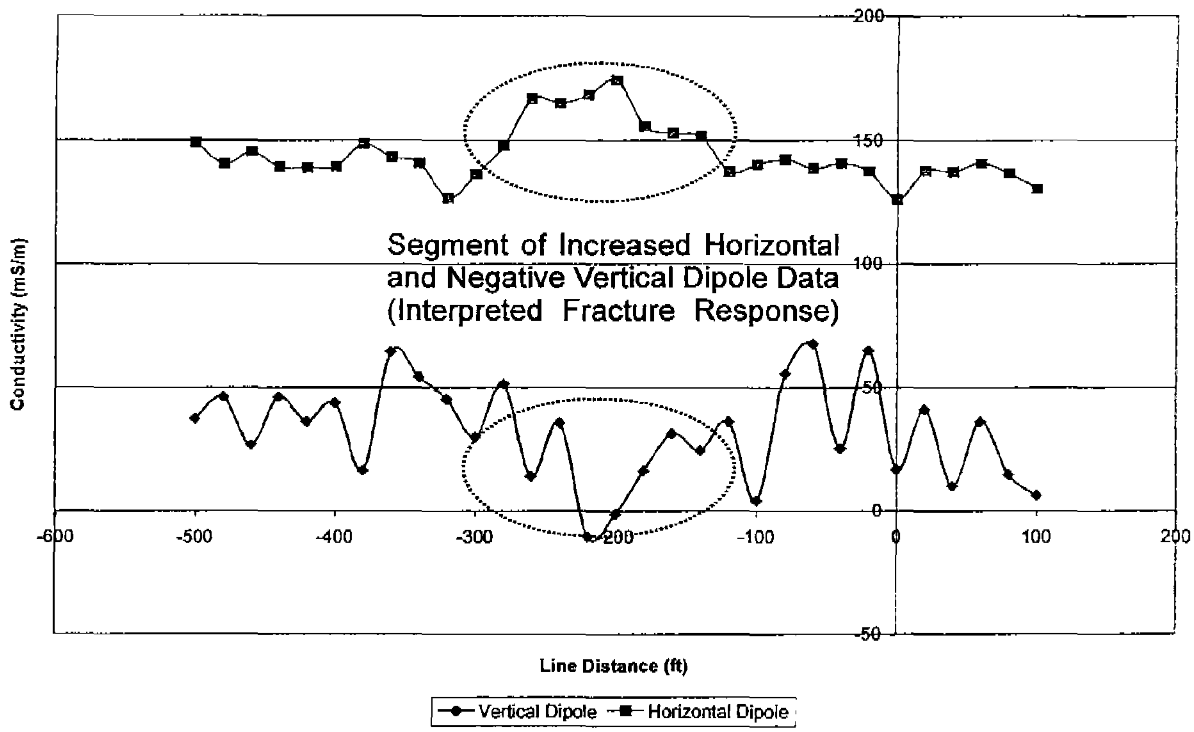

JUDGE'S OFFICE STONEWALL COUNTY, TEXAS	SDII GLOBAL	EXAMPLE OF VLF (UPPER) AND EM34 (LOWER) DATA TRANSECT - AREA B (#2) SALT POLUTION STUDY STONEWALL COUNTY, TEXAS

DESIGNED BY:	CT	PROJECT NO.: 101152C		FIGURE
CHECKED BY:	TLD	DRAWING NO.:		15
DRAWN BY:	JMW	DATE:	07/10/00	

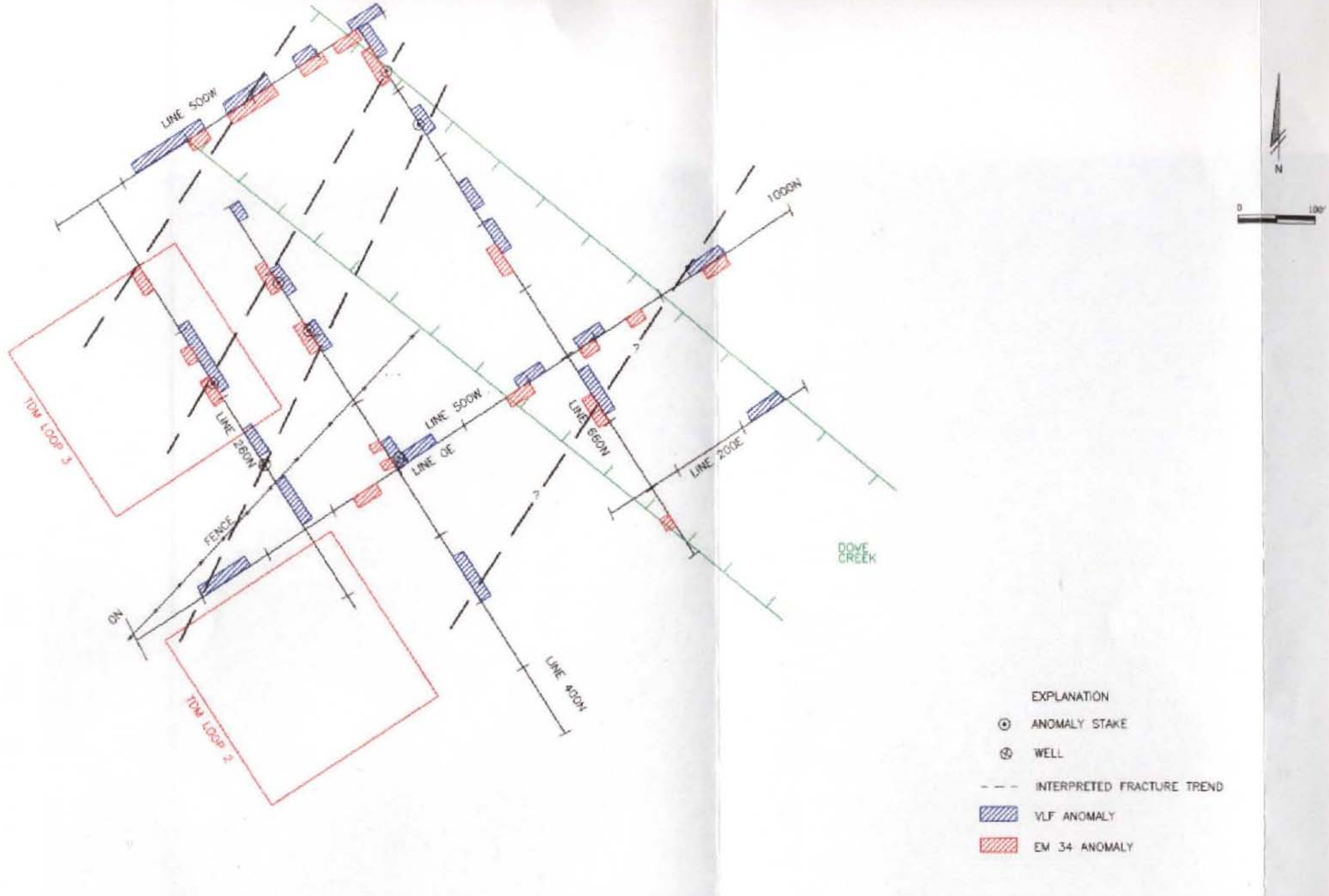

JUDGE'S OFFICE STONEWALL COUNTY, TEXAS	SDII GLOBAL CORPORATION	SURVEY AND SA STO Designed By: T Checked By: T Drawn By: J

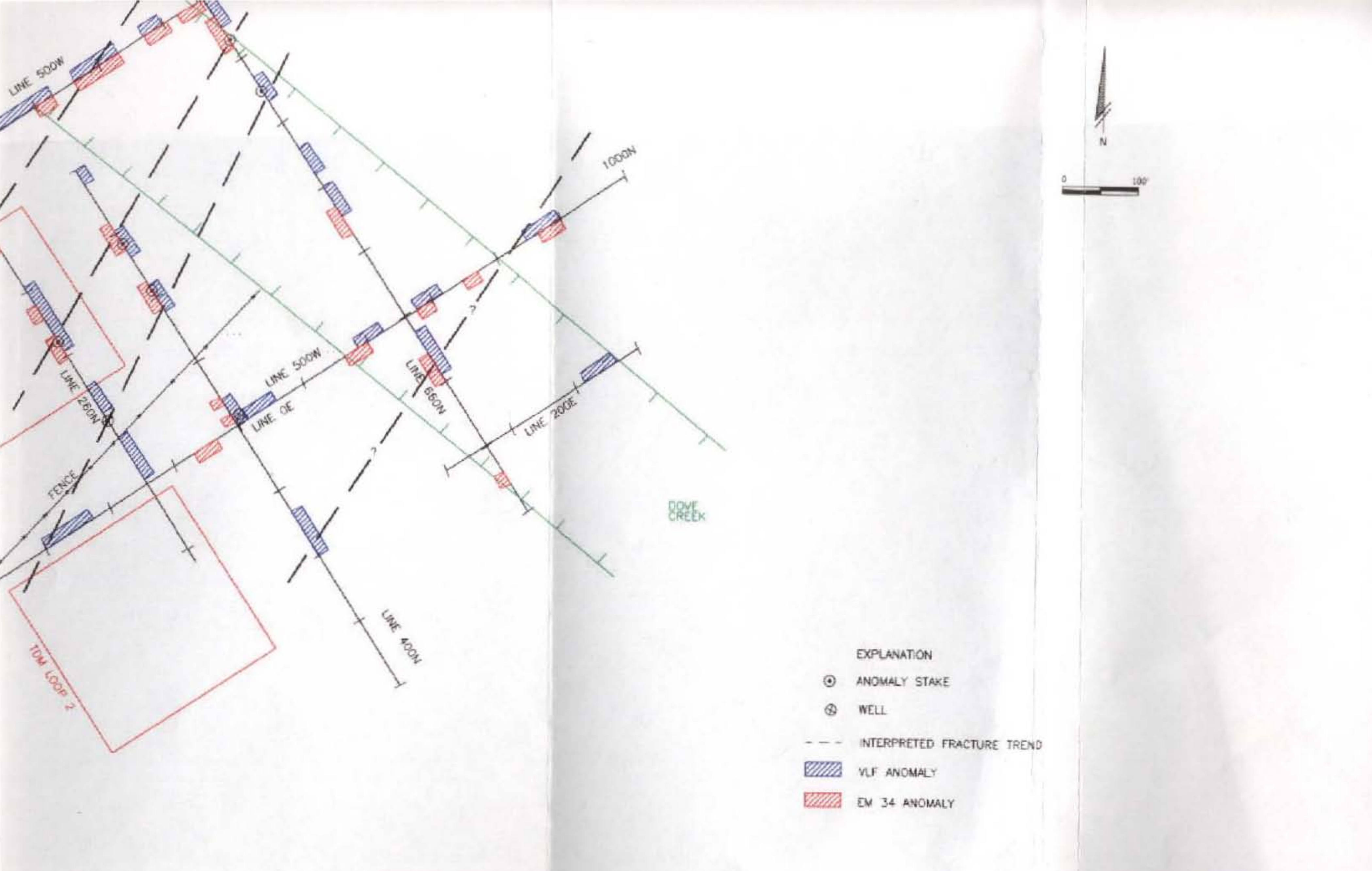

JUDGE'S OFFICE STONEWALL COUNTY, TEXAS	SDII GLOBAL CORPORATION	SURVEY AREA B GEOPHYSICAL LINES AND CONDUCTIVE ANOMALIES SALT POLLUTION STUDY STONEWALL COUNTY, TEXAS					
		Designed By:	TLD	Project No:	1011520	FIGURE
		Checked By:	TLD	Drawing No:	1520-16	
		Drawn By:	JMW	Date:	07/12/00	16

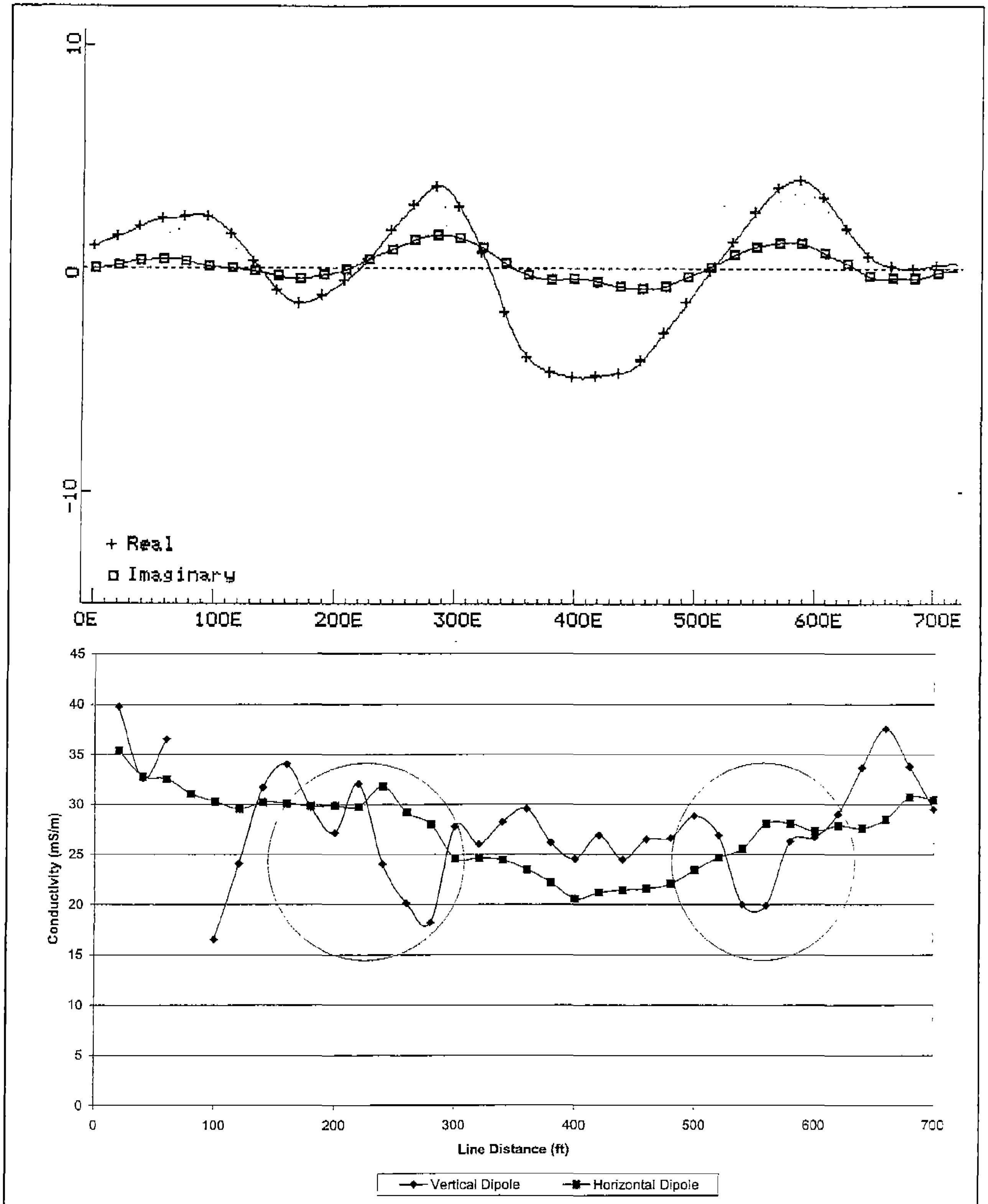

JUDGE'S OFFICE
STONEWALL COUNTY, TEXAS

SDII GLOBAL

EXAMPLE OF VLF (UPPER) AND EM34 (LOWER)
DATA TRANSECT - AREA C
SALT POLUTION STUDY
STONEWALL COUNTY, TEXAS

DESIGNED BY: CT	PROJECT NO.: 1011520	FIGURE 17
CHECKED BY: TLD	DRAWING NO.:	
DRAWN BY: JMW	DATE: 07/10/00	

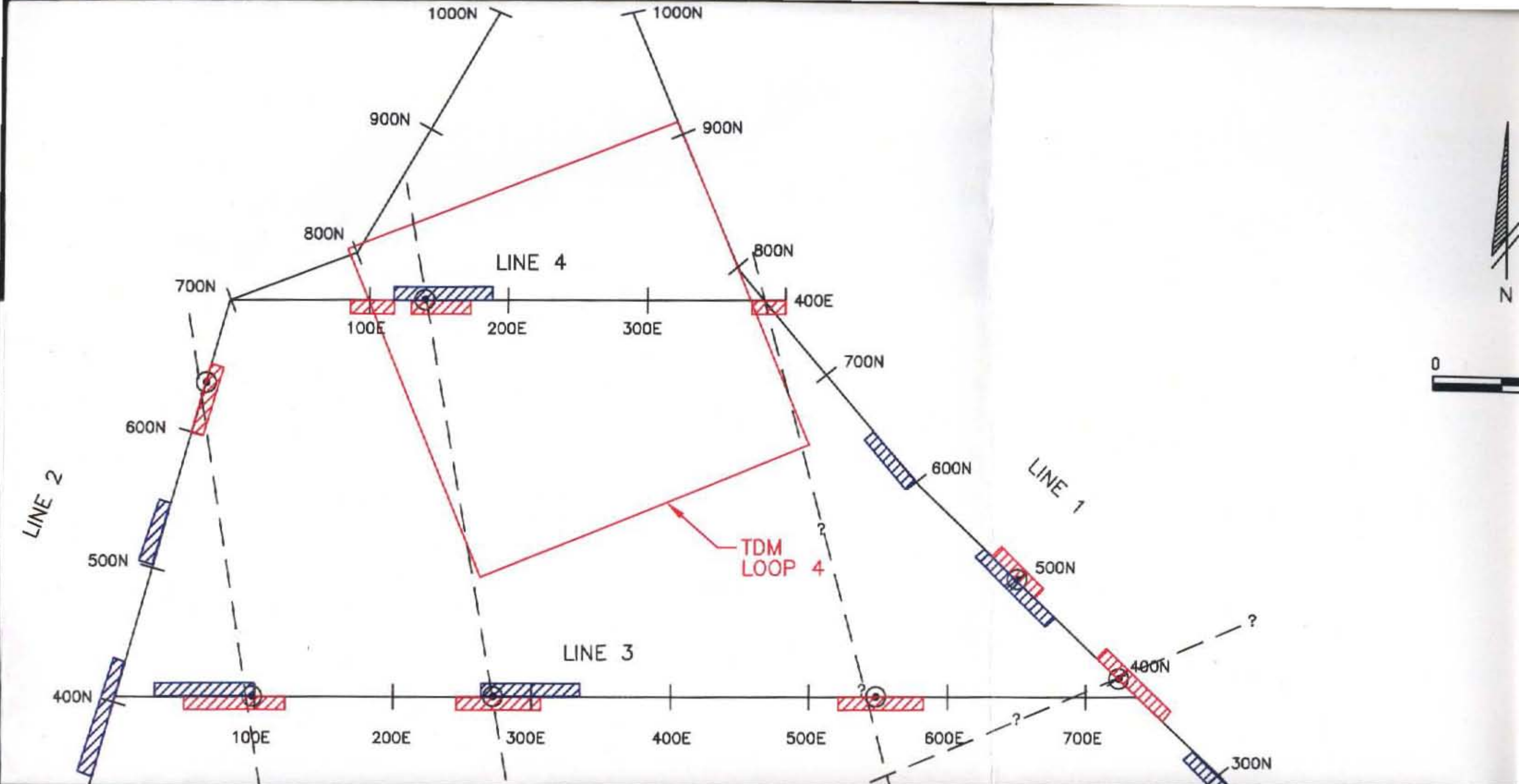

1000N
1000N
900N
900N
800N
800N
LINE 4
700N
100E
200E
300E
400E
700N
600N
600N
LINE 2
LINE 1
500N
TDM
LOOP 4
500N
LINE 3
400N
400N
100E
200E
300E
400E
500E
600E
700E
300N
N
0

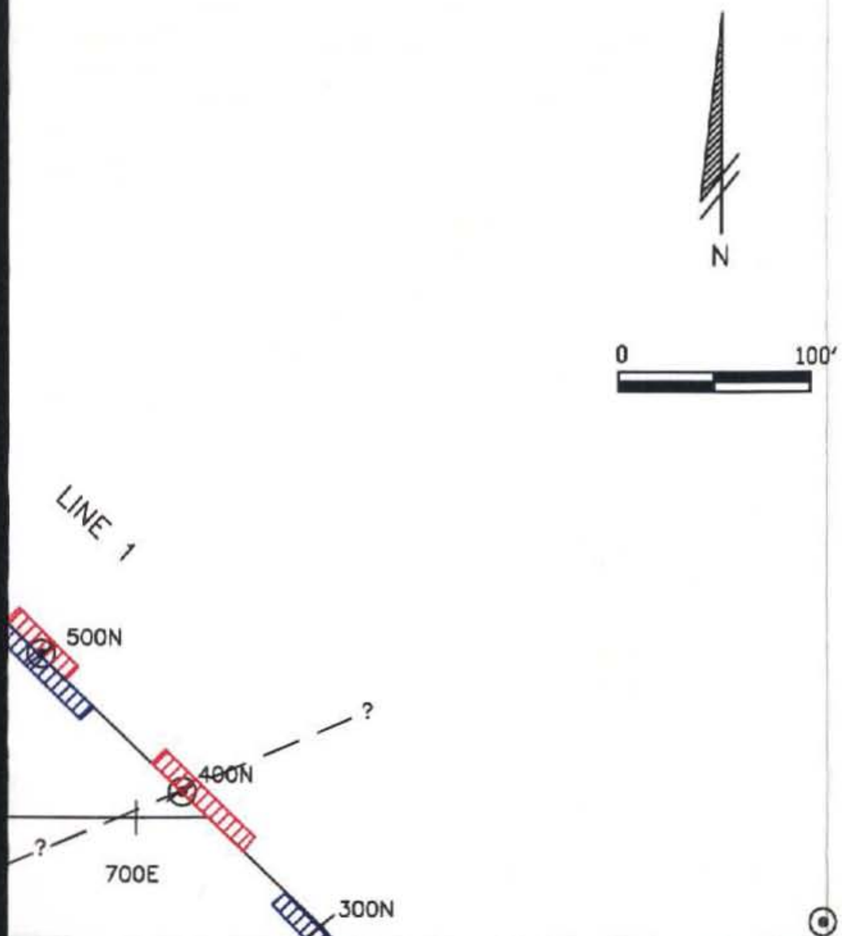

EXPLANATION

ANOMALY STAKE

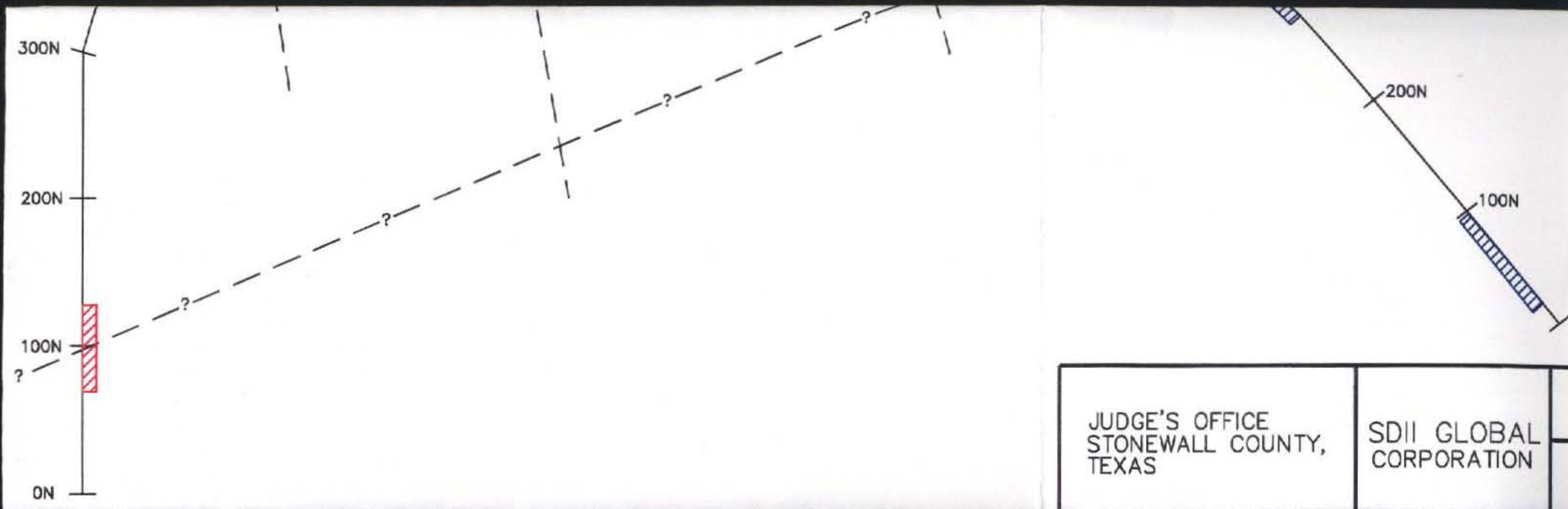

JUDGE'S OFFICE STONEWALL COUNTY, TEXAS	SDII GLOBAL CORPORATION

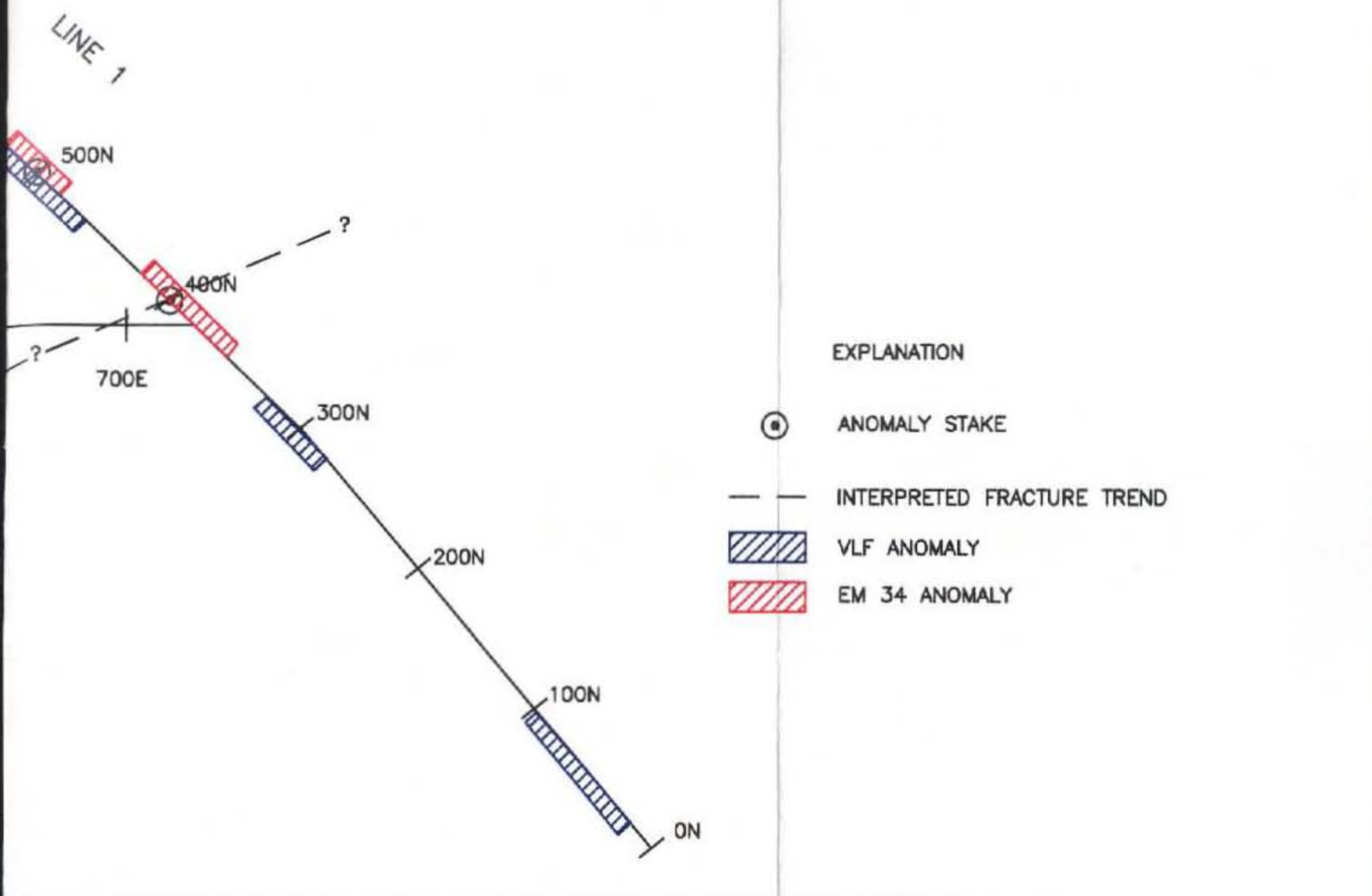

JUDGE'S OFFICE STONEWALL COUNTY, TEXAS	SDII GLOBAL CORPORATION	SURVEY AREA C GEOPHYSICAL LINES AND CONDUCTIVE ANOMALIES SALT POLLUTION STUDY STONEWALL COUNTY, TEXAS				
		Designed By:	TLD	Proj. No.	1011520	FIGURE
		Checked By:	TLD	DWG	1520-18	18
		Drawn By:	JMW	Date:	07/12/00	

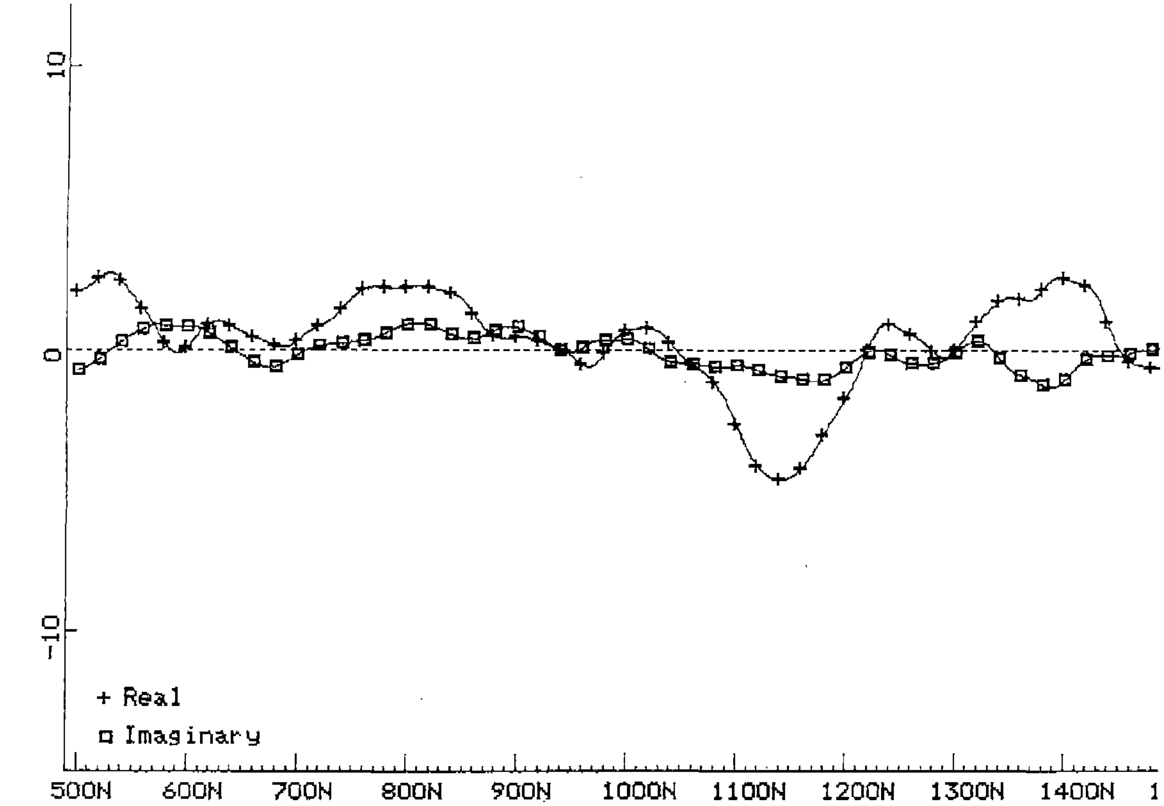

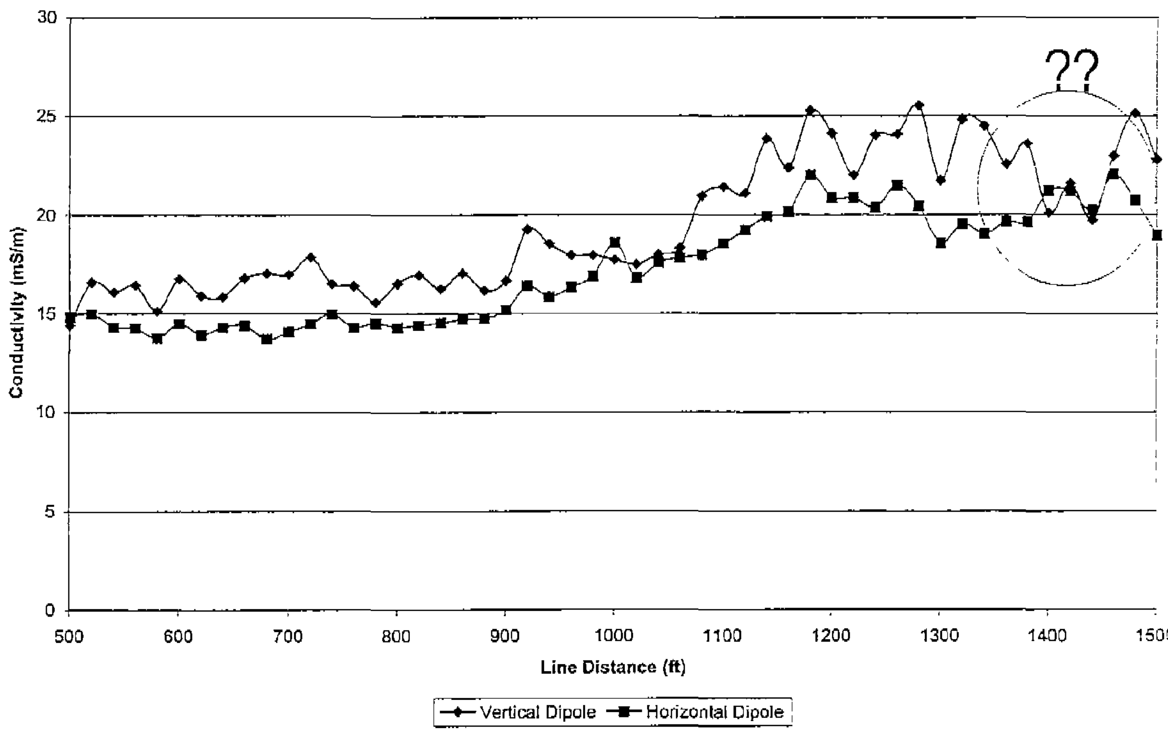

JUDGE'S OFFICE
STONEWALL COUNTY, TEXAS

EXAMPLE OF VLF (UPPER) AND EM34 (LOWER)
DATA TRANSECT - AREA D
SALT POLUTION STUDY
STONEWALL COUNTY, TEXAS

DESIGNED BY: CT	PROJECT NO.: 1011520	FIGURE
CHECKED BY: TLD	DRAWING NO.:	19
DRAWN BY: JMW	DATE: 07/10/00	

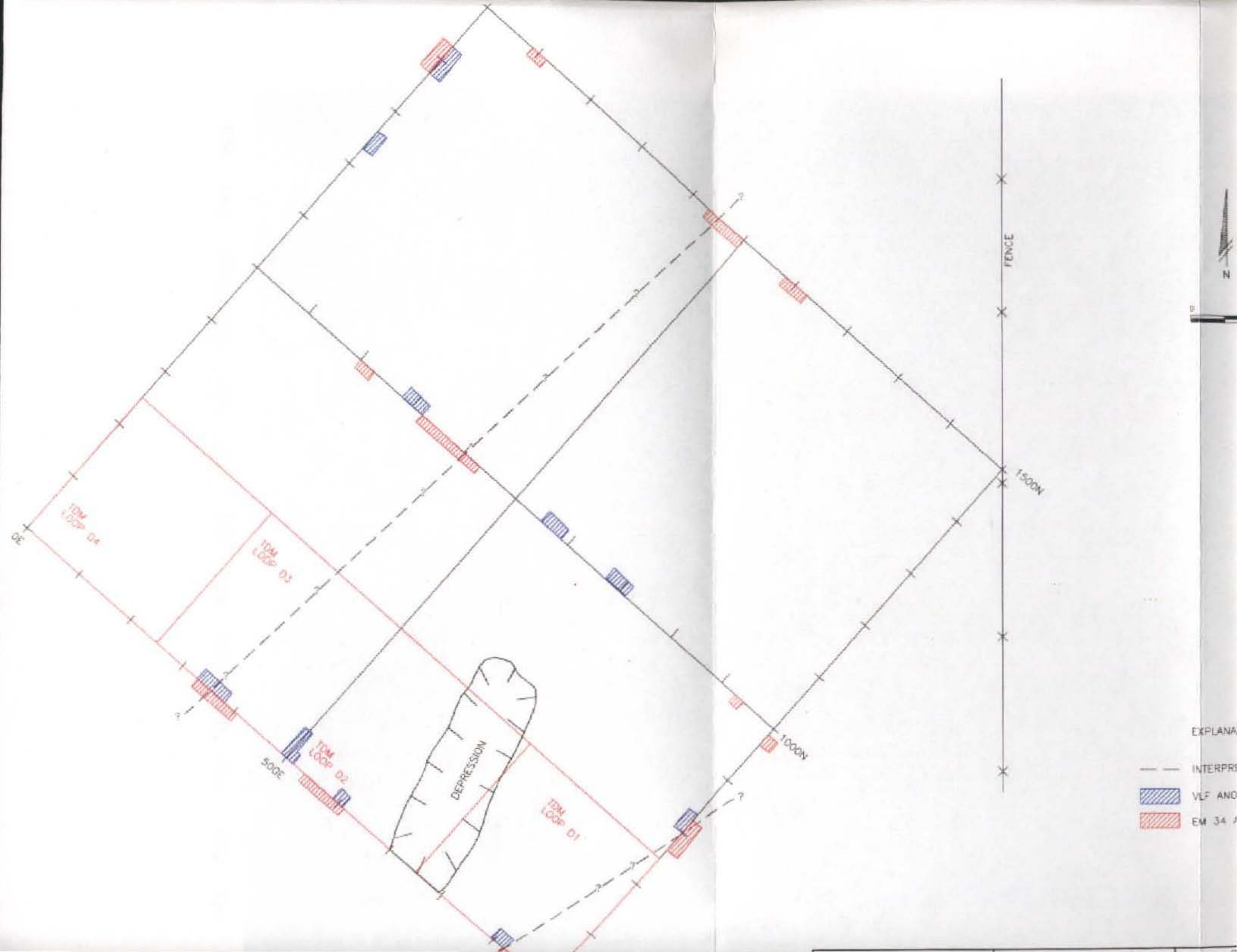
N
FENCE
1500N
1000N
500E
0E
TDM LOOP D1
TDM LOOP D2
TDM LOOP D3
TDM LOOP D4
DEPRESSION
EXPLANA
INTERPR
VLF ANO
EM 34

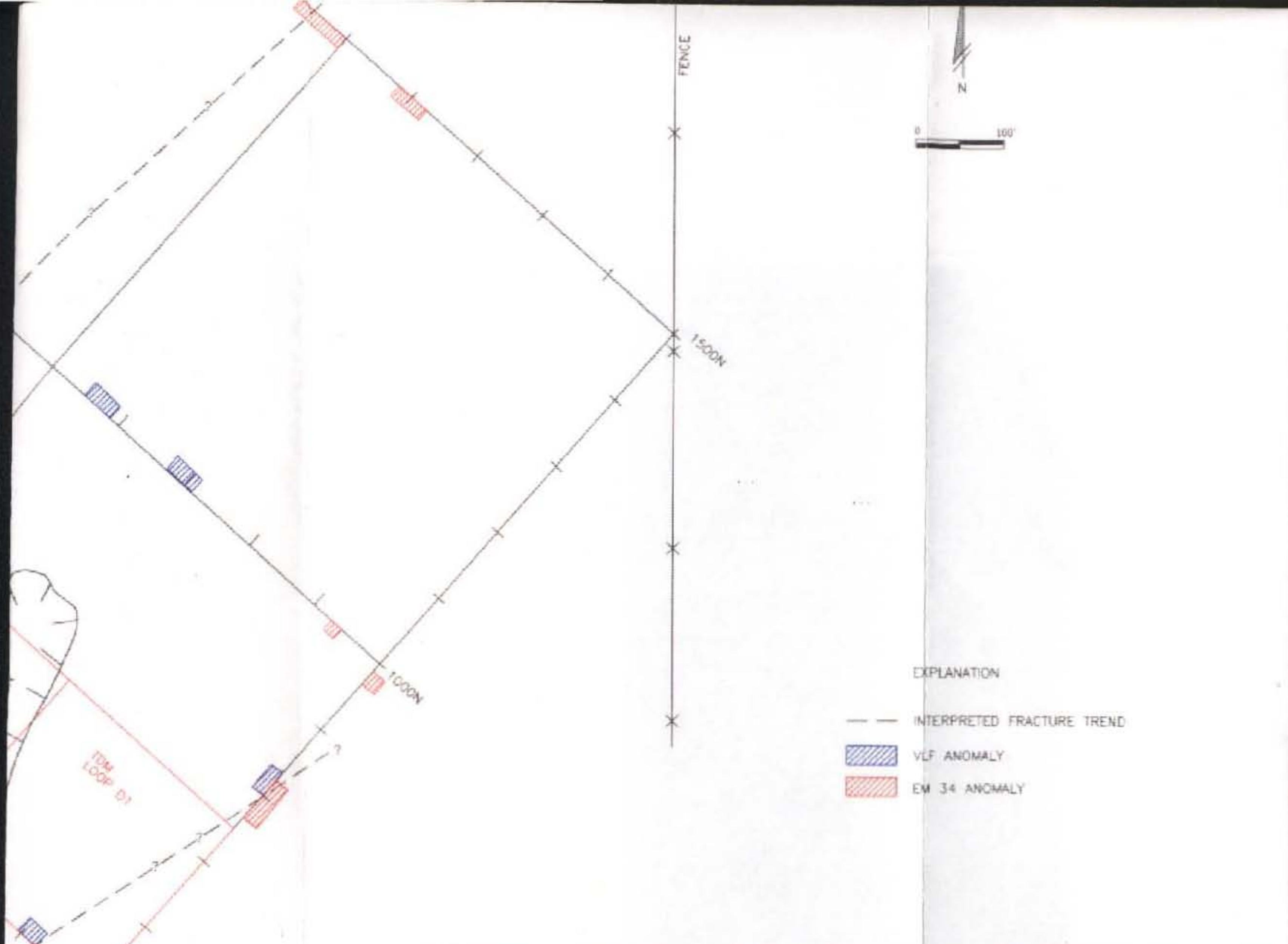

JUDGE'S OFFICE STONEWALL COUNTY, TEXAS	SDII GLOBAL CORPORATION	SURVEY AREA D GEOPHYSICAL LINES AND CONDUCTIVE ANOMALIES SALT POLLUTION STUDY STONEWALL COUNTY, TEXAS				
		Designed By:	TLD	Project No.	1011520	FIGURE
		Checked By:	TLD	Drawing No:	1520-20	20
		Drawn By:	JMW	Date:	07/12/00	

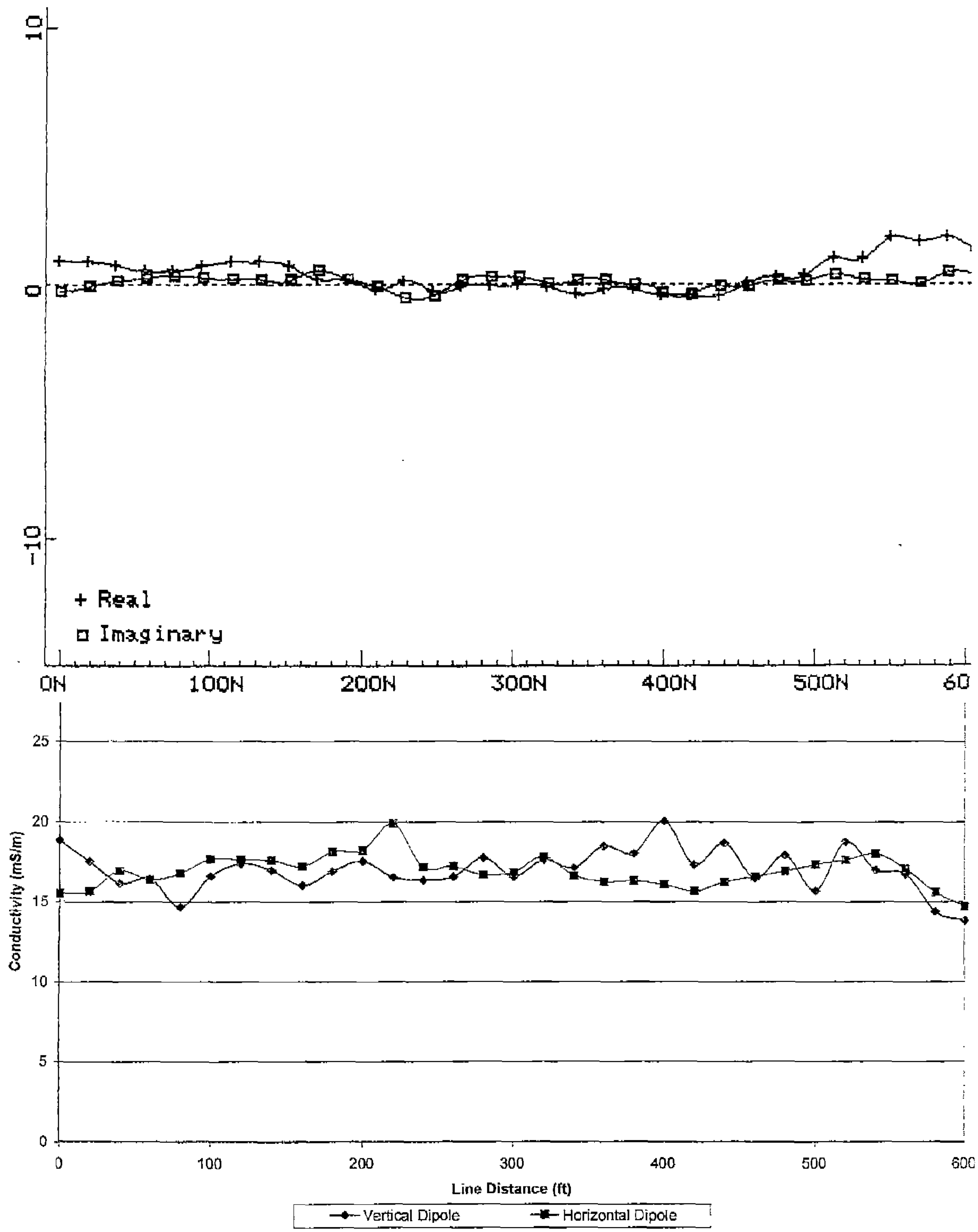

JUDGE'S OFFICE
STONEWALL COUNTY, TEXAS

EXAMPLE OF VLF (UPPER) AND EM34 (LOWER)
DATA TRANSECT - AREA E
SALT POLUTION STUDY
STONEWALL COUNTY, TEXAS

DESIGNED BY: CT	PROJECT NO.:	1011520	FIGURE
CHECKED BY: TLD	DRAWING NO.:		21
DRAWN BY: JMW	DATE:	07/11/00	

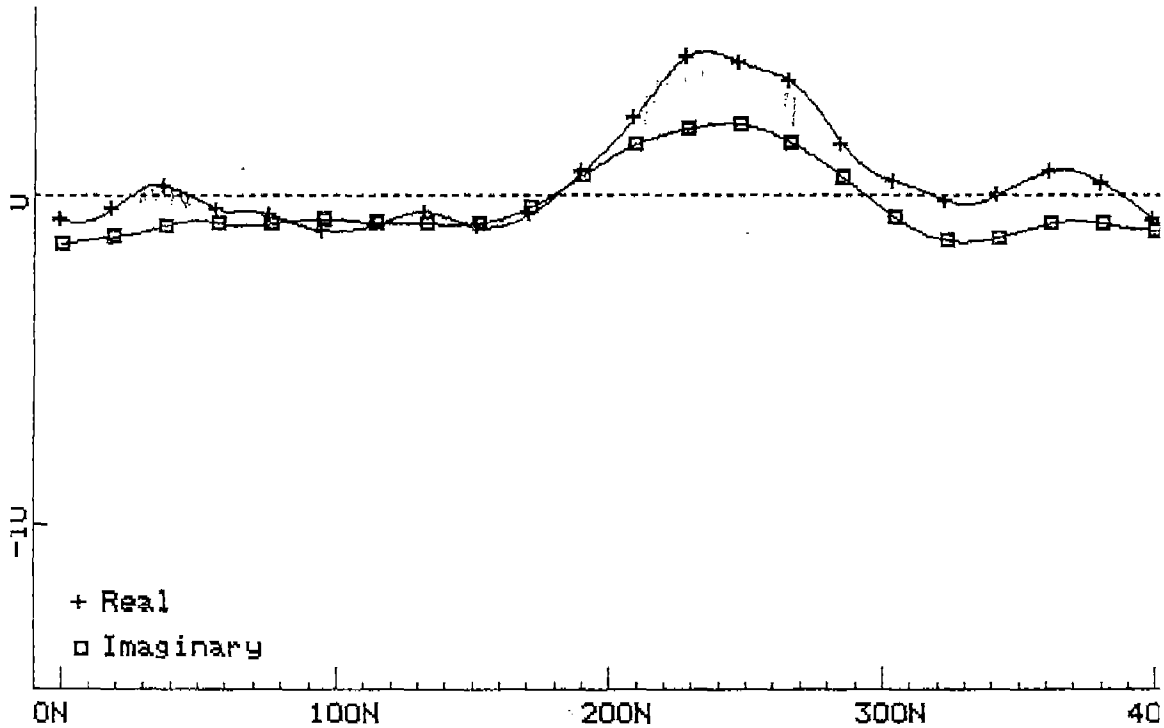

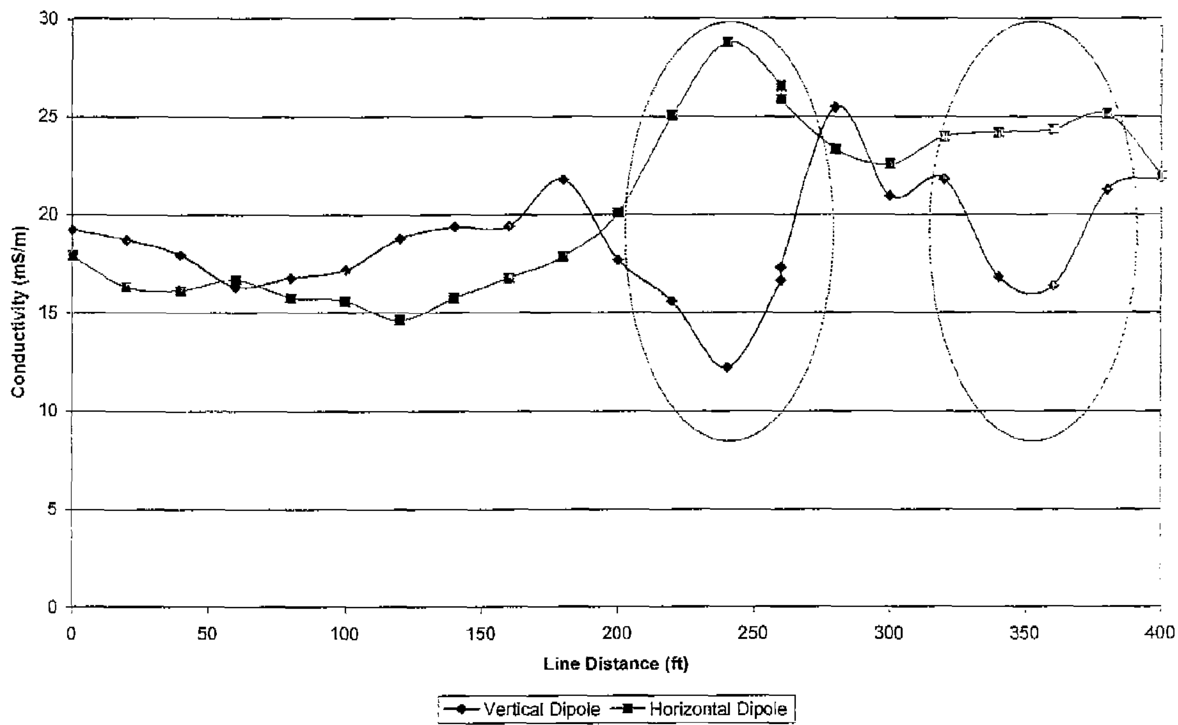

JUDGE'S OFFICE
STONEWALL COUNTY, TEXAS

SDII GLOBAL

EXAMPLE OF VLF (UPPER) AND EM34 (LOWER)
DATA TRANSECT - AREA F
SALT POLUTION STUDY
STONEWALL COUNTY, TEXAS

DESIGNED BY:	CT	PROJECT NO.: 1011520		FIGURE
CHECKED BY:	TLD	DRAWING NO.:		22
DRAWN BY:	JMW	DATE:	07/11/00	

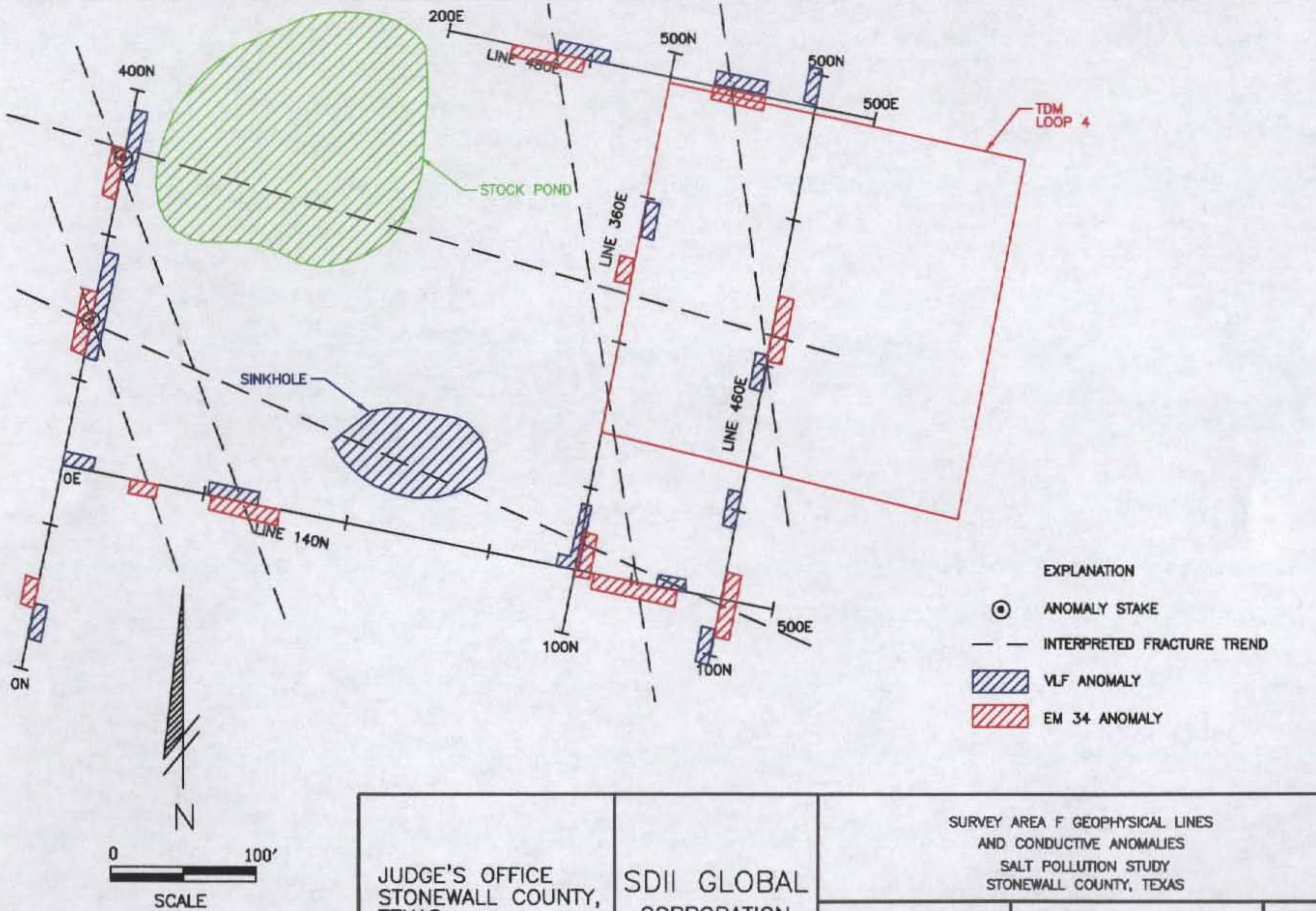

JUDGE'S OFFICE STONEWALL COUNTY, TEXAS	SDII GLOBAL CORPORATION	SURVEY AREA F GEOPHYSICAL LINES AND CONDUCTIVE ANOMALIES SALT POLLUTION STUDY STONEWALL COUNTY, TEXAS				
		DESIGNED BY:	TLD	PROJECT NO.:	1011520	FIGURE
		CHECKED BY:	TLD	DRAWING NO.:	1520-23	23
		DRAWN BY:	JMW	DATE:	07/12/00	

SITE10

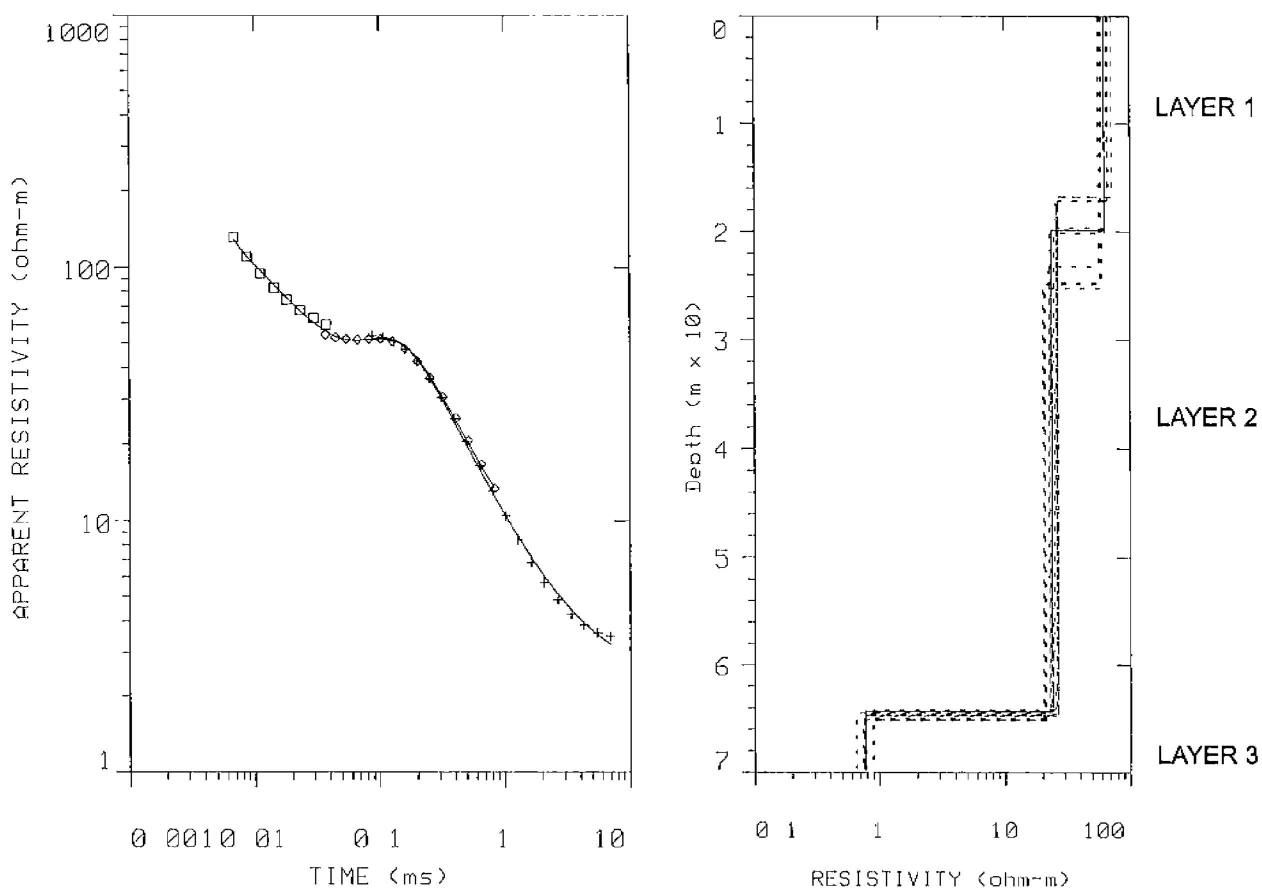

JUDGE'S OFFICE
STONEWALL COUNTY,
TEXAS

GLOBAL

EXAMPLE TDM SOUNDING DATA (LEFT)
AND MODEL INVERSION (RIGHT)
SALT POLLUTION STUDY
STONEWALL COUNTY, TEXAS

DESIGNED BY: CT	PROJECT NO.: 1011520	FIGURE
CHECKED BY: TLD	DRAWING NO.: LOC	24
DRAWN BY: JMW	DATE: 07/11/00	

APPENDIX A

PLOTS OF EM34 DATA

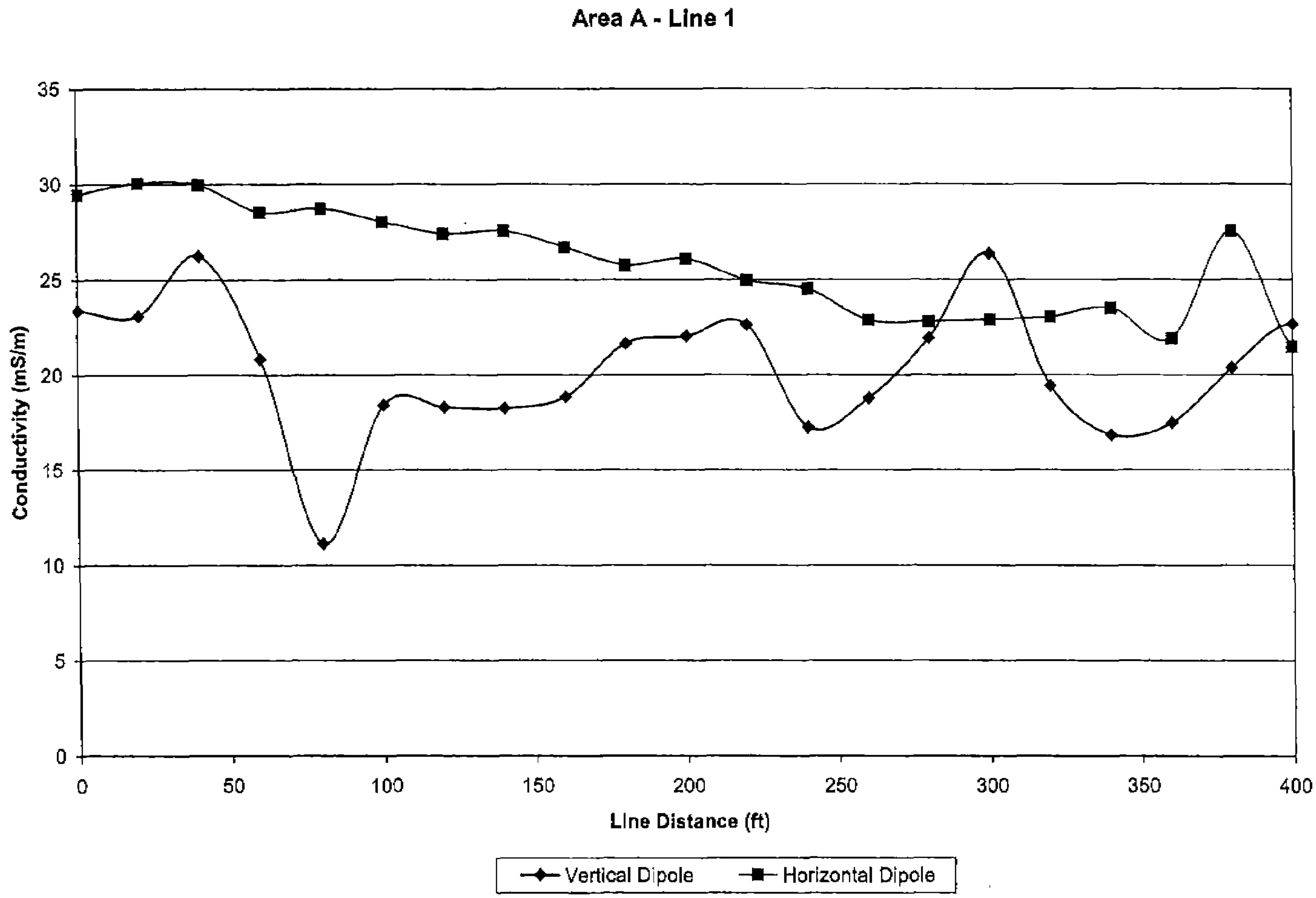

JUDGE'S OFFICE STONEWALL COUNTY, TEXAS		AREA A LINE 1 - EM34 DATA SALT POLLUTION STUDY STONEWALL COUNTY, TEXAS			
		DESIGNED BY: CT	PROJECT NO.: 1011520	FIGURE	
		CHECKED BY: TLD	DRAWING NO.: LOC	A-1	
		DRAWN BY: JMW	DATE: 07/05/00		

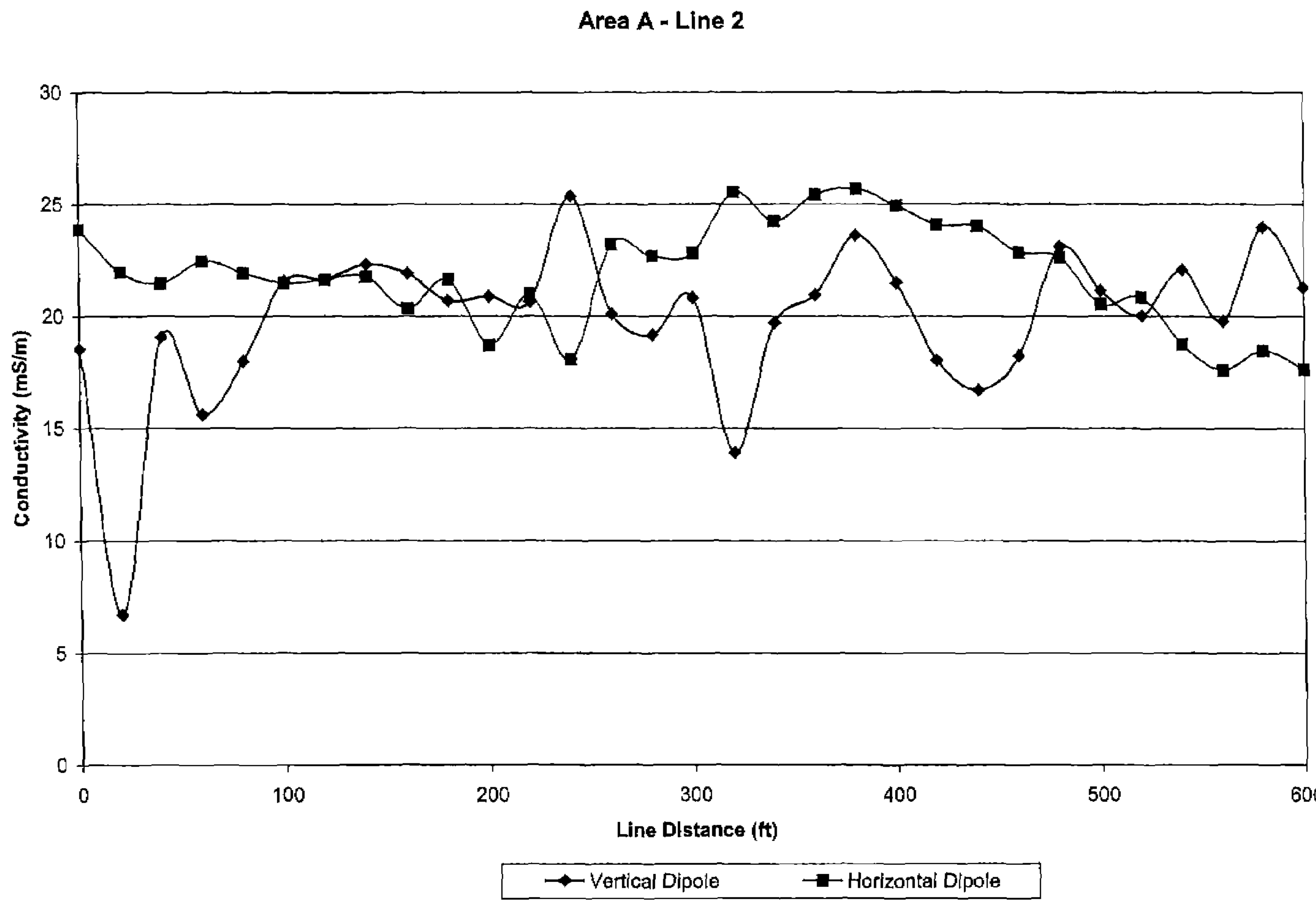

JUDGE'S OFFICE STONEWALL COUNTY, TEXAS	GLOBAL	AREA A LINE 2 - EM34 DATA SALT POLLUTION STUDY STONEWALL COUNTY, TEXAS

DESIGNED BY:	CT	PROJECT NO.:	1011520	FIGURE
CHECKED BY:	TLD	DRAWING NO.:	LOC	A-2
DRAWN BY:	JMW	DATE:	07/05/00	

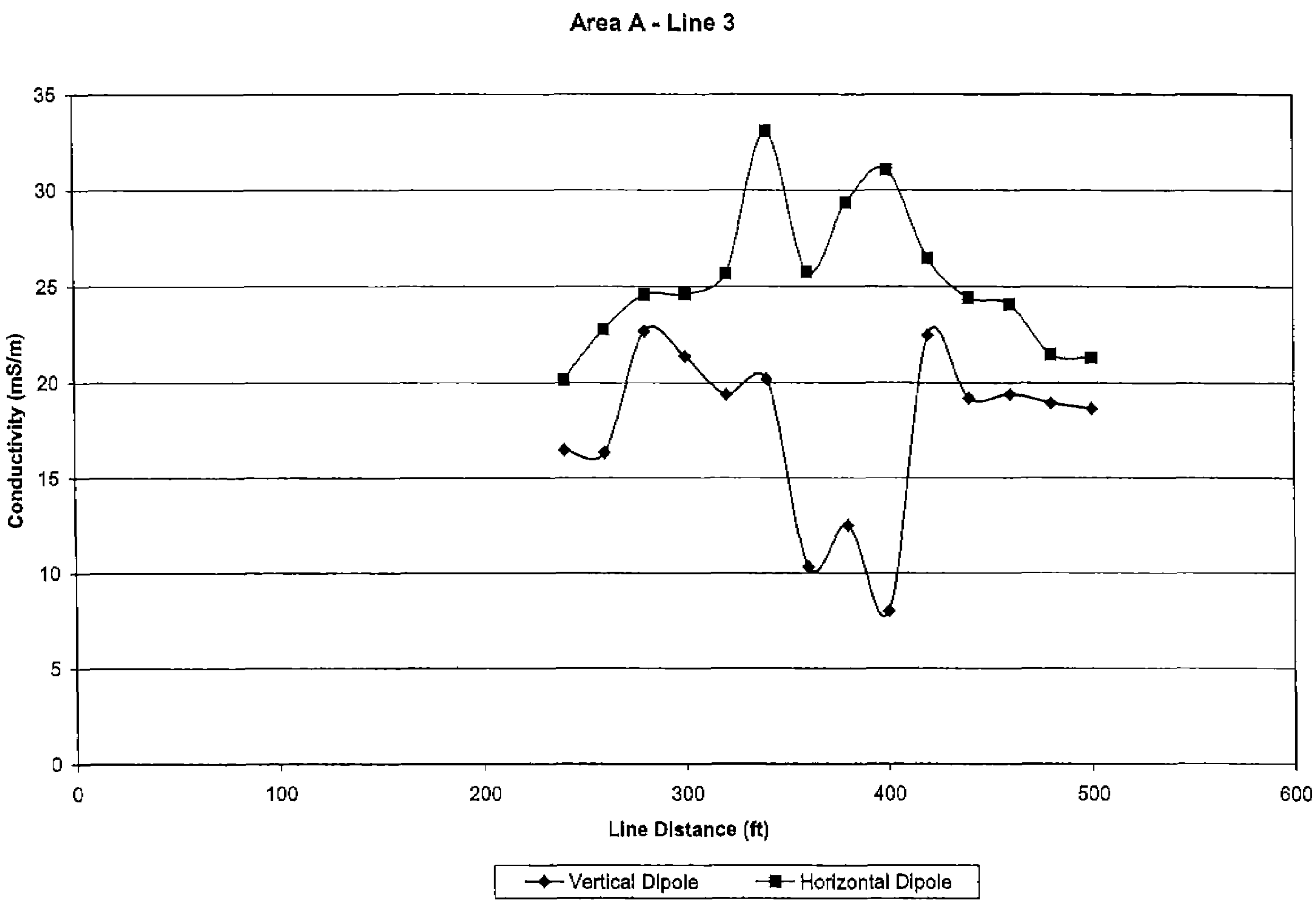

JUDGE'S OFFICE
STONEWALL COUNTY,
TEXAS

AREA A LINE 3 - EM34 DATA
SALT POLLUTION STUDY
STONEWALL COUNTY, TEXAS

DESIGNED BY: CT	PROJECT NO.: 1011520	FIGURE
CHECKED BY: TLD	DRAWING NO.: LOC	A-3
DRAWN BY: JMW	DATE: 07/05/00	

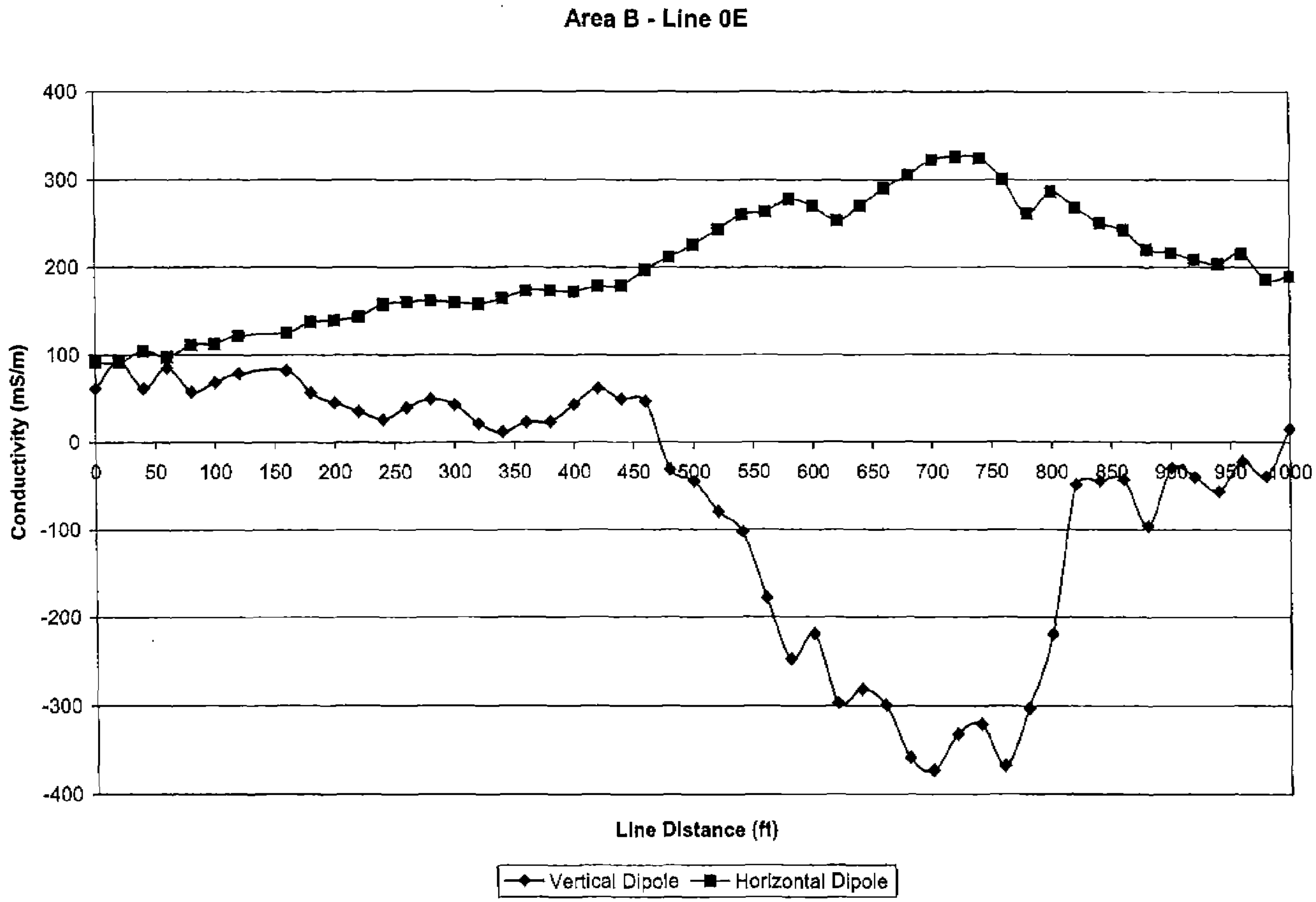

JUDGE'S OFFICE
STONEWALL COUNTY,
TEXAS

AREA B LINE 0E - EM34 DATA
SALT POLLUTION STUDY
STONEWALL COUNTY, TEXAS

DESIGNED BY:	CT	PROJECT NO.:	1011520	FIGURE
CHECKED BY:	TLD	DRAWING NO.:	LOC	A-4
DRAWN BY:	JMW	DATE:	07/05/00	

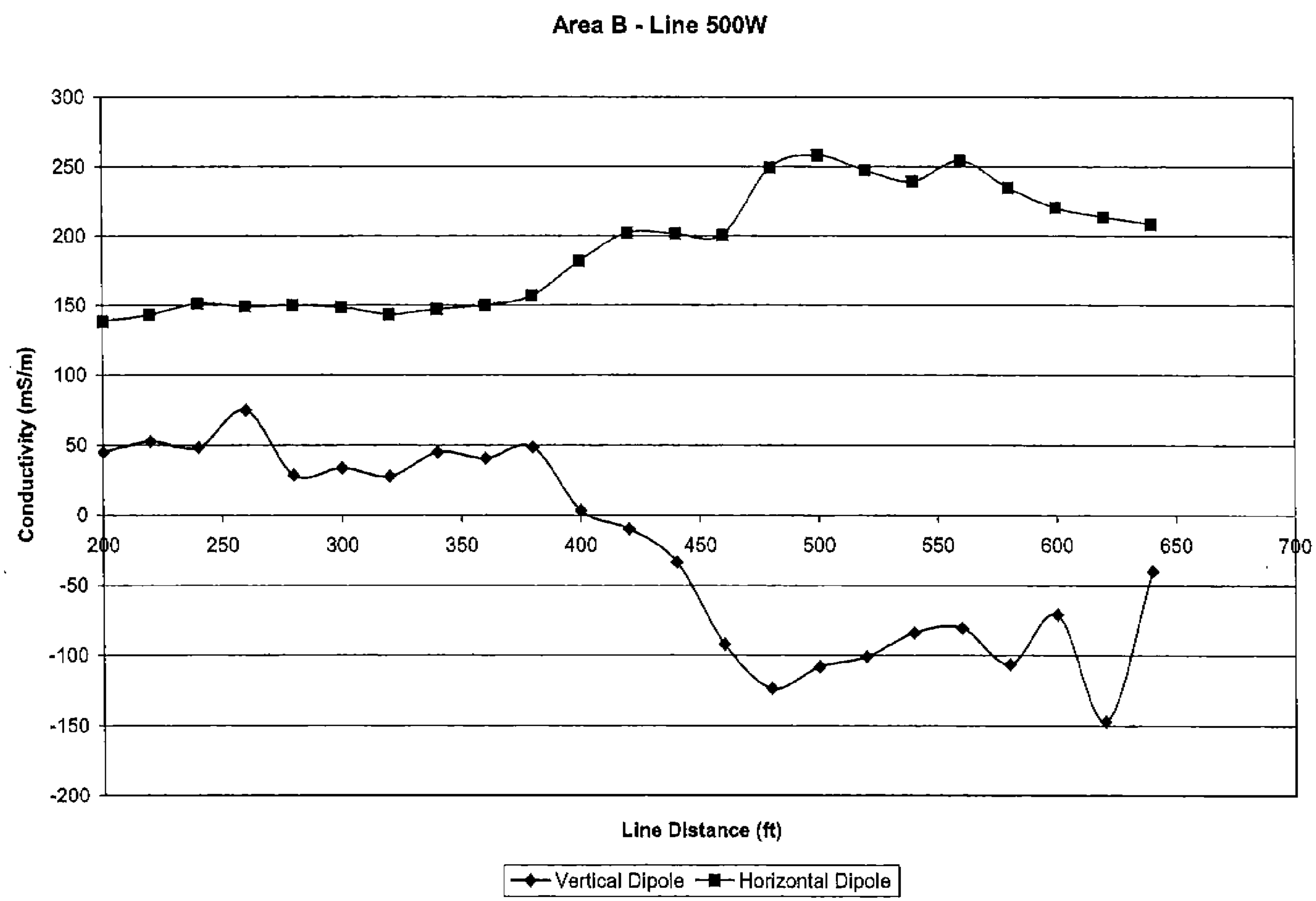

JUDGE'S OFFICE
STONEWALL COUNTY,
TEXAS

AREA B LINE 500W - EM34 DATA
SALT POLLUTION STUDY
STONEWALL COUNTY, TEXAS

DESIGNED BY: CT	PROJECT NO.: 1011520	FIGURE
CHECKED BY: TLD	DRAWING NO.: LOC	A-5
DRAWN BY: JMW	DATE: 07/05/00	

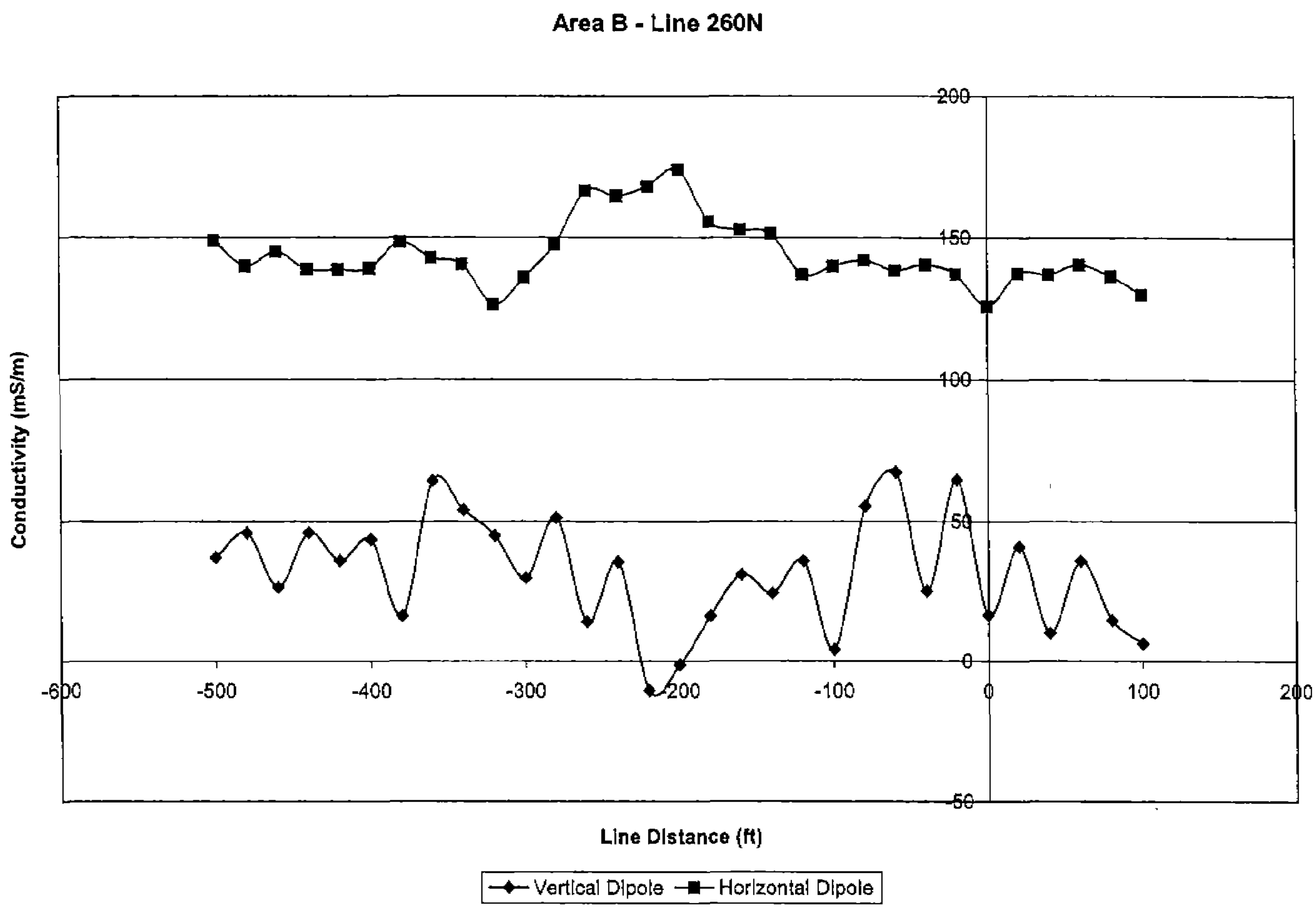

JUDGE'S OFFICE
STONEWALL COUNTY,
TEXAS

AREA B LINE 260N - EM34 DATA
SALT POLLUTION STUDY
STONEWALL COUNTY, TEXAS

DESIGNED BY: CT	PROJECT NO.: 1011520	FIGURE
CHECKED BY: TLD	DRAWING NO.: LOC	A-6
DRAWN BY: JMW	DATE: 07/05/00	

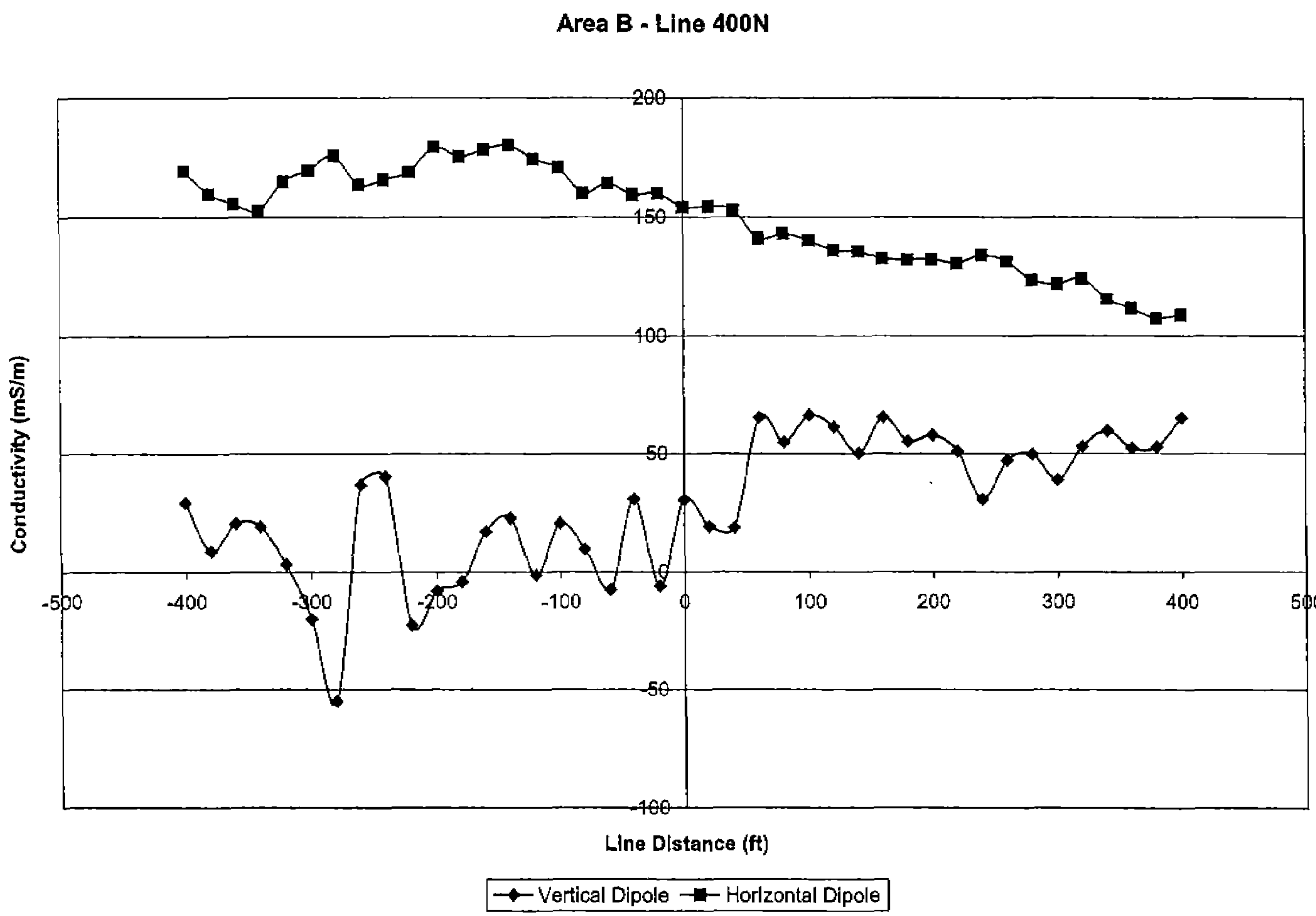

JUDGE'S OFFICE STONEWALL COUNTY, TEXAS		AREA B LINE 400N - EM34 DATA SALT POLLUTION STUDY STONEWALL COUNTY, TEXAS

DESIGNED BY:	CT	PROJECT NO.:	1011520	FIGURE
CHECKED BY:	TLD	DRAWING NO.:	LOC	A-7
DRAWN BY:	JMW	DATE:	07/05/00	

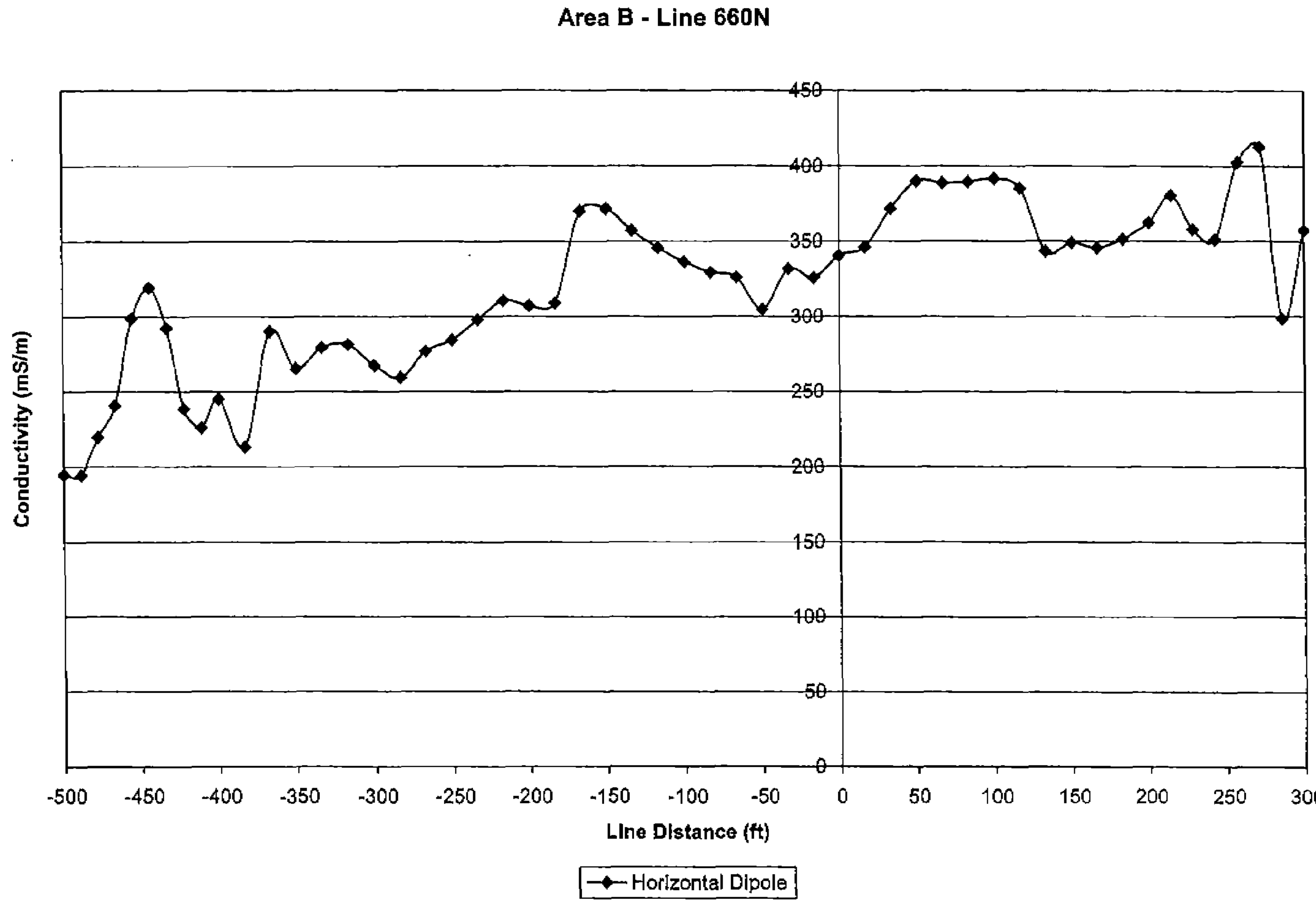

JUDGE'S OFFICE STONEWALL COUNTY, TEXAS	SDII GLOBAL	AREA B LINE 660N - EM34 DATA SALT POLLUTION STUDY STONEWALL COUNTY, TEXAS

DESIGNED BY:	CT	PROJECT NO.:	1011520	FIGURE
CHECKED BY:	TLD	DRAWING NO.:	LOC	A-8
DRAWN BY:	JMW	DATE:	07/05/00	

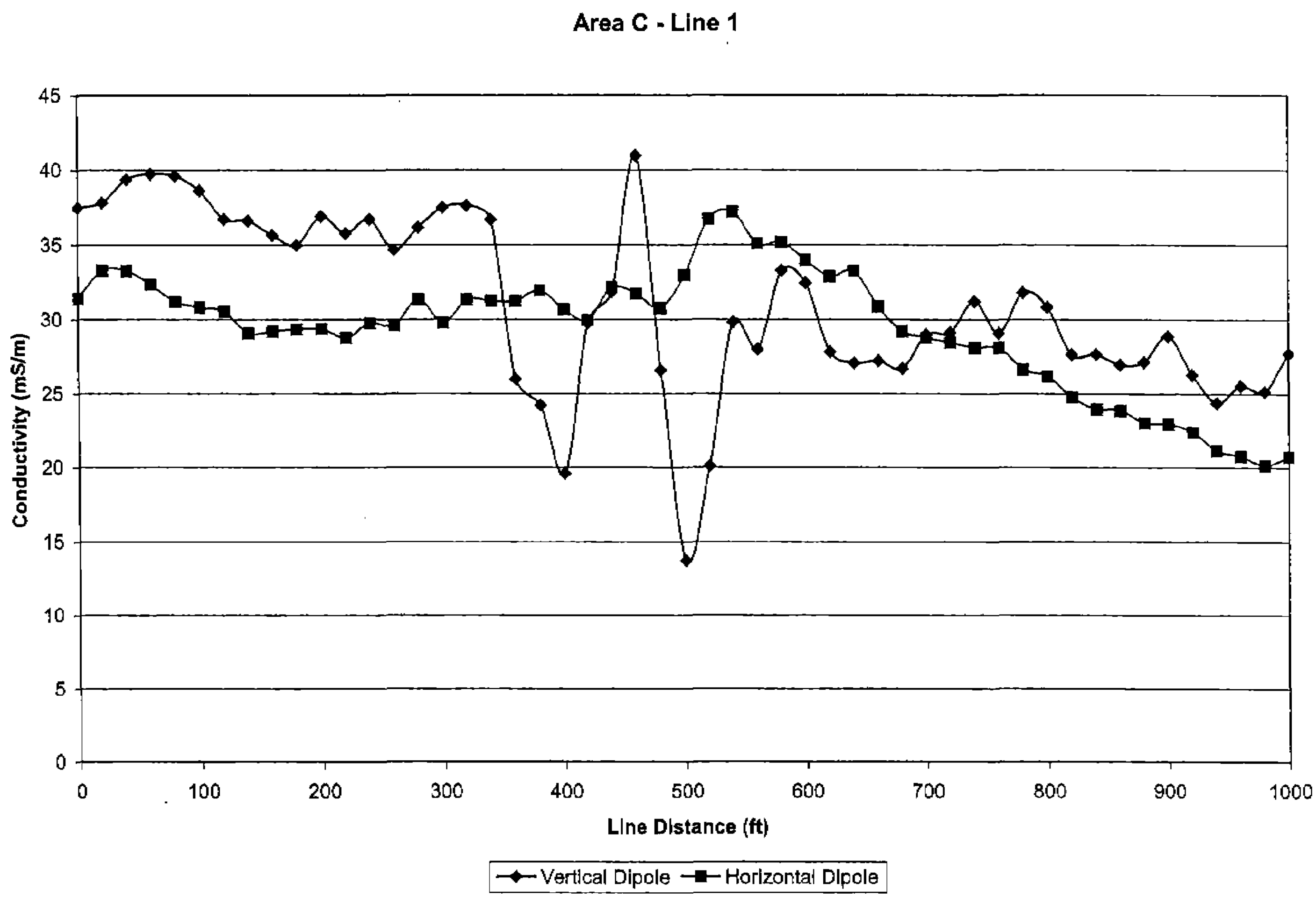

JUDGE'S OFFICE STONEWALL COUNTY, TEXAS	SDII	AREA C LINE 1 - EM34 DATA SALT POLLUTION STUDY STONEWALL COUNTY, TEXAS

DESIGNED BY:	CT	PROJECT NO.:	1011520	FIGURE
CHECKED BY:	TLD	DRAWING NO.:	LOC	A-9
DRAWN BY:	JMW	DATE:	07/05/00	

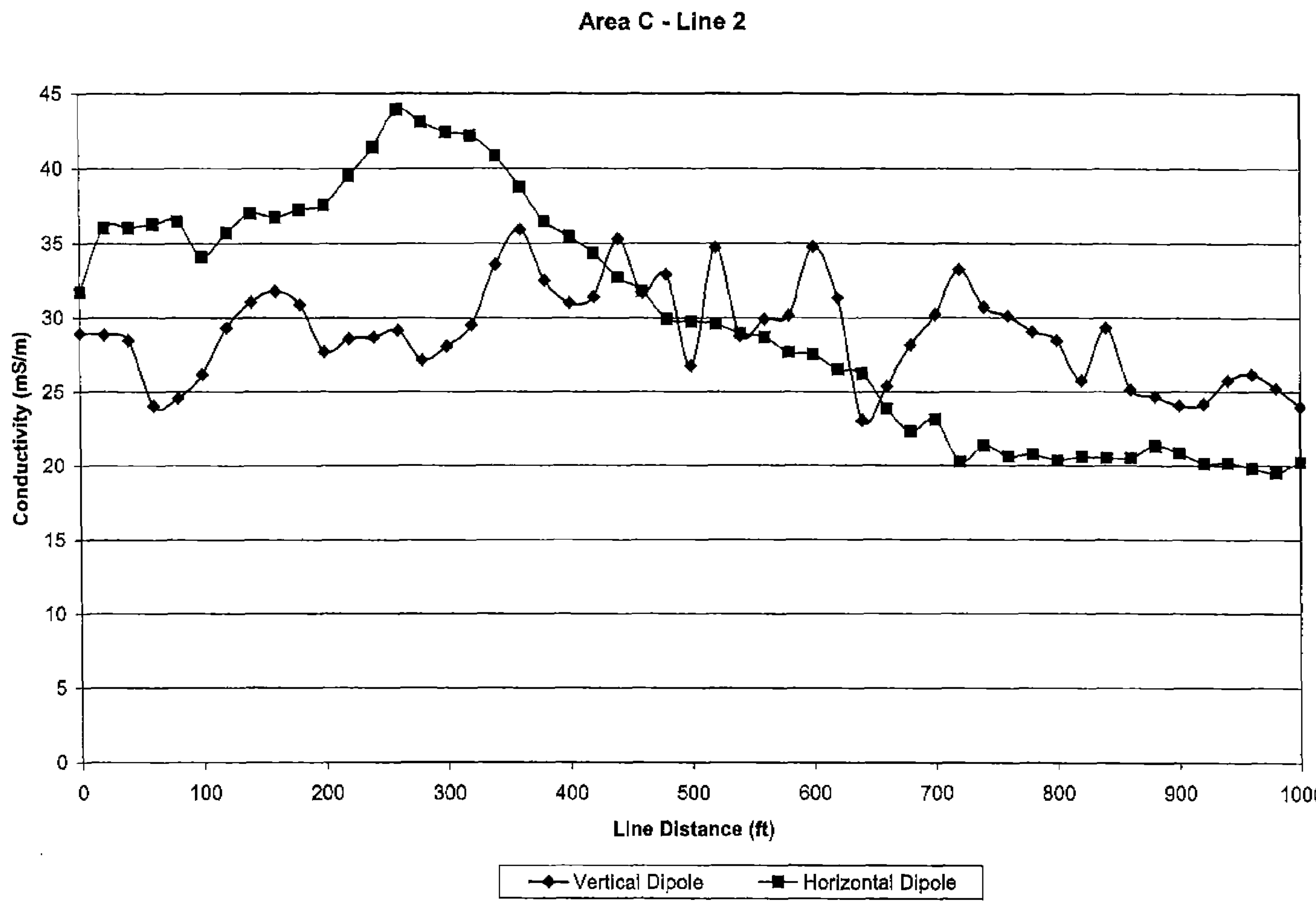

JUDGE'S OFFICE STONEWALL COUNTY, TEXAS	SDII GLOBAL	AREA C LINE 2 - EM34 DATA SALT POLLUTION STUDY STONEWALL COUNTY, TEXAS	
		DESIGNED BY: CT CHECKED BY: TLD DRAWN BY: JMW	PROJECT NO.: 1011520 DRAWING NO.: LOC DATE: 07/05/00	FIGURE A-10

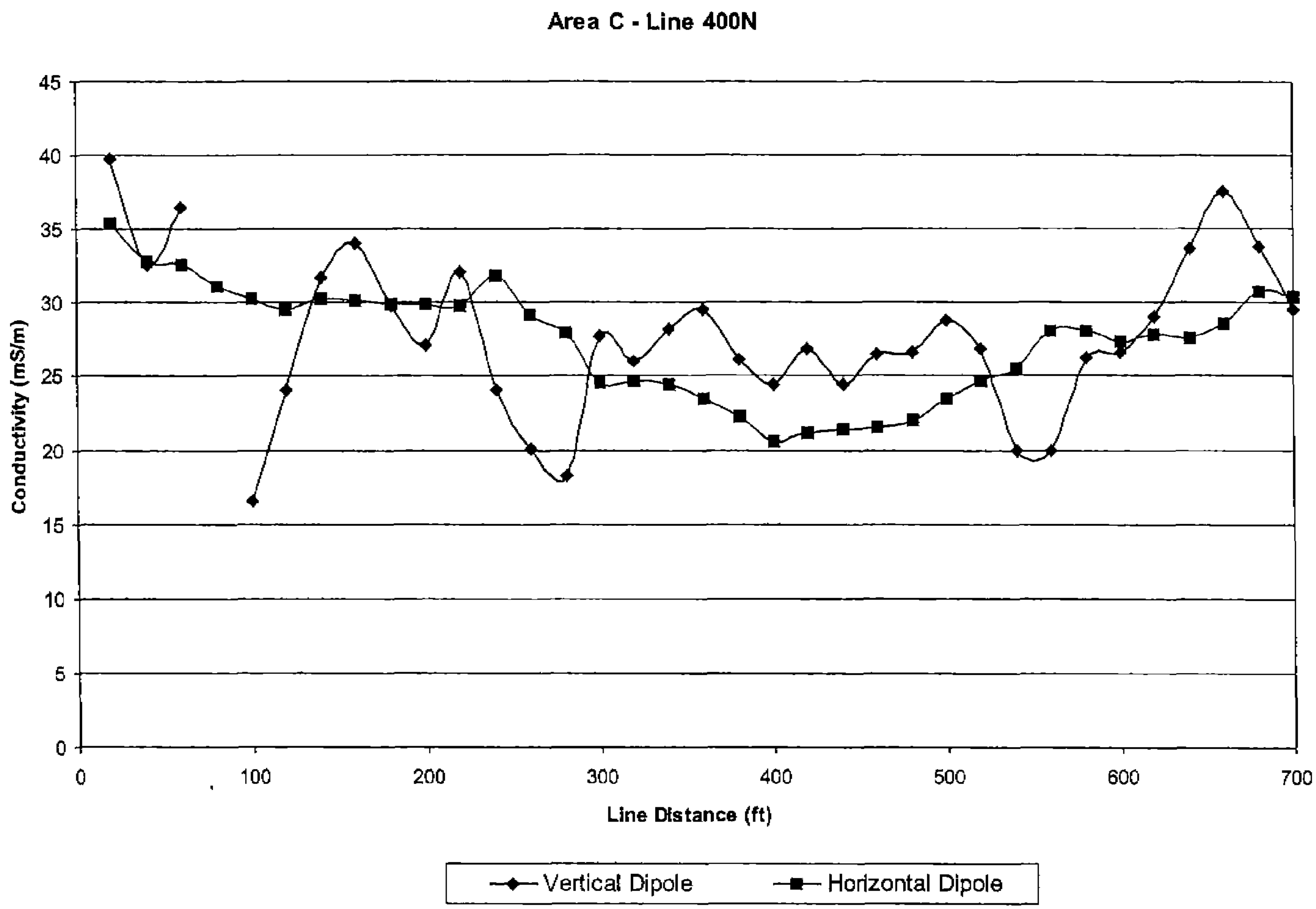

JUDGE'S OFFICE
STONEWALL COUNTY,
TEXAS

AREA C LINE 400N - EM34 DATA
SALT POLLUTION STUDY
STONEWALL COUNTY, TEXAS

DESIGNED BY:	CT	PROJECT NO.:	1011520	FIGURE
CHECKED BY:	TLD	DRAWING NO.:	LOC	A-11
DRAWN BY:	JMW	DATE:	07/05/00	

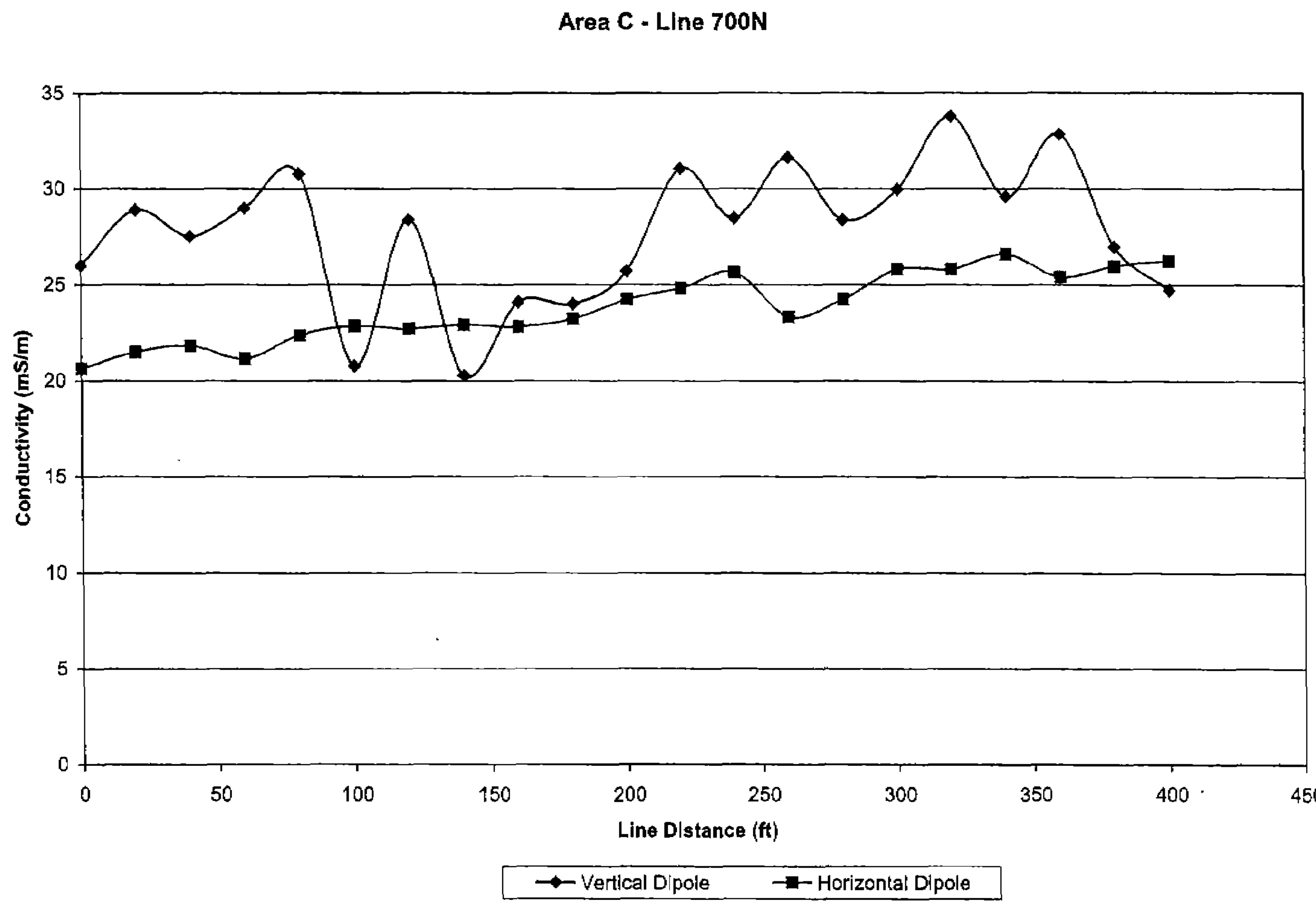

JUDGE'S OFFICE STONEWALL COUNTY, TEXAS		AREA C LINE 700N - EM34 DATA SALT POLLUTION STUDY STONEWALL COUNTY, TEXAS	
		DESIGNED BY: CT CHECKED BY: TLD DRAWN BY: JMW	PROJECT NO.: 1011520 DRAWING NO.: LOC DATE: 07/05/00	FIGURE A-12

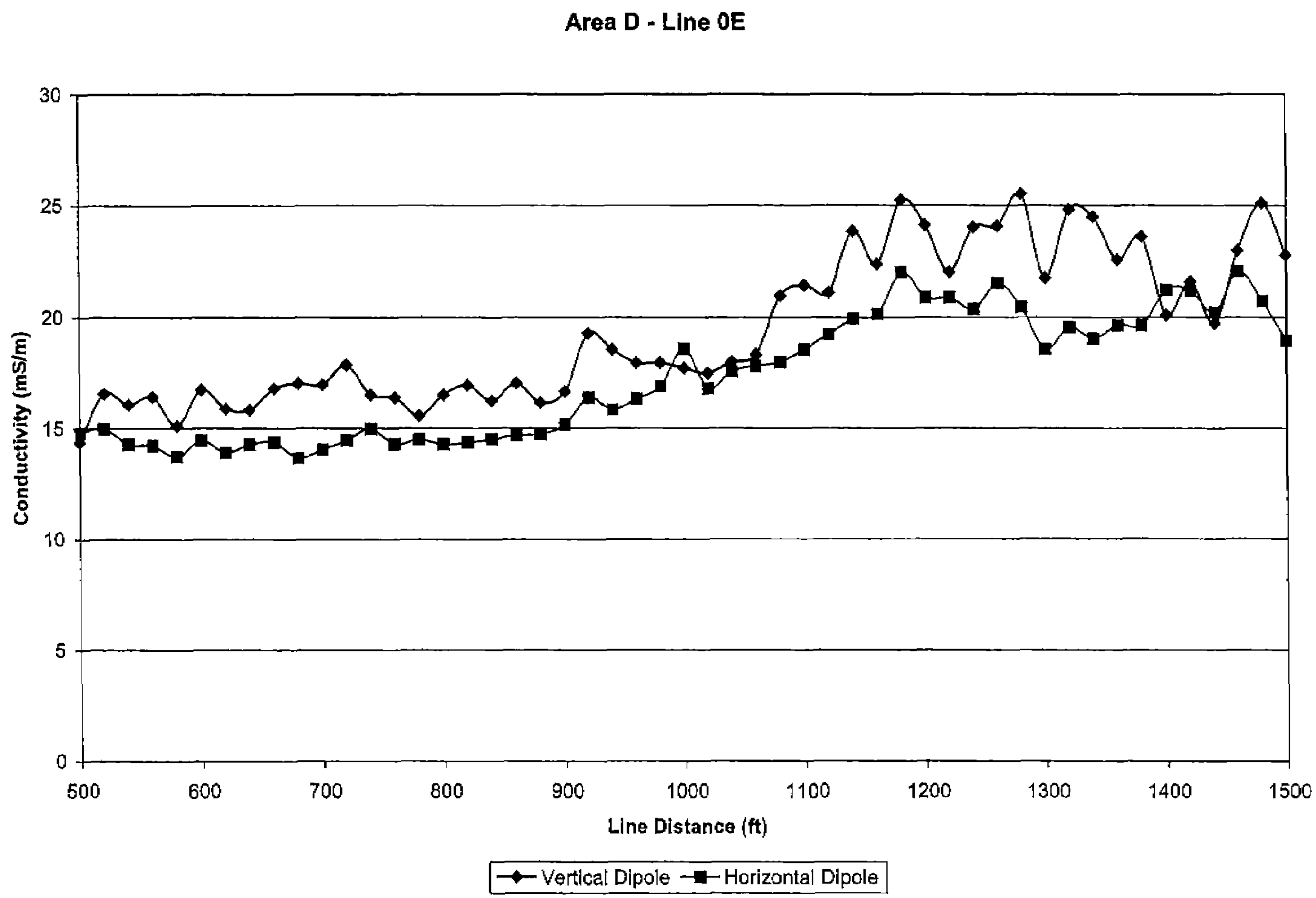

JUDGE'S OFFICE STONEWALL COUNTY, TEXAS	SDII	AREA D LINE 0E - EM34 DATA SALT POLLUTION STUDY STONEWALL COUNTY, TEXAS	
		DESIGNED BY: CT CHECKED BY: TLD DRAWN BY: JMW	PROJECT NO.: 1011520 DRAWING NO.: LOC DATE: 07/05/00	FIGURE A-13

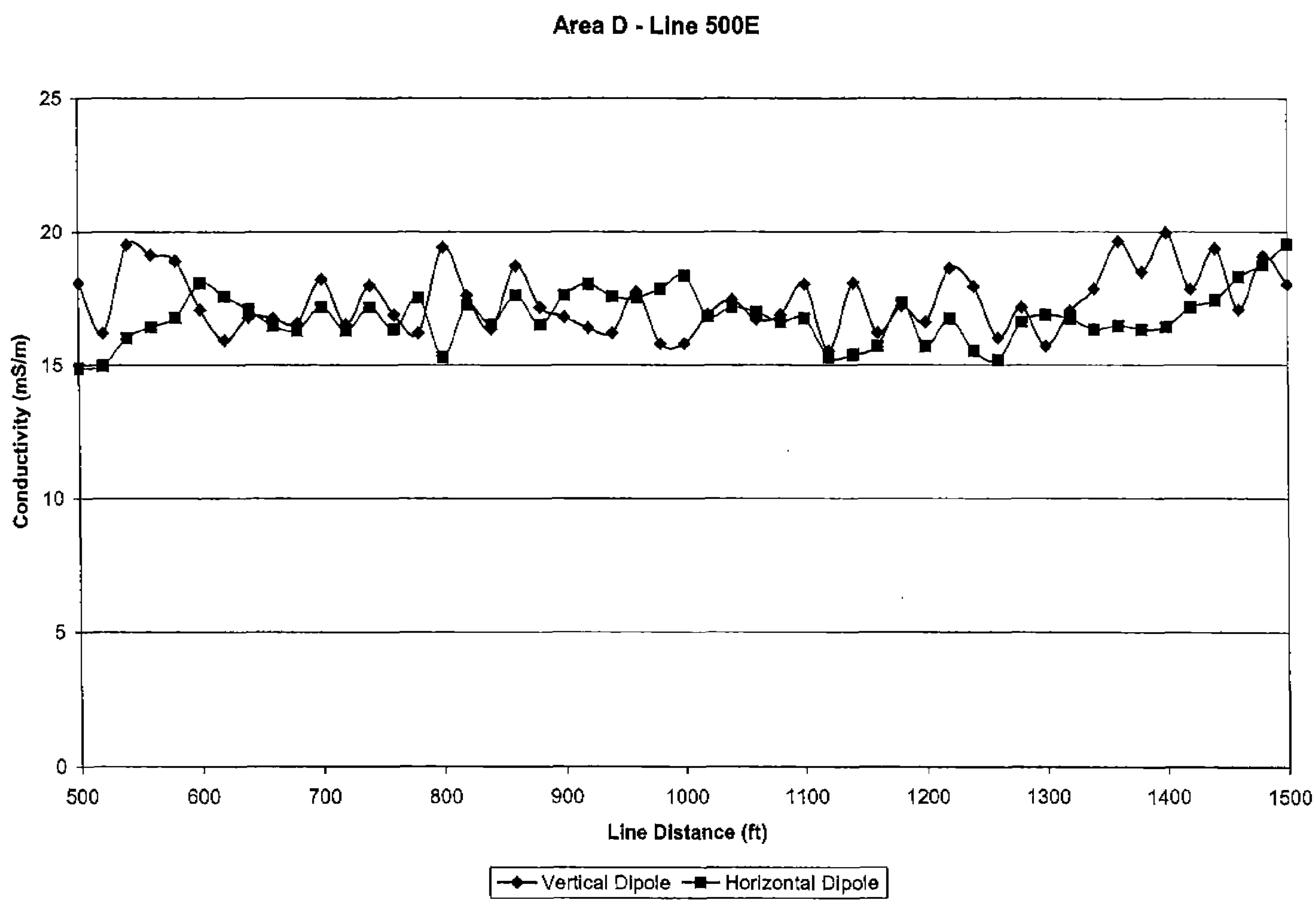

JUDGE'S OFFICE
STONEWALL COUNTY,
TEXAS

SDII GLOBAL

AREA D LINE 500E - EM34 DATA
SALT POLLUTION STUDY
STONEWALL COUNTY, TEXAS

DESIGNED BY:	CT	PROJECT NO.:	1011520	FIGURE
CHECKED BY:	TLD	DRAWING NO.:	LOC	A-14
DRAWN BY:	JMW	DATE:	07/05/00	

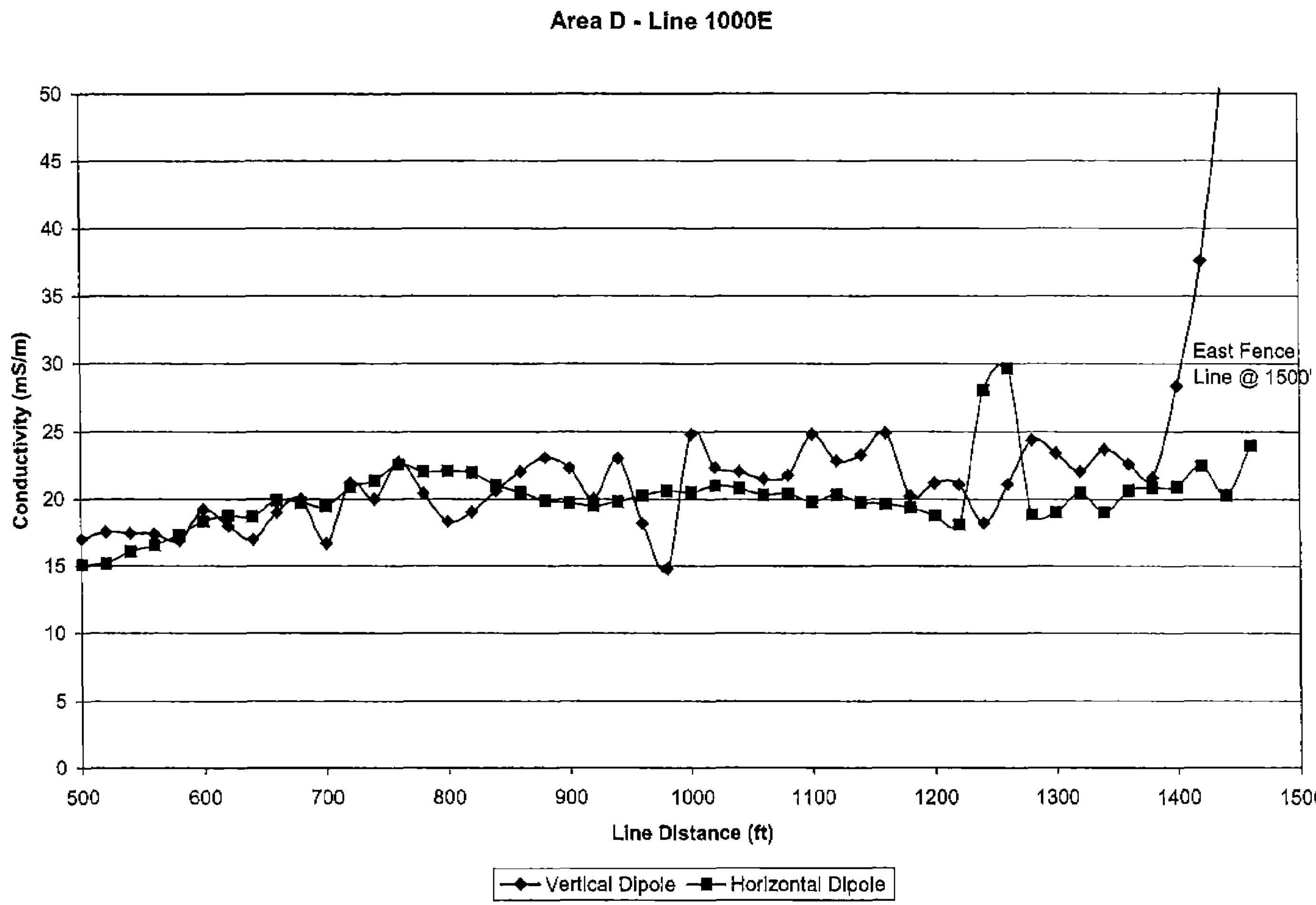

JUDGE'S OFFICE
STONEWALL COUNTY,
TEXAS

AREA D LINE 1000E - EM34 DATA
SALT POLLUTION STUDY
STONEWALL COUNTY, TEXAS

DESIGNED BY: CT	PROJECT NO.: 1011520	FIGURE
CHECKED BY: TLD	DRAWING NO.: LOC	A-15
DRAWN BY: JMW	DATE: 07/05/00	

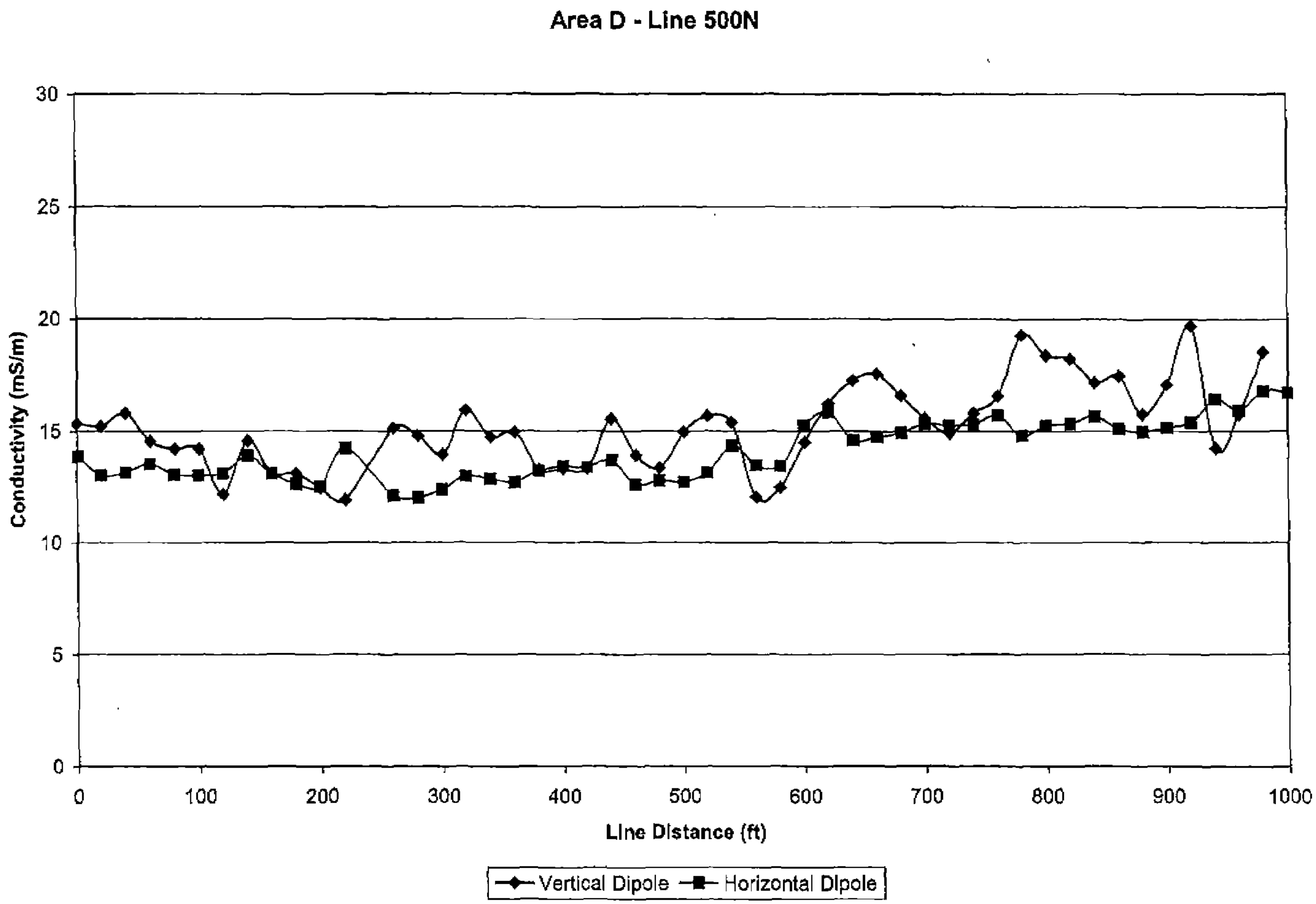

JUDGE'S OFFICE STONEWALL COUNTY, TEXAS	SDII GLOBAL	AREA D LINE 500N - EM34 DATA SALT POLLUTION STUDY STONEWALL COUNTY, TEXAS

DESIGNED BY: CT	PROJECT NO.: 1011520	FIGURE
CHECKED BY: TLD	DRAWING NO.: LOC	A-16
DRAWN BY: JMW	DATE: 07/05/00	

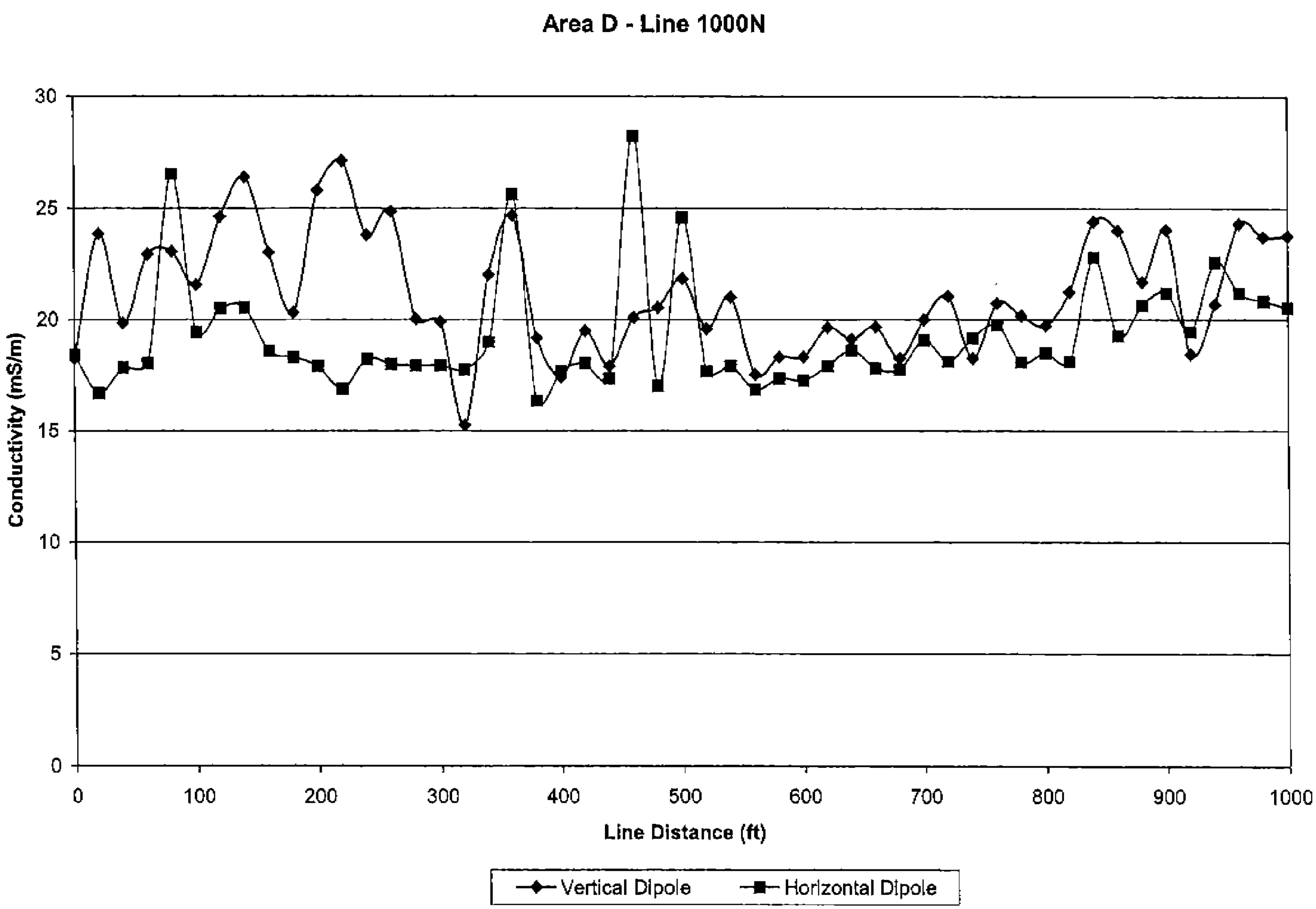

JUDGE'S OFFICE
STONEWALL COUNTY,
TEXAS

AREA D LINE 1000N - EM34 DATA
SALT POLLUTION STUDY
STONEWALL COUNTY, TEXAS

DESIGNED BY: CT	PROJECT NO.: 1011520	FIGURE
CHECKED BY: TLD	DRAWING NO.: LOC	A-17
DRAWN BY: JMW	DATE: 07/05/00	

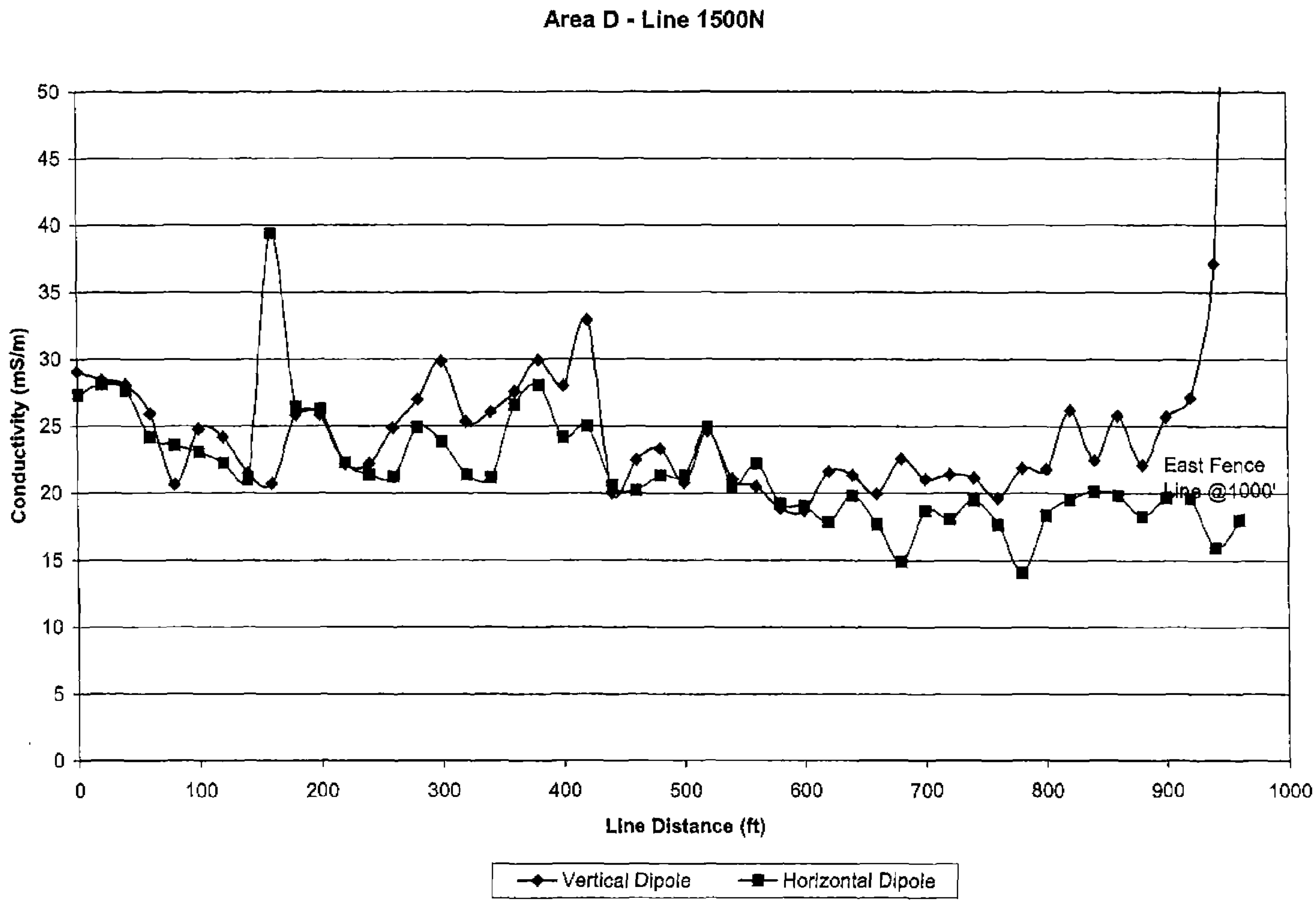

JUDGE'S OFFICE STONEWALL COUNTY, TEXAS		AREA D LINE 1500N - EM34 DATA SALT POLLUTION STUDY STONEWALL COUNTY, TEXAS

DESIGNED BY: CT	PROJECT NO.: 1011520	FIGURE
CHECKED BY: TLD	DRAWING NO.: LOC	A-18
DRAWN BY: JMW	DATE: 07/05/00	

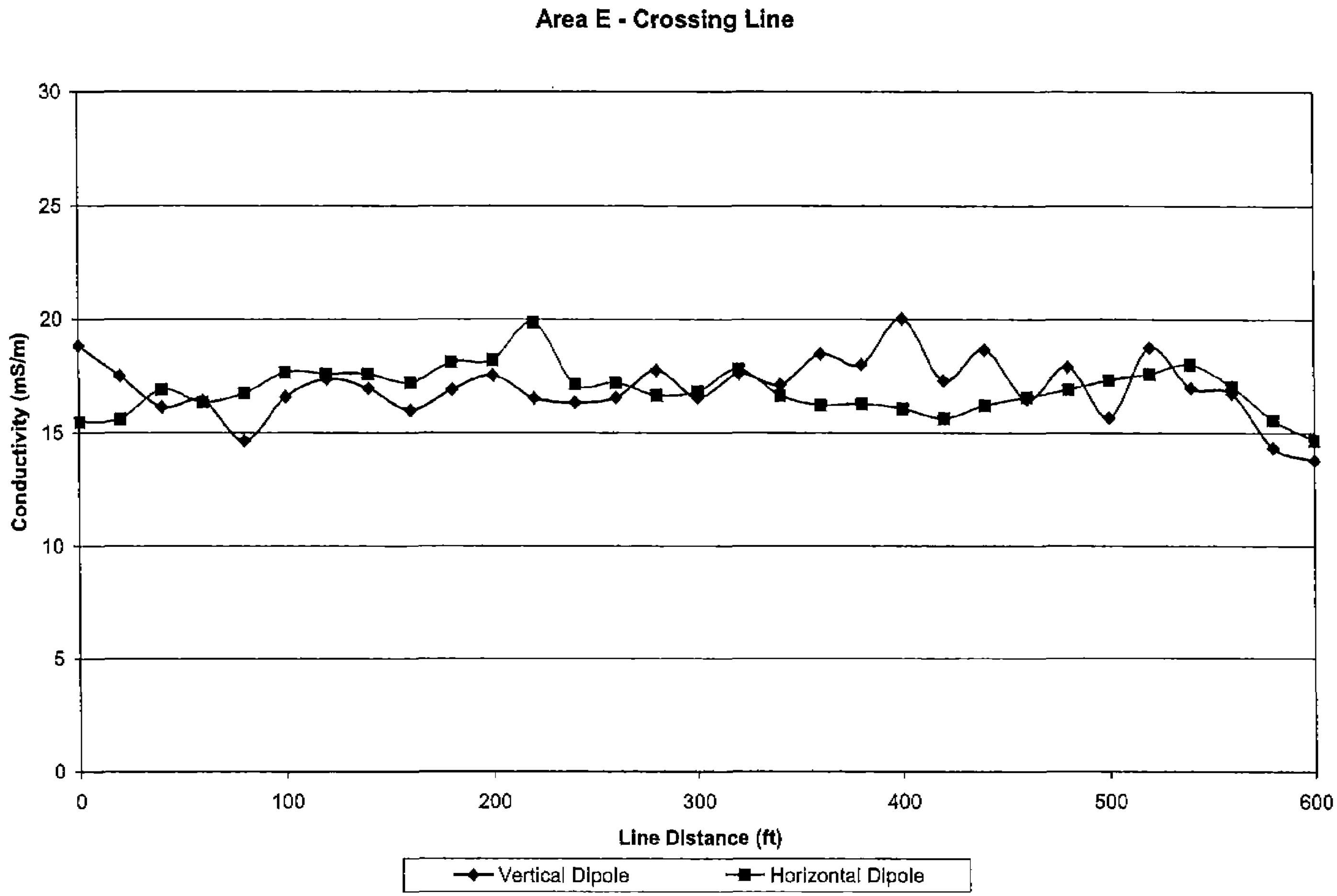

JUDGE'S OFFICE STONEWALL COUNTY, TEXAS	SDII GLOBAL	AREA E LINE 1 - EM34 DATA SALT POLLUTION STUDY STONEWALL COUNTY, TEXAS	
DESIGNED BY: CT CHECKED BY: TLD DRAWN BY: JMW	PROJECT NO.: 1011520 DRAWING NO.: LOC DATE: 07/05/00	FIGURE A-19	

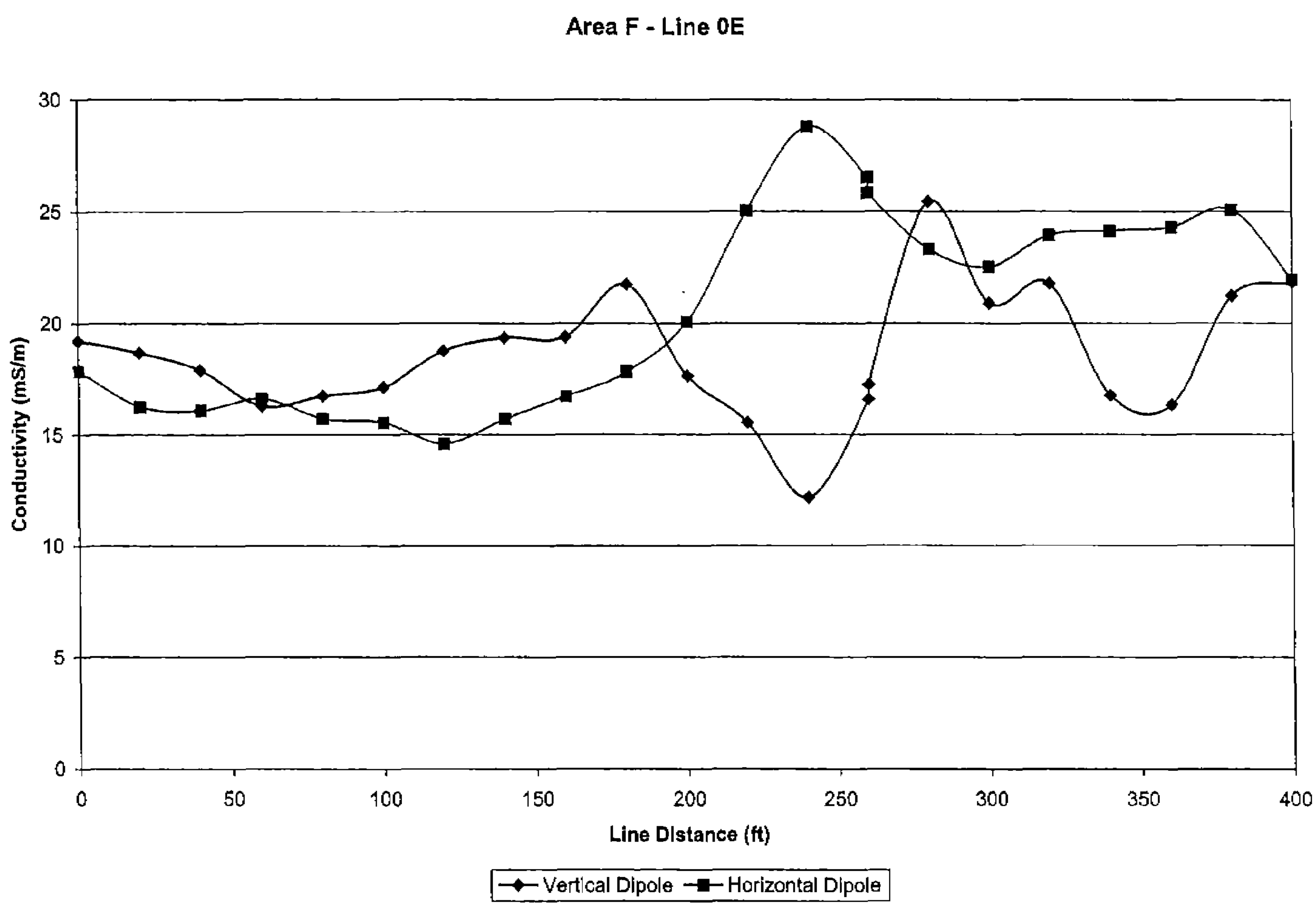

JUDGE'S OFFICE
STONEWALL COUNTY,
TEXAS

AREA F LINE 0E - EM34 DATA
SALT POLLUTION STUDY
STONEWALL COUNTY, TEXAS

DESIGNED BY: CT	PROJECT NO.: 1011520	FIGURE
CHECKED BY: TLD	DRAWING NO.: LOC	A-20
DRAWN BY: JMW	DATE: 07/06/00	

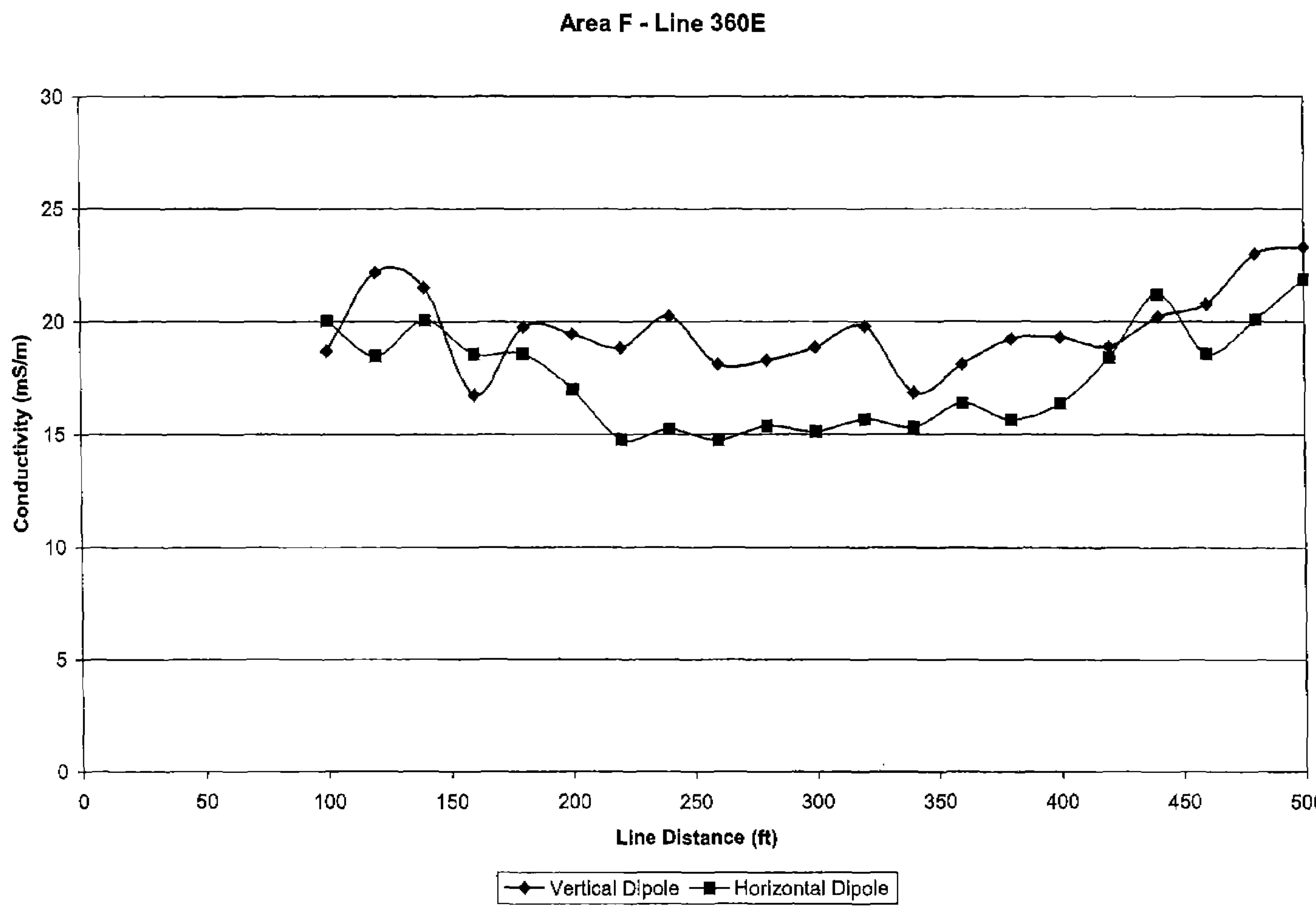

JUDGE'S OFFICE STONEWALL COUNTY, TEXAS	SDII GLOBAL	AREA F LINE 360E - EM34 DATA SALT POLLUTION STUDY STONEWALL COUNTY, TEXAS		
		DESIGNED BY: CT CHECKED BY: TLD DRAWN BY: JMW	PROJECT NO.: 1011520 DRAWING NO.: LOC DATE: 07/06/00	FIGURE A-21

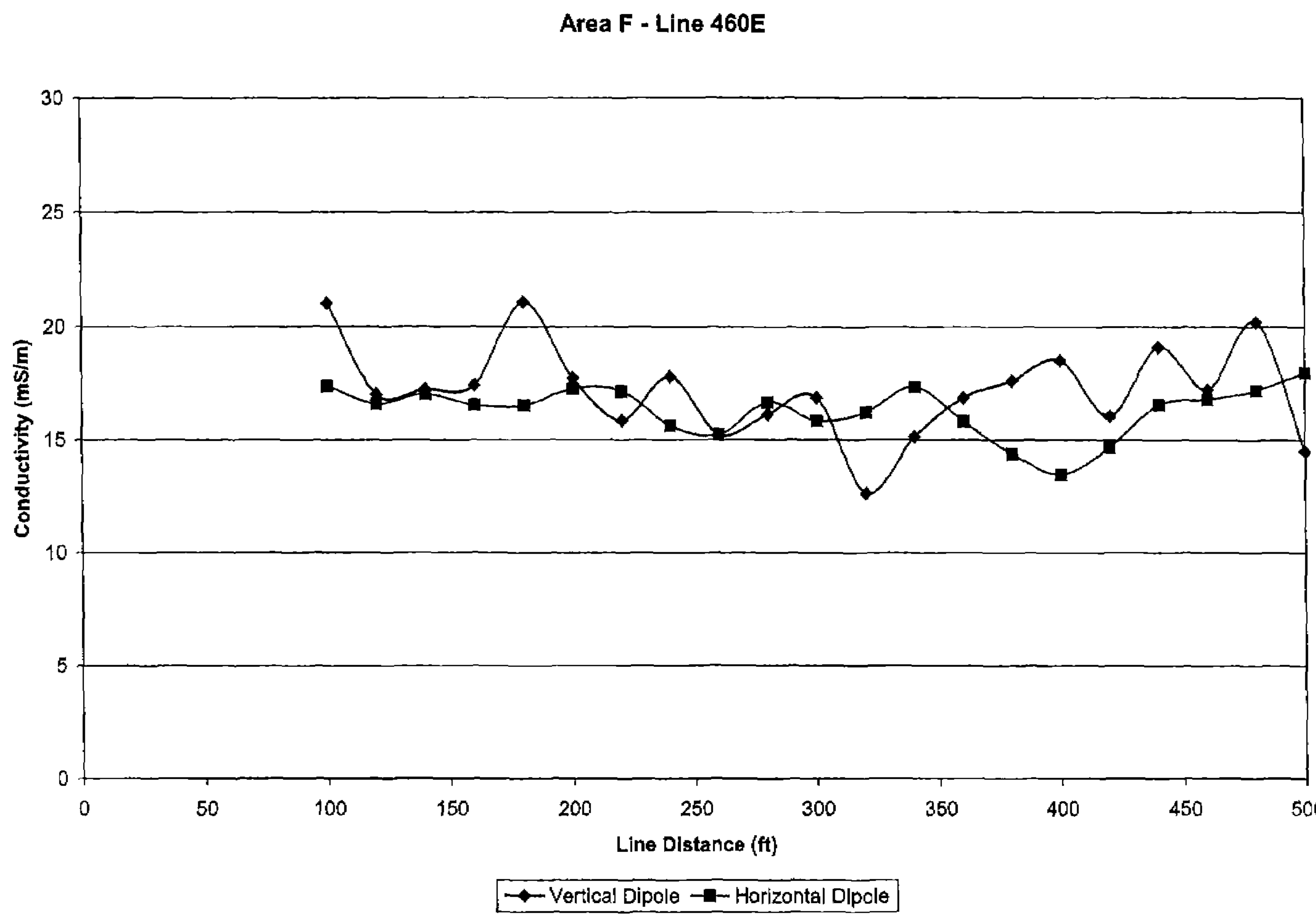

JUDGE'S OFFICE STONEWALL COUNTY, TEXAS	SDII GLOBAL	AREA F LINE 460E - EM34 DATA SALT POLLUTION STUDY STONEWALL COUNTY, TEXAS

DESIGNED BY: CT	PROJECT NO.: 1011520	FIGURE
CHECKED BY: TLD	DRAWING NO.: LOC	A-22
DRAWN BY: JMW	DATE: 07/06/00	

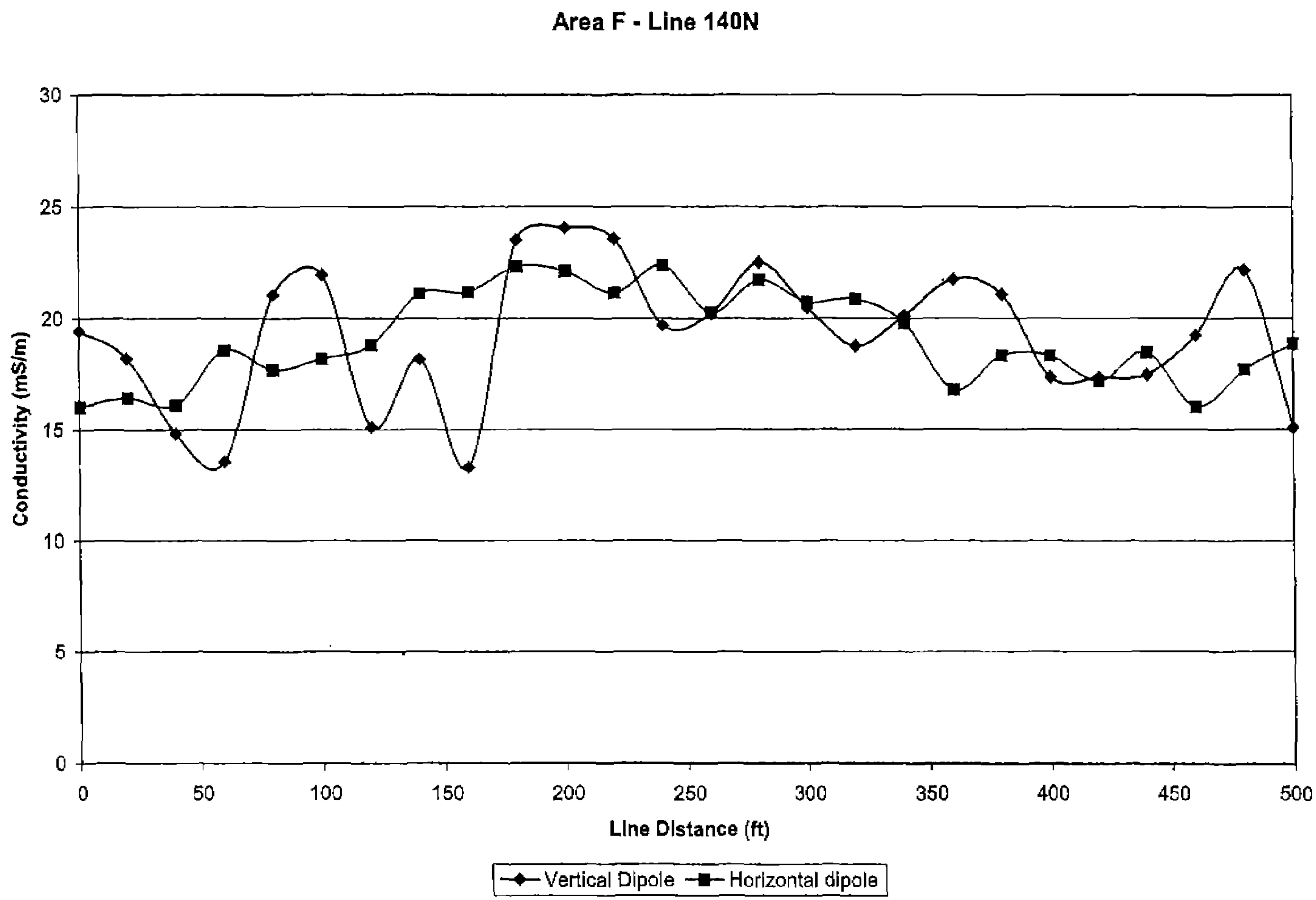

JUDGE'S OFFICE STONEWALL COUNTY, TEXAS		AREA F LINE 140N - EM34 DATA SALT POLLUTION STUDY STONEWALL COUNTY, TEXAS		
		DESIGNED BY: CT CHECKED BY: TLD DRAWN BY: JMW	PROJECT NO.: 1011520 DRAWING NO.: LOC DATE: 07/06/00	FIGURE A-23

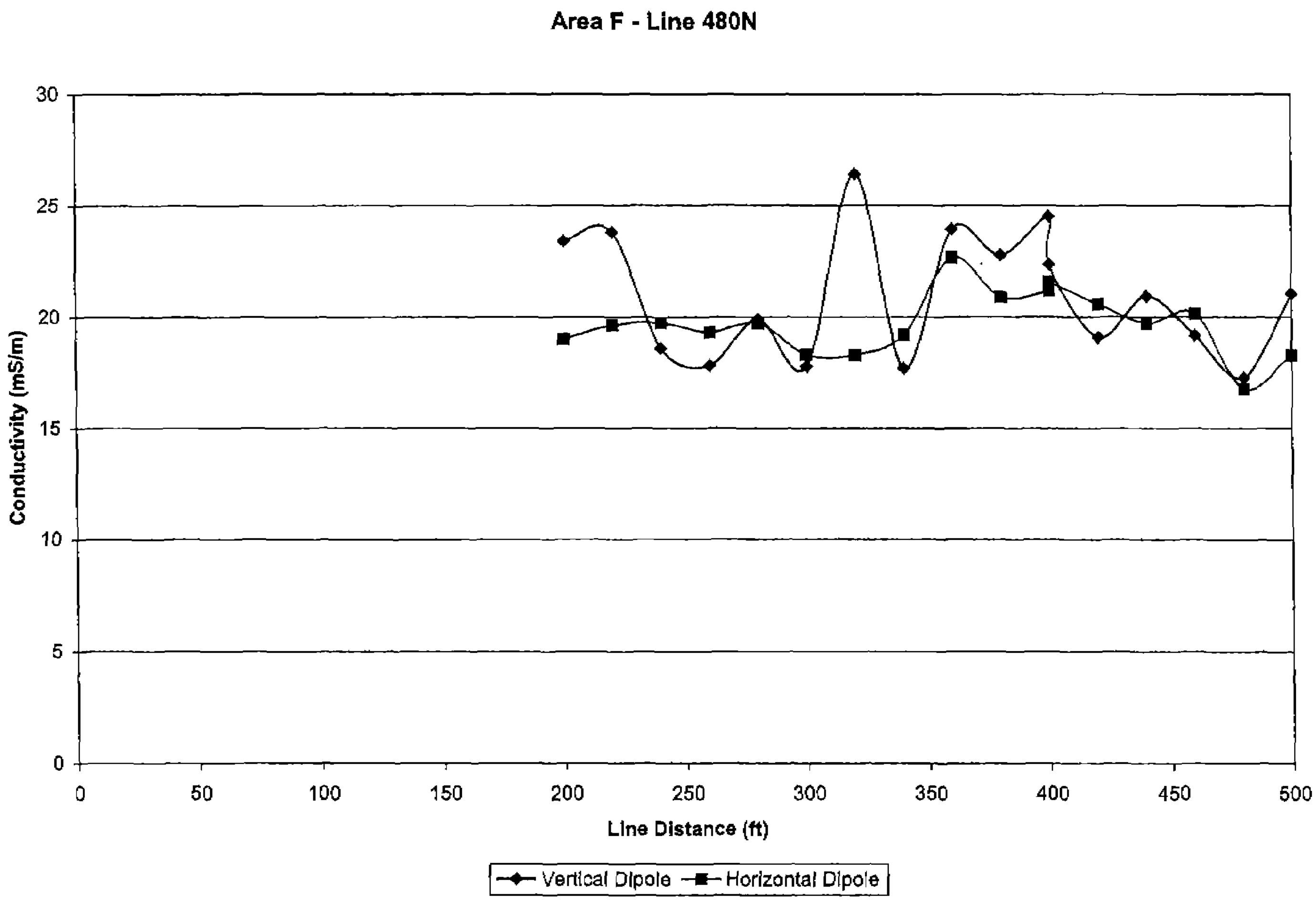

JUDGE'S OFFICE STONEWALL COUNTY, TEXAS	SDII GLOBAL	AREA F LINE 480N - EM34 DATA SALT POLLUTION STUDY STONEWALL COUNTY, TEXAS		
		DESIGNED BY: CT CHECKED BY: TLD DRAWN BY: JMW	PROJECT NO.: 1011520 DRAWING NO.: LOC DATE: 07/06/00	FIGURE A-24

APPENDIX B

PLOTS OF PROCESSED VLF DATA

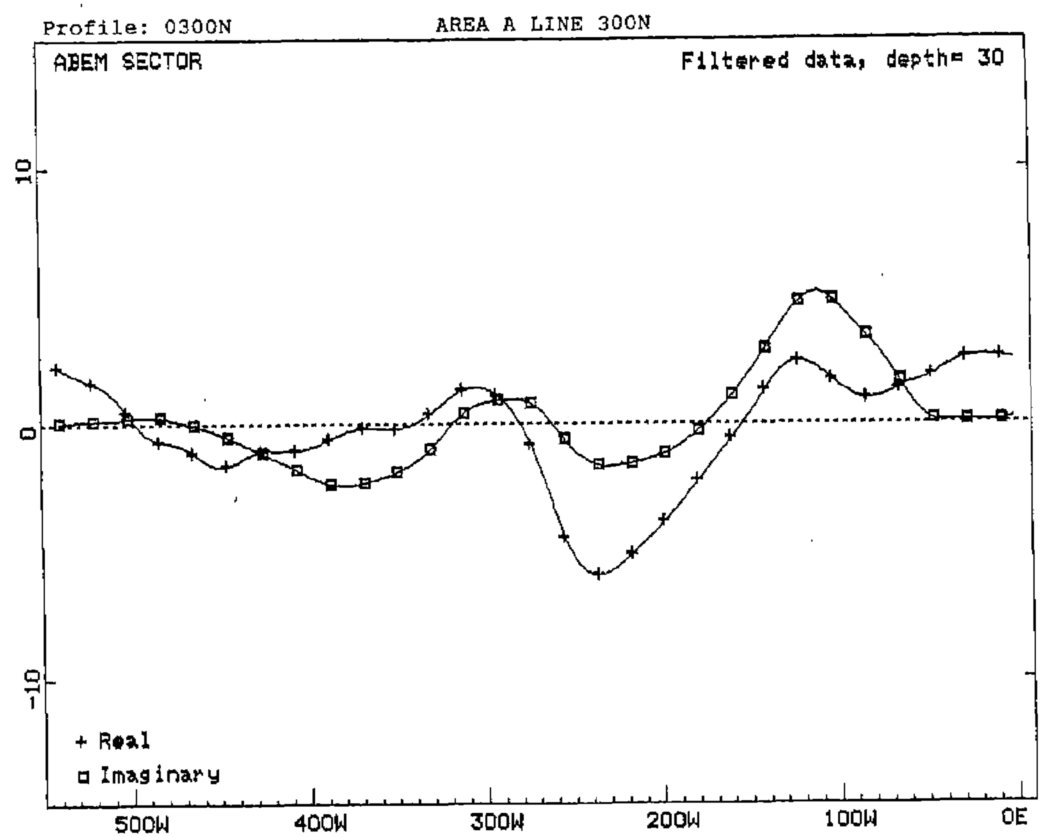

JUDGE'S OFFICE STONEWALL COUNTY, TEXAS	SDII GLOBAL	AREA A LINE 1 - VLF DATA SALT POLLUTION STUDY STONEWALL COUNTY, TEXAS		
		DESIGNED BY: CT CHECKED BY: TLD DRAWN BY: JMW	PROJECT NO.: 1011520 DRAWING NO.: LOC DATE: 07/05/00	FIGURE B-1

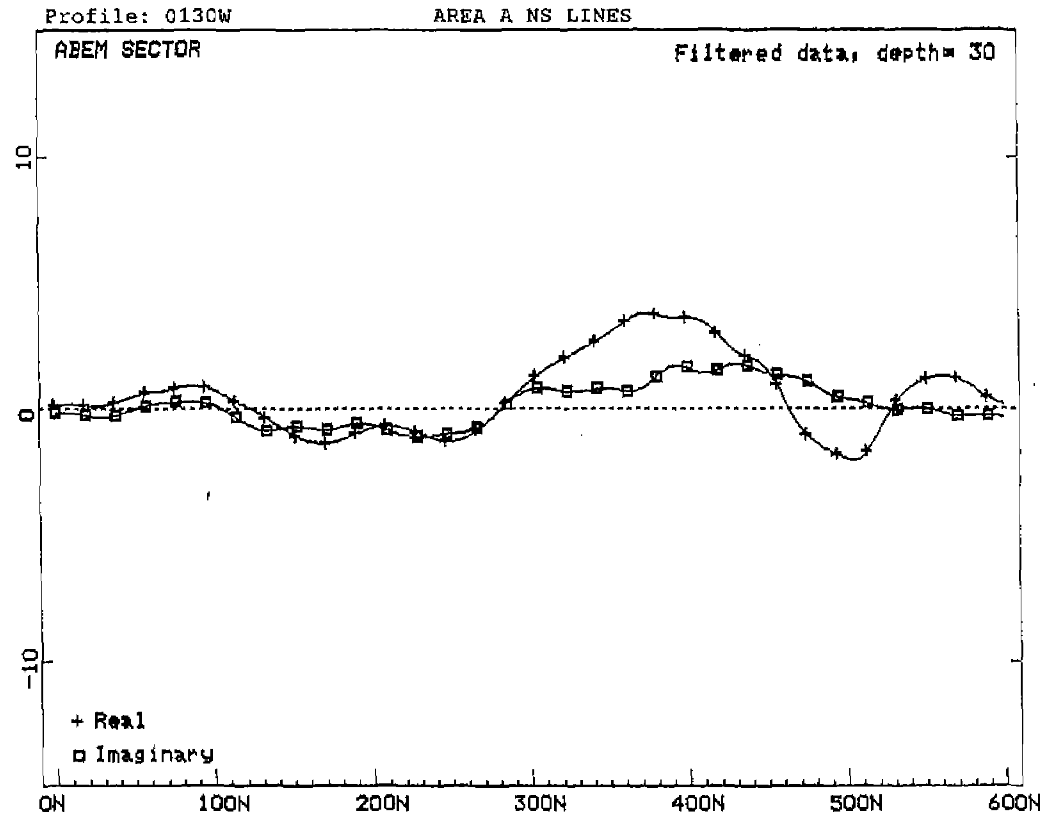

JUDGE'S OFFICE STONEWALL COUNTY, TEXAS	SDII GLOBAL	AREA A LINE 2 - VLF DATA SALT POLLUTION STUDY STONEWALL COUNTY, TEXAS	
		DESIGNED BY: CT CHECKED BY: TLD DRAWN BY: JMW	PROJECT NO.: 1011520 DRAWING NO.: LOC DATE: 07/05/00	FIGURE B-2

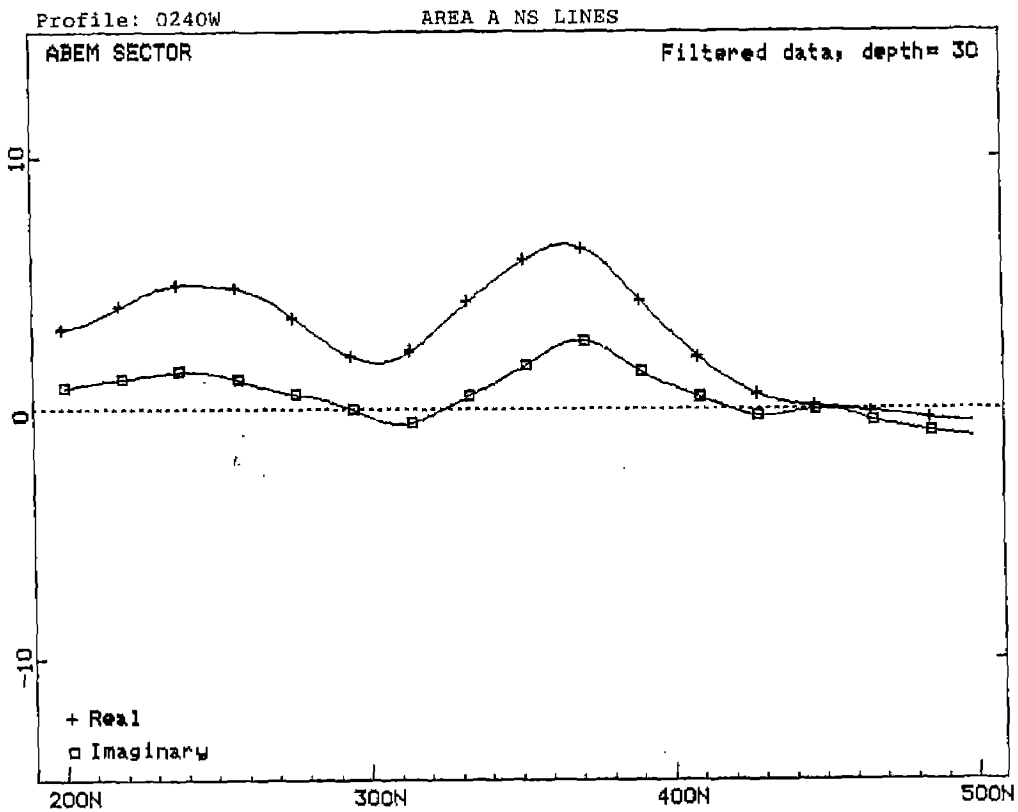

JUDGE'S OFFICE
STONEWALL COUNTY,
TEXAS

AREA A LINE 3 - VLF DATA
SALT POLLUTION STUDY
STONEWALL COUNTY, TEXAS

DESIGNED BY: CT	PROJECT NO.: 1011520	FIGURE
CHECKED BY: TLD	DRAWING NO.: LOC	B-3
DRAWN BY: JMW	DATE: 07/05/00	

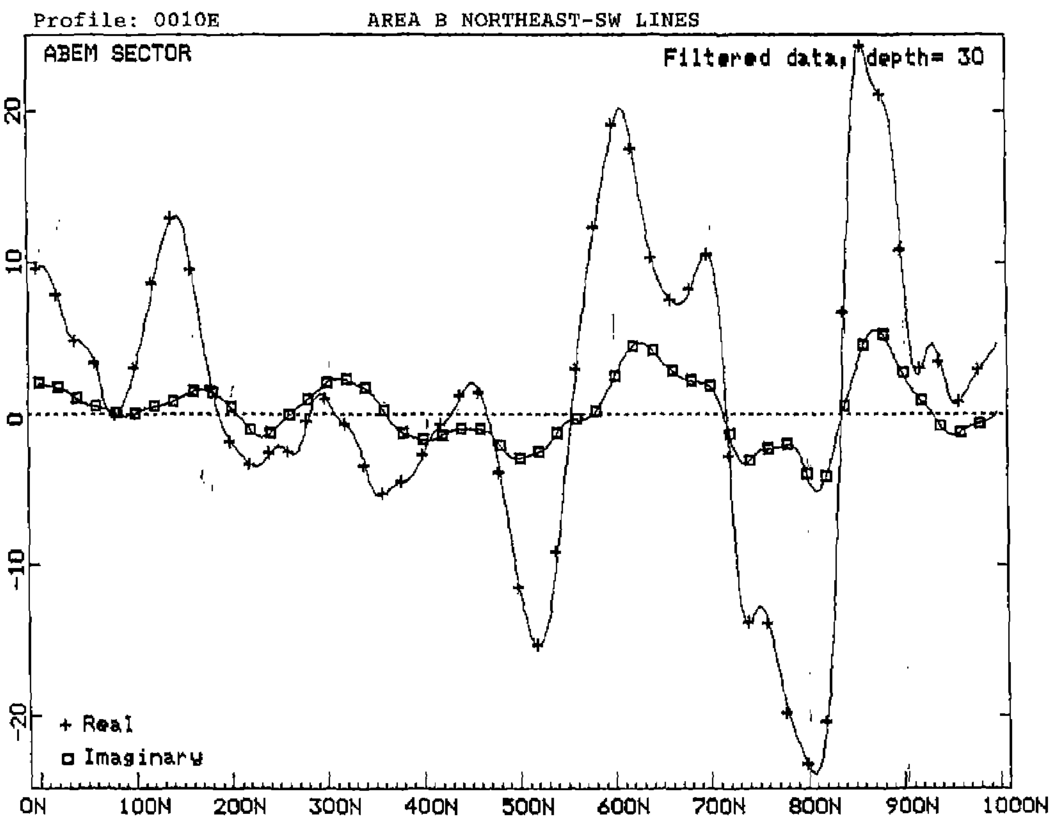

JUDGE'S OFFICE
STONEWALL COUNTY, TEXAS

SDII GLOBAL

AREA B LINE 0E - VLF DATA
SALT POLLUTION STUDY
STONEWALL COUNTY, TEXAS

DESIGNED BY:	CT	PROJECT NO.:	1011520	FIGURE
CHECKED BY:	TLD	DRAWING NO.:	LOC	B-4
DRAWN BY:	JMW	DATE:	07/05/00	

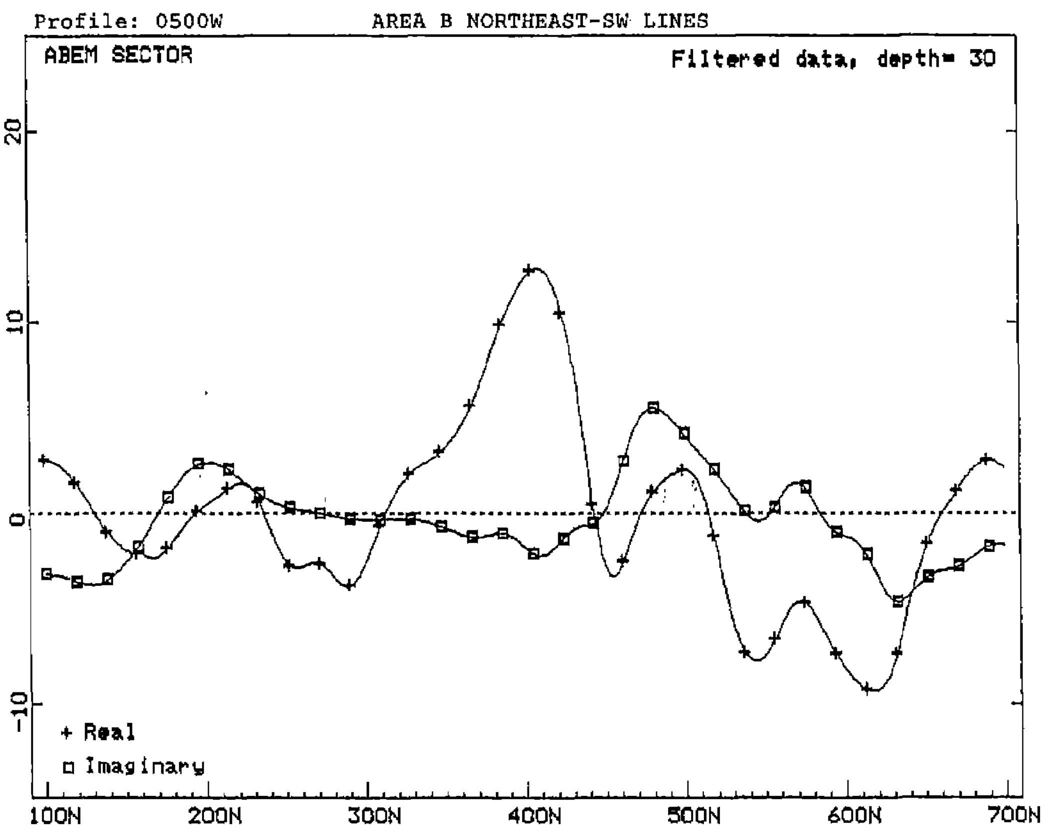

JUDGE'S OFFICE
STONEWALL COUNTY,
TEXAS

SDII GLOBAL

AREA B LINE 500W - VLF DATA
SALT POLLUTION STUDY
STONEWALL COUNTY, TEXAS

DESIGNED BY: CT	PROJECT NO.: 1011520	FIGURE
CHECKED BY: TLD	DRAWING NO.: LOC	B-5
DRAWN BY: JMW	DATE: 07/05/00	

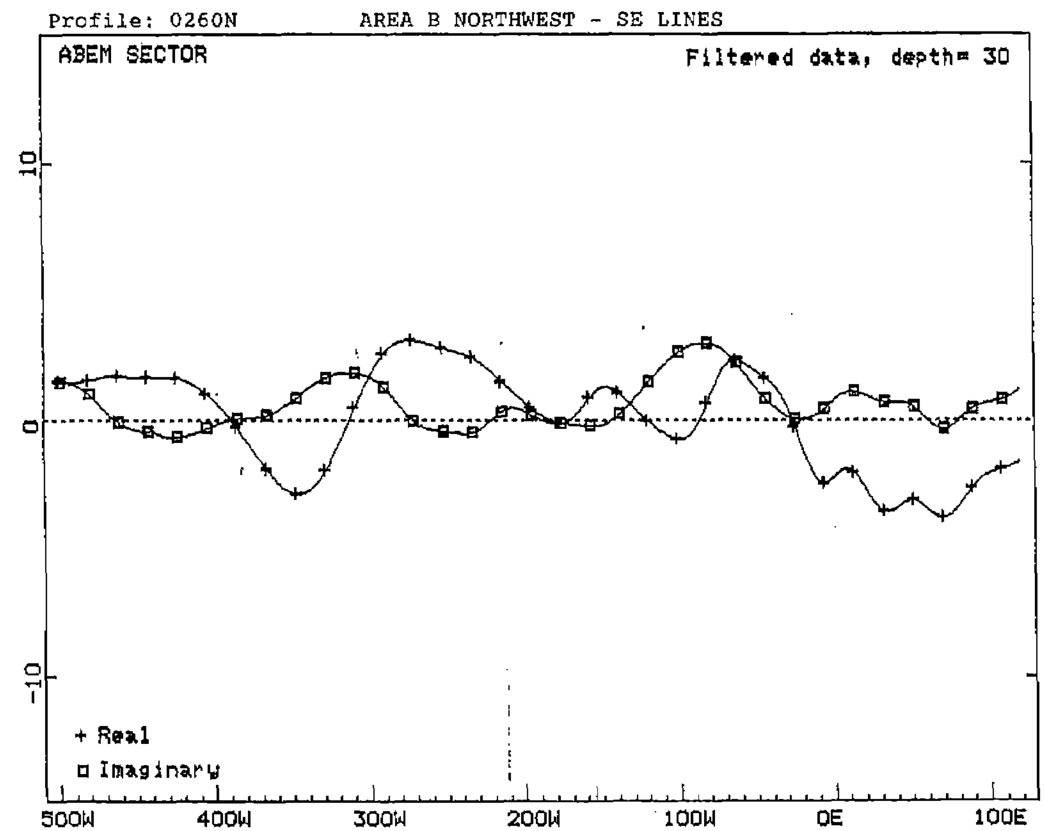

JUDGE'S OFFICE
STONEWALL COUNTY,
TEXAS

AREA B LINE 260N - VLF DATA
SALT POLLUTION STUDY
STONEWALL COUNTY, TEXAS

DESIGNED BY:	CT	PROJECT NO.:	1011520	FIGURE
CHECKED BY:	TLD	DRAWING NO.:	LOC	B-6
DRAWN BY:	JMW	DATE:	07/05/00	

Profile: 0400N AREA B NORTHWEST - SE LINES

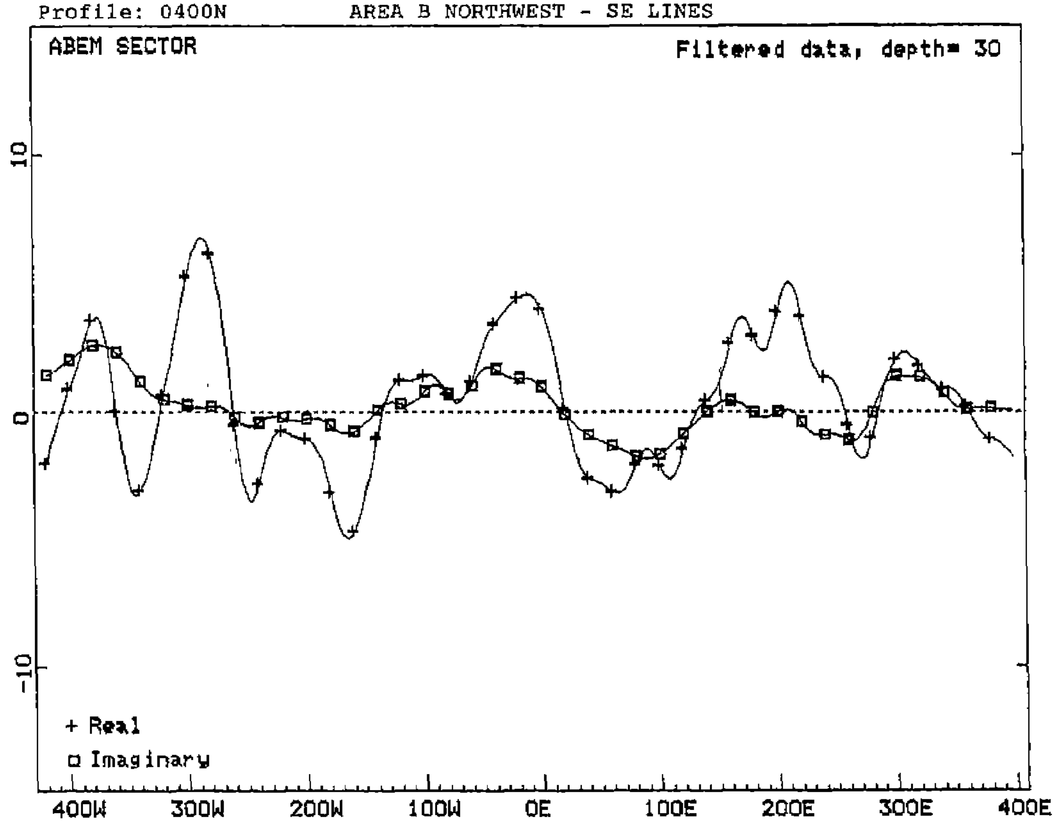

JUDGE'S OFFICE STONEWALL COUNTY, TEXAS	SDII GLOBAL	AREA B LINE 400N - VLF DATA SALT POLLUTION STUDY STONEWALL COUNTY, TEXAS	
		DESIGNED BY: CT CHECKED BY: TLD DRAWN BY: JMW	PROJECT NO.: 1011520 DRAWING NO.: LOC DATE: 07/05/00
			FIGURE B-7

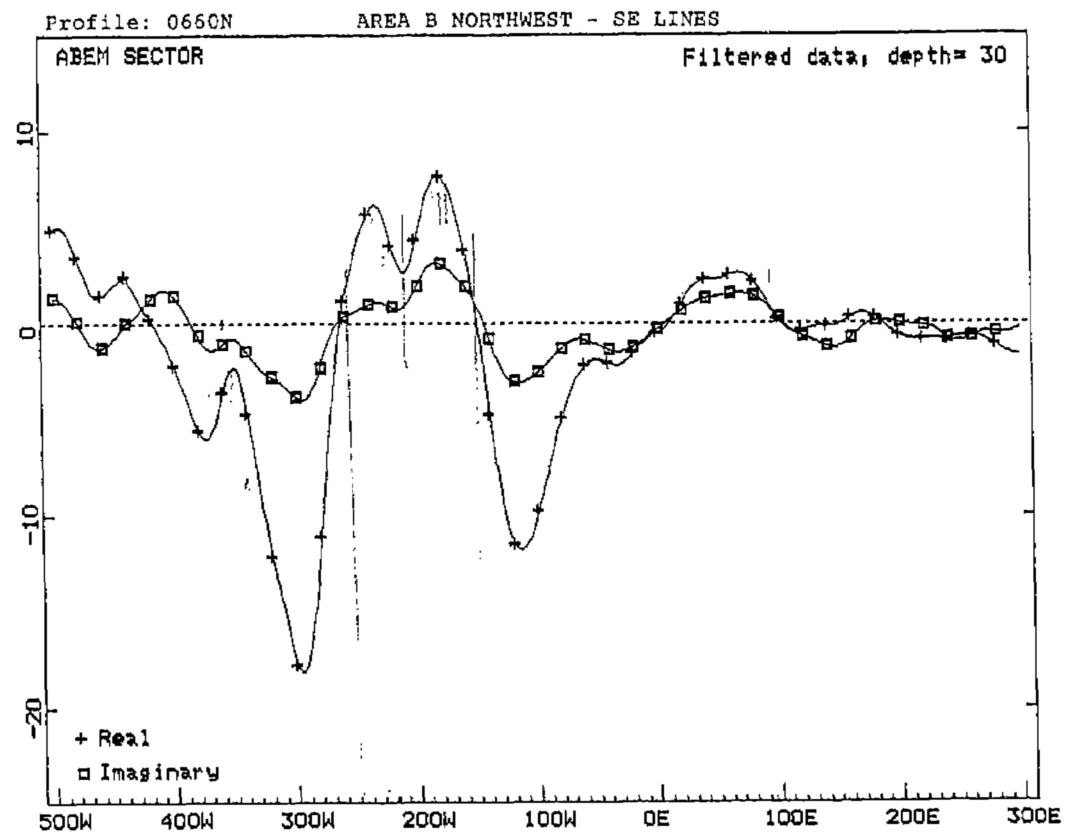

JUDGE'S OFFICE
STONEWALL COUNTY, TEXAS

AREA B LINE 660N - VLF DATA
SALT POLLUTION STUDY
STONEWALL COUNTY, TEXAS

DESIGNED BY: CT	PROJECT NO.:	1011520	FIGURE
CHECKED BY: TLD	DRAWING NO.:	LOC	B-8
DRAWN BY: JMW	DATE:	07/05/00	

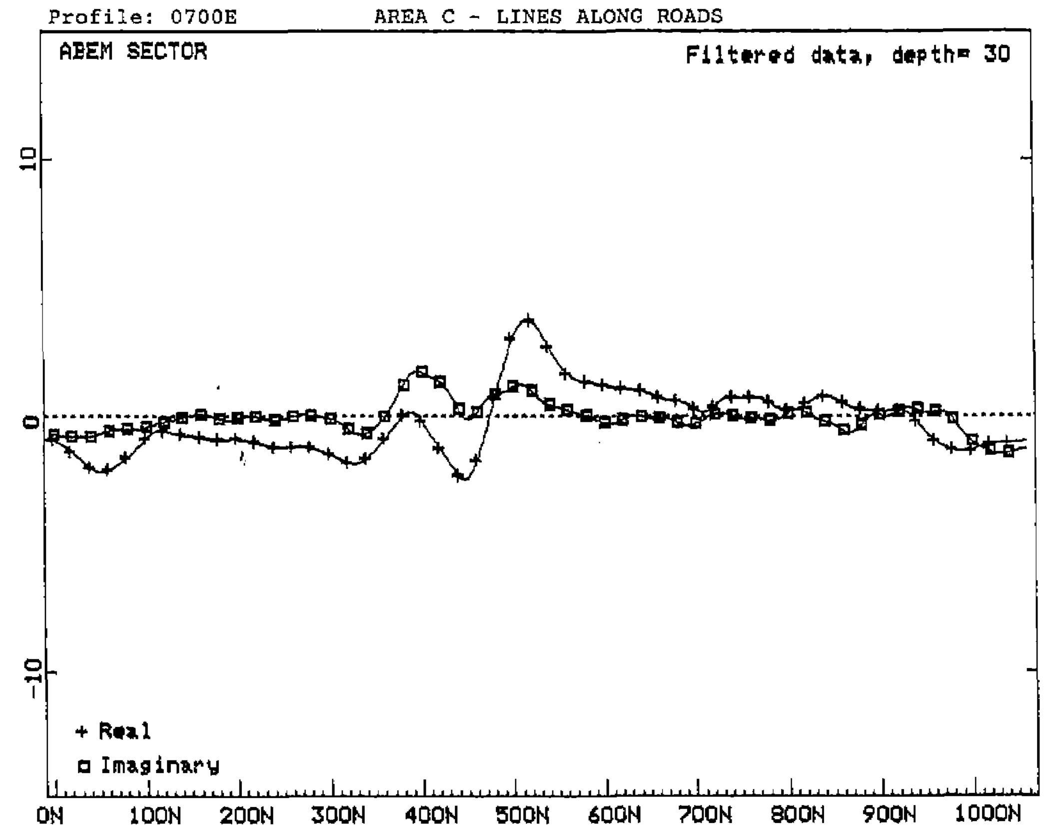

JUDGE'S OFFICE STONEWALL COUNTY, TEXAS	AREA C LINE 1 - VLF DATA SALT POLLUTION STUDY STONEWALL COUNTY, TEXAS		
	DESIGNED BY: CT CHECKED BY: TLD DRAWN BY: JMW	PROJECT NO.: 1011520 DRAWING NO.: LOC DATE: 07/05/00	FIGURE B-9

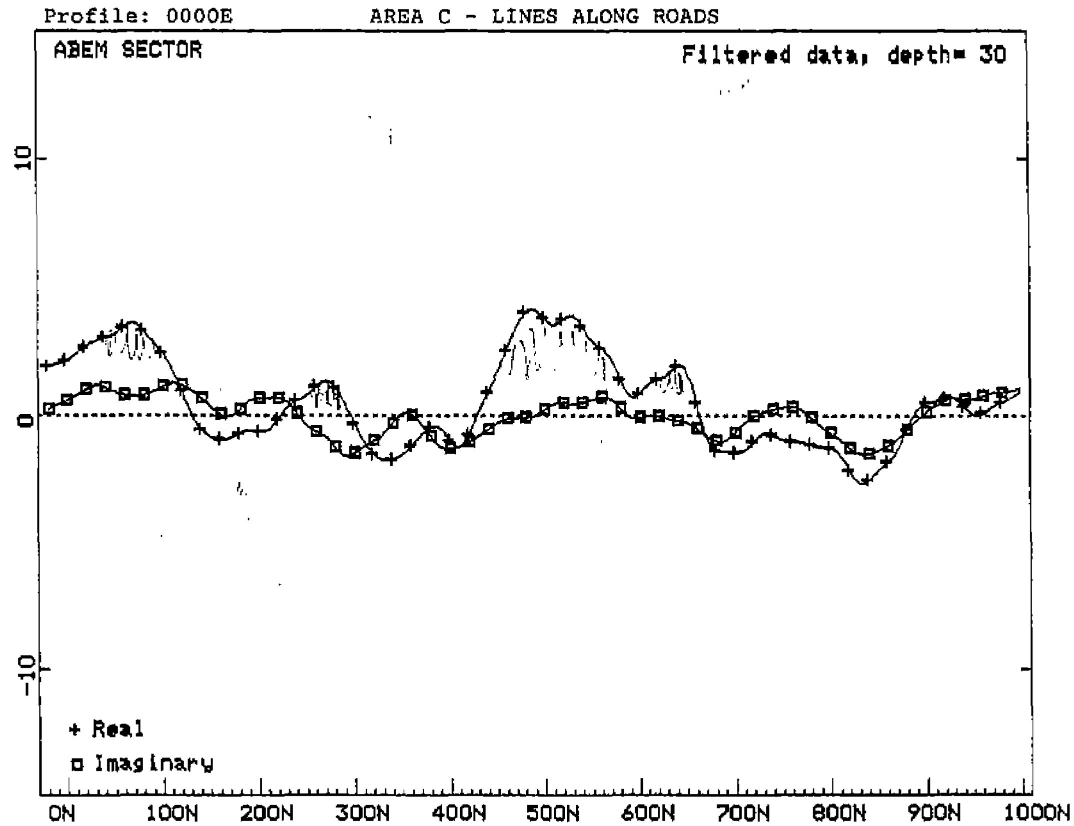

JUDGE'S OFFICE
STONEWALL COUNTY, TEXAS

AREA C LINE 2 - VLF DATA
SALT POLLUTION STUDY
STONEWALL COUNTY, TEXAS

DESIGNED BY: CT	PROJECT NO.: 1011520	FIGURE
CHECKED BY: TLD	DRAWING NO.: LOC	B-10
DRAWN BY: JMW	DATE: 07/05/00	

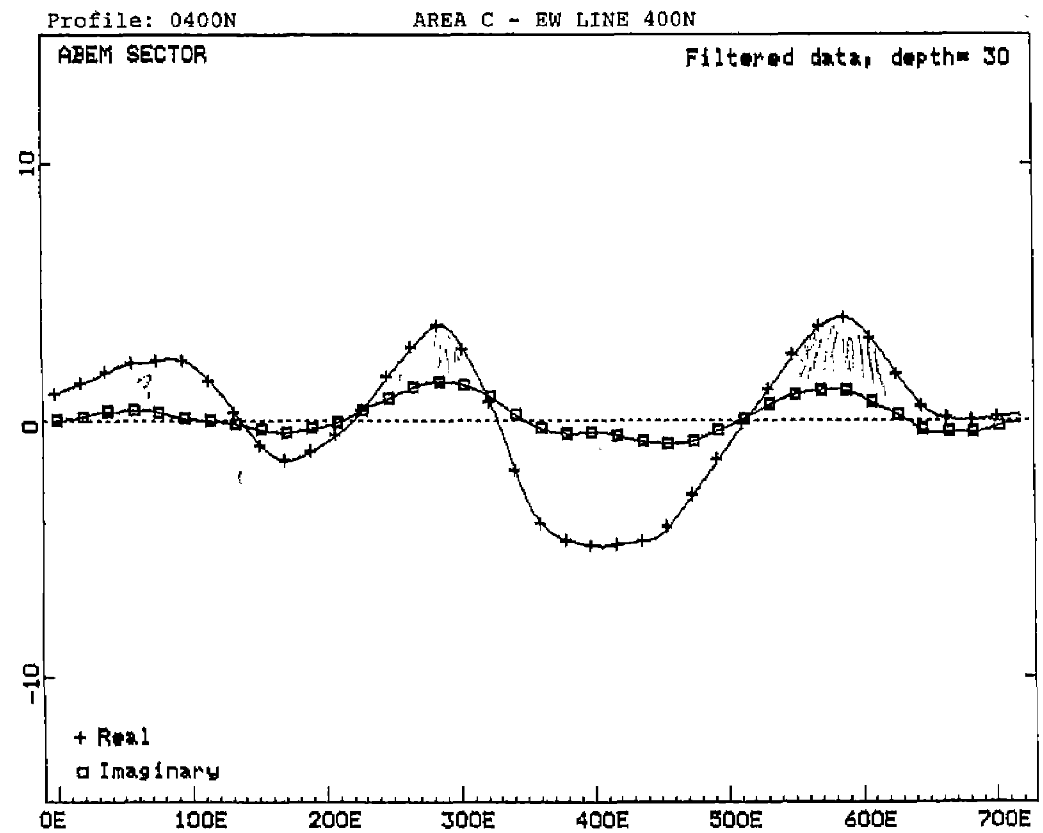

JUDGE'S OFFICE
STONEWALL COUNTY,
TEXAS

AREA C LINE 400N - VLF DATA
SALT POLLUTION STUDY
STONEWALL COUNTY, TEXAS

DESIGNED BY:	CT	PROJECT NO.:	1011520	FIGURE
CHECKED BY:	TLD	DRAWING NO.:	LOC	B-11
DRAWN BY:	JMW	DATE:	07/05/00	

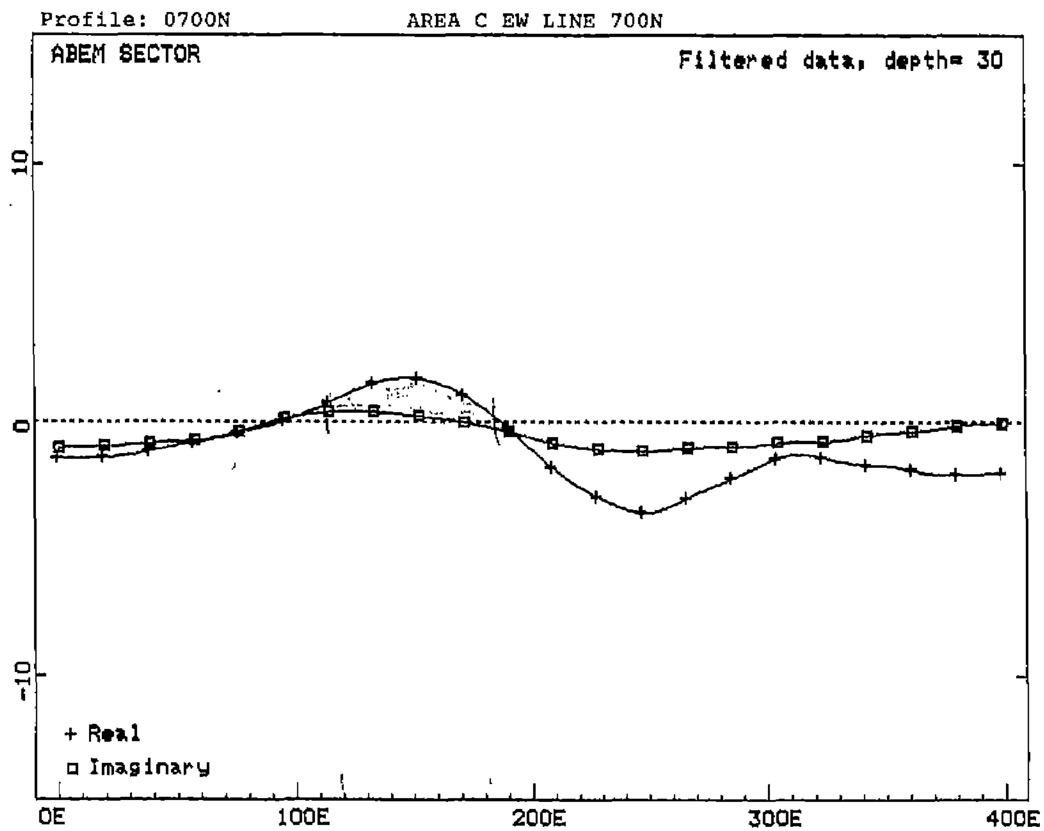

JUDGE'S OFFICE
STONEWALL COUNTY,
TEXAS

AREA C LINE 700N - VLF DATA
SALT POLLUTION STUDY
STONEWALL COUNTY, TEXAS

DESIGNED BY: CT	PROJECT NO.:	1011520	FIGURE
CHECKED BY: TLD	DRAWING NO.:	LOC	B-12
DRAWN BY: JMW	DATE:	07/05/00	

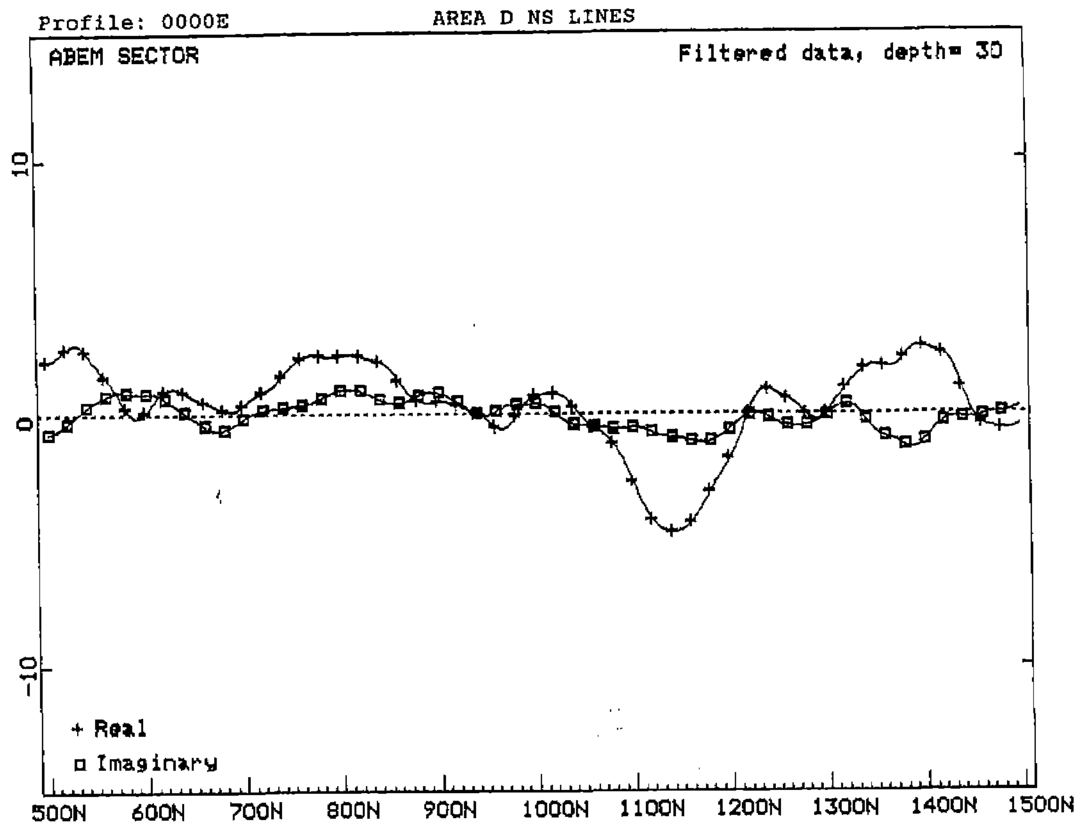

JUDGE'S OFFICE
STONEWALL COUNTY,
TEXAS

SDII GLOBAL

AREA D LINE 0E - VLF DATA
SALT POLLUTION STUDY
STONEWALL COUNTY, TEXAS

DESIGNED BY: CT	PROJECT NO.: 1011520	FIGURE
CHECKED BY: TLD	DRAWING NO.: LOC	B-13
DRAWN BY: JMW	DATE: 07/05/00	

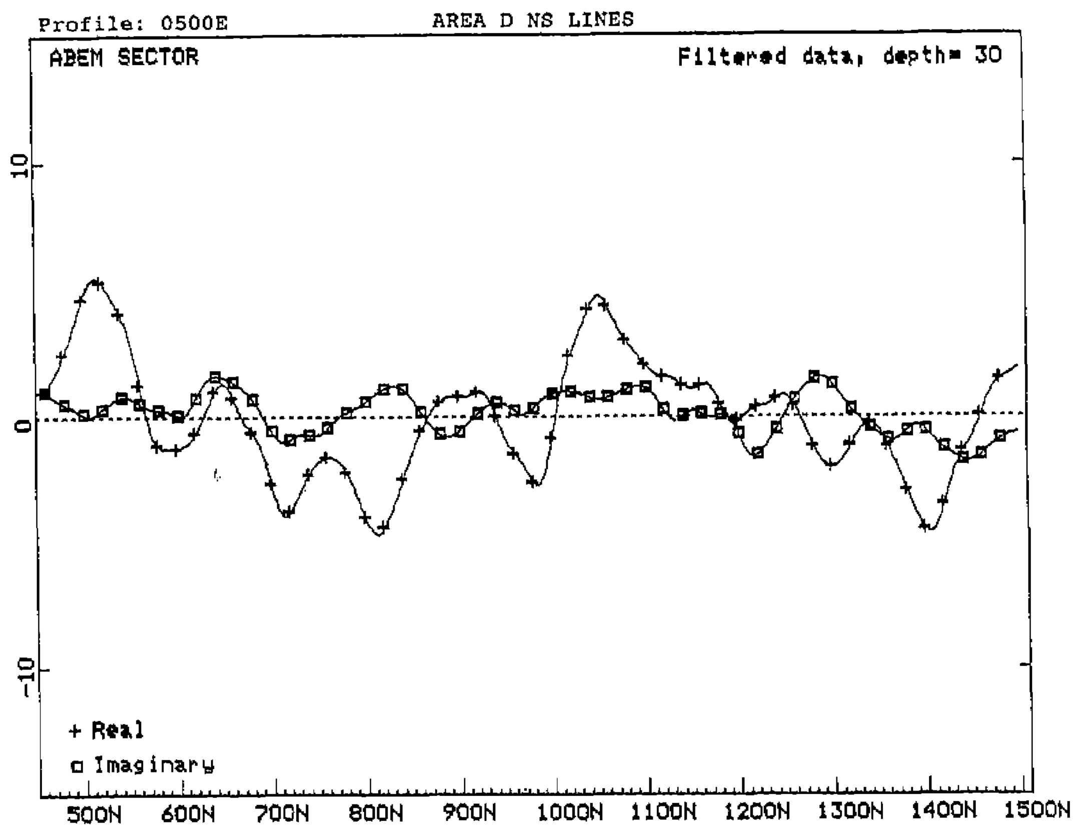

JUDGE'S OFFICE STONEWALL COUNTY, TEXAS	SDII GLOBAL	AREA D LINE 500E - VLF DATA SALT POLLUTION STUDY STONEWALL COUNTY, TEXAS

DESIGNED BY:	CT	PROJECT NO.:	1011520	FIGURE
CHECKED BY:	TLD	DRAWING NO.:	LOC	B-14
DRAWN BY:	JMW	DATE:	07/05/00	

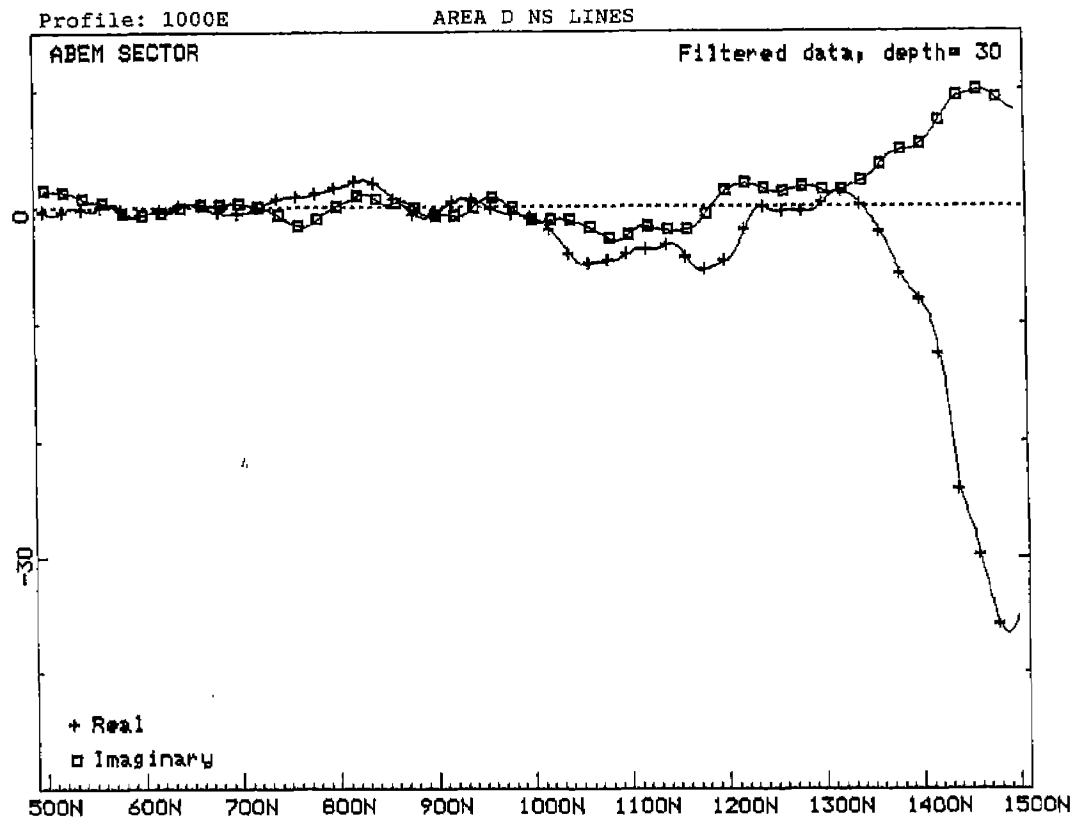

JUDGE'S OFFICE STONEWALL COUNTY, TEXAS	SDII GLOBAL	AREA D LINE 1000E - VLF DATA SALT POLLUTION STUDY STONEWALL COUNTY, TEXAS	
DESIGNED BY: CT CHECKED BY: TLD DRAWN BY: JMW	PROJECT NO.: 1011520 DRAWING NO.: LOC DATE: 07/05/00	FIGURE B-15	

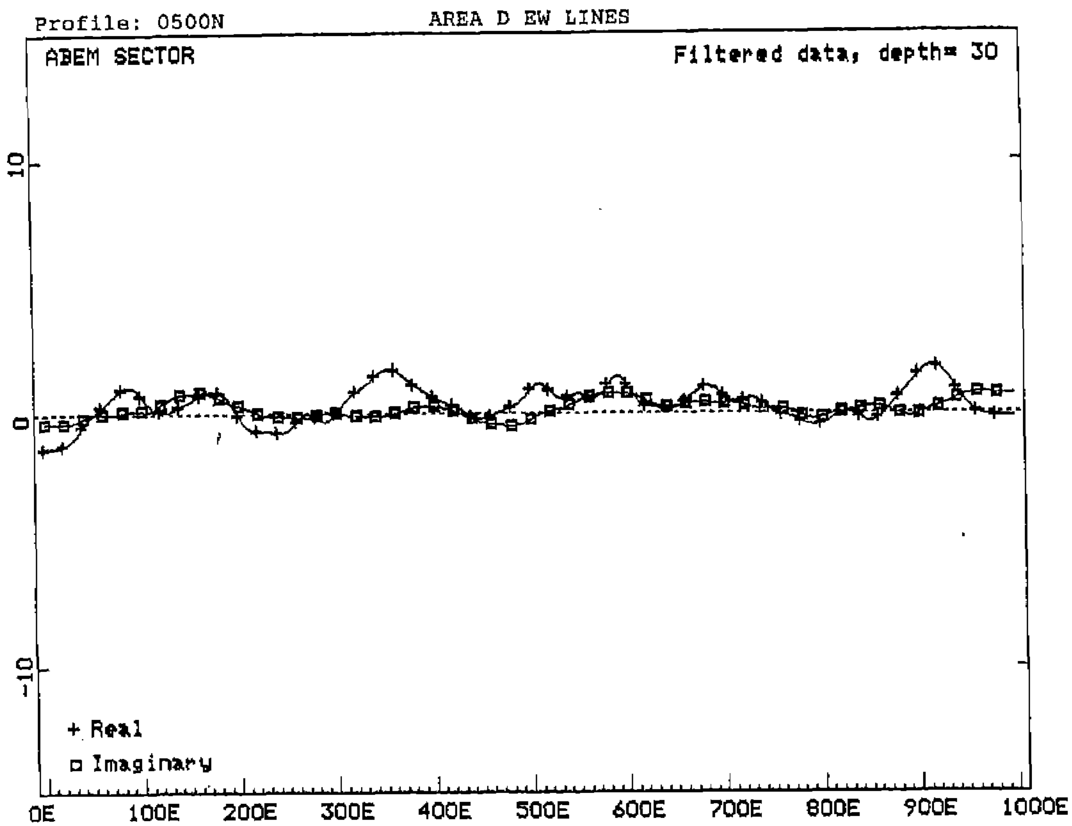

JUDGE'S OFFICE
STONEWALL COUNTY,
TEXAS

AREA D LINE 500N - VLF DATA
SALT POLLUTION STUDY
STONEWALL COUNTY, TEXAS

DESIGNED BY:	CT	PROJECT NO.:	1011520	FIGURE
CHECKED BY:	TLD	DRAWING NO.:	LOC	B-16
DRAWN BY:	JMW	DATE:	07/05/00	

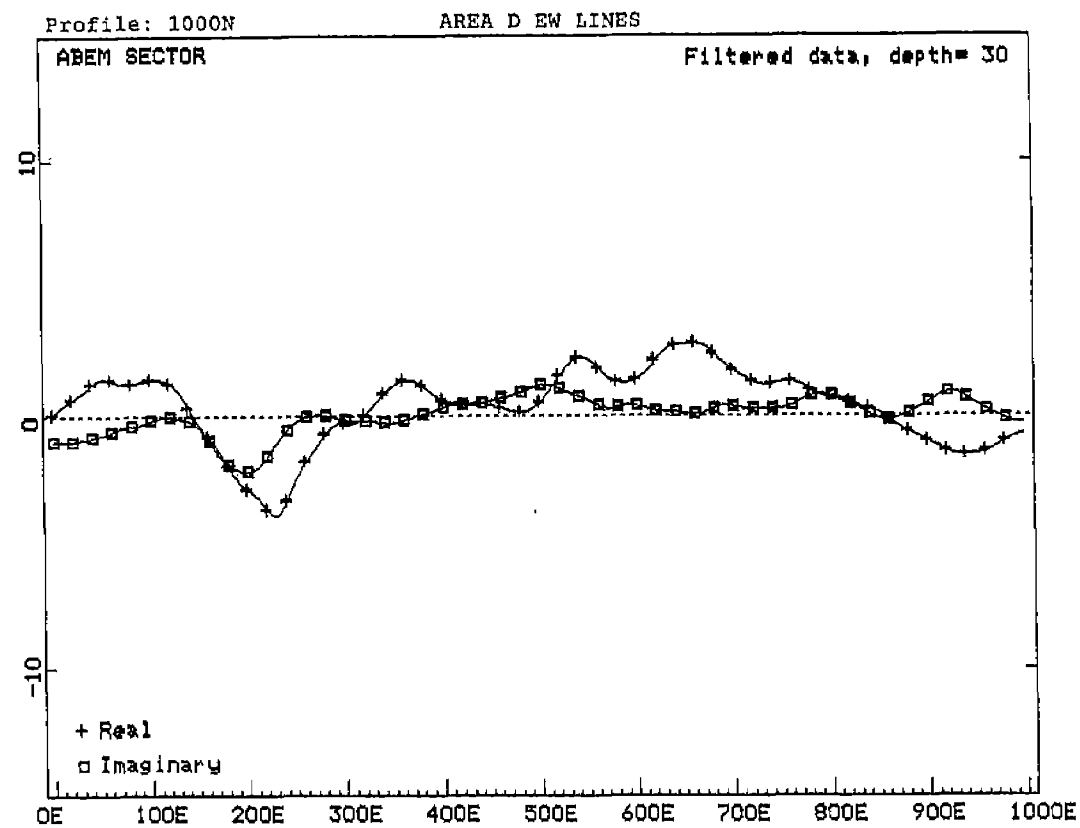

JUDGE'S OFFICE
STONEWALL COUNTY, TEXAS

AREA D LINE 1000N - VLF DATA
SALT POLLUTION STUDY
STONEWALL COUNTY, TEXAS

DESIGNED BY:	CT	PROJECT NO.:	1011520	FIGURE
CHECKED BY:	TLD	DRAWING NO.:	LOC	B-17
DRAWN BY:	JMW	DATE:	07/05/00	

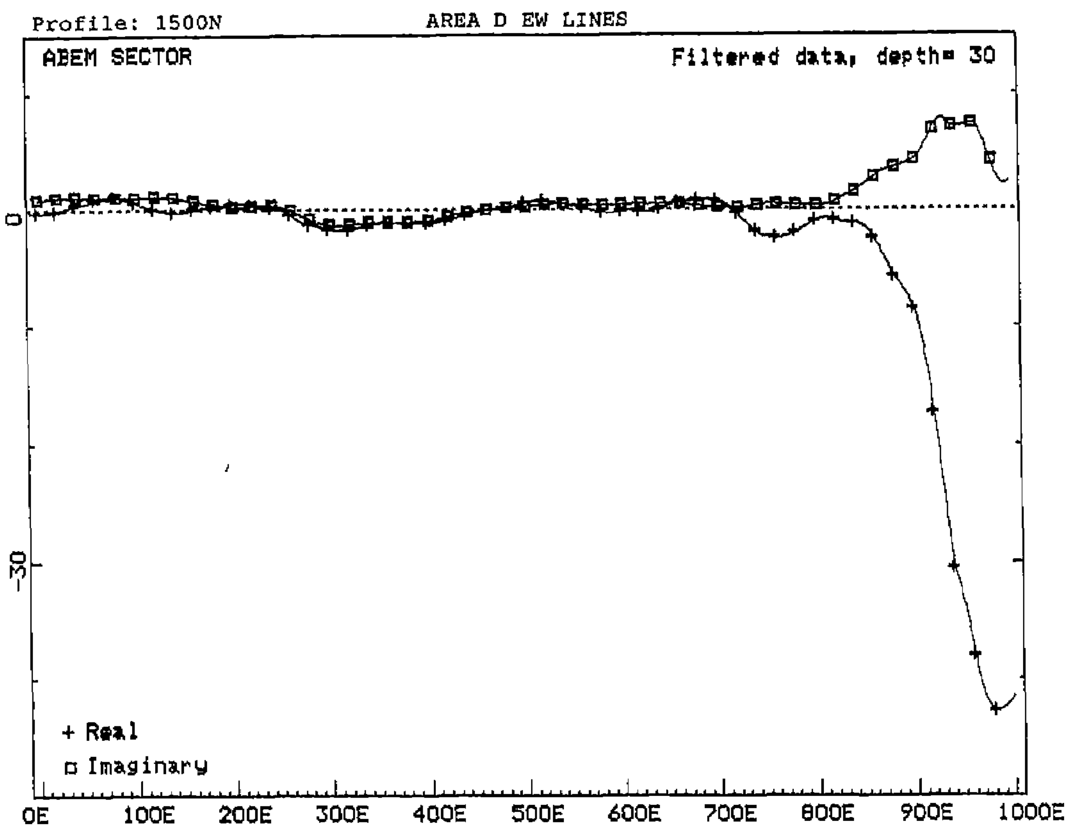

JUDGE'S OFFICE
STONEWALL COUNTY,
TEXAS

AREA D LINE 1500N - VLF DATA
SALT POLLUTION STUDY
STONEWALL COUNTY, TEXAS

DESIGNED BY:	CT	PROJECT NO.:	1011520	FIGURE
CHECKED BY:	TLD	DRAWING NO.:	LOC	B-18
DRAWN BY:	JMW	DATE:	07/05/00	

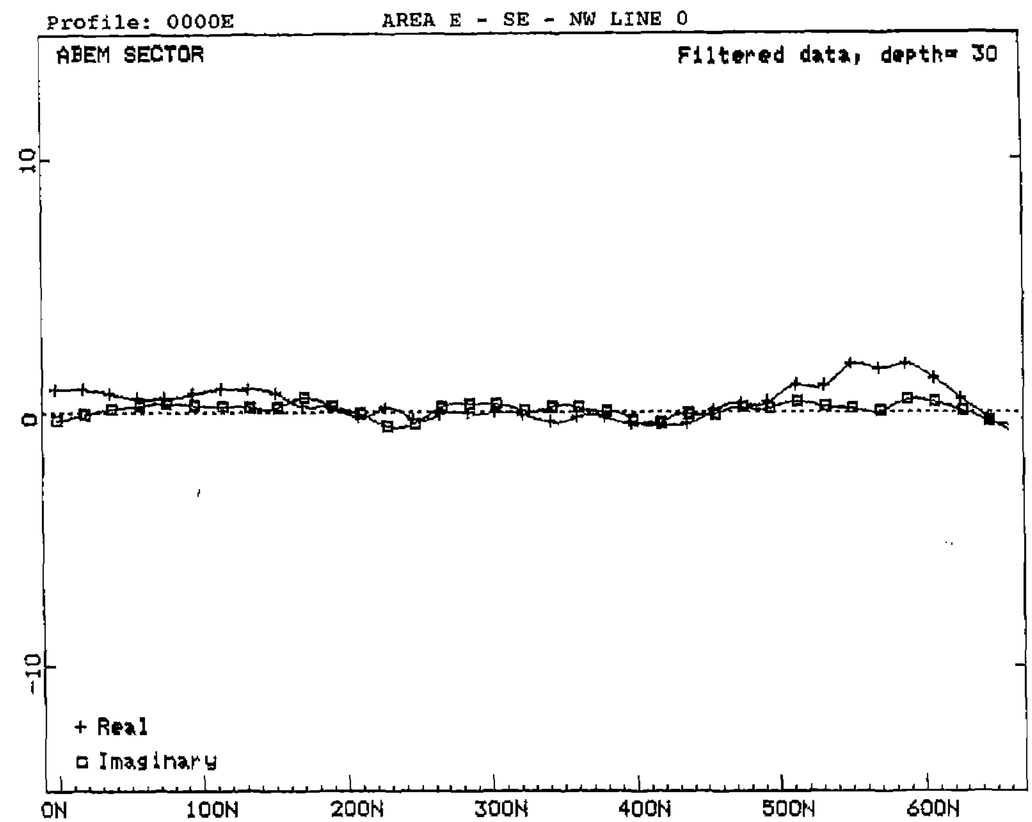

JUDGE'S OFFICE STONEWALL COUNTY, TEXAS		AREA E LINE 1 - VLF DATA SALT POLLUTION STUDY STONEWALL COUNTY, TEXAS	
		DESIGNED BY: CT CHECKED BY: TLD DRAWN BY: JMW	PROJECT NO.: 1011520 DRAWING NO.: LOC DATE: 07/05/00	FIGURE B-19

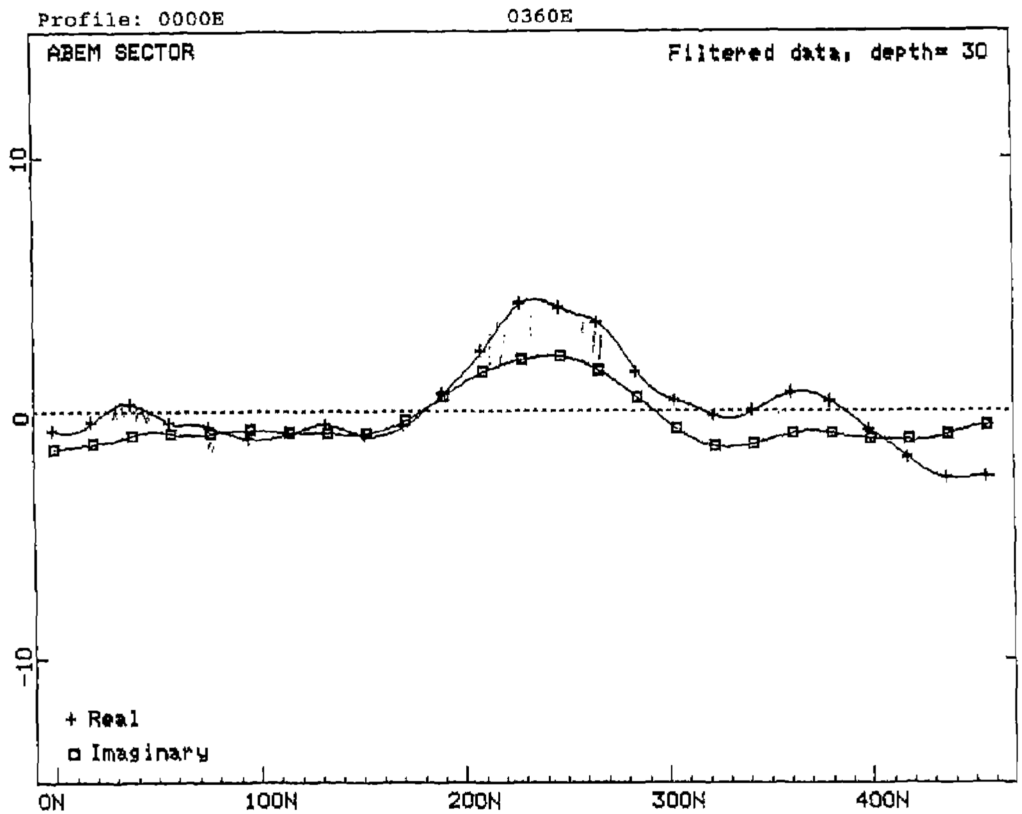

JUDGE'S OFFICE
STONEWALL COUNTY, TEXAS

AREA F LINE 0E - VLF DATA
SALT POLLUTION STUDY
STONEWALL COUNTY, TEXAS

DESIGNED BY:	CT	PROJECT NO.:	1011520	FIGURE
CHECKED BY:	TLD	DRAWING NO.:	LOC	B-20
DRAWN BY:	JMW	DATE:	07/06/00	

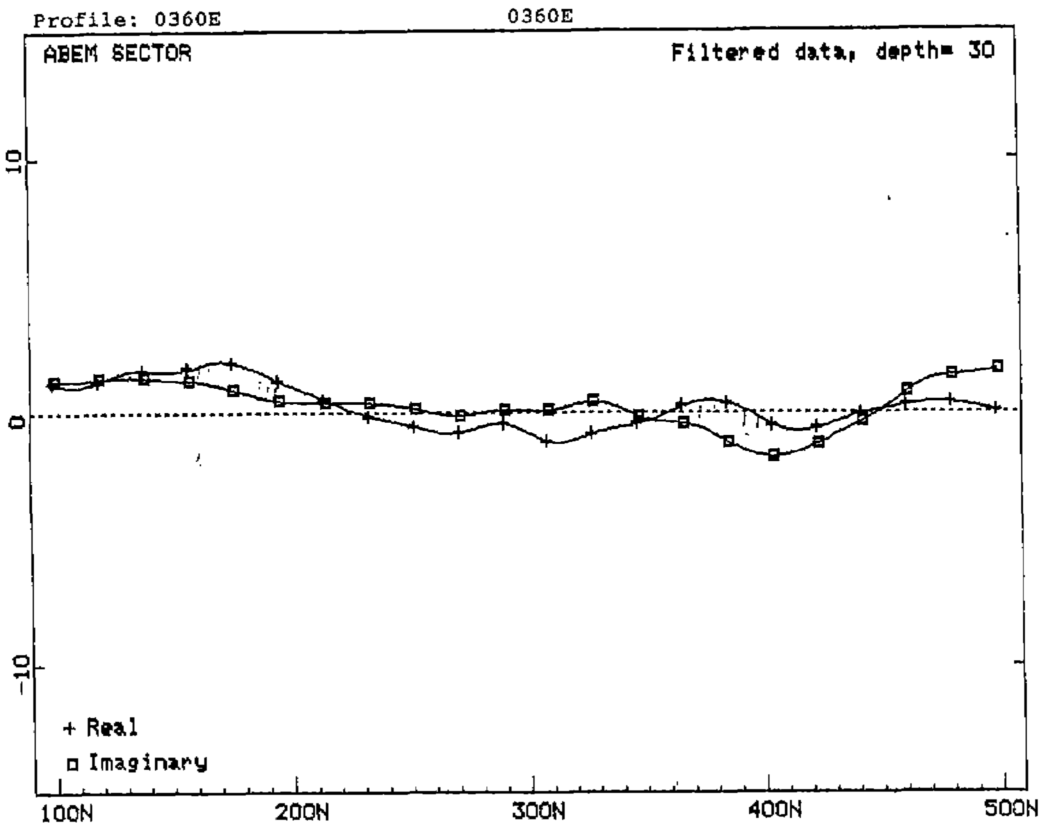

JUDGE'S OFFICE STONEWALL COUNTY, TEXAS	SDII	AREA F LINE 360E - VLF DATA SALT POLLUTION STUDY STONEWALL COUNTY, TEXAS

DESIGNED BY:	CT	PROJECT NO.:	1011520	FIGURE
CHECKED BY:	TLD	DRAWING NO.:	LOC	B-21
DRAWN BY:	JMW	DATE:	07/06/00	

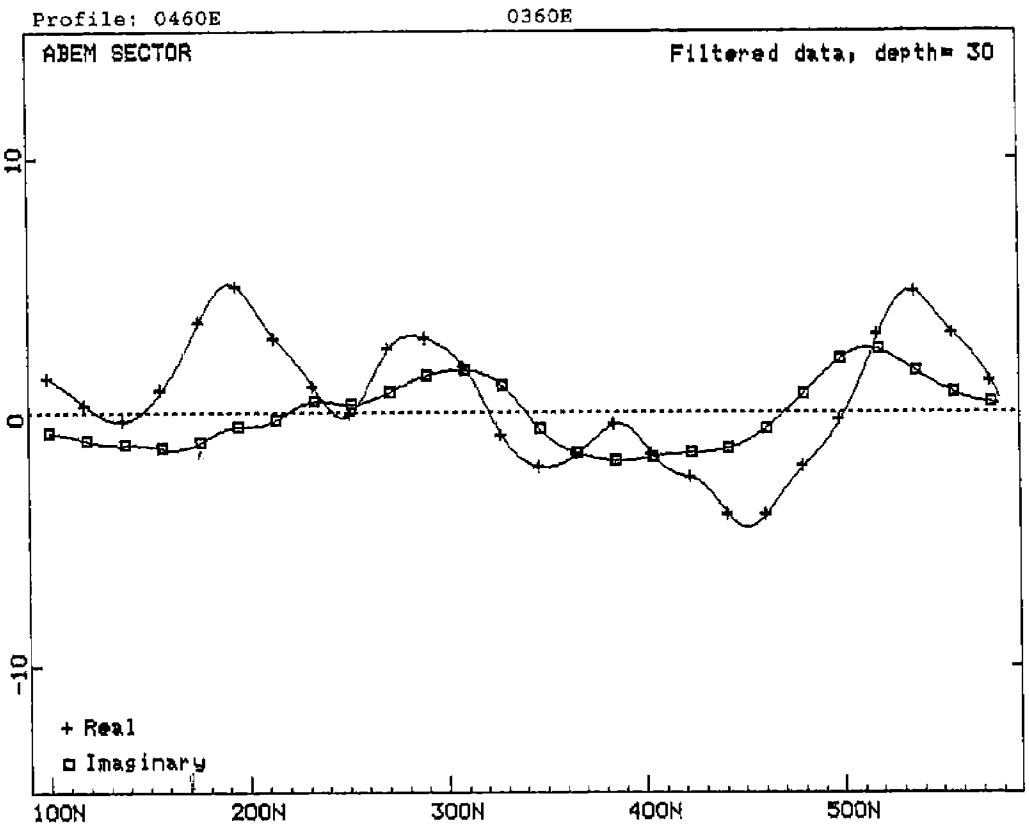

JUDGE'S OFFICE
STONEWALL COUNTY,
TEXAS

AREA F LINE 460E - VLF DATA
SALT POLLUTION STUDY
STONEWALL COUNTY, TEXAS

DESIGNED BY:	CT	PROJECT NO.:	1011520	FIGURE
CHECKED BY:	TLD	DRAWING NO.:	LOC	B-22
DRAWN BY:	JMW	DATE:	07/06/00	

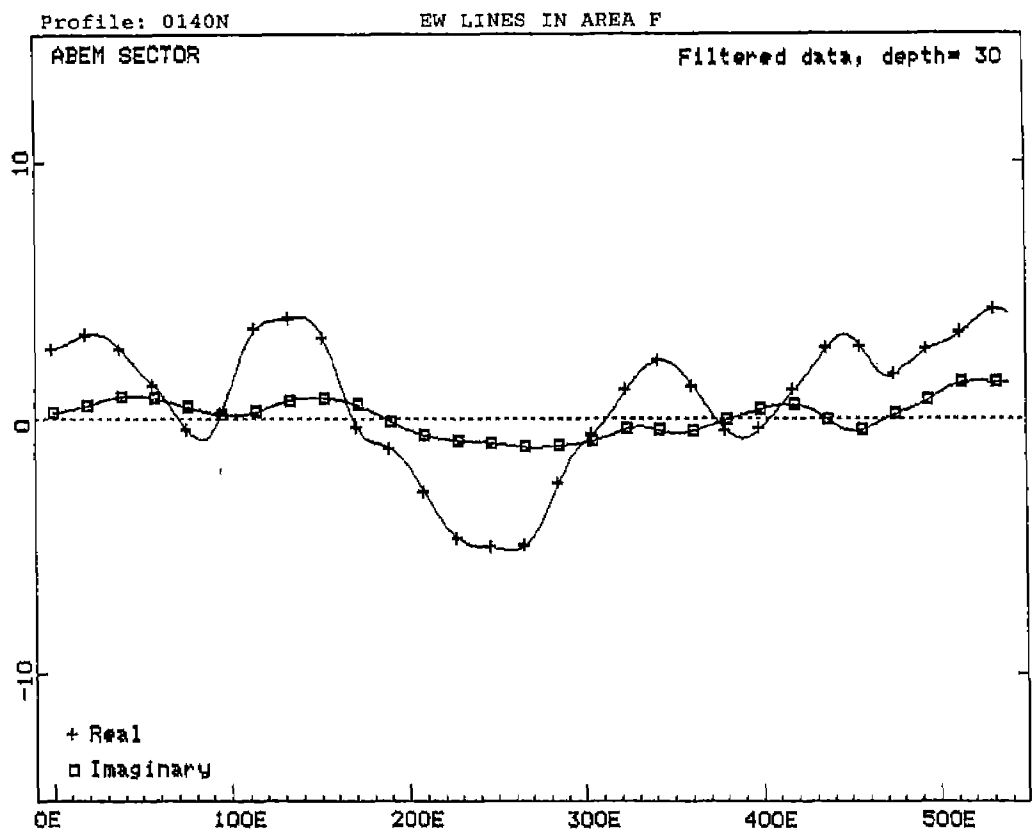

JUDGE'S OFFICE STONEWALL COUNTY, TEXAS	SDII GLOBAL	AREA F LINE 140N - VLF DATA SALT POLLUTION STUDY STONEWALL COUNTY, TEXAS	
		DESIGNED BY: CT CHECKED BY: TLD DRAWN BY: JMW	PROJECT NO.: 1011520 DRAWING NO.: LOC DATE: 07/06/00	FIGURE B-23

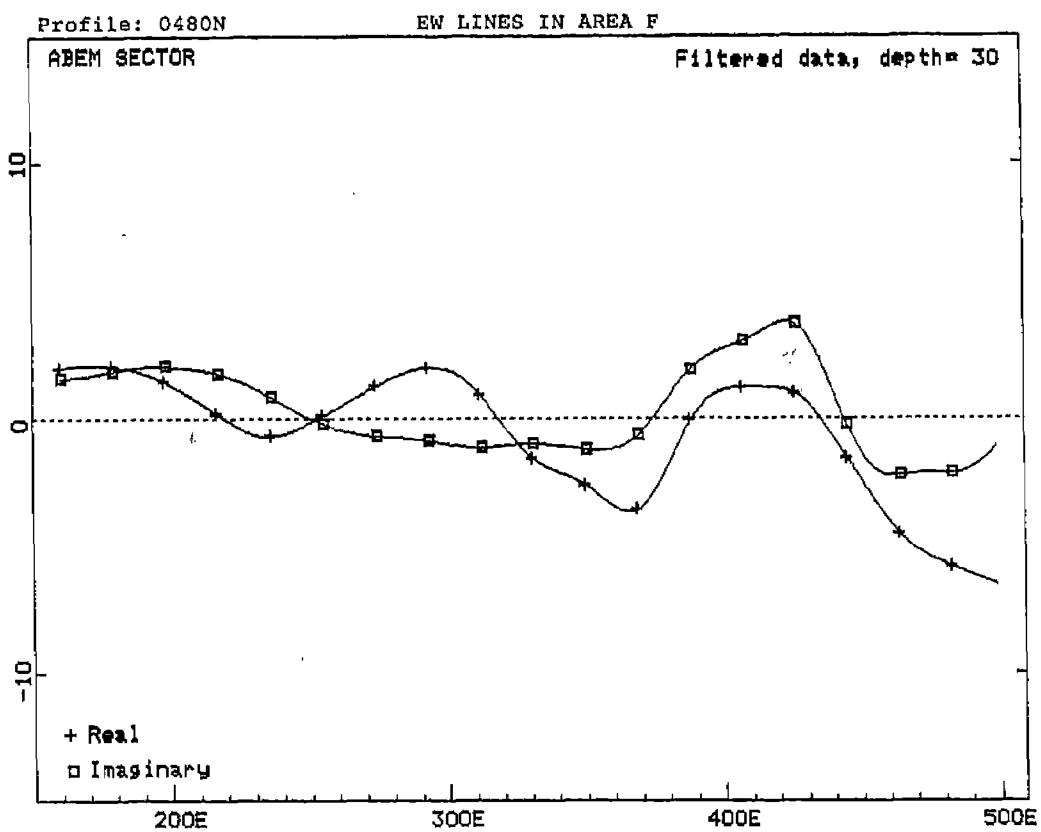

JUDGE'S OFFICE
STONEWALL COUNTY,
TEXAS

AREA F LINE 480N - VLF DATA
SALT POLLUTION STUDY
STONEWALL COUNTY, TEXAS

DESIGNED BY:	CT	PROJECT NO.:	1011520	FIGURE
CHECKED BY:	TLD	DRAWING NO.:	LOC	B-24
DRAWN BY:	JMW	DATE:	07/06/00	

APPENDIX C

PLOTS OF PROCESSED TDM DATA AND MODELS

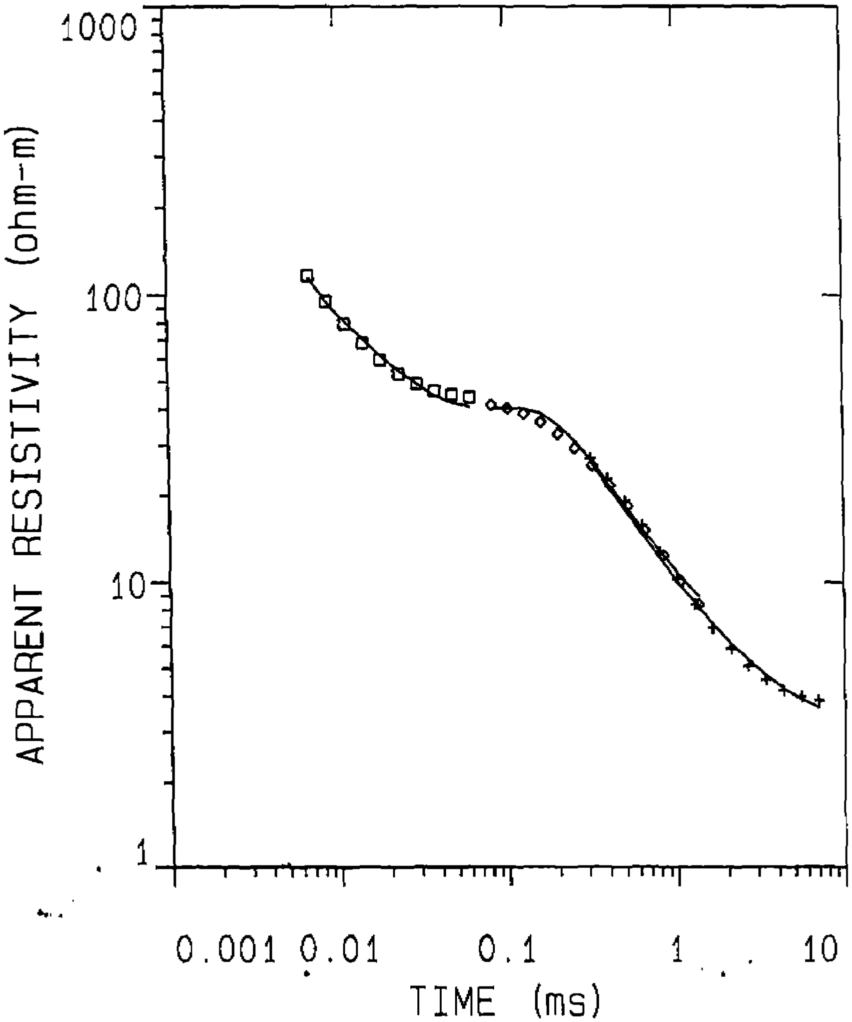

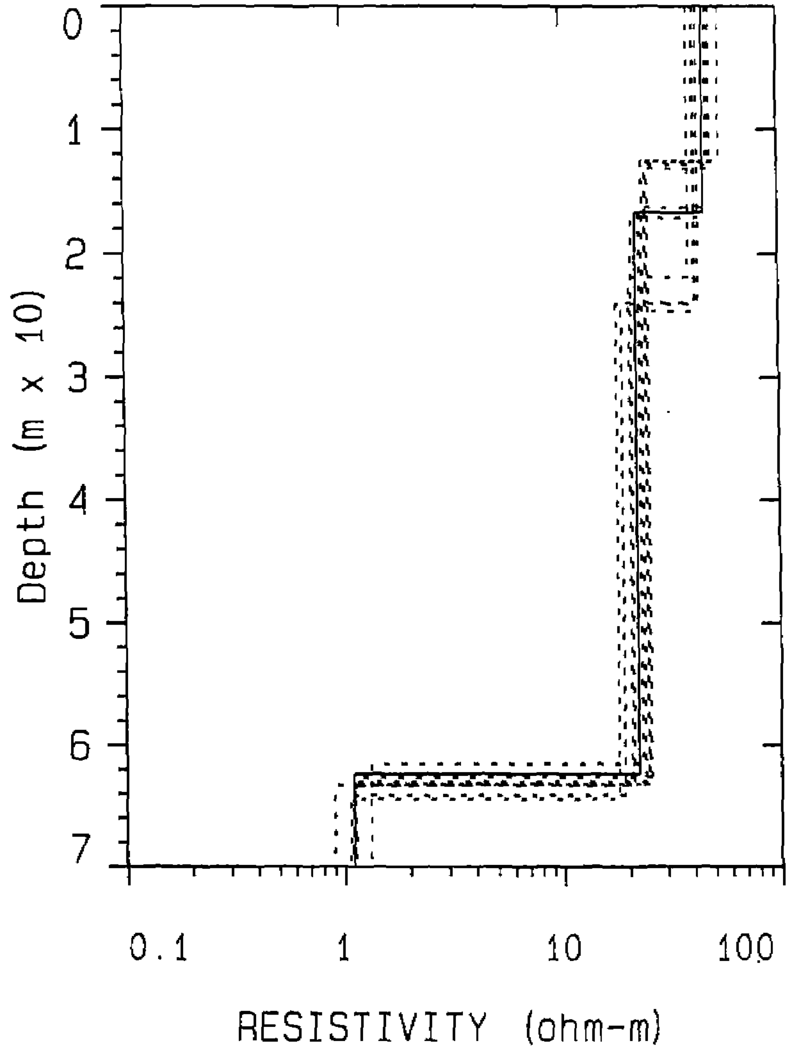

Stonewall County		Salt Pollution Study
Subsurface Detection		Site A Stonewall County, TX
Data Set: SITE1	Date: JUN-05-00	
Equipment: Geonics PROTEM	Sounding: 1	Azimuth:

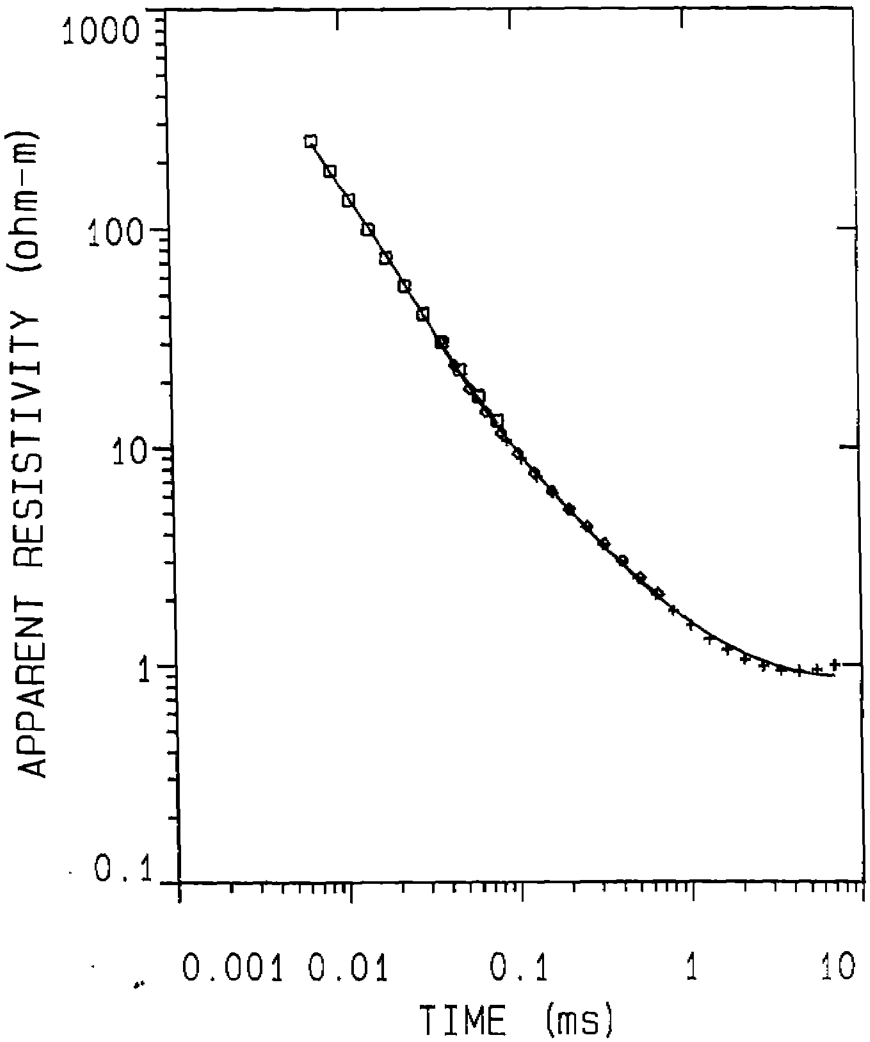

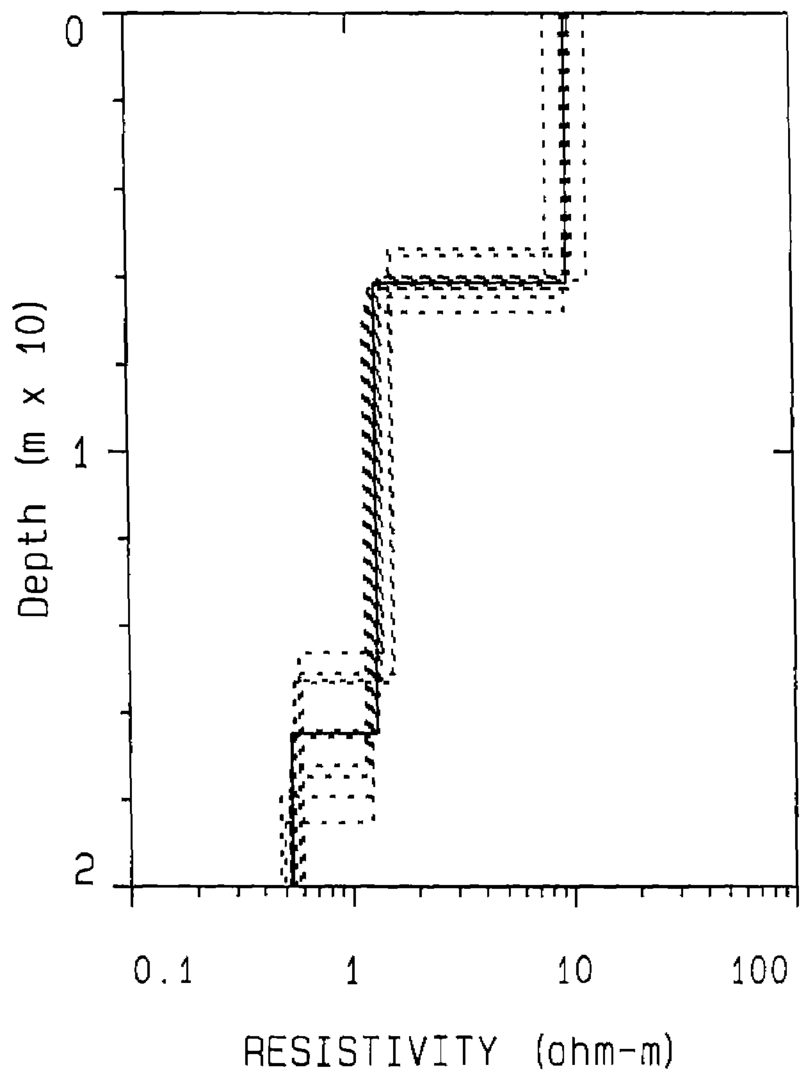

Stonewall County		Salt Pollution Study
Subsurface Detection		Site B (1) Stonewall County, TX
Data Set: SITE2	Date: JUN-05-00	
Equipment: Geonics PROTEM	Sounding: 1	Azimuth:

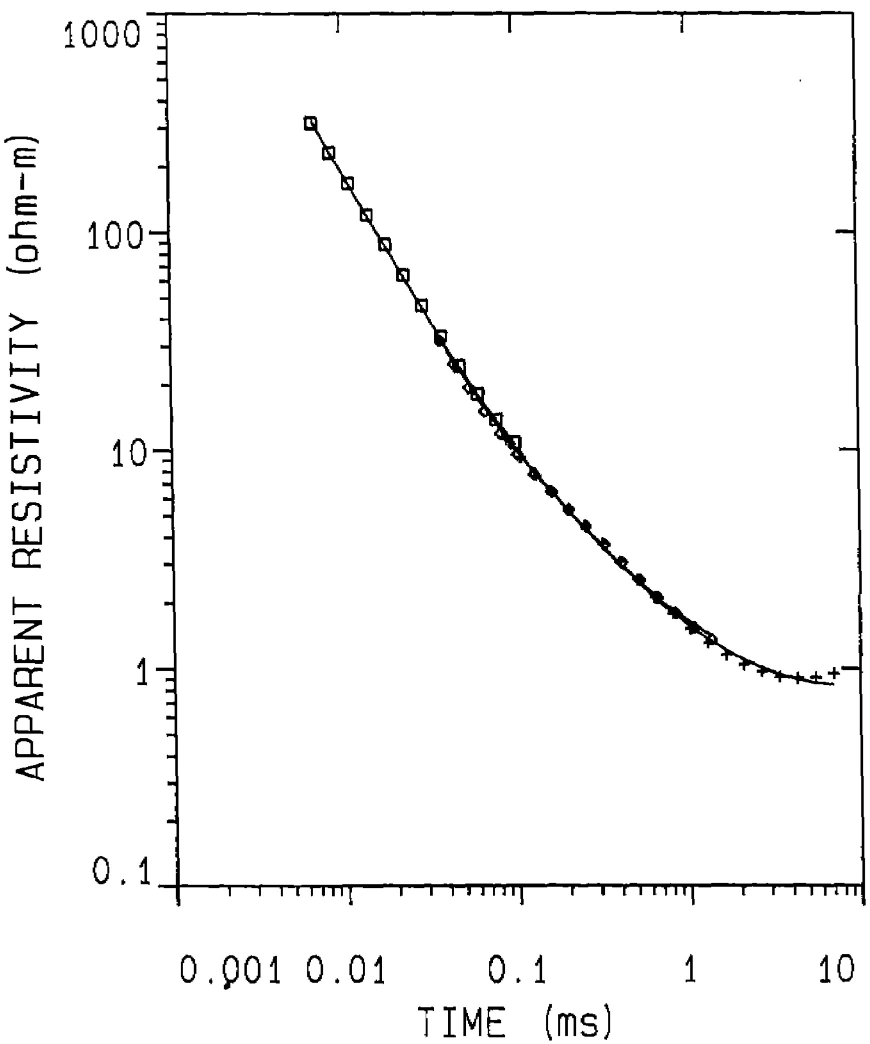

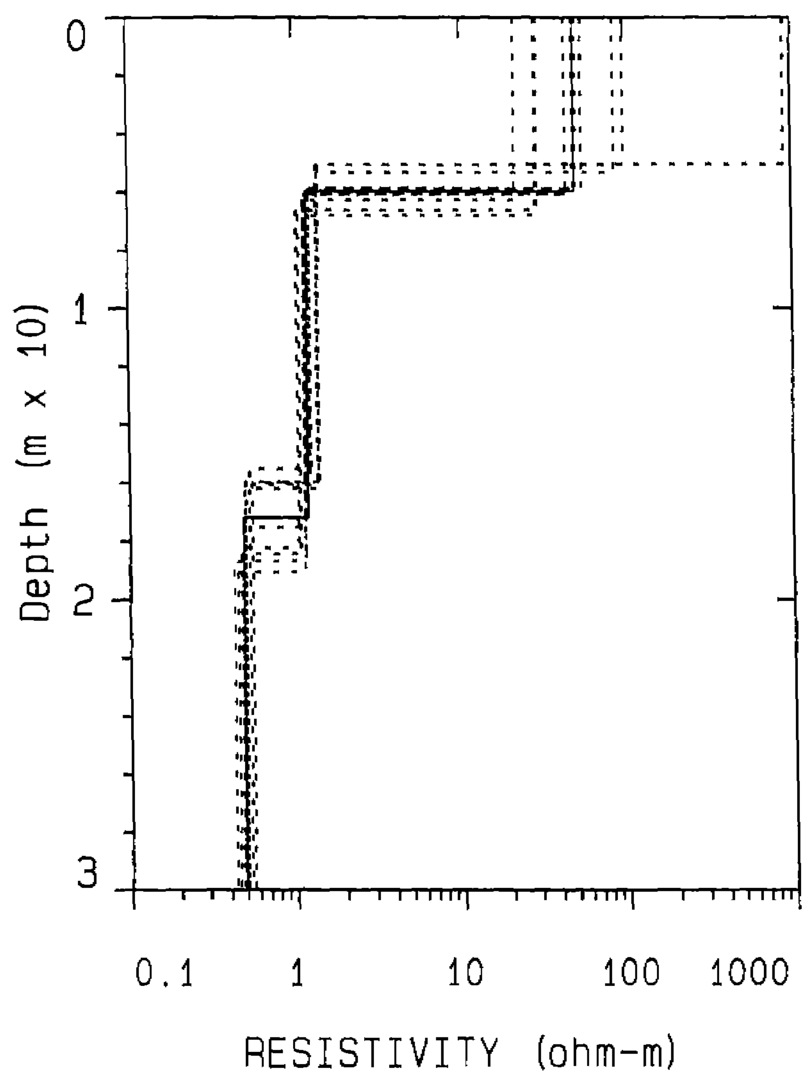

Stonewall County		Salt Pollution Study
Subsurface Detection		Site B (2) Stonewell County, TX
Data Set: SITE3	Date: JUN-05-00	
Equipment: Geonics PROTEM	Sounding: 1	Azimuth:

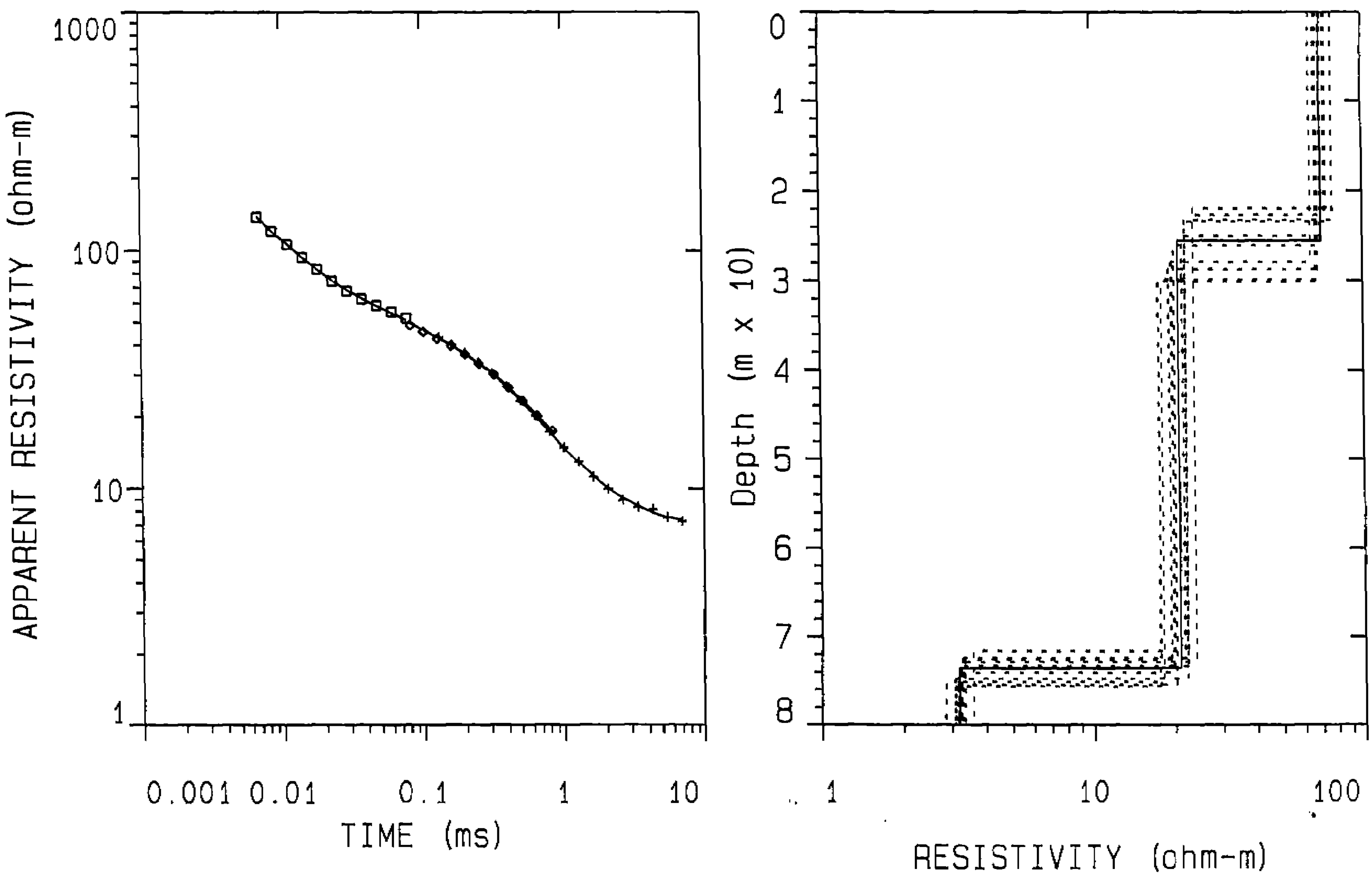

Stonewall County		Salt Pollution Study
Subsurface Detection		Site F Stonewell County, TX
Data Set: SITE4	Date: JUN-05-00	
Equipment: Geonics PROTEM	Sounding: 1	Azimuth:

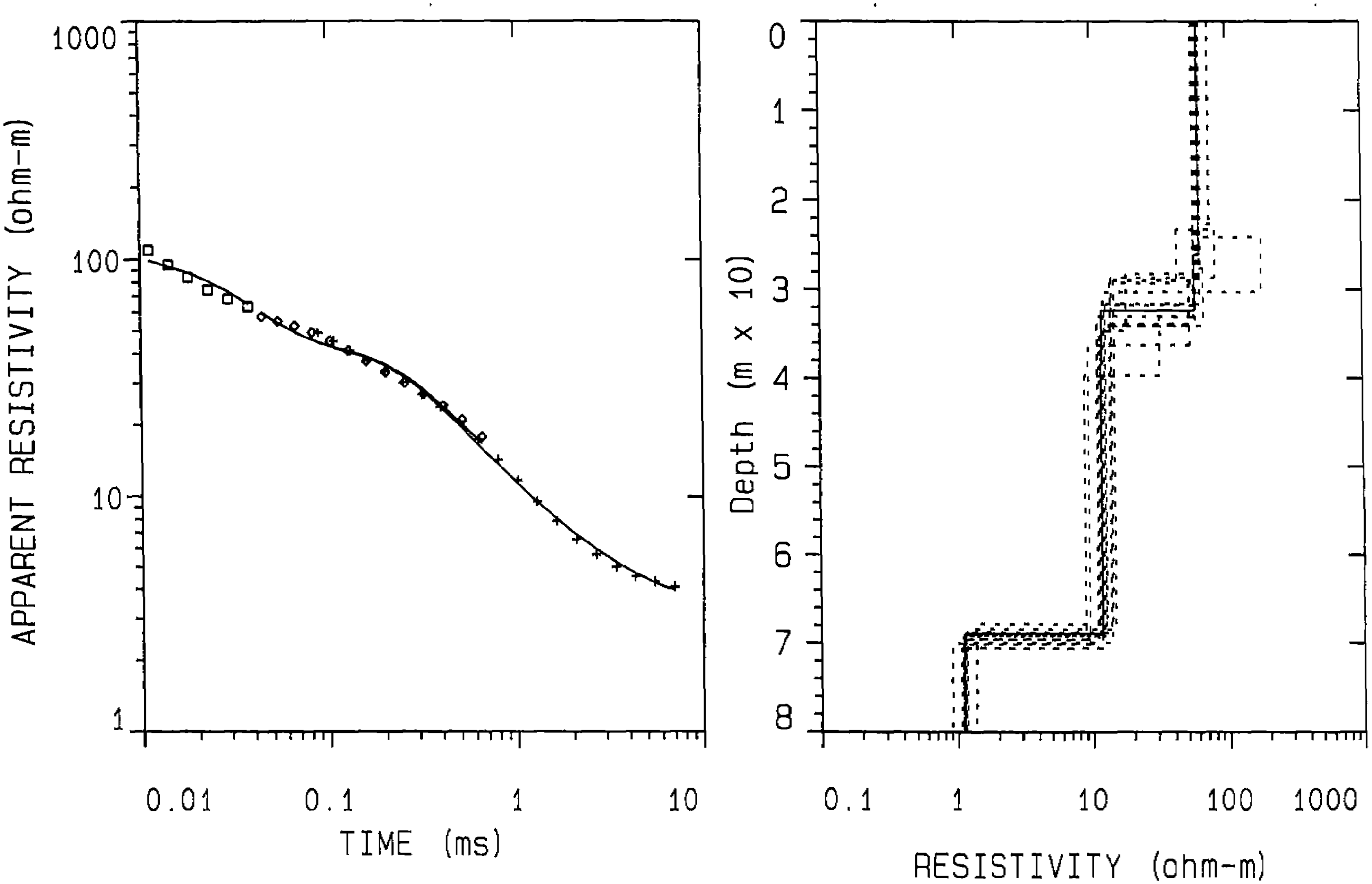

Stonewall County		Salt Pollution Study
Subsurface Detection		Site E Stonewall County, TX
Data Set: SITE5	Date: JUN-05-00	
Equipment: Geonics PROTEM	Sounding: 1	Azimuth:

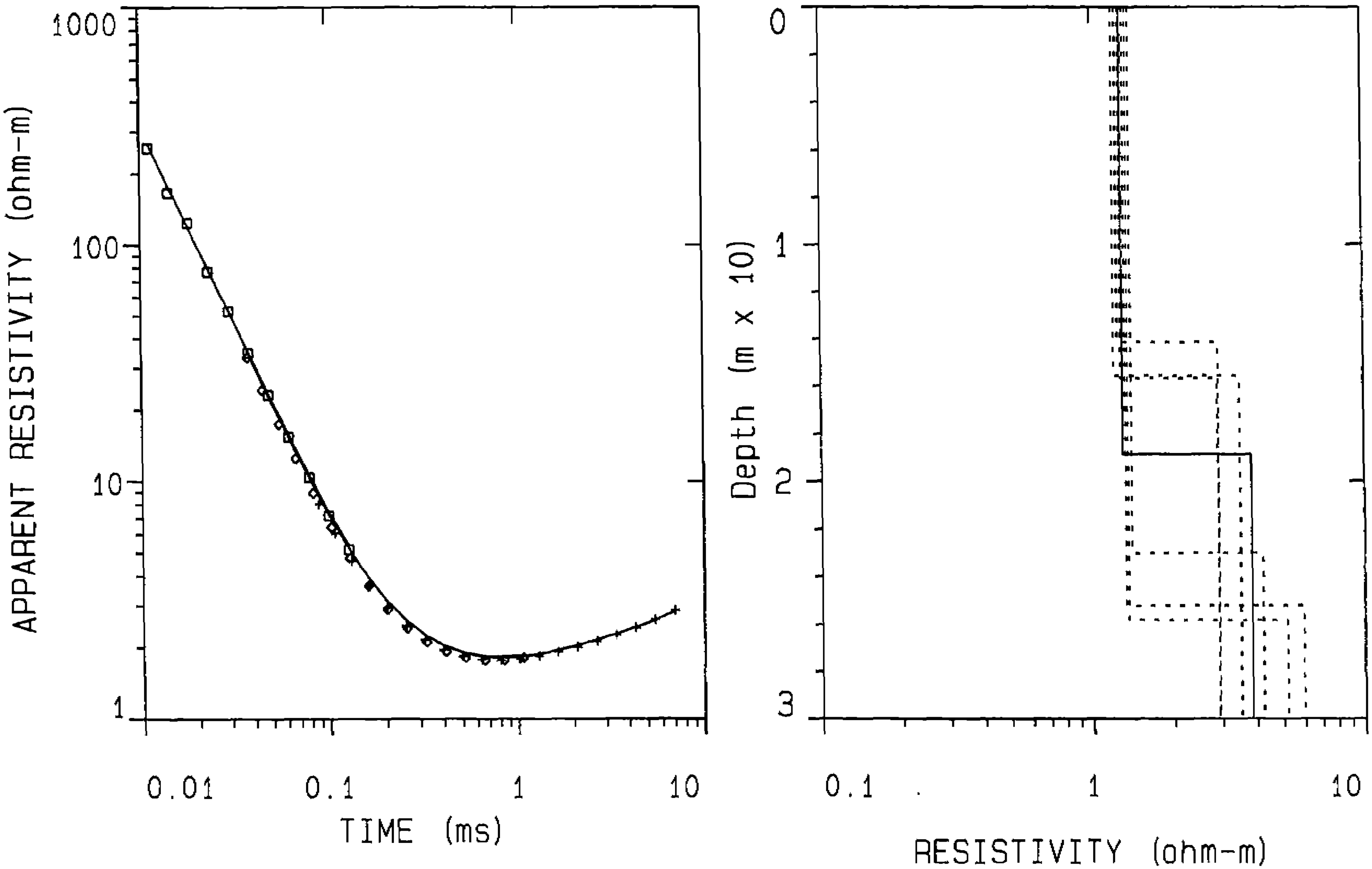

Stonewall County		Salt Pollution Study
Subsurface Detection		Low Water Crossing Stonewall County, TX
Data Set: SITE6	Date: JUN-06-00	
Equipment: Geonics PROTEM	Sounding: 1	Azimuth:

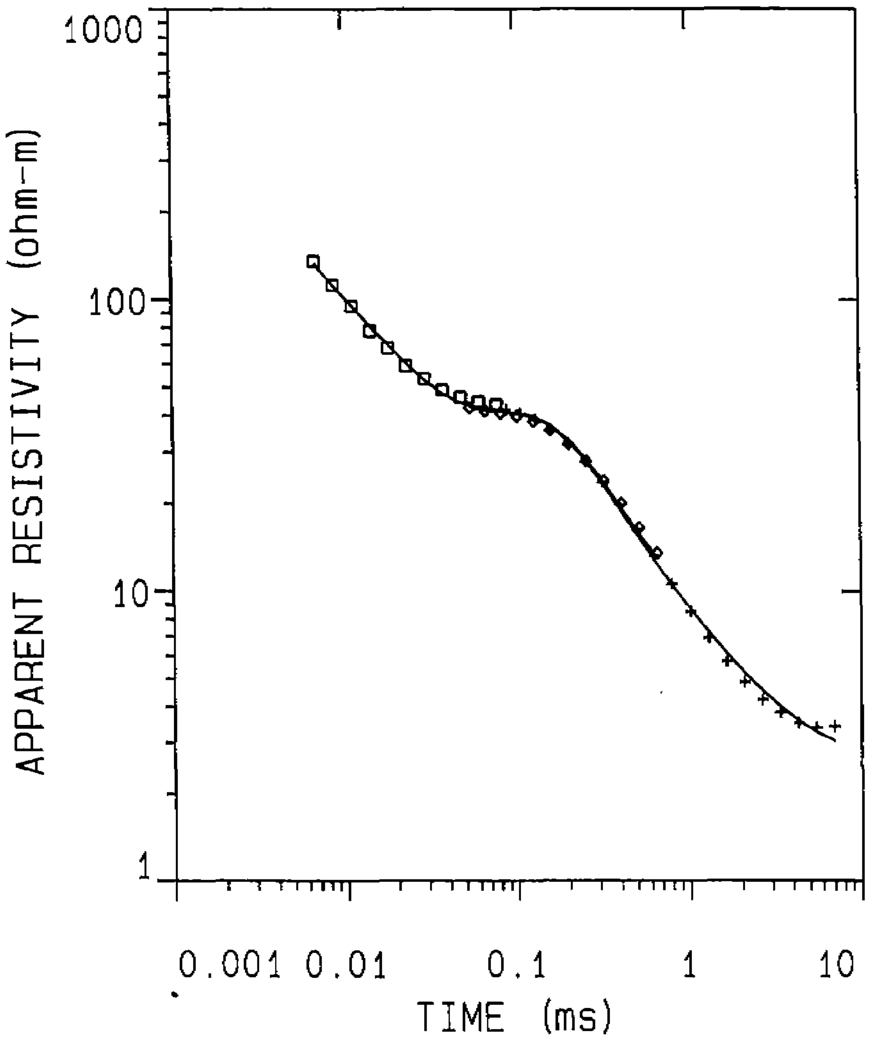

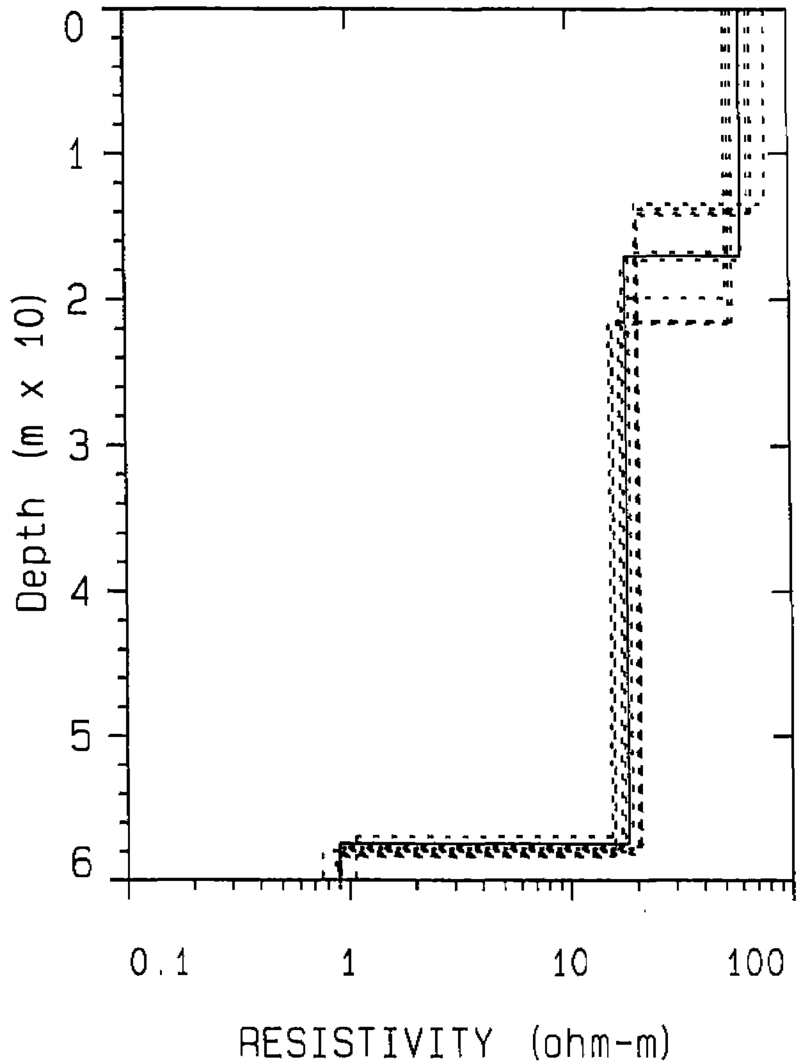

Stonewall County		Salt Pollution Study
Subsurface Detection		Well One Location Stonewall County, TX
Data Set: SITE7	Date: JUN-06-00	
Equipment: Geonics PROTEM	Sounding: 1	Azimuth:

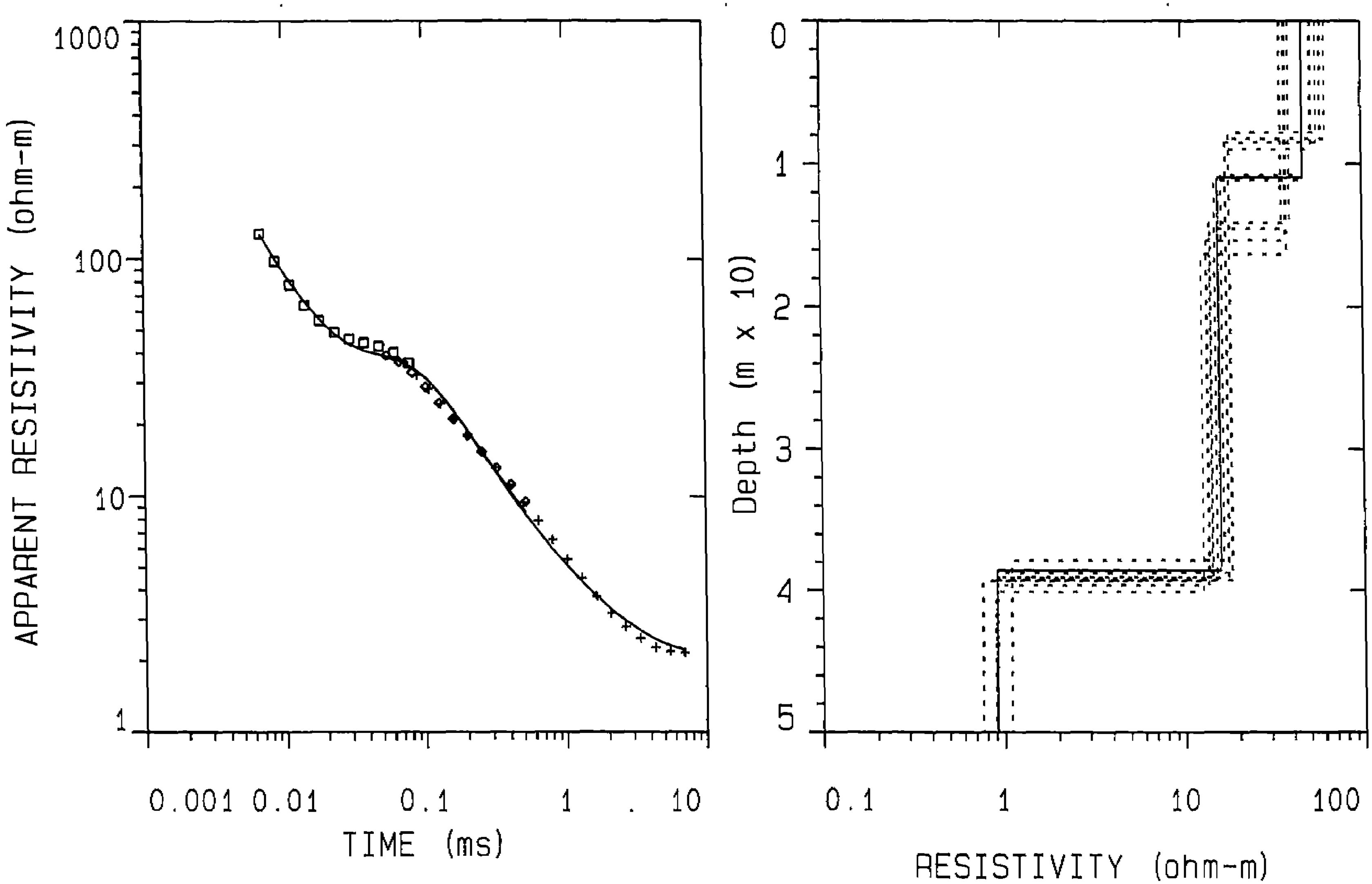

Stonewall County		Salt Pollution Study
Subsurface Detection		SITE C Stonewall County, TX
Data Set: SITE8	Date: JUN-06-00	
Equipment: Geonics PROTEM	Sounding: 1	Azimuth:

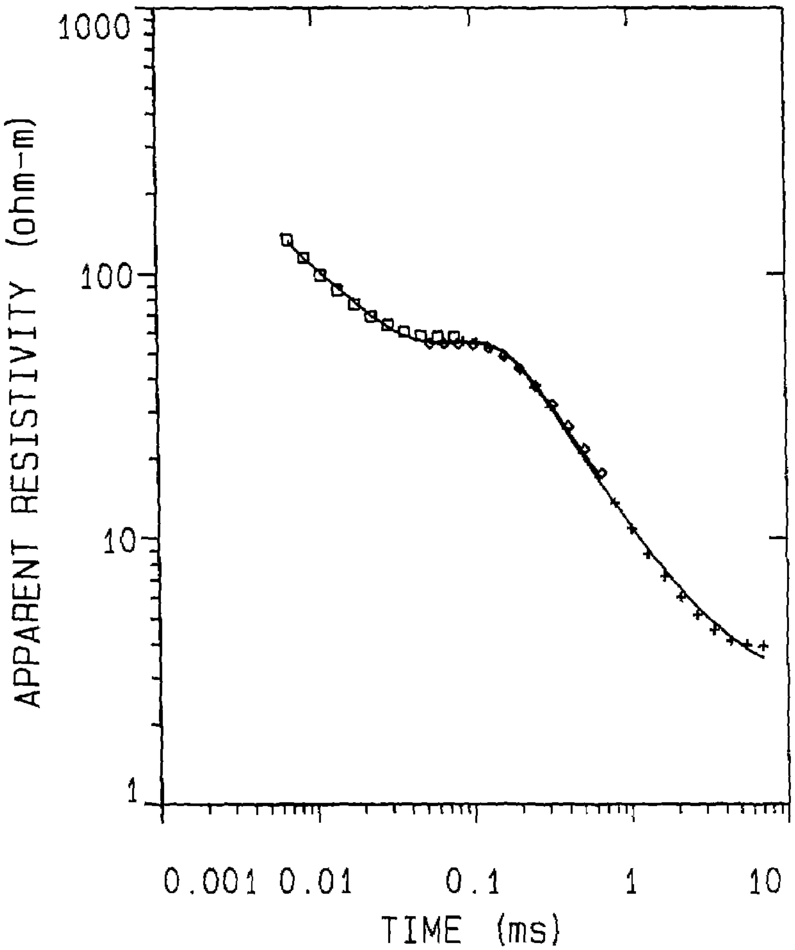

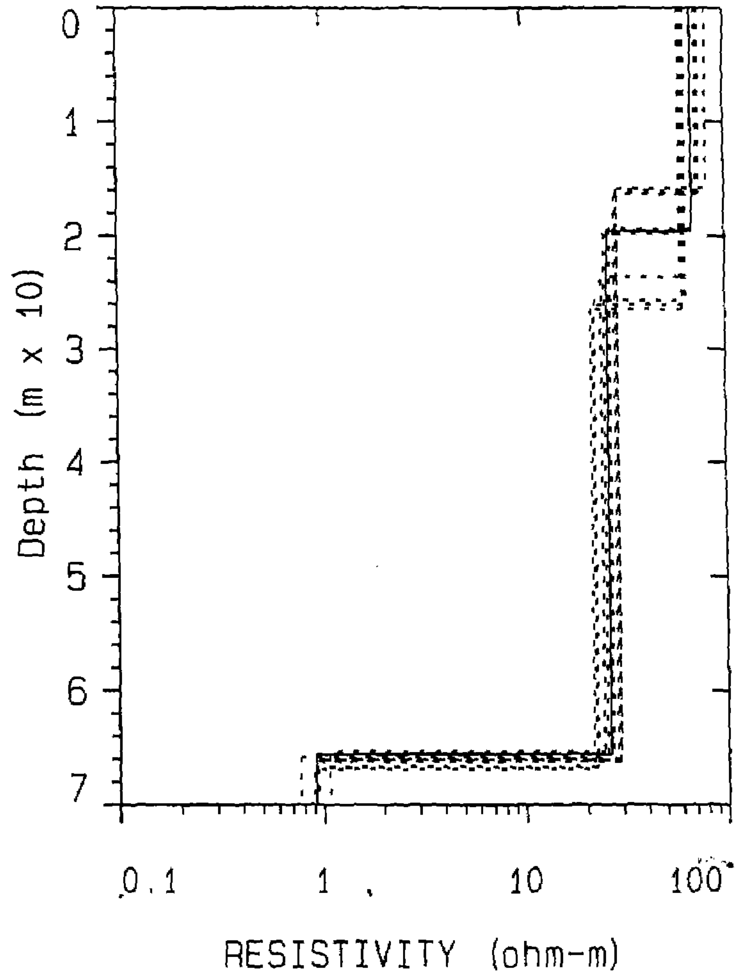

Stonewall County		Salt Pollution Study
Subsurface Detection		SITE D-1 Stonewall County, TX
Data Set: SITE9	Date: JUN-06-00	
Equipment: Geonics PROTEM	Sounding: 1	Azimuth:

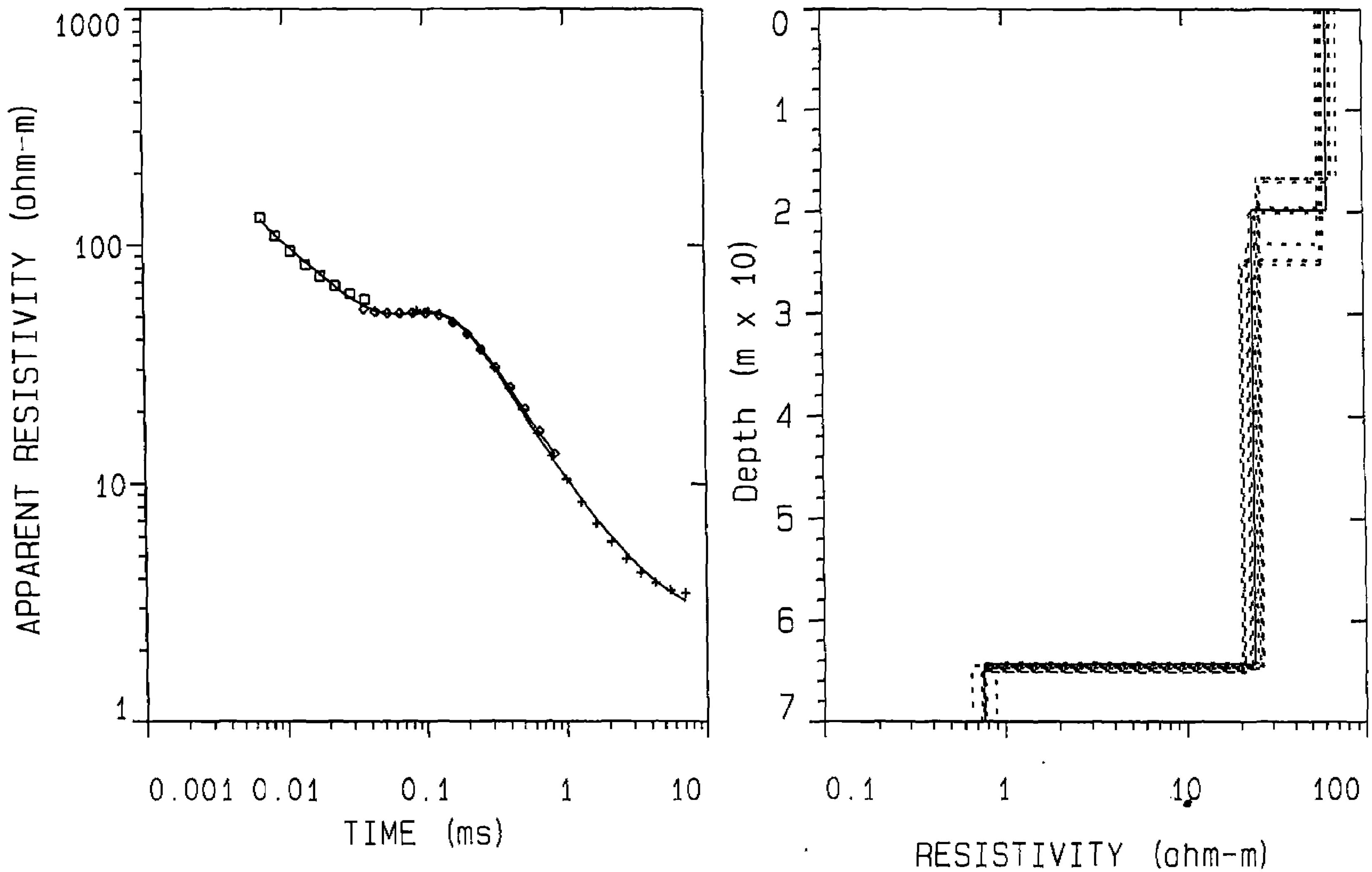

Stonewall County		Salt Pollution Study
Subsurface Detection		SITE D-2 Stonewall County, TX
Data Set: SITE10	Date: JUN-06-00	
Equipment: Geonics PROTEM	Sounding: 1	Azimuth:

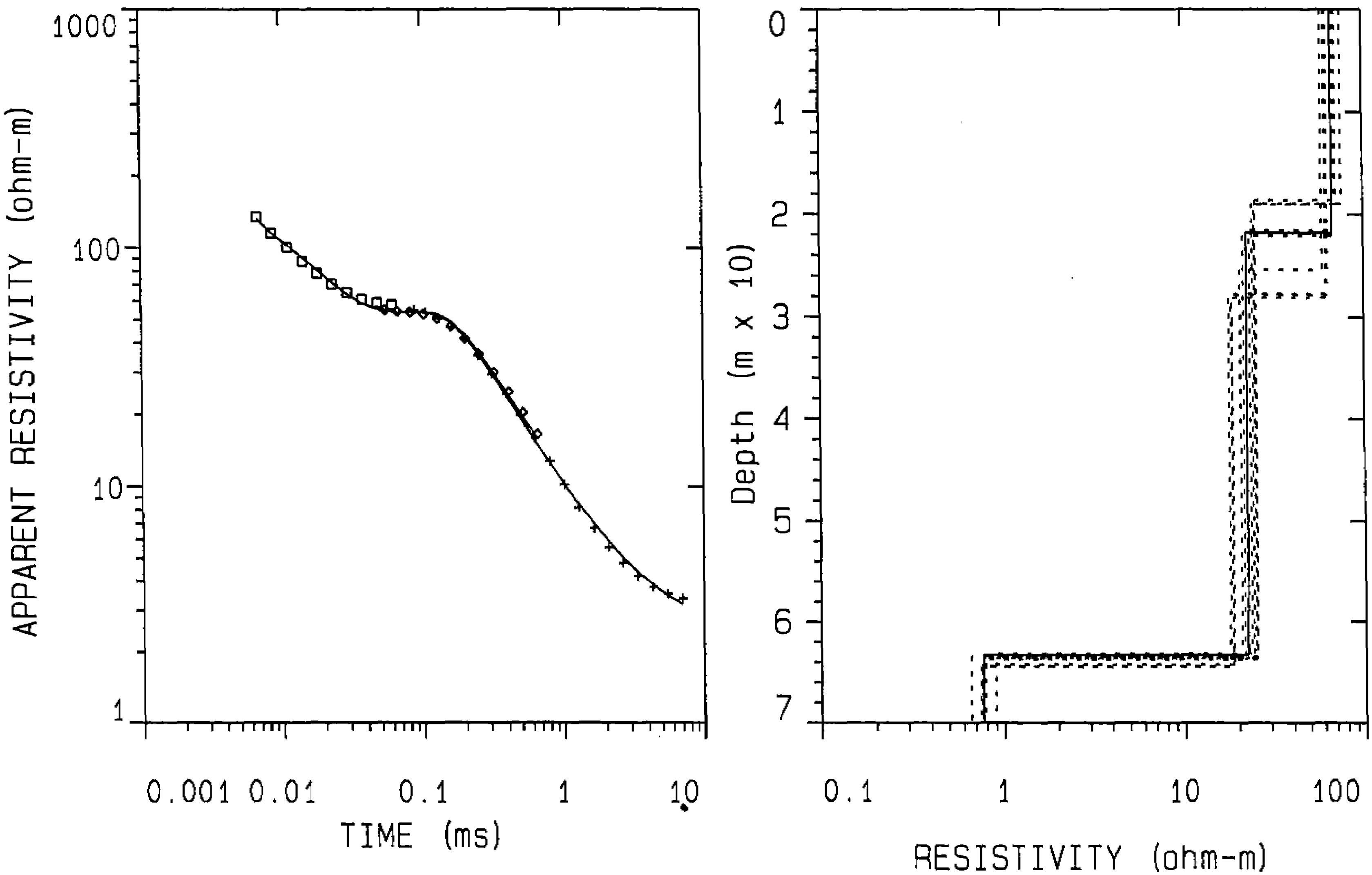

Stonewall County		Salt Pollution Study
Subsurface Detection		SITE D-3 Stonewall County, TX
Data Set: SITE11	Date: JUN-06-00	
Equipment: Geonics PROTEM	Sounding: 1	Azimuth:

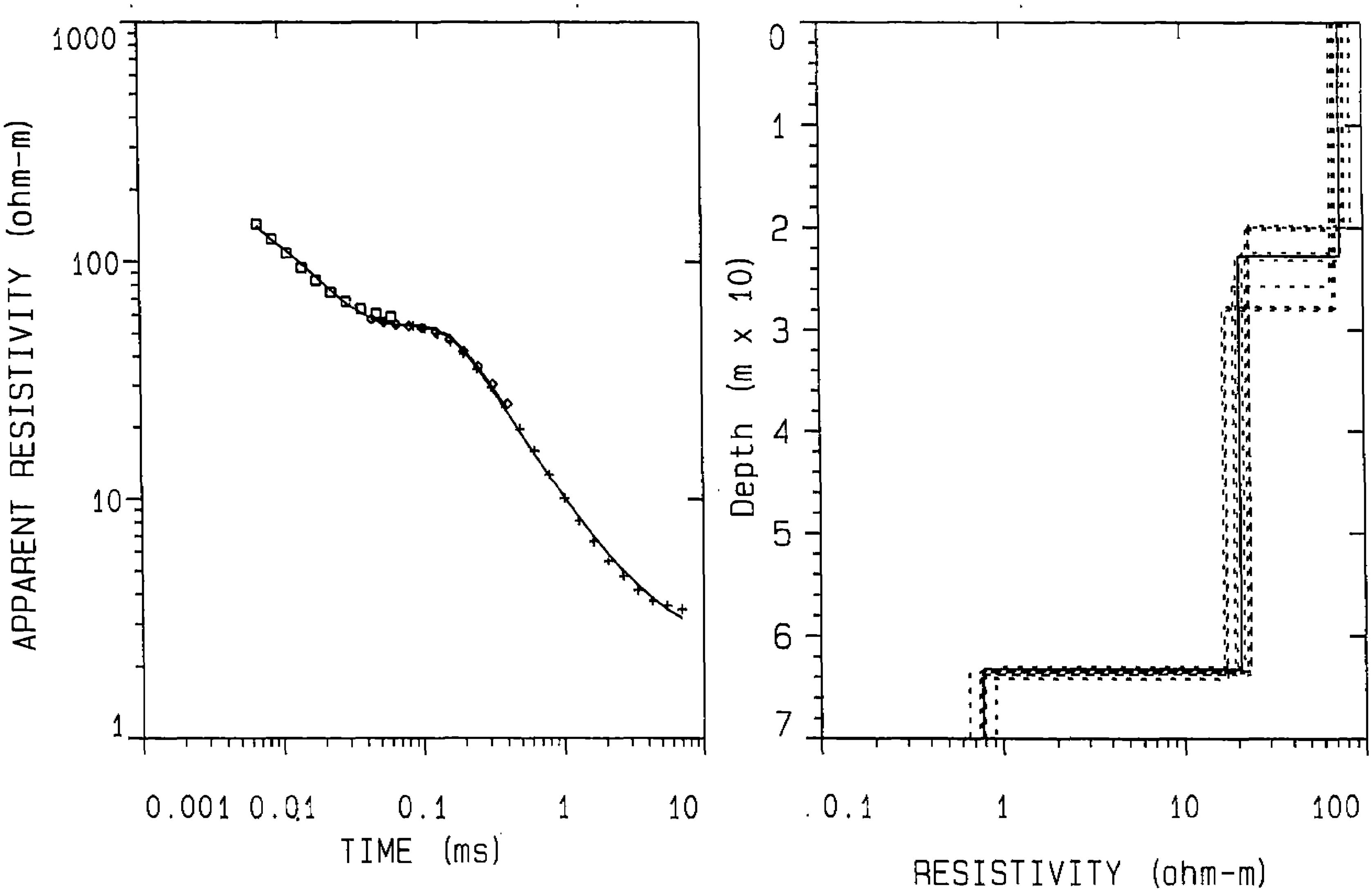

Stonewall County	Salt Pollution Study
Subsurface Detection	SITE D-4 Stonewall County, TX
Data Set: SITE12 / Date: JUN-06-00	
Equipment: Geonics PROTEM / Sounding: 1	Azimuth:

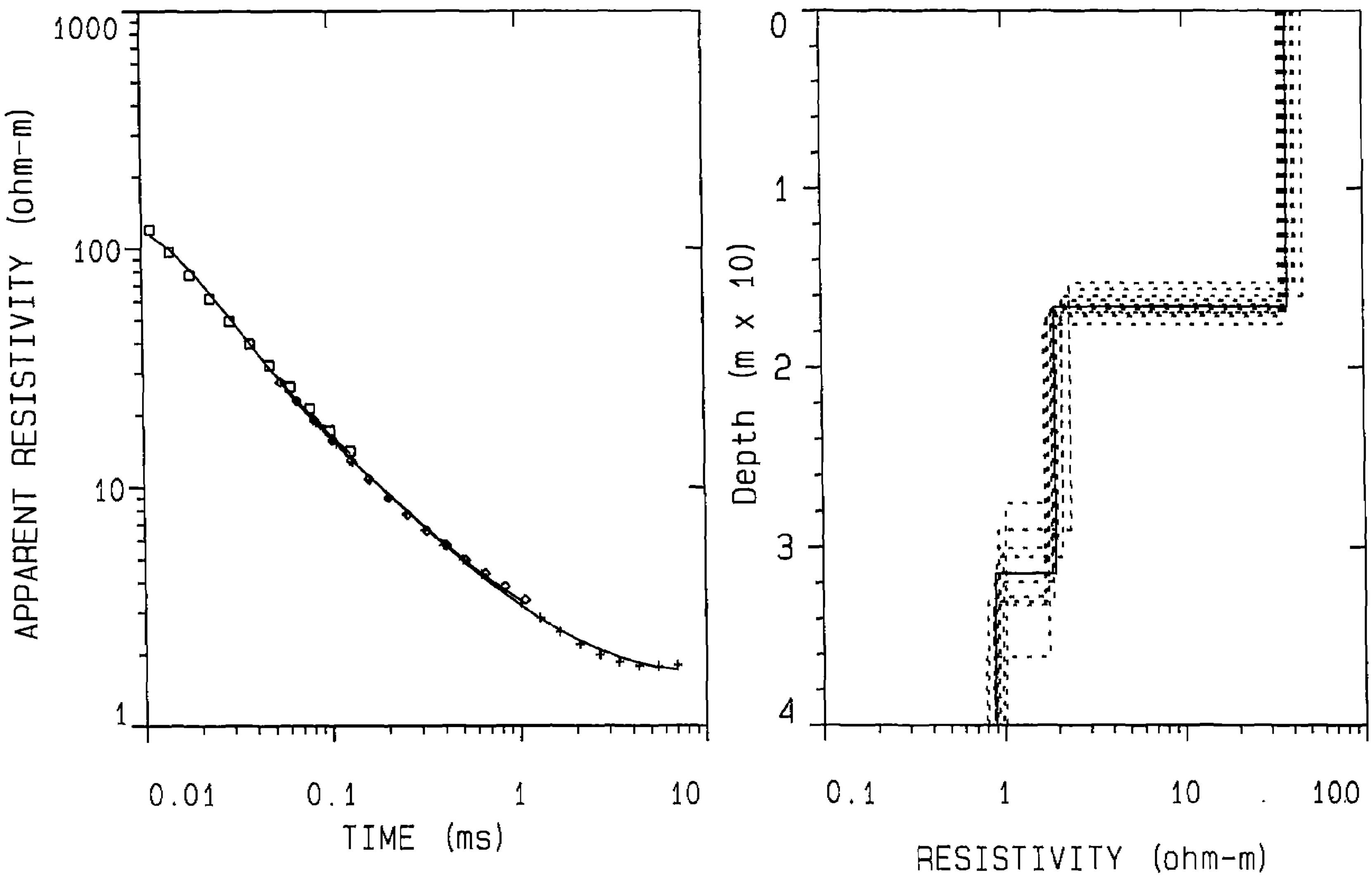

Stonewall County		Salt Pollution Study
Subsurface Detection		Site 13 Stonewall County, TX
Data Set: SITE13	Date: JUN-07-00	
Equipment: Geonics PROTEM	Sounding: 1	Azimuth:

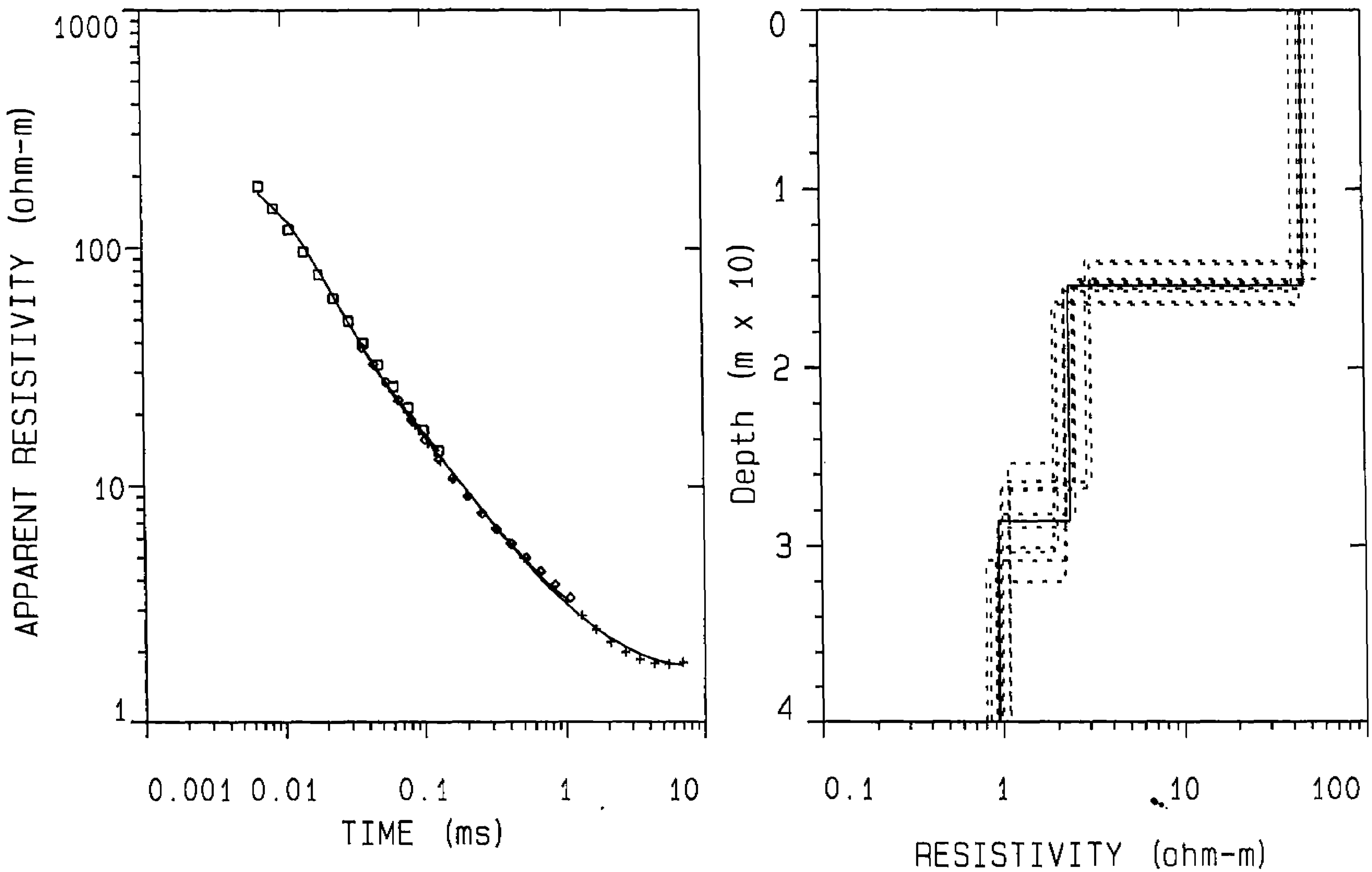

Salt Pollution Study	
Subsurface Detection	
Data Set: SITE14	Date: JUN-07-00
Equipment: Geonics PROTEM	Sounding: 1

Salt Pollution Study

Site 14
Stonewall County, TX

Azimuth:

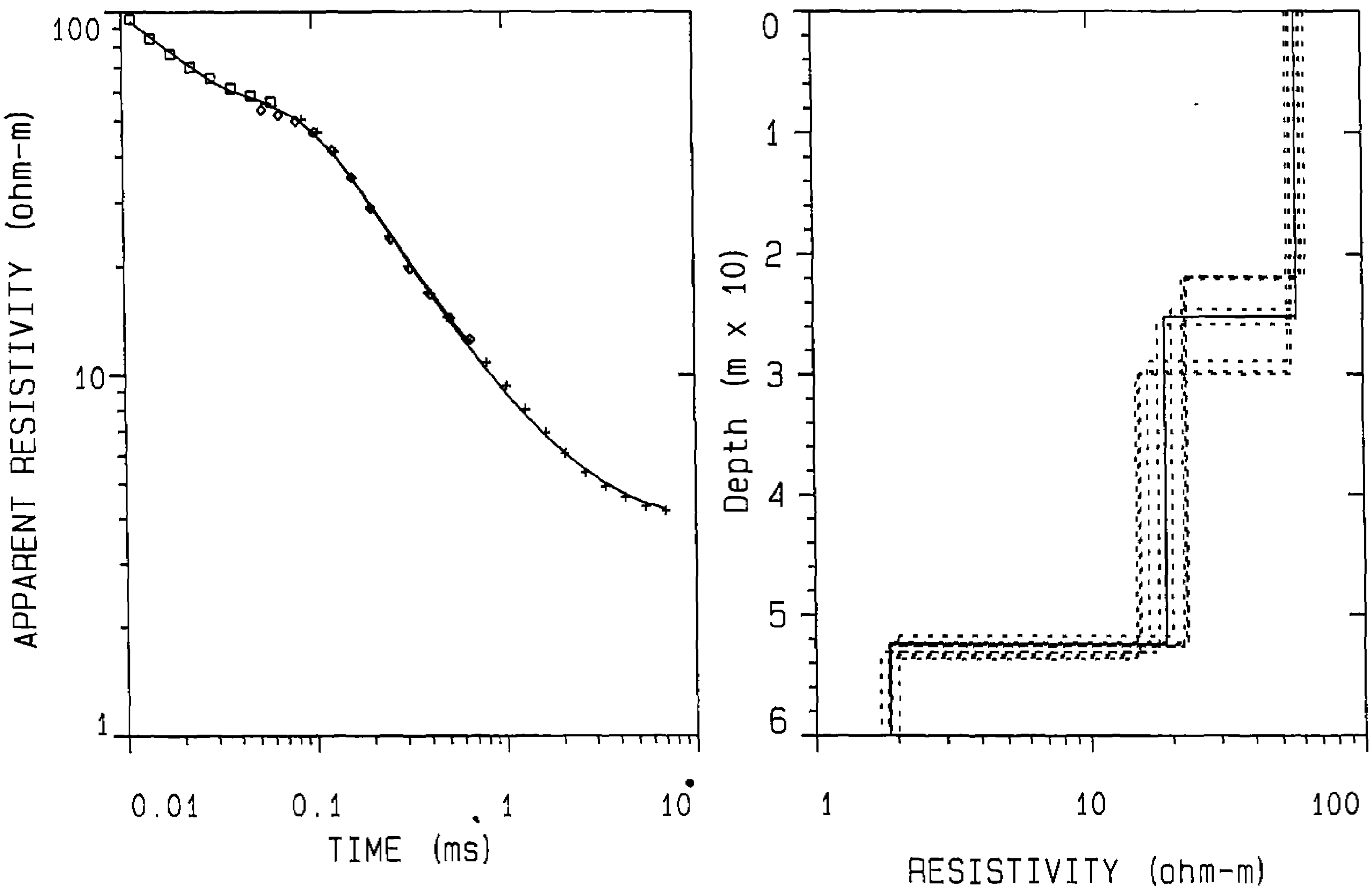

Stonewall County		Salt Pollution Study
Subsurface Detection		Site 15 Stonewall County, Tx
Data Set: SITE15	Date: JUN-07-00	
Equipment: Geonics PROTEM	Sounding: 570	Azimuth:

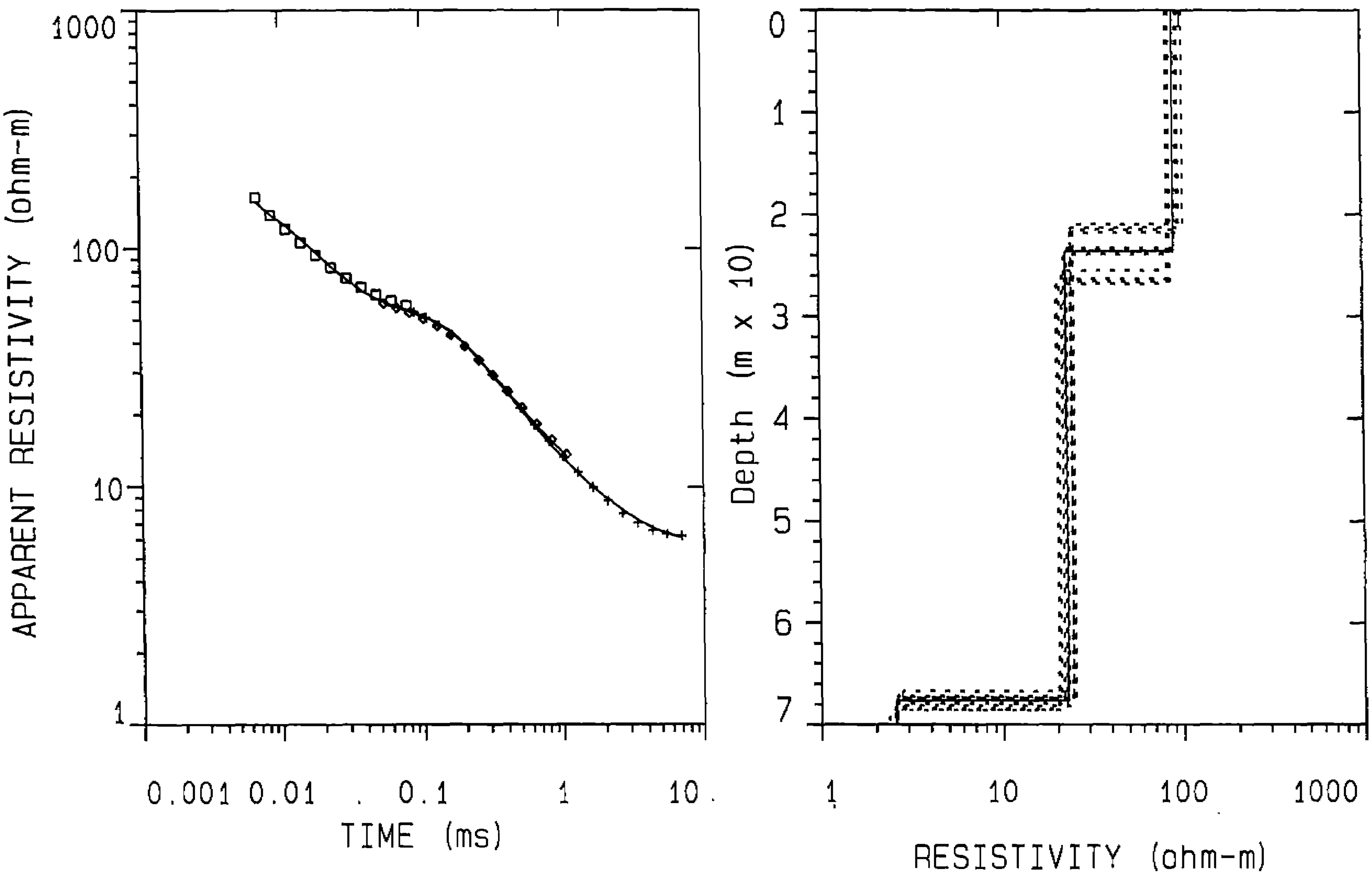

Stonewall County		Water Quality Assessment
Subsurface Detection		SITE 16 Stonewall County, TX
Data Set: SITE16	Date: JUN-07-00	
Equipment: Geonics PROTEM	Sounding: 1	Azimuth:

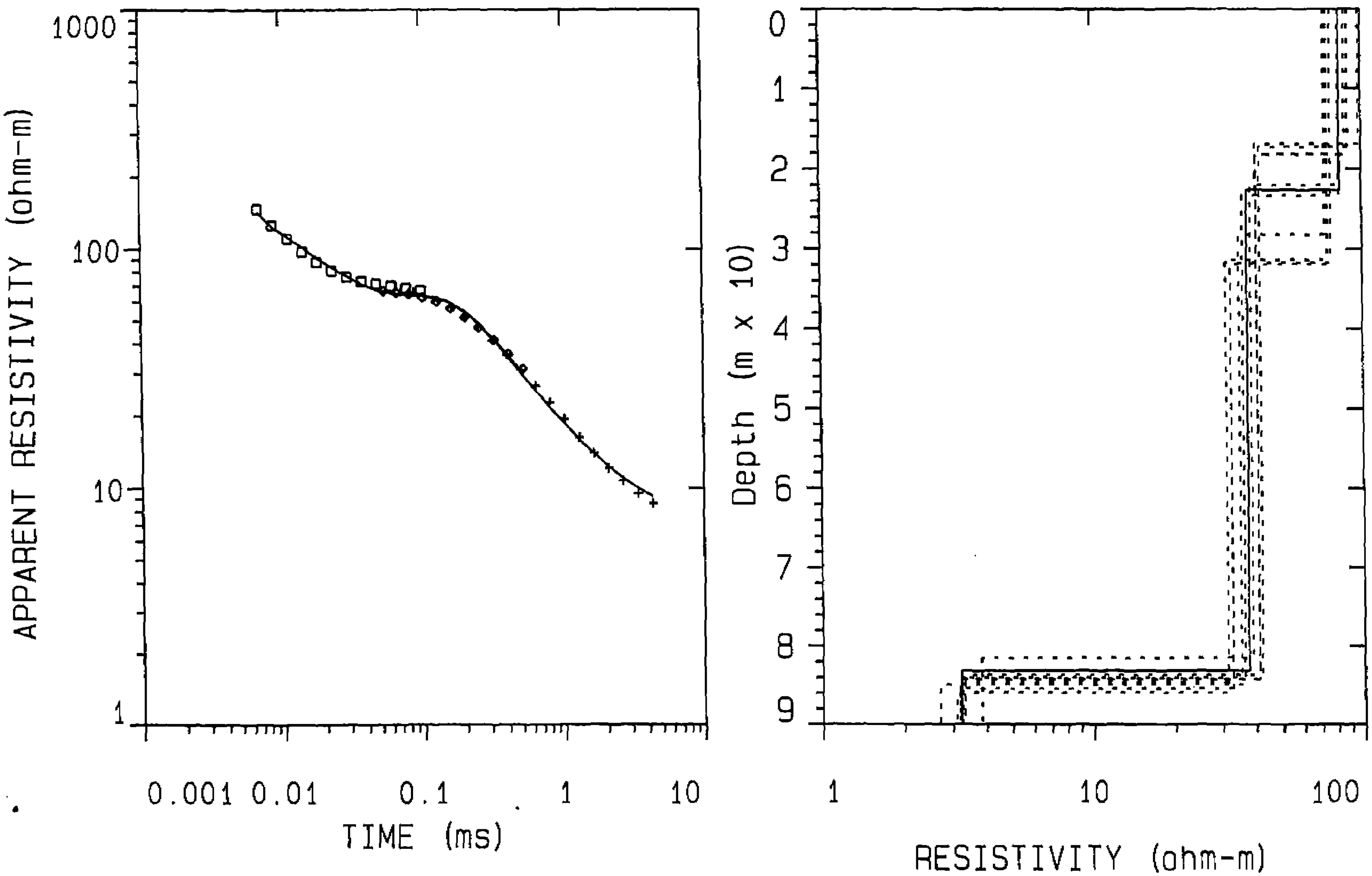

Stonewall County		Salt Pollution Study
Subsurface Detection		Site 17 Stonewall County, TX
Data Set: SITE17	Date: JUN-07-00	
Equipment: Geonics PROTEM	Sounding: 1	Azimuth:

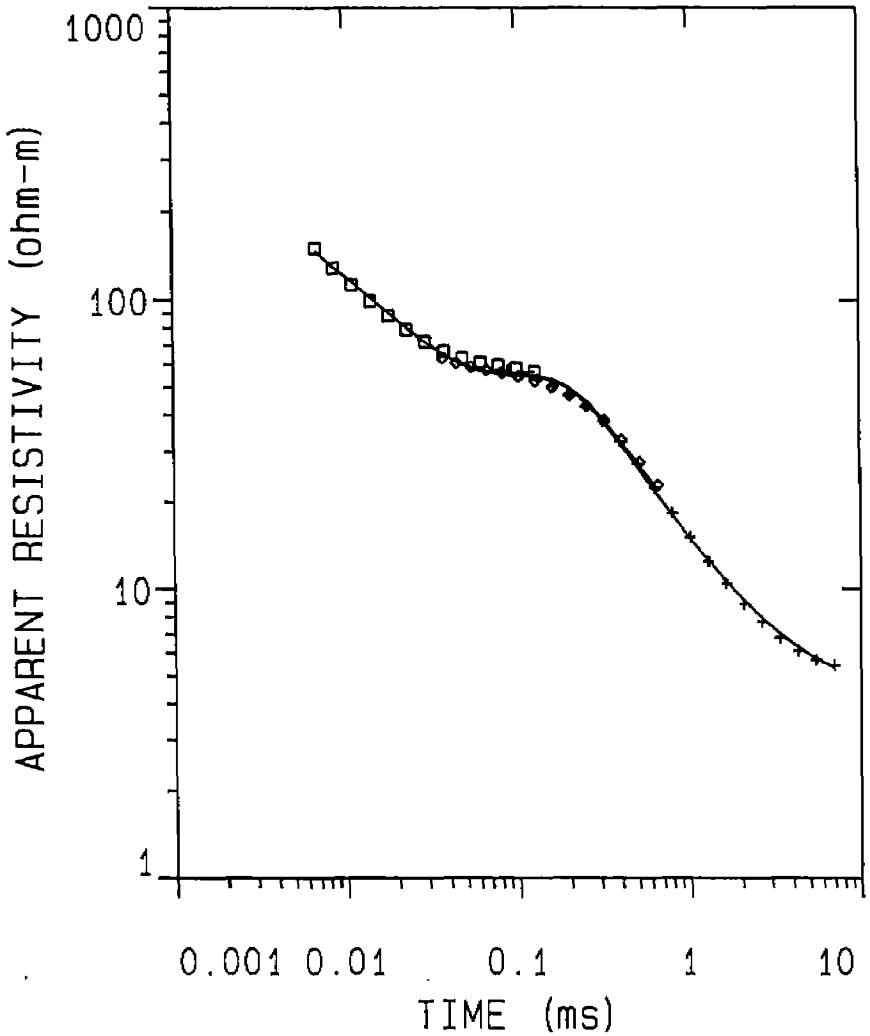

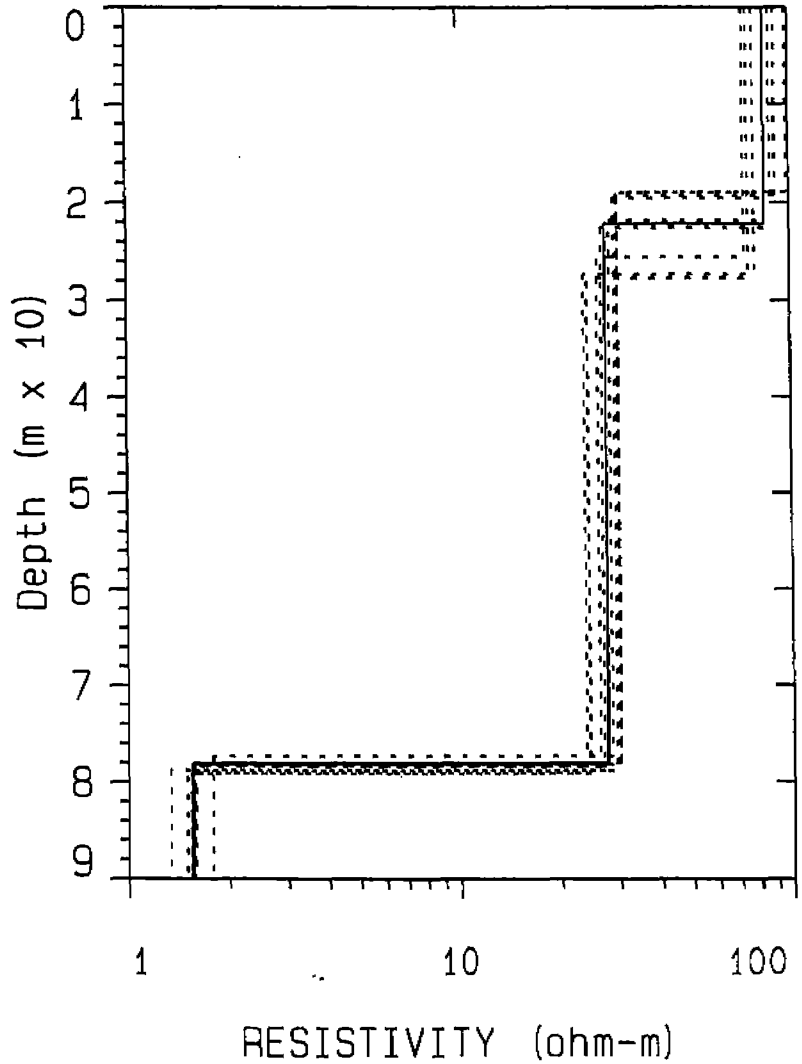

Stonewall County		Salt Pollution Study
Subsurface Detection		Site 18 Stonewall County, TX
Data Set: SITE18	Date: JUN-07-00	
Equipment: Geonics PROTEM	Sounding: 1	Azimuth:

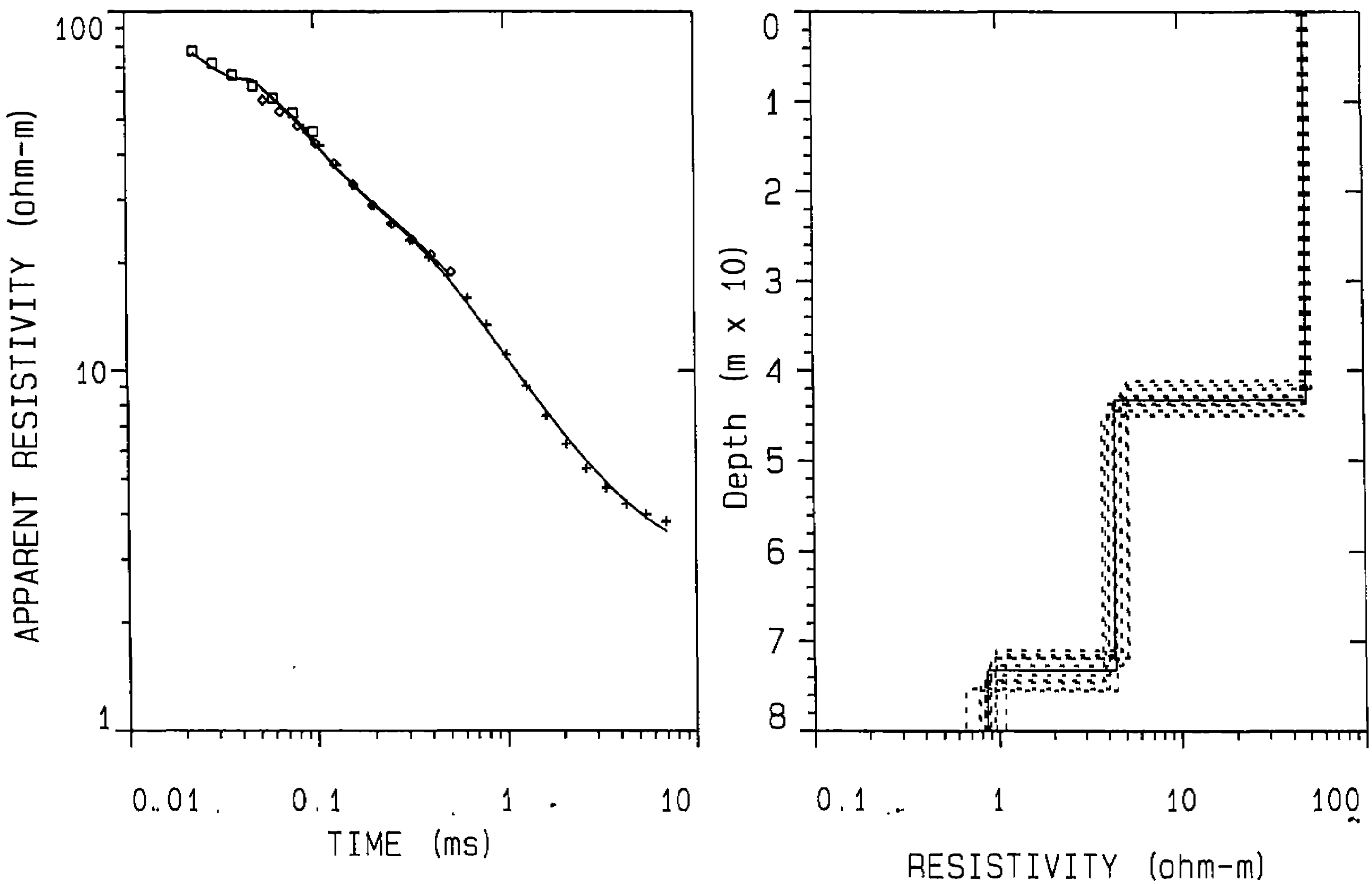

Stonewall County		Salt Pollution Study
Subsurface Detection		Site 19 Stonewall County, TX
Data Set: SITE19	Date: JUN-07-00	
Equipment: Geonics PROTEM	Sounding: 1	Azimuth:

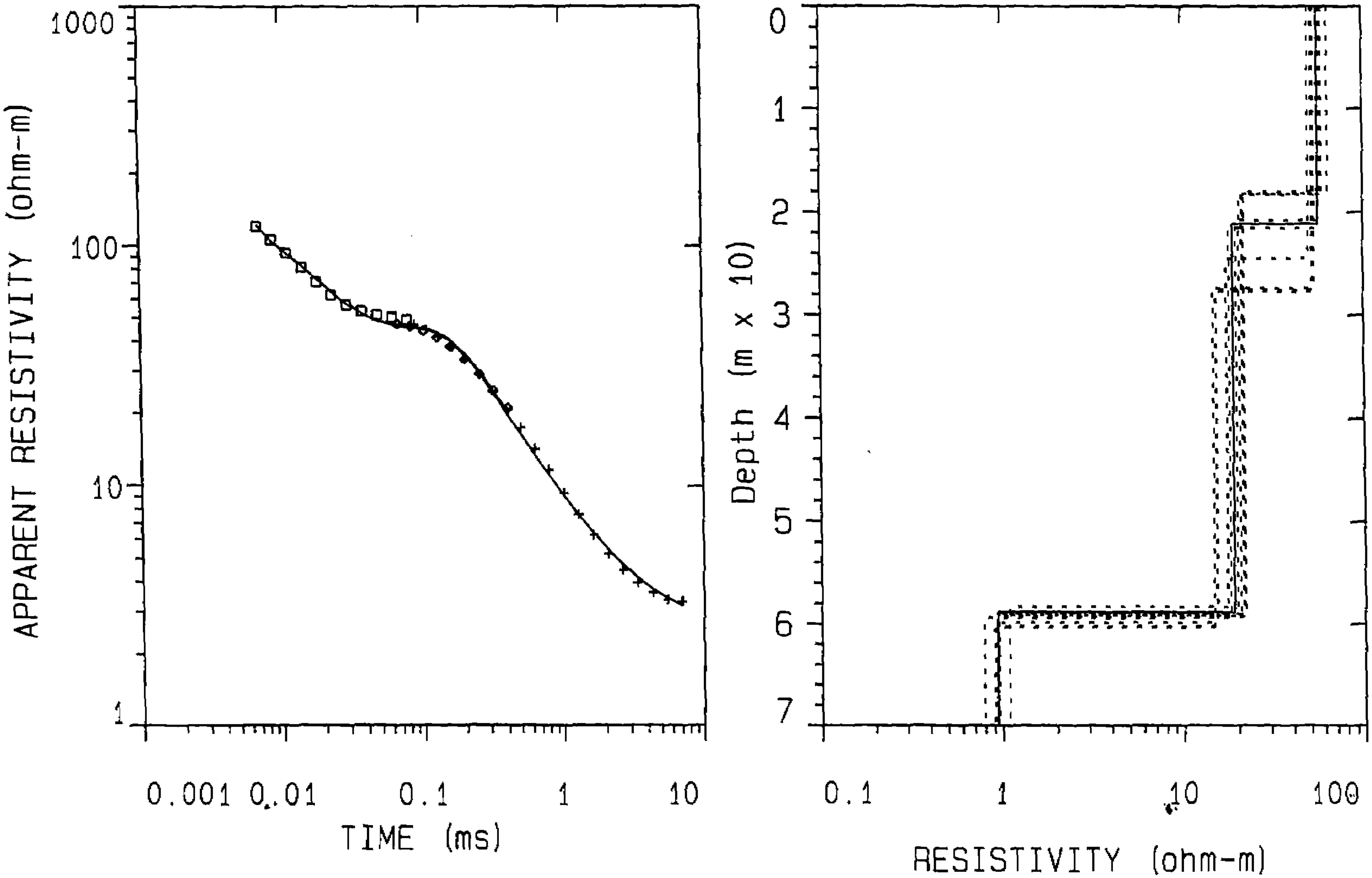

Stonewall County		Salt Pollution Study
Subsurface Detection		Site 20 Stonewall County, TX
Data Set: SITE20	Date: JUN-07-00	
Equipment: Geonics PROTEM	Sounding: 1	Azimuth:

BRAZOS RIVER

NATURAL SALT POLLUTION

CHLORIDE CONTROL

PROJECT

PREPARED FOR

STONEWALL COUNTY
BRAZOS RIVER AUTHORITY
U. S. ECONOMIC DEVELOPMENT
ADMINISTRATION

BY

R.W. RODGERS
RWR ASSOCS.
RICHMOND, TEXAS

BRAZOS RIVER CHLORIDE CONTROL PROJECT

TABLE OF CONTENTS

BRAZOS RIVER CHLORIDE CONTROL PROJECT

SUMMARY

Rocks of Middle and Late Permian age crop out within the Rolling Plains in narrow north-south trending belts. Halite-bearing rocks are abundant in these formations in the subsurface to the west. Salt springs and seeps occur along large streams and some tributaries within the outcrop area, with large salt flats occurring at major discharge points. Dove Creek Salt Flat, located in northwestern Stonewall County, is the site of spring discharges that contribute approximately one half of the total salt load of the Salt Fork Brazos River. The brine springs discharge through major fracture systems in the Grayburg Formation (Eskota Gypsum and Childress Dolomite), and the Dog Creek Formation.

Wells drilled to intercept the brine should be located along these major fractures, and at fracture intersection points. The wells will be located approximately one mile to the west of Dove Creek Salt Flat at locations determined from the geological and geophysical surveys.

The Grayburg and Dog Creek Formations dip to the west at approximately twenty five (25) feet per mile. Drainage patterns in these near-flat lying rocks would normally be dendritic in form, given the soft unconsolidated character of the shales and interbedded sands. However, the conversion of anhydrite to gypsum in the Eskota Gypsum has resulted in the interbedded gypsums becoming thicker and more consolidated. The scarp-forming Childress Dolomite and the gypsum beds are sufficiently resistant to cause a modified rectangular drainage pattern to develop (Figs. 1-3). An analysis of the drainage patterns from topographic maps, aerial photographs, photomosaics, and field studies resulted in six (6) localities being determined to conduct the geophysical surveys (Figs.1-4). These six (6) localities all meet the necessary criteria for a well location, including; number and size (length) of intersecting fracture trends, depth to the probable aquifer/aquiclude, relationship to the strike of the Childress Dolomite (aquifer/aquiclude), accessibility (terrain conditions) for drilling rig operations, and distance to Dove Creek for discharge of produced brine waters during field testing.

BRAZOS RIVER CHLORIDE CONTROL PROJECT

SECTION 1

SCOPE OF WORK

GEOLOGIC FIELD INVESTIGATION- Conduct a geologic field investigation in conjunction with a detailed analysis of aerial photographs and maps of the Salt Flat Area, to specifically define the regional fracture pattern geometry to provide site specific information to conduct the geophysical surveys. This will be accomplished by the following:

- Conducting a site specific geologic field investigation in the Salt Flat area;
- Assembling and analyzing topographic and geologic maps of the area to define the fracture patterns;
- Assembling and analyzing aerial photographs of the area to define the fracture patterns

Deliverables: Provide specific map locations of probable fracture intersections in order to facilitate conducting the geophysical survey program.

BRAZOS RIVER CHLORIDE CONTROL PROJECT

TASK 1-COMPLETE GEOLOGIC FIELD WORK, FINALIZE AERIAL PHOTO ANALYSIS TO DETERMINE FRACTURE INTERSECTION LOCATIONS FOR THE ELECTROMAGNETIC SURVEYS, AND IDENTIFY AREAS FOR FURTHER INVESTIGATION.

PROCEDURES

1- Site specific geologic field investigation in the Salt Flat area to determine the best-available potential well locations: based on both map and aerial photo analysis in conjunction with the field investigation. Field work was done during the Spring of 2000. Outcrops of the Eskota Gypsum were examined for evidence of fracture orientations which could be mapped. Small fractures in the Eskota shales, held open by large selenite gypsum crystals, were mapped, compared and correlated with the fracture trends determined from the topographic maps and air photos. Outcrops of the Childress Dolomite were examined in the area to the east of Salt Flat, and projected in cross-section to the study area in order to determine its position in the subsurface in the study area. (Geologic Atlas of Texas-Lubbock Sheet, 1:250,000).

2- Analyze aerial photos of the region, including: regional aerial photos provided by the U.S. Department of Agriculture, and stereo pairs of the area. Additionally, a regional photomosaic (1in.=1400 ft.) constructed specifically for this project was utilized. Prominent drainage patterns, defined by long, very narrow channels, were noted on the aerial photos. These features were much easier to define from the photos than from the topographic maps. These drainage features were examined in the field for any evidence that would indicate vertical movement of water, such as collapse structures, or former collapse areas. One such area was noted along the drainage connecting Locality F and Locality D areas (Fig. 6).

3- Analyze topographic maps. The Southerland Canyon (site specific), Seven Diamond L, and Lover's Resort - U.S.G.S. 1:24,000 (1in.=2000ft.) Topographic maps were used. (Figs. 1-1A-1B).

In order to determine possible fracture orientations and trends, the drainage patterns of Dove Creek, Salt Creek, Haystack Creek, Salt Croton Creek, and their tributaries were examined for directional trends. In order to make the examination more objective, specific characteristics of the drainage patterns were measured.

These included:

a- stream length(s) of trends.

b- grouping by stream length.

c- grouping trends by total number of streams of specific (minimum) lengths.

d- determining stream order number (Horton Analysis) to define trends of specific lengths.

e- plotting the drainage trends on the topographic maps.

f- plotting the trends on acrylic overlays in order to extend the trends to determine potential intersection points. Plotting these trends resulted in six (6) locations where at least three (3) or more major fracture trends intersected within the areas which met all the criteria for well locations (Fig.2).

g- the aerial photomosaic was used to define the most prominent photolinears, and to note any trends in the outcrop pattern of the Childress Dolomite (possible aquifer/ aquaclude) and the Eskota Gypsum which might indicate evidence of fracturing or faulting (Fig.6). There is no evidence of any faulting in the area.

h- structure contours of the Childress Dolomite were plotted on the topographic map, (Fig 3.) and the probable depth to the aquifer/aquiclude, Childress Dolomite and associated fractured shales, at each potential fracture intersection was determined

BRAZOS RIVER CHLORIDE CONTROL PROJECT

FRACTURE INTERSECTION LOCATIONS-

Six (6) fracture intersection locations were defined which met the necessary criteria for a well location (Fig. 2), including:
a- number and size (length) of intersecting fracture trends
b- depth to probable aquifer/aquiclude
c- relationship to the strike of the Childress Dolomite (aquifer/aquiclude)
d- accessibility (terrain conditions) for drilling rig operations.
e- distance to Dove Creek for discharge of produced brine waters during field testing

The geographic position of these intersections (latitude/longitude) was determined, and provided for the geophysical investigation team. (Fig. 4)

Three (3) different geophysical investigations were conducted at each of these sites. These included: EM 34-Terrain Conductivity, VLF-Very Low Frequency EM, and Time Domain EM.

The EM 34 and VLF surveys were designed to define the trend and location of near- vertical brine-filled fractures. The Time Domain EM is designed to determine the depth and thickness of variations of layers in the subsurface, including variations in groundwater chemistry and depth to the deep-brine aquifer.

Additionally, ten (10) other locations, associated with fracture trends, were mapped using the Time Domain EM in order to define the geometry of the Childress Dolomite.

Based on the field investigations, seventeen (17) anomalies were staked in the field to define potential fracture traces, and potential well locations (Fig.6).

BRAZOS RIVER CHLORIDE CONTROL PROJECT

GEOLOGY

Dove Creek Salt Flat is located within the Low Rolling Plains of North-Central Texas, on the eastern edge of the Permian Basin. Rocks of Middle and Late Permian age crop out in narrow north-south trending belts. In the study area, the Grayburg Formation, Eskota Gypsum and Childress Dolomite, forms the surface terrain, and is underlain by fractured shales of the Dog Creek Formation. The interbedded shales and gypsums of the Eskota, and the dolomites and poorly-cemented sandstones of the Childress form a topography dominated by deep canyons and local upland flats. The flats are typically formed on one of the four main gypsum zones in the Eskota. The Childress Dolomite crops out to the east of the study area where it forms prominent ledges in the canyons.

The Grayburg and Dog Creek Formations dip to the west at approximately twenty-five (25) feet per mile. Drainage patterns in these near-flat lying rocks would normally be dendritic in form, given the soft unconsolidated character of the shales and interbedded sands. However, the conversion of anhydrite to gypsum in the Eskota Gypsum has resulted in the interbedded gypsum beds becoming thicker and more consolidated. The scarp-forming Childress Dolomite and the gypsum beds are sufficiently resistant to result in a modified rectangular drainage pattern (Figs.1, 1A, 1B, 5, 6). These fracture trends appear to follow earth's regmatic fracture pattern. There are a number of gypsum caves in the region which are formed along major fractures. At Locality F, a large sinkhole has developed in the Eskota Gypsum. Fracture trend projections (Fig.2) located an area at Locality D where a large collapse structure is forming.

Halite-bearing rocks are abundant in the subsurface to the west of the study area. Dissolution of the halite has resulted in salt springs and seeps which discharge along large streams and some tributaries, with large salt flats occurring at major discharge points. The brine springs discharge through major fracture systems in the Grayburg and Dog Creek Formations.

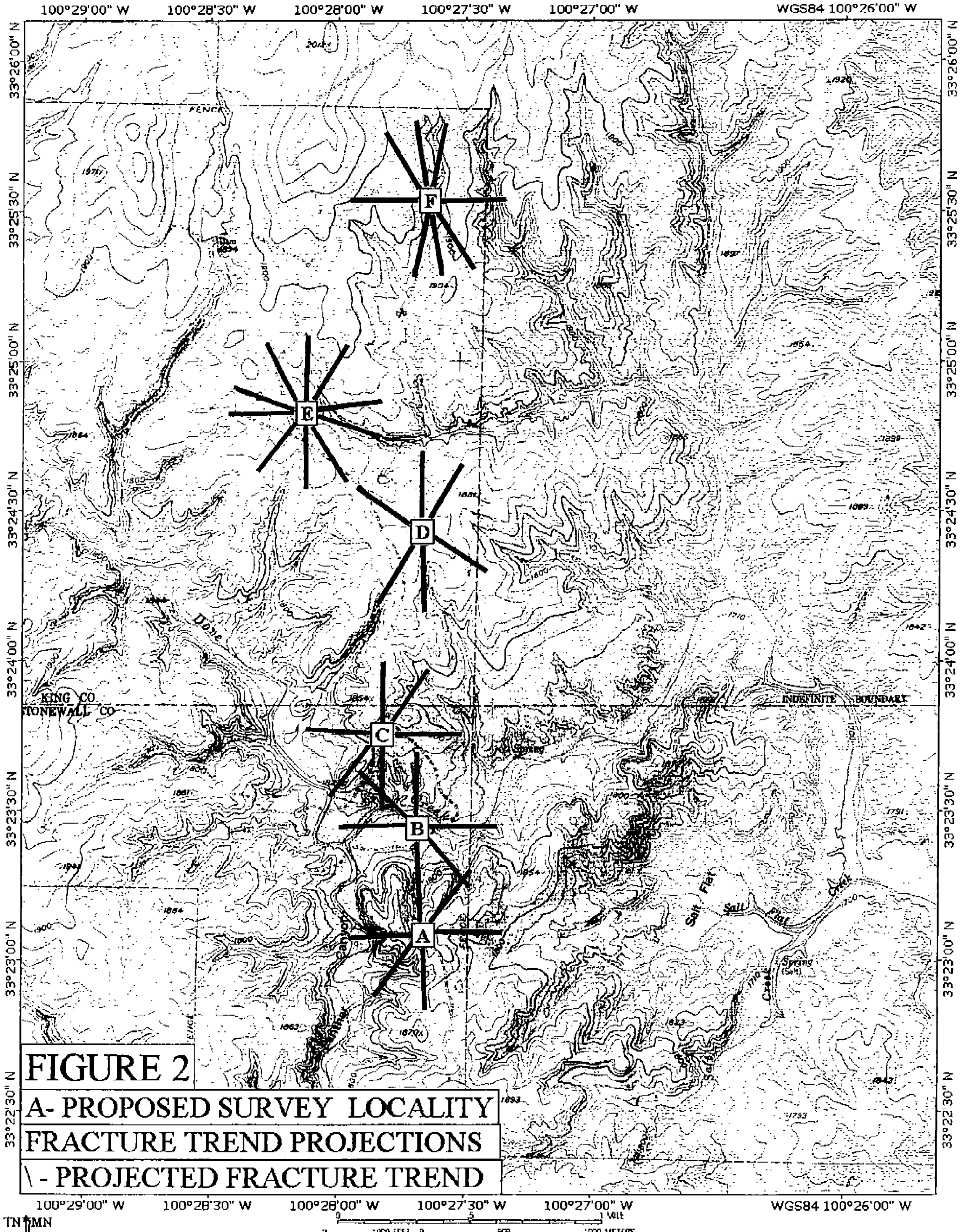

FIGURE 2

A- PROPOSED SURVEY LOCALITY

FRACTURE TREND PROJECTIONS

\ - PROJECTED FRACTURE TREND

Printed from TOPO! ©2001 National Geographic Holdings (www.topo.com)

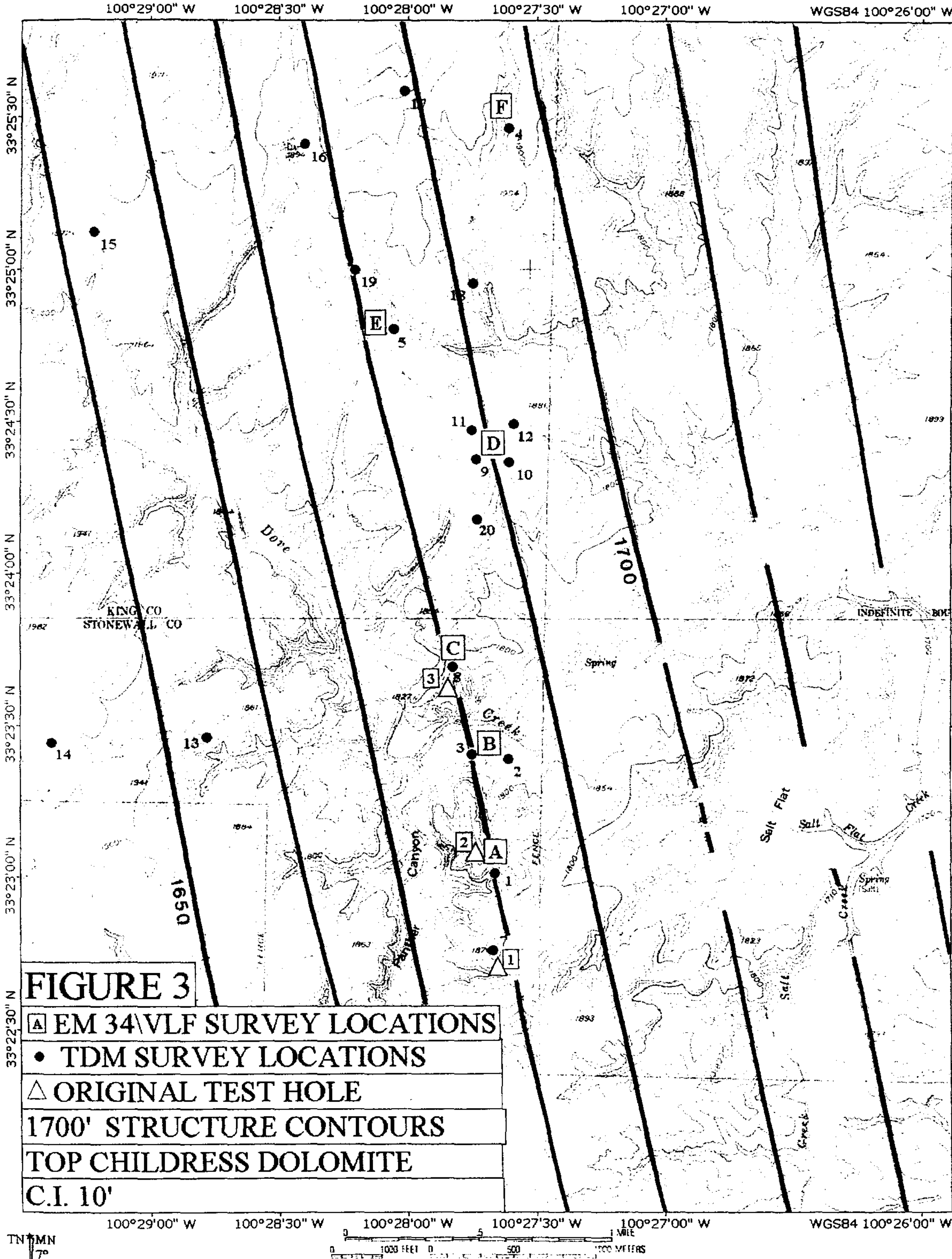

Printed from TOPO! ©2001 National Geographic Holdings (www.topo.com)

BRAZOS RIVER CHLORIDE CONTROL PROJECT

FIG. 4

LOCALITY POINTS- SOUTHERLAND CANYON
USGS TOP. MAP 1: 24,000 SCALE

LOCALITY

A 100 deg. 27' 38" W
33 deg. 23' 05" N

B 100 deg. 27' 38" W
33 deg. 23' 27" N

C 100 deg. 27' 41" W
33 deg. 23' 40" N

D 100 deg. 27' 35" W
33 deg. 24' 26" N

E 100 deg. 28' 04" W
33 deg. 24' 46" N

F 100 deg. 27' 06" W
33 deg. 25' 45" N

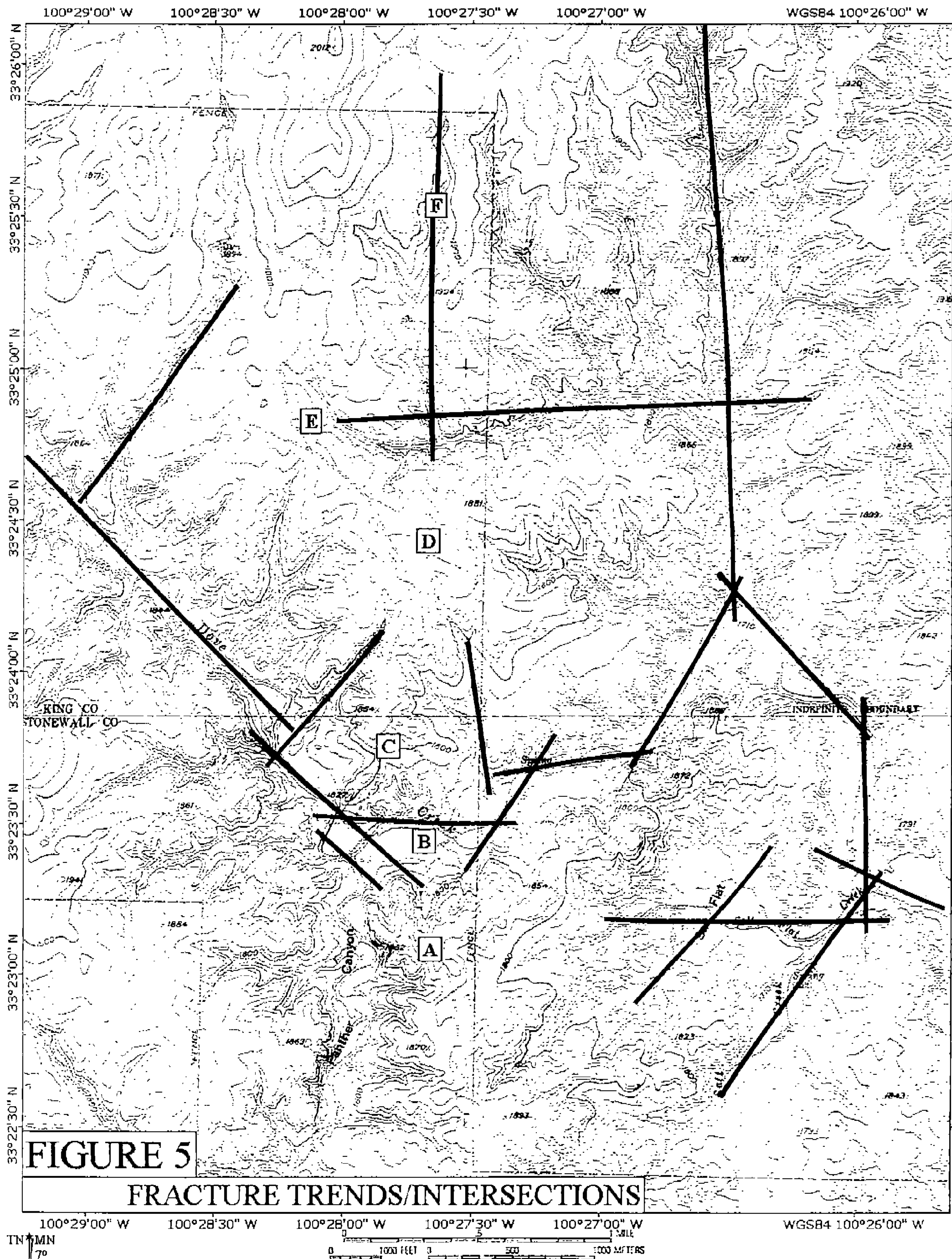

FIGURE 5

FRACTURE TRENDS/INTERSECTIONS

Printed from TOPO! ©2001 National Geographic Holdings (www.topo.com)

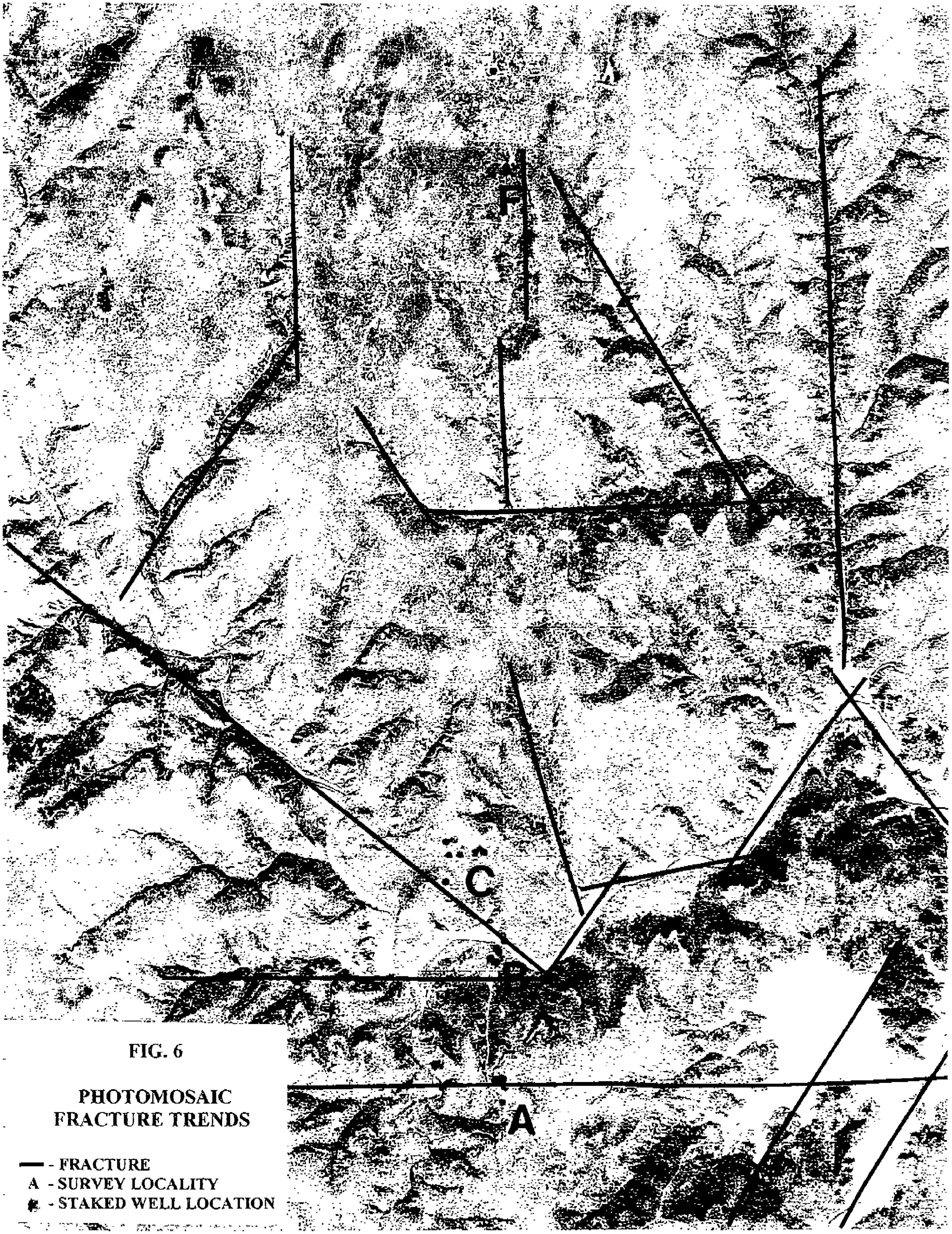

FIG. 6

PHOTOMOSAIC
FRACTURE TRENDS

BRAZOS RIVER CHLORIDE CONTROL PROJECT

LOCALITY DESCRIPTIONS

A- Locality A is in proximity to the first test well drilled in the first phase of the project in 1998. The first well drilled at this site showed potential for substantial brine flow before being lost due to drilling conditions. Two subsequent tests did not show this flow potential. It was believed that the first attempt may have been in, or close to, a possible fracture. This area was originally chosen because it is immediately west of, and downdip, from the Salt Flat. The area shows two prominent trends, one which is N 30 deg. E, and is in line with a section of Dove Creek where the nearest salt spring is located. The other trends slightly west of north, and is in line with Area B and C. There are also prominent E-W drainages just to the to the south and to the north of Locality A. Depth to the brine aquifer is estimated to be approximately 160 ft.

B- Locality B is in the floodplain of Dove Creek, and includes the area where a well blowout occurred in the 1950's. Reports indicate that this well flowed substantial quantities of brine before being plugged and abandoned. Three prominent trends were observed at this locality. The trend N 45-50 deg. W follows a prominent trend of Dove Creek. A prominent E-W trend is also affecting the flow of, and drainage into, Dove Creek. A trend which is slightly west of north was observed from the maps and air photos, and also from field observations. Depth to the brine aquifer is estimated to be approximately 45 ft.

C- Locality C is located to the north of Dove Creek, and is near the area where the northernmost test well was drilled in 1998. The prominent N-S trend is present, as well as the E-W trend which is in line with the salt spring located to the east on Dove Creek. Depth to the brine aquifer is estimated to be approximately 120 ft.

D- Locality C is located to the north of Dove Creek on an upland flat. Three very prominent trends, and two less prominent trends were projected into this locality. A N 30-35 deg. E trend, a N 55-60 W trend, and a very prominent N-S trend were noted. The N-S trend is in line with the drainage that connects to the prominent sink hole at Locality F. When this locality was field checked, features indicating the formation of a prominent sink hole were also observed There is a pronounced depression with large blocks of the Upper Eskota Gypsum bowed up in the center. This indicates that the downward movement in the area is creating a space problem causing the gypsum to be fractured and displaced. There is good field evidence that there is a prominent subsurface drainage from the north flowing south toward Dove Creek. Depth to the brine aquifer is approximately 190 ft.

E- Locality E is the westernmost of the localities. There are several prominent trends Which project into the area. N 75-80 deg E, N 30 deg. E, N 65-70 deg. W, N 30 deg. W, and N-S. No surface features were observed at this locality. Certainly nothing similar to Locality D, although the area is in an upland flat similar to D. The area is covered by unconsolidated silts and sands in the Eskota, making it difficult to define local features. The pronounced E-W fracture trend following the rapidly developing very narrow, deep canyon, which flows into the N-S drainage which flows from Locality F toward Dove Creek (Fig. 6). Depth to the brine aquifer is approximately 175 ft.

F- Locality F is the northernmost of the localities. There are three prominent trends which project into the area. N 30-35 deg. W, N 10 deg. E, and N 10 deg. W. A trend, E-W, was observed in fractures on outcrops at the locality. A very large, deep sinkhole with a pronounced E-W trend at depth is located in the area. The sinkhole was explored to a depth of approximately 130 ft. This is the highest elevation of any of the localities, and it appears that a pronounced N-S surface drainage that enters the fracture system at this point and then drains south to Dove Creek begins in this area. Depth to the brine aquifer is approximately 205 ft.